TESIS DE LA UNIVERSIDAD DE ZARAGOZA

2020

116

Roberto Castro Muñoz

# Preparation and characterization of mixed matrix membranes for gas separation and pervaporation

Departamento

Ingeniería Química y Tecnologías del Medio Ambiente

Director/es

Fila, Vlastimil

Coronas Ceresuela, Joaquín

Drioli, Enrico



ISSN 2254-7606

Prensas de la Universidad Universidad Zaragoza



ISSN 2254-7606

Universidad Zaragoza
1542

Tesis Doctoral

# PREPARATION AND CHARACTERIZATION OF MIXED MATRIX MEMBRANES FOR GAS SEPARATION AND PERVAPORATION


Autor

Roberto Castro Muñoz

Director/es

Fila, Vlastimil
Coronas Ceresuela, Joaquín
Drioli, Enrico

**UNIVERSIDAD DE ZARAGOZA**

Ingeniería Química y Tecnologías del Medio Ambiente


2019

UNIVERSITY OF
CHEMISTRY AND TECHNOLOGY
PRAGUE

UNIVERSITÀ
DELLA CALABRIA

Universidad
Zaragoza

# Preparation and characterization of mixed matrix membranes for gas separation and pervaporation

## DISSERTATION


| | |
|---|---|
| AUTHOR | **MSc. Roberto Castro Muñoz** |
| SUPERVISOR | **doc. Dr. Ing. Vlastimil Fíla**<br>**Prof. Enrico Drioli**<br>**Prof. Joaquin Coronas** |
| STUDY PROGRAMME | Chemistry and Chemical Technologies |
| FIELD OF STUDY | Inorganic Technology |
| YEAR | **2019** |

VYSOKÁ ŠKOLA
CHEMICKO-TECHNOLOGICKÁ
V PRAZE

UNIVERSITÀ
DELLA CALABRIA

Universidad
Zaragoza

# Příprava a charakterizace membrán se smíšenou matricí pro separaci plynů a pervaporaci

## DISERTAČNÍ PRÁCE


| | |
|---|---|
| AUTOR | **MSc. Roberto Castro Muñoz** |
| ŠKOLITEL | **doc. Dr. Ing. Vlastimil Fíla**<br>**Prof. Enrico Drioli**<br>**Prof. Joaquin Coronas** |
| STUDIJNÍ PROGRAM | Chemie a chemické technologie |
| STUDIJNÍ OBOR | Anorganická technologie |
| ROK | **2019** |

“To Mexico“

“To *my mom (Silvia Muñoz Ramírez), father (Sergio Castro Elizalde †), brothers (Jorge, Daniel, Angel) to support me all the time*”

“*Kochanie (Miss Gontarek)… kocham cie”*

“I know that I know nothing” …….. *Socrates*

# Summary

The main aim of this research work was to develop mixed matrix membranes (MMMs), which may provide superior performance compared to the base pristine polymers, for two different types of membrane-based technologies (e.g. gas separation and pervaporation). In the first part of the thesis, the enhancement of $CO_2$ permeation of a commercial polymer, like Matrimid®5218 polyimide, was aimed. At this point, it is proposed, for the first time, the preparation of ternary MMMs based on the filling ZIF-8 nanoparticles (33.83 ± 6.2 nm) into Matrimid®-PEG 200 blend. The MMMs were tested at fixed feed composition (equimolar mixture $CO_2$: $CH_4$) and different feed pressures (from 2 to 8 bar). The MMMs were characterized using SEM, EDX, DSC, and TGA. The results indicate that the incorporation of 30 wt.% of ZIF-8 nanoparticles leads to increase of $CO_2$ permeability in binary (up to 31.47 Barrer) and ternary MMMs (up to 33.12 Barrer); pointing out that the addition of PEG and ZIF-8 enhanced the $CO_2$ permeability (more than 4-folds) comparing to the neat Matrimid® membranes (7.16 Barrer).

The use of this commercial Matrimid®5218 polyimide, as a hydrophilic polymer, has been also extended to other membrane technology (e.g. pervaporation). The potentiality of this polyimide deals with the separation of organic-organic azeotropic mixtures. Herein, Matrimid® membranes were prepared and tested, for the first time, in pervaporation (PV) separation of azeotropic methanol (MeOH)- methyl *tert*-butyl ether (MTBE) mixture (14.3 and 85.7%, respectively). The PV experiments were carried out at different feed temperatures (25-45ºC) and vacuum pressures (0.0538, 0.2400, 2.1000 mbar) at permeate side. The results pointed out that the feed temperature (in the range of 25-45 ºC) affected mainly the MeOH permeation producing an increasing on its permeate flux and separation factor as well. Importantly, the best performances of Matrimid® were found at 45 ºC and 0.054 mbar, where a permeate flux and a separation factor of about 0.073 kg $m^{-2}$ $h^{-1}$ and 21.16, respectively, were reached.

In the last part of this thesis, the enhancement of another commercial polymer, like poly(vinyl alcohol) (PVA), was proposed for PV applications. In this way, a highly

hydrophilic inorganic material, like graphene oxide (GO), was successfully prepared and incorporated into a cross-linked PVA matrix. The MMMs were tested for the dehydration of ethanol (10:90 wt.% water-ethanol), monitoring their performance in terms of total permeate flux, components fluxes, as well as their separation factor. The effect of filler was analyzed by doubling the GO content (at 0.5, 1.0, and 2.0 wt.%) in the MMMs. Furthermore, the membranes were characterized by FESEM, DSC, TGA, XRD, measurements of degree of swelling, water contact angle, and mechanical properties. The best performance of such MMMs (containing 1 wt.% of GO) was found at 40 ºC, displaying a separation factor of 263 and a permeate flux of about 0.137 $kg \cdot m^{-2} \cdot h^{-1}$ (in which 0.133 $kg \cdot m^{-2} \cdot h^{-1}$ corresponds to water). This result represents a 75 % enhancement of the original permeation rate of pristine cross-linked PVA membranes.

Finally, this work reports the enhancement of two commercial polymers (such as Matrimid®5218 polyimide and poly(vinyl alcohol) (PVA)). It is important to mention that such polymers were chosen according to their consolidation in large-scale production and their near application at industrial scale. In general, the chapters also address the literature reviews to select each case of study, and thus to be attended during this research (e.g. $CO_2/CH_4$ and MeOH-MTBE separations as well as ethanol dehydration). Moreover, this thesis provides relevant insights into the suitable preparation procedures to reach high performing MMMs.

# Souhrn

Hlavním cílem této práce bylo vyvinout membrány se směsnou matricí (mixed matrix membranes, MMMs) použitelné při separaci plynu a pervaporaci, které by měly ve srovnání s čistými polymerními materiály lepší vlastnosti. První část práce je zaměřena na zlepšení permeace $CO_2$ v komerčně dostupném polyimidu Matrimid®5218. V rámci této studie byly připraveny dvousložkové MMMs na bázi Matrimid/ZIF-8 a ternární MMMs kombinující Matrimid, PEG 200 a ZIF-8. Ternární MMMs byly připraveny vnášením nanočástic ZIF-8 (33.83 ± 6.2 nm) do směsi Matrimid®-PEG 200 a tato kombinace složek byla vyzkoušena a ověřena vůbec poprvé. Membrány byly testovány při separaci ekvimolární binární směsí $CO_2$: $CH_4$ za různých tlaků (od 2 do 8 bar). Přítomnost 30 % hmot. nanočástic ZIF-8 vedla ke zvýšení permeability $CO_2$ jak v binárních MMMs (až 31.47 Barrer) tak i v ternárních MMMs (až 33.12 Barrer). Z porovnání uvedených hodnot vyplývá, že přídavek ZIF-8 vede k významnému zvýšení permeability $CO_2$ (více než čtyřikrát) oproti membránám z čistého Matrimidu (7.16 Barrer). Přídavek PEG vykazuje synergický efekt s ZIF-8 a vede k dalšímu zvýšení permeability, které však již není tak významné.

Komerčně dostupný hydrofilní polyimid Matrimid®5218 byl testován v další membránové technologii, pervaporaci. Potenciální aplikace tohoto materiálu spočívá zejména v separaci organických azeotropických směsí. V této práci byly také poprvé použity a testovány Matrimidové membrány v pervaporační separaci azeotropické směsi metanol (MeOH)/metyl-terc-butyleter (MTBE) (obsah MEOH 14.3 % hmot.). Pervaporační experimenty byly provedeny při různých teplotách nástřiku (24-45 °C) a při tlacích na straně permeátu blízkých vakuu (0.0538, 0.2400, 2.1000 mbar). Teplota nástřiku ovlivňuje zejména permeaci MeOH, která vede ke zvýšení jeho permeátového toku a současně i separačního faktoru. Nejlepší separační vlastnosti vykazovala tato membrána při vstupní teplotě 45 °C a tlaku na straně permeátu 0.054 mbar, kdy bylo dosaženo toku permeátu 0.073 kg $m^{-2}$ $h^{-1}$ a hodnoty separačního faktoru 21.16.

V poslední části práce bylo navrženo zlepšení separačních vlastností dalšího komerčně dostupného polymeru na bázi polyvinylalkoholu (PVA) pro využití v pervaporaci. Vysoce hydrofilní anorganický materiál, oxid grafenu (GO), byl úspěšně připraven a inkorporován do zesíťované PVA matrice. Takto připravené membrány byly testovány při dehydrataci etanolu (10:90 % hmot. voda-etanol) a jejich výkon byl určen měřením toku permeátu, toku jednotlivých složek a separačního faktoru. Vliv přidaného plniva byl zkoumán zdvojnásobením obsahu GO (na 0.5, 1.0 a 2.0 % hmot.) v MMMs. Membrány byly charakterizovány pomocí metod FESEM, DSC, TGA, XRD a současně byl měřen stupeň botnání, kontaktní úhel vody a mechanické vlastnosti. Nejlepších vlastností dosáhly membrány s obsahem GO 1 % hmot. při 40 °C, kdy byl naměřen separační faktor 263 a tok permeátu 0.137 $kg \cdot m^{-2} \cdot h^{-1}$ (v němž 0.133 $kg \cdot m^{-2} \cdot h^{-1}$ připadá na vodu). Tento výsledek představuje zlepšení původní permeační rychlosti membrán z čistého zesíťovaného PVA o 75 %.

V závěru lze říci, že v této práci jsou popsány metody vhodné k přípravě vysoce účinných MMMs a navrženy MMMs na bázi dvou komerčně dostupných polymerů (polyimidu Matrimid®5218 a PVA), které vykazují oproti čistým polymerům významné zlepšení. Je důležité zmínit, že tyto polymery byly vybrány z důvodu jejich vysokokapacitní výroby a možnosti využití v průmyslovém měřítku. Součástí této práce jsou i kapitoly shrnující relevantních poznatky z odborné literatury pro každou řešenou oblast, na kterou se práce zaměřuje (např. $CO_2/CH_4$ a MeOH-MTBE separace a dehydratace etanolu).

# Resumen

El objetivo principal de esta investigación fue desarrollar membranas de matriz mixta (MMMs) que pueda proveer un rendimiento superior que los polímeros puros para dos diferentes tipos de tecnologías de membranas (por ejemplo separación de gas y pervaporación). En la primera parte de esta tesis, el mejoramiento de la permeación de $CO_2$ de un polímero commercial, como la polimida Matrimid®5218, fue abordada. En este punto, fue propuesta por primera vez la preparación de MMMs ternarias rellenando nanopartículas ZIF-8 (33.83 ± 6.2 nm) en la mezcla Matrimid®-PEG 200. Las MMMs fueron probadas a diferentes composiciones (50:50) y presiones de alimentación (de 2 a 8 bar). Las MMMs fueron también caracterizadas usando SEM, EDX, DSC, and TGA. Los resultados indicaron que la incorporación del 30 %p/p de nanopartículas condujo a incrementar la permeabilidad al $CO_2$ en las MMM binarias (hasta 31.47 Barrer ) y ternarias (hasta 33.12 Barrer); destacando que la adición del PEG y el ZIF-8 mejoró la permeabilidad al $CO_2$ (mas de tres veces) en comparación con las membranas Matrimid® puras (7.16 Barrer).

El uso de esta poliimida comercial Matrimid®5218, como un polímero hidrofílico, ha sido también extendido a otra tecnología de membrane (por ejemplo la pervaporación). La potencialidad de esta polimida se relaciona con la separación de mezclas azeotrópicas orgánicas-orgánicas. En este punto, membranas de Matrimid®5218 fueron preparadas y probadas por primera vez en separación por pervaporación (PV) de la mezcla azeotrópica methanol (MeOH)- metil terc-butil éter (MTBE) (14.3 y 85.7%p/p, respectivamente). Los experimentos PV fueron llevados acabo a diferentes temperaturas (25-45ºC) y presiones de vacío (0.0538, 0.2400, 2.1000 mbar) en el permeado. Los resultados destacan que la temperatura (en el rango de 25-45 ºC) afectó principalmente la permeación del MeOH, produciendo un incremento en su flujo de permeado y el factor de separación también. Los mejores rendimientos de Matrimid® fueron a 45 ºC y 0.054 mbar, donde un flujo de permeado y un factor de separación de alrededor de 0.073 kg $m^{-2}$ $h^{-1}$ y 21.16, respectivamente, fueron alcanzados.

En la última parte de esta tesis, el mejoramiento de otro polímero comercial, como el alcohol de polivinilo (PVA), fue propuesto para aplicaciones de PV. De este modo, un material altamente hidrofílico, como el óxido de grafeno (GO), fue existosamente preparado e incorporado en una matriz de PVA reticulado. Las MMM fueron probadas para la deshidratación de etanol (10:90 %p/p agua-etanol) monitoreando su rendimiento en terminus de flujo total de permeado, flujo por componentes, así como su factor de separación. El efecto del relleno fue analizado duplicando el contenido del GO (a 0.5, 1.0, and 2.0 %p/p) en las MMMs. Además, las membranas fueron caracterizadas por FESEM, DSC, TGA, XRD, grado de hinchamiento, ángulo de contacto con agua, y propiedades mecánicas. El mejor rendimiento de dichas MMMs (conteniendo 1 %p/p de GO) fue encontrado a 40 ºC, mostrando un factor de separación de 263 y un flujo de permeado de alrededor de 0.137 $kg \cdot m^{-2} \cdot h^{-1}$ (en el cual 0.133 $kg \cdot m^{-2} \cdot h^{-1}$ corresponde a agua). Este resultado representa una mejora del 75 % de la tasa de permeación original de las membranas reticuladas de PVA pura.

Finalmente, este trabajo reporta el mejoramiento de dos polímeros comerciales (tales como poliimida Matrimid®5218 y alcohol de polivinilo). Es importante mencionar que tales polímeros fueron selecionados acorde a su consolidación en producción a grande escala y su aplicación cercana a escala industrial. En general los capítulos también abordan revisiones de literatura para seleccionar cada caso de estudio y así ser atendidos durante esta investigación (por ejemplo separaciones $CO_2/CH_4$ y MeOH-MTBE, así como deshidratación de etanol). Además, esta tesis provee puntos relevantes en procedimientos de preparación adecuados para obtener MMMs con buen rendimiento.

# Riassunto

Lo scopo principale del presente lavoro è stato lo sviluppo di membrane a matrice mista (MMMs) in grado di mostrare prestazioni superiori rispetto ai classici polimeri puri, in due tipi di processi a membrana: separazione di gas e pervaporazione. La prima parte della tesi è stata incentrata sul miglioramento della permeazione alla $CO_2$ in membrane preparate con il polimero commerciale Matrimid® 5218. E' stata pertanto proposta, per la prima volta, le preparazione di MMMs basate sull'incorporazione di nanoparticelle ZIF-8 (33.83 ± 6.2 nm) all'interno di un blend polimerico costituito da Matrimid® e polietilenglicole (PEG) 200. Le MMMs ottenute sono state testate ad una composizione fissa (50:50) e differenti pressioni ( da 2 a 8 bar). Le MMMs sono state inoltre caratterizzate attraverso SEM, EDX, DSC e TGA. I risultati indicano che l'incorporazione del 30 %p/p di nanoparticelle ZIF-8 porta ad un aumento della permeabilità alla $CO_2$ nelle MMMs preparate con Matrimid®+PEG fino a 31.47 Barrer, e per quelle preparate con Matrimid®+PEG+ZIF-8 fino a 33.12 Barrer; mostrando come l'aggiunta di PEG e ZIF-8 aumenti la permeabilità alla $CO_2$ (più di 3 volte) rispetto alle membrane preparate solo con Matrimid (7.16 Barrer).

L'uso della polimmide Matrimid® 5218, come polimero idrofilico, è stato, inoltre, esteso in un altro processo a membrana quale la pervaporazione. Le potenzialità di questa polimmide sono state valutate in una separazione azeotropica organico/organico. Le membrane in Matrimid® sono state infatti testate, per la prima volta, in pervaporazione per la separazione della miscela costituita da metanolo (MeOH) e metil-tert-butiletere (MTBE) (14.3 e 85.7 %p/p, rispettivamente). I test sono stati condotti a differenti temperature (25-45°C) e differenti pressioni lato vuoto (0.0538, 0.2400, 2.1000 mbar). I risultati hanno mostrato che la temperatura della soluzione di alimentazione (nel range 25-45°C) influisce maggiormente sulla permeazione del MeOH producendo un aumento del suo flusso parziale e quindi della sua selettività. Le migliori prestazioni della membrana in Matrimid® sono state trovate alla temperatura di 45°C ed alla pressone lato vuoto di 0.054 mbar, dove il flusso totale ed il fattore di separazione sono stati rispettivamente di 0.073 kg $m^{-2}$ $h^{-1}$ e 21.16.

L'ultima parte del presente lavoro ha riguardato il miglioramento delle prestazioni in pervaporazione di un altro polimero commerciale: il polivinil alcol (PVA). Un materiale idrofilico inorganico, quale l'ossido di grafene (GO), è stato, pertanto, preparato ed incorporato nella matrice polimerica di una membrana in PVA. Le MMMs così preparate sono state testate nella deidratazione di etanolo dalla acqua (10:90 %p/p acqua:etanolo) valutando le loro prestazioni in pervaporazione in termini di flusso totale, flussi parziali e selettività. L'effetto del filler GO è stato valutato variandone la concentrazione (0.5, 1 e 2 %p/p) all'interno delle MMMs. Inoltre, le membrane sono state caratterizzate attraverso FESEM, DSC, TGA, XRD, angolo di contatto e proprietà meccaniche. Le migliori prestazioni di tali MMMs (contenenti l'1% p/p di GO) sono state trovate alla temperatura di 40°C, dove hanno mostrato una selettività di 263 ed un flusso totale di circa 0.137 kg $m^{-2}$ $h^{-1}$ (di cui 0.133 kg $m^{-2}$ $h^{-1}$ è stato il contributo del flusso parziale all'acqua). Questi risultati riflettono un miglioramento del 75% rispetto alle membrane preparate unicamente con PVA.

Concludendo, questo lavoro riporta il miglioramento delle prestazioni di due polimeri: Matrimid® 5218 e PVA. È importante ricordare che tali polimeri sono stati selezionati sulla base della loro produzione ed applicazione su ampia scala. I vari capitoli affrontano inoltre gli studi già riportati in letteratura selezionando per ogni applicazione un caso-studio (separazione $CO_2/CH_4$, MeOH/MTBE ed acqua/etanolo). Inoltre, la tesi fornisce importanti risultati ed informazioni sui metodi migliori per la preparazione di MMMs altamente performanti.

# TABLE OF CONTENTS

# *Chapter 1*

## Introduction

Nowadays, membrane-based technologies are one of the emerging processes used for separating of different types of mixtures in liquid and gas state; such technologies have been used in many industrial applications. This is due to the fact that membrane technologies offer high selectivity (depending on the membrane material), relatively easy scale-up and operating facilities, and low energy-consumption [1]. Being the latest, the most relevant in terms of cost overall production process at large scale. If the feed mixtures are in gas state, it is obvious to address membrane gas separation, which is able to selectively separate a gas from complex mixtures. It is likely that the main application of membrane gas separation deals with the purification of natural gas (removal of $CO_2$) based on its attractive market, followed by hydrogen recovery, oxygen enrichment from air (medical devices) and nitrogen enrichment from air [2–4].

On the other hand, if the feed mixtures are in liquid state, and the necessity comprises the removal of traces of one target compound, pervaporation (PV) is surely a potential candidate to carry out such purification step. Furthermore, PV offers several advantages in separating heat-sensitive azeotropic mixtures such as *i)* mild operating conditions and simple control of process by handling of the operating parameters like permeate vacuum pressure, feed flow and temperature; *ii)* no emission to the environment due to the absence of additional streams; *iii)* no use of additional chemicals to the feed stream, thus reducing the cost of disposal pollution agents; and of course, *iv)* low energy requirements in comparison with conventional processes (e.g. distillation) [5].

However, to date, it is well-known that these processes (membrane gas separation and pervaporation) can compete with current conventional processes, however, according to the long term stability, high price of specific polymers, and some features of the existing polymeric materials, their consolidation is still compromised. In fact, the high selective polymers do not demonstrate high permeability values, and high permeable polymers

are not selective enough. The aim of this research is to provide new perspectives of improving commercial polymeric materials for the preparation of membranes for gas separation and pervaporation. Today, one of the current approaches aiming the enhancement of membrane performance is the incorporation of organic-inorganic materials, which can provide a synergistic effect on membranes and thus generate superior performing membranes. Fundamentally, the mixed matrix membranes (MMMs) combine the strengths of inorganic and polymeric membranes to ideally reach an enhanced performance. The selection of the polymeric material for gas separation application (focused to $CO_2/CH_4$ separation) was carried out by attending the current necessity of research community. According to our literature review [6], the industrial Matrimid® 5218 polyimide has been the most sought polymer in the preparation of membranes for gas separation. Based on the characteristics of the polymer, Matrimid® offers high selectivity but low permeability towards $CO_2/CH_4$ separation, such typical feature makes it to be restricted by the so-called upper bound in a log-log plot of selectivity against permeability, well-known as Robeson relationship [7–9]. The strategy applied in this work implies two synergistic steps, i) to blend Matrimid® with an additive which may provide better $CO_2$ permeability. In this case, polyethylene glycol (PEG) has shown strong evidence that improves the $CO_2$ transport. In particular, the polar ether segments (ethylene oxide units) of PEG interact positively with $CO_2$ molecules by dipole-quadrupole interactions, leading the transport through the membranes [10,11]. Afterwards, the blend membranes were used ii) to prepare MMMs. Indeed, ZIF-8 has been widely proposed for multicomponent gas separations containing $CO_2$ and $CH_4$ [12,13], this because ZIF-8 is thermally stable and able to absorb small gas molecules, such as hydrogen and carbon dioxide ($CO_2$) with apparent thermal stability. In this framework, the present study evaluates the effect of the addition of PEG 200 into Matrimid® using ZIF-8 filler in order to improve their $CO_2$ permeation and $CO_2/CH_4$ separation.

The second part of the thesis is focusing on the development and testing of membranes in pervaporation processes. The potential industrial applications of pervaporation are targeted in the separation of azeotropic organic-organic mixtures, as Methanol (MeOH)-methyl *tert*-butyl ether (MTBE). The MTBE is commercially used to produce a lead-free gasoline aiming the reduction of air pollution. MTBE is formed by reacting MeOH with isobutylene; however, the azeotropic mixture at a composition of 14.3 wt.% MeOH and 85.7 wt.% MTBE is produced and further purification is needed. Thereby, using the

hydrophilic nature of Matrimid®, the application of Matrimid® 5218 polyimide in this system is proposed, for the first time, in this work.

The PV also finds its industrial application for the dehydration of organics (mainly isopropanol and ethanol) [14–16]. At this point, the dehydration of organics has to be performed by using hydrophilic polymers. The poly(vinyl alcohol) (PVA) is the only polymer applied industrially, e.g. by DeltaMem AG (http://www.deltamem.ch), to perform such separations. The improvement of crosslinked-PVA membranes by embedding a hydrophilic material, like graphene oxide (GO), is the last scope of this research. Highly oxygenated GO having hydroxyl and epoxy functional groups on their basal planes, in addition to carbonyl and carboxyl groups located at the sheet edges [17] could provide a high hydrophilic profile to the matrix material and enhance the separation performance. These MMMs based on cross-linked PVA and GO were tested for the dehydration of ethanol.

The literature review, providing an overview and future directions in the field of MMMs, the theoretical background and clear strategies related about how to meet the preparation of compelling MMMs are given for the each above-mentioned gas separation and pervaporation applications.

# *Chapter 2*

# Literature review: Matrimid®5218 mixed matrix membranes for gas separation

## 2.1.Introduction

Over the last decades, different polymers have been employed as continuous phase for preparing selective membranes for gas separation. Today, some of these materials have been consolidated commercially; however, the necessity to improve the performance (in terms of permeability/selectivity) of polymeric membranes above Robeson's upper bound has been conducted by blending polymers, use of additives, implementation new methods, development of new materials and coating films, development of mixed matrix membranes, and so on. One of the most recent approaches is the use of polymers such as polyimides, which have demonstrated, to provide remarkable gas separation performance using the attempts aforementioned. Belong of them the industrially produced polymer Matrimid® 5218 have proven the exceptional properties in this domain. In this chapter the current state-of-the-art of the use of Matrimid® 5218 in preparation of membrane for gas separation is provided. The progress in this field is summarized and discussed chronologically in two periods, decade (from 1998 to 2008) and current (from 2009 up to now) frameworks. This contribution leads to take a complete and compelling overview of the state-of-the-art based on Matrimid. Furthermore, the main approaches, aim of study, gas separation evaluated, main techniques used for membrane characterization, main supplier of the polymer, main secondary materials for blending, fillers incorporated into the matrix, and remarks on the carried out studies are summarized in detail. Finally, the prospects and future trends on the use of Matrimid® 5218 for membrane applications, which became as a starting point of this thesis, are denoted.

### 2.2.Mixed matrix membranes

Mixed matrix membranes (MMMs) have been defined as mixtures of inorganic particles (as filler material) in a polymeric matrix. **Figure 2.1** shows the scheme for a typical MMM used for gas separation. According to [18], the MMM can contain two or more different materials of distinct properties such as:

- Different chemical nature,
- Containing a separating layer made of a continuous phase (usually a polymer),
- Embedding a second dispersed phase,
- Different selectivity and permeation flux.

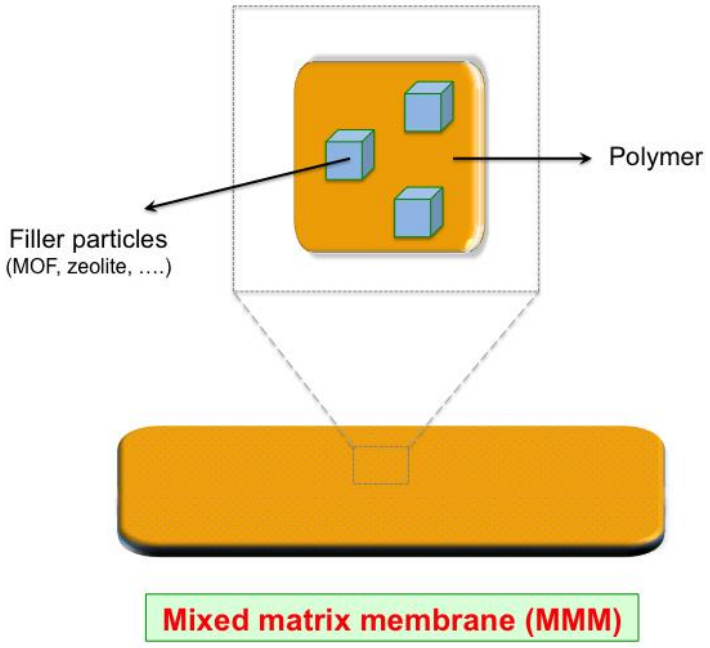


**Figure 2.1.** Schematic description of a mixed matrix membrane for gas separation.

In theory, the MMMs exhibit the excellent gas separation properties of inorganic materials and combine desirable mechanical properties with the economical processing capacity of polymers [19]. Chemical industries have used several mixed matrix membranes (MMMs) for different types of applications such as oxygen enrichment of air, hydrogen recovery, removal of volatile components from gas effluent streams, separation of $CO_2$ from natural gas and separation of greenhouse gases [9], [20]. Moreover, the membrane engineering is working on development of new membrane polymers as well as organic/inorganic hybrid materials in order to improve the existing

membranes and expand their application. The gas separation process efficiency depend upon [21]:

- Material (permeability, separation factors),
- Membrane structure and thickness (permeance),
- Membrane configuration (flat, hollow fiber, etc.)
- Module and system design.

The gas transport in polymeric membranes (two mechanisms: solution diffusion and sorption) is influenced by several polymer properties, such as morphology, free volume content, intersegmental chain spacing (d-spacing), orientation, cross- linking, polymer polarity, presence of defects, thermal processing history, glass transition temperature, average molecular weight, molecular weight distribution, composition, degree of crystallization, and types of crystallites [22]. The membrane properties as permeability and selectivity play an important role in the economic framework of the gas separation membrane process. According to Bernardo *et al.* [23] the *Permeability (P)* is defined as the rate at which any compound permeates through a membrane; which depends upon a thermodynamic factor (partitioning of species between feed phase and membrane phase) and a kinetic factor (diffusion in a dense membrane or surface diffusion in a microporous membrane). The permeability of component A ($P_A$) is then the product of the solubility coefficient ($S_A$, thermodynamic parameter), and the diffusion coefficient ($D_A$, kinetic parameter), according to Eq. (1):

$$P_A = S_A D_A \tag{1}$$

The permeability ($P_A$) of the membrane could be calculated from the following measured parameters:

$$P_A = \frac{Q_A l}{\Delta P A} \tag{2}$$

where $Q_A$ is the flow of gas "A", $\Delta P$ is the transmembrane pressure drop, $l$ is the effective thickness of the membrane and A is the surface area of the membrane [22]. The gas permeability values are normally given in Barrers, where 1 Barrer means 1 $x10^{-10}$ ($cm^3$ (STP) $\cdot$ cm / $cm^2 \cdot s \cdot$ cmHg) [24].

On the other hand, the *Selectivity (α)* is the ability of a membrane to accomplish a given separation (relative permeability of the membrane for the feed species). Selectivity is a

key parameter to achieve high product purity at high recovery [23]. The selectivity (or perm-selectivity) $\alpha_{AB}$ is the ratio of the permeability of penetrant "A" with respect to the permeability of a second permeant "B":

$$\alpha_{AB} = \frac{P_A}{P_B} = \frac{S_A}{S_B}\frac{D_A}{D_B} \tag{3}$$

In order to achieve the gas separation by MMMs, different polymers are applied as main matrix whereas some varieties of particles have been included in the role of fillers, trying to overcome the Robeson's upper bound; e.g. for $O_2/N_2$ and $CO_2/CH_4$ separations using zeolite as filler is possible [25]. According to the advances of MMMs for gas separation, the aim is completely focusing to develop matrixes that provide better characteristics than the existing. Concerning to the last asseveration, **Figure 2.2** shows the desired region pursuit in the MMMs based on Robeson curve [25].

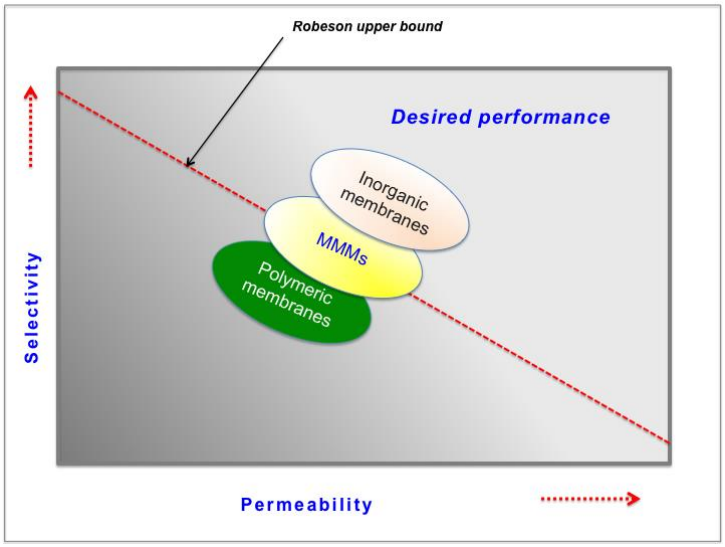


**Figure 2.2.** Comparison on desired selectivity and permeability in MMMs, inorganic and polymeric membranes by Robeson upper bound.

The most common of fillers such as zeolites, carbon molecular sieves, silica, molecular organic frameworks (MOFs) (such as ZIF-8, UiO-66, HKUST-1, etc.) and even carbon nanotubes have been used for this purpose. In case of ZIF-8 seems to be most studied filler in MMMs due to its hydrophobic profile, which is favorably compatible with hydrophobic polymers. It is important to note that some other factors influencing the mixed matrix membrane fabrication, Dong *et al.* [26] described that fabrication of a mixed matrix membrane must overcome several challenges in order to obtain the

desired morphology, gas separation properties and mechanical/chemical stability. Those challenges include: *(i)* to achieve a homogeneous dispersion of particles in the polymer matrix so as to avoid the loss of selectivity as a result of agglomeration, *(ii)* to ensure a defect-free polymer/inorganic particle interface thus guaranteeing the membrane integrity as well as the separation performance, and *(iii)* to properly select the polymer and inorganic materials not only on the basis of good separation properties but also on the compatibility between them. Indeed, the performance of membranes based on zeolitic-imidazolate framework (ZIF) / polymers also depends on the interface region between the bulk polymer and zeolite surface. Generally, the modification of the interface is necessary to achieve increase above those of the pure polymer. These interfaces of ZIFs occupy an extremely small volume fraction (less than 10% of membrane volume); but it seems to have a significant effect on the separation performance of MMMs.

According to the description of Bastani *et al.* [22], **Figure 2.3** shows the schematic diagram of various structures at the polymer/zeolite interface region. Case 1 shows a homogenous blend of polymer and sieve as ideal interphase morphology. While, Case 2 corresponds to a region in the external polymer phase as a result of shrinkage stresses generated during solvent removal, which named polymer chains rigidification.

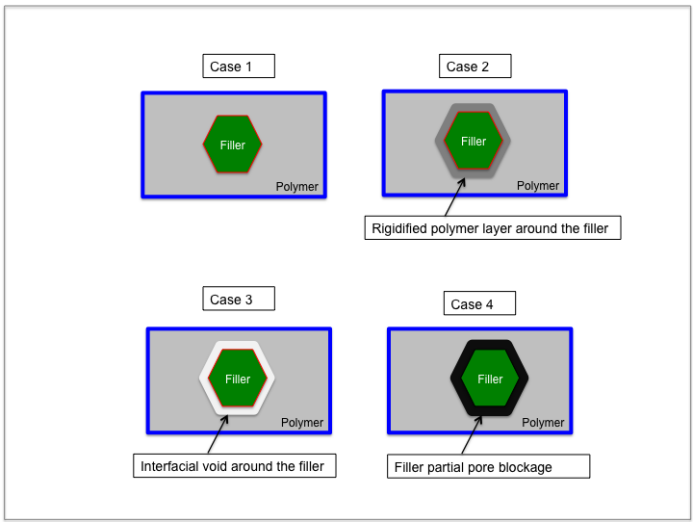


**Figure 2.3.** Representation of various structures at the polymer/ zeolite interface region. Adapted from Bastani *et al.* [22].

In Case 3 indicates poor compatibility between molecular sieve and polymer matrix or ‘‘sieve-in-a-cage’’ morphology, which cause the formation of voids at the interfacial

region. Case 4 represents a situation in which the surface pores of the zeolites have been partially sealed by the rigidified polymer chains. The idea behind mixed matrix membranes is to create micro and nanocomposites, as well as new hybrid membranes whose effective transport properties are a synergistic combination of the inherent properties of the pure components.

## 2.3.General methodologies for preparing MMMs based on polymers

According to Aroon *et al.* [20], there are usually three different methods to elaborate MMM's based on polymeric matrix and fillers, which are used to have better distribution of the inorganic fillers due to it is common to present agglomerating in the fabrication. The methods are described as [18]: A) Inorganic fillers are dispersed in the solvent and blended for specific time, and later the polymer is added **(Figure 2.4A)**; B) The base polymer is added into the solvent and mixed; then the inorganic fillers are added in the polymeric solution **(Figure 2.4B)**. Finally, C) the inorganic fillers are dispersed in solvent and mixed during predetermined time. The polymer is dissolved in another solvent separately. The suspension containing the fillers is later added to the polymeric solution **(Figure 2.4C)**.

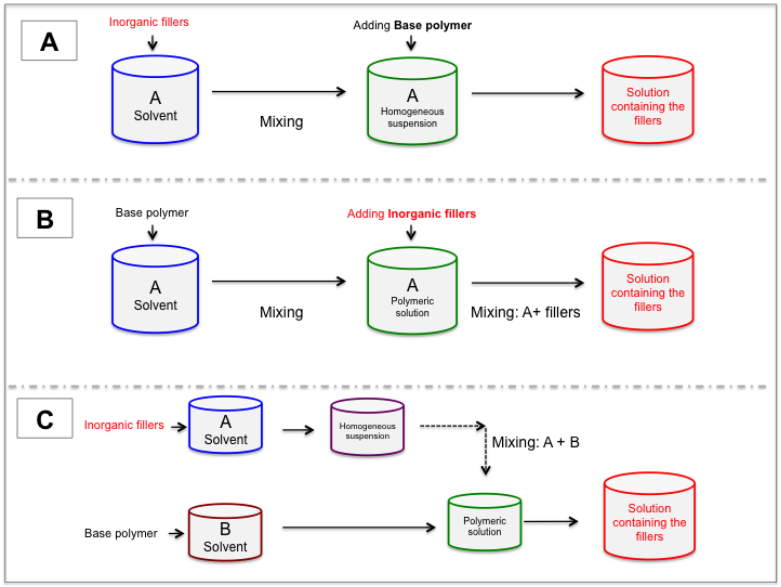


**Figure 2.4.** Common methods used for fabricating MMMs.

The final solutions containing the fillers are well known as "Dope solution" (**Figures 2. 4A, B & C**); which are later commonly processed by *phase-inversion method* in order to elaborate the membranes. This method is generally carrying out by three different methodologies such as i) dry process, ii) wet process and, iii) wet/dry process (**Figure 2.5**), it is necessary to use previously a casting step (the dope solutions are spread or poured on a flat glass plate).

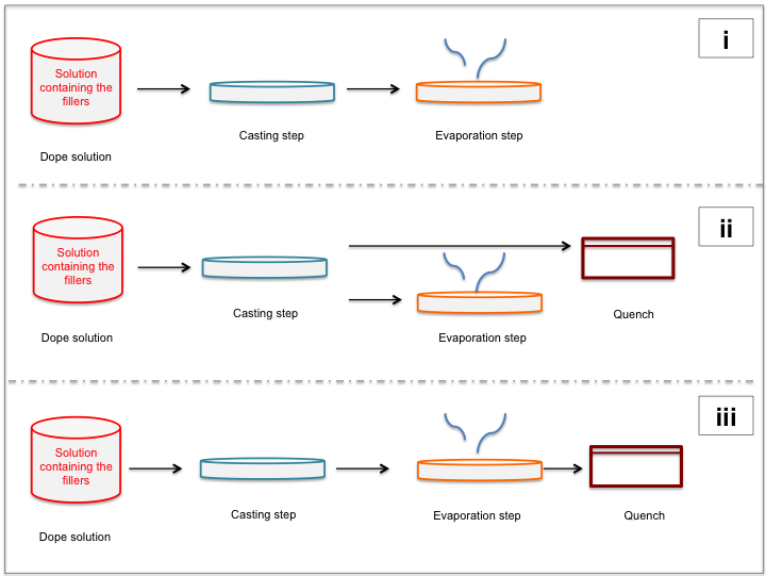


**Figure 2.5.** General description of the phase-inversion method.

The solvent evaporation in the three methodologies is needed. The wet and dry processes are different if the application of non-solvent coagulant is used to submerge the casting plate [19].

### 2.4.Current materials used as fillers in polymeric membranes.

Several materials have been used as fillers in polymeric MMMs; the most common that have been evaluated are zeolites (e.g. zeolite A, ZSM-5, Zeolite-13X, Zeolite-KY), porous titanosilicates, ordered mesoporous silica (e.g. Silicalite-1, SAPO-34, MCM-41 and 48, SBA-11, 12 and 15,), nonporous silica, carbon nanotubes, carbon molecular sieves (CMSs), MOFs (e.g. ZIF-7, ZIF-8, MIL-96 and 100, MOF-5 and 177, Cu-TPA, $Cu_3(BTC)_2$, Cu-BPY-HFS, $Zn(pyrz)_2(SiF_6)$), and lamellar materials (e.g. JDF-L1, AlPO, SAMH-3) [6,27]. Currently, the most applied is the ZIF families due to they are intrinsically more compatible with glassy polymers as compared to other molecular sieves. In addition, they comprise a subset of metal–organic frameworks (MOFs) with

exceptional thermal and chemical stability, further making them attractive for mixed matrix applications [4]. Specifically, ZIF-8 has been the most studied filler of this family, it possesses six-ring-cages with aperture size (3.4 A) that is close to the molecule size of many gases with economic interests (e.g. $H_2$, $CO_2$, $O_2$, $N_2$, $C_2H_4$, $C_3H_6$, $C_2H_6$, $C_3H_8$, and $CH_4$); which permit a readily absorb small gas molecules, such as hydrogen, carbon dioxide [28]. ZIF-8 also exhibits a high surface area of 1300-1600 $m^2/g$ that allow obtaining good performances in gas separation. In last 5 years, ZIF-8 was applied into composite membranes as well as MMM to evaluate the separation of different gases.

### 2.5.Current approaches of membranes based on Matrimid®.

Matrimid is a high glass transition ($T_g$) polymer, and aromatic amorphous thermoplastic polyimide comprised of 3,3'-4,4'-benzophenone tetracarboxylic dianhydride (BTDA) and diaminophenylindane (DAPI) monomers [29] (see **Figure 2.6**). This polyimide is one of the most popular polyimide materials studied for gas separation and chemical modifications; nevertheless, its studying is currently carried out because presents good processability and superior combination in selectivity and permeability [30]. Furthermore, the good solubility of Matrimid in common organic solvents allows it to be solution processed, which is a requirement for fabrication into a gas separation membrane. Matrimid has the best combination of $CO_2$ permeability and $CO_2/CH_4$ selectivity in comparison with other commercial polymers such as PSF, TB-BisA-PC, and Aramid [31]. These characteristics permit to have new developments in the framework of MMMs for gas separation based on Matrimid.

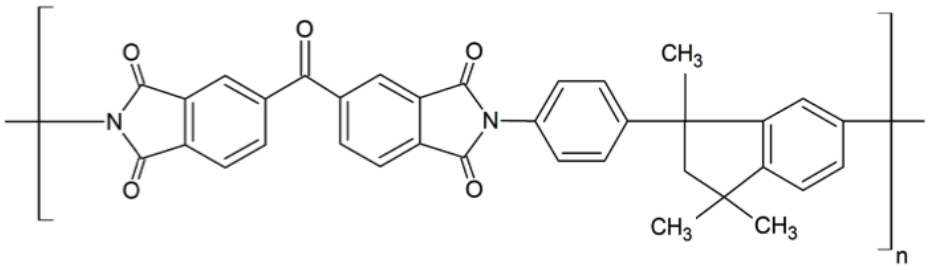


**Figure 2.6.** Chemical structure of Matrimid®: BTDA–DAPI (3,3'-4, 4'-benzophenone tetracarboxylic dianhydride and diaminophenylindane) polyimide [29].

Arron *et al.* [20] showed that Matrimid MMMs demonstrated a separation performance close to the known Robeson upper bound. Today, the mixing of Matrimid with other type of membrane materials has been done. Yong *et al.* [32] have been developed membranes in which PIM-1 was added to Matrimid® polymer. This study demonstrated that both materials are partially miscible, as well as PIM-1/ Matrimid® blends permit an increasing on permeability values about of 25 % and 77% for 5 and 10 wt.% of PIM-1, respectively. Indeed, the highest permeability was achieved for $CO_2$ using the $CO_2/CH_4$ mixture for matrix with 30 wt.% of PIM-1. On the other hand, the adding of 5-30% of Matrimid® into PIM-1 matrix induced the decreasing in selectivity values. In the same framework, the use of PIM-1/Matrimid® blend can be used for fabricating hollow fiber membranes, which may present high performance for $CO_2/CH_4$, $O_2/N_2$ and $CO_2/N_2$ separations [33]. The membranes containing 5 and 10 wt.% of PIM-1 increase the $CO_2$ permeation around 78% and 146%, respectively. According to the authors, the polymeric membranes based on PIM-1/Matrimid® have potential to be considered for gas natural purification, air separation and $CO_2$ separation. **Table 2.1** (pg. 17) reports and summarizes a chronological overview of the current approaches of MMMs using Matrimid® as continuous phase.

In the last decade, the incorporation of organic/inorganic materials is a successful approach to improve the gas transport properties of Matrimid. Metal organic frameworks (MOF) have been one of the preferred candidates for this application. The MOFs demonstrating high chemical stability, impressive surface area, and good polymer compatibility consist of inorganic metals and organic linkers. In fact, the functional groups of the organic ligands and the metal ions associated with the secondary building units may facilitate interactions with the polymer, producing defect-free MMMs. Perez *et al.* [34] successfully incorporated metal organic framework (MOF-5) particles into Matrimid matrix and reported an improvement in permeability (up 120 %) of pure Matrimid, keeping constant the initial selectivity of the polymer. This considerable increment in permeability is fully attributed to the porosity of the nanocrystals. The addition of MOFs can also improve thermal and mechanical properties of Matrimid membranes. i.e., $[Cu_3(BTC)_2]$ was added into Matrimid, showing an enhancement of mechanical properties (tensile strength and dynamic storage modulus) and an increase on permeation and selectivities for $CO_2/CH_4$ and $CO_2/N_2$ [35]. According to Li *et al.* [36], the use of another organic/inorganic hybrid material like POSS® Octa Amic acid improved the $CO_2/CH_4$ separation performance of pure

Matrimid up to 70%. Furthermore, it was demonstrated a very good compatibility between POSS® particles and PI, due to the intermolecular hydrogen bond between the carboxylic group of POSS® and Matrimid. A sub-class of MOFs like zeolitic imidazolate frameworks (ZIFs) was used as filler in Matrimid-based MMMs. Matrimid/ZIF-8 MMMs demonstrated an improvement on selectivity values for several gas pairs such as $H_2/O_2$, $H_2/CO_2$, $H_2/CH_4$, $CO_2/CH_4$, $CO_2/C_3H_8$, and $H_2/C_3H_8$; while the permeability values obtained for all gases increased with the ZIF-8 content. Many authors have been supported this statement [28,37,38]. The authors suggested ZIF-8 as a promising material for gas separations at higher pressures and temperatures, at which most industrial gas separation processes are conducted. Diestel *et al.* [38] incorporated other barely used MOF; ZIF-90 for MMMs. This filler considerably enhanced the $H_2/CO_2$ separation factor (9.5) in comparison with pure Matrimid (3.5); whereas ZIF-8 led to increase the $H_2$ permeability maintaining the separation factor with minimal changes.

Different inorganic particles such as aerosil silica 200, zeolites (4A, 13X and ZSM-5), carbon nanotube (CNT), TS-1, POP-2, ETS-10, and carbon molecular sieve (CMS) were used as fillers, which enhanced slightly the performance of Matrimid; mainly for $CO_2/CH_4$, $CO_2/N_2$, $O_2/N_2$, and $H_2/N_2$ [39–45]. The studies demonstrated the capability of Matrimid to incorporate different types of particles. In spite of this, the addition of zeolitic fillers does not always guarantee the improvement of the separation properties. Dorosti *et al.* [46] applied ZSM-5 into PSF/Matrimid blend and achieved high permeabilities for some gases ($CH_4$, $N_2$, $O_2$, and $CO_2$) in comparison with the unfilled membranes, but they were not capable to overcome the $CO_2/CH_4$ and $O_2/N_2$ selectivities reached with pure Matrimid membrane. The same polymer blend was used to incorporate silicate-1; and the enhancement on permeability was reported too. These MMMs presented higher selectivities than the neat membrane for $H_2/CH_4$, $CO_2/N_2$, and $O_2/N_2$ mixtures, with values of 180.0, 41.7, and 8.5, respectively [47]. Whereas, using silica into PSF/Matrimid blend showed a $CO_2/CH_4$ selectivity of 61.0, which is an excellent performance in comparison to the other attempts [48]. Generally, the addition of nanoparticles is expected to increase the permeability due to the increase in free volume fraction of polymer matrix, chain packing disruption and the increment of diffusivity through the porous materials. These phenomena have been confirmed by Moghadam *et al.* [49] and Peydayesh *et al.* [50]. They added $TiO_2$ and SAPO-34

nanoparticles respectively, into a Matrimid matrix. The $CO_2$ permeability increased 2.45 fold-times compared to the neat Matrimid membrane in case of $TiO_2$ nanoparticles addition. The nanoparticles also improved the separation efficiency of $CO_2$ with respect to $CH_4$. However, MMMs did not overcome the Robeson upper bound [49]. Concerning to Peydayesh's study, MMMs containing SAPO-34 zeolite showed higher $CO_2/CH_4$ selectivity around 67.0. Dorosti *et al.* [51] improved the $CO_2/CH_4$ selectivity from 28.2 in pure Matrimid up to 51.8 with 15% of MIL-53. The results obtained in this study are closer to the Robeson trade-off. The main goal of the addition of fillers in Matrimid membranes is to improve the gas separation properties of the polymer. However, other advantages of MMMs over polymeric membranes have been disclosed. The use of MOFs (like MIL-53 (Al), ZIF-8, $Cu_3BTC_2$) tends to suppress the $CO_2$ plasticization phenomenon [13], MOF particles hinder the mobility of the polymer chain. In addition, these MOFs maintain large separation factors ($CO_2/CH_4$) over a wide pressure range. The suppression of $CO_2$ plasticization was also achieved by the addition of a mesoporous material like Fe(BTC) [52], where an increment of 62% of $CO_2/CH_4$ separation factor in gas binary mixture was obtained. The permeability improvement for both gases was achieved too. Perm-selectivity enhancement is attributed to the strong increase in the sorption due to present Fe (BTC) particles. The chemical modification of the fillers is also a current approach in synthesis of MMMs. i.e., Chen *et al.* [53] carried out the chemical grafted modification of zeolite (AU/EMT intergrowth zeolite) to prepare MMMs with cross-linked Matrimid (by addition of APTMDS) matrix. Properties of the filler, such as surface density, micropore volume or $CO_2$ adsorption capacity, were changed due to the surface modification. Pure Matrimid membrane presented a $CO_2/CH_4$ selectivity of 28.0. After the addition of the modified zeolite, as well as the cross-linking of the polymer, the resulting MMMs showed an increase in selectivity value up to 41.4. Mesoporous silica spheres (MCM-41) were also functionalized with sulfonic acid ($-SO_3H$) groups; these functionalized Matrimid MMMs showed up to 31% increase in $CO_2$ permeability and 14% increase in $CO_2/CH_4$ selectivity [54]; basically, the polar groups ($-SO_3H$) tend to increase the $CO_2$ solubility in membranes due to interact with the $CO_2$ quadrupole [54]. Rodenas *et al.* [55] applied the chemical modification of MIL-53 (production of $NH_2$-MIL-53(Al) nanoparticles); which led a $CO_2$ permeability increment (up to 70% higher than neat Matrimid) in the MMMs, while the $CO_2/CH_4$ separation factor (around 30.0-35.0) is slightly increasing, Chen *et al.* [56] also enhanced the $CO_2$ permeability of Matrimid membranes using

$NH_2$-MIL-53(Al). In order to improve the separation performance of MMMs, two different approaches can be used: *i)* chemical modification of the surface of filler and *ii)* chemical modification of the structure of the polymer matrix. Furthermore, synthesis of novel fillers is a current challenge too. Amooghin *et al.* [57] developed a novel MMMs incorporating micro- and nano-porous sodium zeolite-Y. These MMMs demonstrated an outstanding performance for $CO_2/CH_4$ separations; the $CO_2$ permeability was increased more than two-fold whereas separation factor showed an enhancement of 20 % (from 36.3 in Matrimid to 43.3 in MMMs).

Loloei *et al.* [58] added ZMS-5 as fillers and PEG 200 to produce ternary mixed matrix membranes. These Matrimid/PEG 200/ZMS-5 membranes revealed that the $CO_2$ permeability and $CO_2/CH_4$ selectivity of pure Matrimid was significantly enhanced. The $CO_2$ permeability of the ternary MMMs (Matrimid/PEG (95:5) + 5 wt.% ZSM-5) increased about 50% (from 7.68 to 11.53 Barrer) and $CO_2/CH_4$ selectivity about 72% (from 34.9 to 60.1) comparing to pure Matrimid. The novelty on the synthesis of hybrid ternary membranes can be a promising approach to develop new membranes with better performances.

**Table 2.1.** Recent applications of Matrimid in the preparation of MMMs for gas separation

| *Filler* | *Aim of the study* | *Supplier of Matrimid ®* | *Evaluated application* | *Techniques used for Membrane characterization* | *Measurement type:* | *Permeation performance:* | *Selectivity or separation factor:* | *Remark of the study* | *Reference* |
|---|---|---|---|---|---|---|---|---|---|
| MOF-5 | -Incorporation of MOF-5 nanoparticles into Matrimid® matrix for the gas separation in binary mixture. | Ciba Specialty Chemicals | -Permeability: $N_2$, $O_2$, $CH_4$, $CO_2$, and $H_2$<br>-Separation in binary mixture: $H_2/CO_2$, $CH_4/N_2$, and $CO_2/CH_4$ | • XRD<br>• SEM<br>• TGA<br>• MOF-5 BET analysis | Single gas permeation<br>Conditions: 2 atm, 35 ◦C | At 30 wt. % filler loading:<br>$H_2$: 53.8 Barrer<br>$N_2$: 0.5 Barrer<br>$O_2$: 4.1 Barrer<br>$CH_4$: 0.4 Barrer<br>$CO_2$: 20.2 Barrer | At 30 wt. % filler loading:<br>$H_2/CH_4$ :120.0<br>$N_2/CH_4$ :0.8<br>$CO_2/CH_4$ :44.7<br>$O_2/N_2$ :7.9<br>$H_2/CO_2$:2.6 | 30 wt% MMM, the permeabilities of the tested gases increased by 120% while the ideal selectivities remained constant compared to Matrimid® membrane. | [34] |
| $[Cu_3(BTC)_2]$ | -Incorporation of nanoparticles into Matrimid® matrix for the gas permeation and binary mixture separation. | Huntsman | -Permeability: $N_2$, $CH_4$, and $CO_2$<br>-Separation in binary mixture: $CO_2/N_2$, and $CO_2/CH_4$ | • TGA<br>• BET analysis of MOF<br>• XRD<br>• SEM | Gas binary mixture separation<br>Conditions: 10 bar, 35 ◦C, feed composition (35:65) | At 30 wt. % filler loading:<br>$CO_2$: 17 GPU<br>$CO_2$: 19 GPU | At 30 wt. % filler loading:<br>$CO_2/CH_4$ :24<br>$CO_2/N_2$ :24 | Improvement in thermal and mechanical properties of membranes with $[Cu_3(BTC)_2]$ loadings.<br>Increment for permeance and $CO_2/CH_4$ and $CO_2/N_2$ selectivity was observed. | [35] |
| POSS® | -Compatibility between inorganic filler and PI.<br>-Generation of hybrid POSS®–Matrimid®–$Zn^{2+}$ nanocomposite membrane for separation of natural gas | Vantico Inc | -Permeability: $N_2$, $CH_4$, $O_2$ and $CO_2$<br>-Separation in binary mixture $CO_2/CH_4$ | • SEM<br>• XRD<br>• DSC<br>• BET analysis of POSS | Single gas permeation<br>Conditions: 10 atm, 35 ◦C. | At 20 wt. % filler loading:<br>$N_2$: 0.1 Barrer<br>$O_2$: 1.3 Barrer<br>$CH_4$: 0.1 Barrer<br>$CO_2$: 5.3 Barrer | At 20 wt. % filler loading:<br>$CO_2/CH_4$ :37.2<br>$O_2/N_2$: 6.9 | The hybrid POSS®-Matrimid®–$Zn^{2+}$ nanocomposite membrane (20 wt% POSS®–Matrimid®–0.3M $ZnCl_2$), increases the selectivity of $CO_2/CH_4$ and $O_2/N_2$ around 70 and 30 %, respectively. | [36] |
| ZIF-8 | -Synthesis of ZIF-8/Matrimid® MMMs for separation of several gas pairs. | Ciba Specialty Chemicals | -Permeability: $N_2$, $CH_4$, $O_2$, $C_3H_8$, $H_2$ and $CO_2$<br>-Separation in binary mixture: $H_2/O_2$, $H_2/CO_2$, $H_2/CH_4$, $CO_2/CH_4$,$CO_2/C_3H_8$, and $H_2/C_3H_8$ | • SEM<br>• XRD<br>• FTIR-ATR<br>• TGA<br>• BET analysis of ZIF-8 | Single gas permeation<br>Conditions: 200 Torr, 35 ◦C. | At 50 wt. % filler loading:<br>$H_2$: 19 Barrer<br>$N_2$: 0.2 Barrer<br>$O_2$: 1 Barrer<br>$CH_4$: 0.1 Barrer | At 50 wt. % filler loading:<br>$CO_2/CH_4$ :124.8<br>$H_2/CO_2$: 3.8 | The ideal selectivities of gas pairs containing small gases, such as $H_2/O_2$, $H_2/CO_2$, $H_2/CH_4$, $CO_2/CH_4$, $CO_2/C_3H_8$, and $H_2/C_3H_8$, showed improvement with the 50 wt.% ZIF-8 loading. | [28] |

**Table 2.1.** Recent applications of Matrimid in the preparation of MMMs for gas separation (continued)

| *Filler* | *Aim of the study* | *Supplier of Matrimid ®* | *Evaluated application* | *Techniques used for Membrane characterization* | *Measurement type:* | *Permeation performance:* | *Selectivity or separation factor:* | *Remark of the study* | *Reference* |
|---|---|---|---|---|---|---|---|---|---|
| IR MOF-1 | -Predicted performance of new MOF/Matrimid<br>combinations for $CO_2/CH_4$ separations | Huntsman | -Permeability: $CH_4$, $H_2$, $N_2$ and $CO_2$<br>-Ideal selectivity: $CO_2/CH_4$,$CH_4/N_2$, $H_2/CO_2$, $H_2/CH_4$, $H_2/N_2$, | • XRD<br>• SEM<br>• TGA<br>• MOF-5 BET analysis | Single gas permeation<br>Conditions: 2 atm, 35 ◦C. | At 30 wt. % filler loading:<br>$CO_2$:18 Barrer<br>$CH_4$: 0.2 Barrer | At 30 wt. % filler loading:<br>$CO_2/CH_4$ :35 | It was examined how polymeric membranes for gas separations can be enhanced by using metal organic framework materials. | [59] |
| • Aerosil silica 200<br>• Zeolite 4A<br>• ZSM-5<br>• CNT<br>• CMS | -Preparation and characterization of MMMs based on Matrimid® using different types of fillers. | Huntsman | -Permeability: $CH_4$, and $CO_2$<br>-Ideal selectivity: $CO_2/CH_4$ | • SEM<br>• TGA<br>• DSC | Single gas permeation<br>Conditions: 10 bar, 30 ◦C. | At 15 wt. % zeolite 4A:<br>$CO_2$: 5.9 Barrer<br>$CH_4$: 0.1 Barrer<br>At 10 wt. % CNT:<br>$CO_2$: 1.0 Barrer<br>$CH_4$: 0.1 Barrer | At 15 wt. % zeolite 4A:<br>$CO_2/CH_4$ :43<br>At 10 wt. % CNT:<br>$CO_2/CH_4$ :11<br>At 10 wt. % CNT:<br>$CO_2/CH_4$ :48 | Good contact was observed between fillers and polymer matrices.<br>All the fillers enhanced slightly performance of Matrimid® for $CO_2/CH_4$ separation. | [39] |
| ZSM-5 | -Preparation and characterization of MMMs based on PSF/Matrimid®.<br>-Effect ZSM-5 particles in the PSF/Matrimid matrix. | Huntsman | -Permeability: $CH_4$, $N_2$, $O_2$, and $CO_2$<br>-Ideal selectivity: $O_2/N_2$, $CO_2/CH_4$ | • SEM<br>• TGA<br>• FTIR | Single gas permeation<br>Conditions: 2-5 bar, 35 ◦C. | At 10 wt. % filler loading:<br>$N_2$: 0.2 Barrer<br>$O_2$: 0.7 Barrer<br>$CH_4$: 0.3 Barrer<br>$CO_2$: 1.5 Barrer | At 10 wt. % filler loading:<br>$CO_2/CH_4$ :4.4<br>$O_2/N_2$: 3.0 | MMMs showed higher permeability than the pure polymer membranes. But the selectivity was not improved. | [46] |
| $TiO_2$ | -Study the effect of $TiO_2$ nanoparticles addition into Matrimid®. | Huntsman LLC Corp. | -Permeability: $CH_4$, $N_2$, $O_2$, He and $CO_2$<br>-Ideal selectivity: $CO_2/N_2$, $He/N_2$, $O_2/N_2$, $CO_2/CH_4$, $H_2/CO_2$ | • SEM<br>• TEM<br>• AFM<br>• FTIR | Single gas permeation<br>Conditions: 2-5 bar, 35 ◦C. | At 25 wt. % filler loading:<br>$N_2$: 1.4 Barrer<br>$O_2$: 2.5 Barrer<br>$CH_4$: 1.8 Barrer<br>$CO_2$: 12.5 Barrer | At 25 wt. % filler loading:<br>$CO_2/N_2$ :10<br>$O_2/N_2$: 3.0<br>$CO_2/CH_4$: 9.0 | The $TiO_2$ nanoparticles incorporation improved membrane performance for $CO_2/CH_4$ separation. The performance was closed to the Robeson bound. | [49] |

**Table 2.1.** Recent applications of Matrimid in the preparation of MMMs for gas separation (continued)

| *Filler* | *Aim of the study* | *Supplier of Matrimid ®* | *Evaluated application* | *Techniques used for Membrane characterization* | *Measurement type:* | *Permeation performance:* | *Selectivity or separation factor:* | *Remark of the study* | *Reference* |
|---|---|---|---|---|---|---|---|---|---|
| Silicalite-1 | -Preparation and characterization of MMMs based on PSF/Matrimid® blend. | Huntsman Advanced Materials | -Separation in binary mixture: $H_2/CH_4$, $CO_2/N_2$, and $O_2/N_2$ | • SEM<br>• BET analysis of Silicate-1<br>• DSC<br>• FTIR<br>• TEM | Gas binary mixture separation<br>Conditions: 245 kPa, 35 ◦C, feed composition (50:50) | At 8 wt. % filler loading:<br>$H_2$: 38.4 Barrer<br>$CO_2$: 18.7 Barrer<br>$O_2$: 12.8Barrer | At 8 wt. % filler loading:<br>$H_2/CH_4$: 180<br>$CO_2/N_2$: 39.8<br>$O_2/N_2$: 8.5 | Permeability improvements are due to the disruption of the polymer chains, the space present in each hollow silicate-1 spheres contributes too.<br>MMMs membranes presented higher selectivities for $H_2/CH_4$, $CO_2/N_2$, and $O_2/N_2$ mixtures than pure membrane. | [47] |
| Silica spheres | -Prepare, characterize and test and mesoporous silica filled Matrimid membranes for $H_2/CH_4$ separations. | Huntsman Advanced Materials | -Separation in binary mixture: $H_2/CH_4$, $CO_2/N_2$, and $O_2/N_2$ | • SEM<br>• TEM<br>• TGA<br>• Tg determination<br>• XRD | Gas binary mixture separation<br>Conditions: 400 kPa, 35 ◦C, feed composition (50:50) | At 8 wt. % filler loading:<br>$H_2$: 48.9 Barrer<br>$CH_4$: 0.3 Barrer | At 8 wt. % filler loading:<br>$H_2/CH_4$: 155.3 | The permeability of the selective gas increases with the filler, whereas the selectivity has a maximum at 8 wt. % filler loading. | [47] |
| • Zeolite 4A<br>• ZSM-5<br>• Zeolite 13X | -Effect of zeolite content in Matrimid® dense films<br>-Modelling of MMMs by Maxwell and modified Maxwell models | Vantico Inc | -Permeability: $H_2$, $N_2$, He and $CO_2$<br>-Ideal selectivity: $CO_2/N_2$, $He/N_2$, $H_2/He$, $H_2/CO_2$ | • SEM | Single gas permeation<br>Conditions: 10 bar, 25 ◦C. | At 30 wt. % zeolite 13X:<br>$H_2$: 178 Barrer<br>$CO_2$: 378 Barrer<br>$N_2$: 185 Barrer<br>He: 111 Barrer | At 30 wt. % zeolite 13X:<br>$CO_2/N_2$: 67.1<br>At 30 wt. % zeolite 4A:<br>$CO_2/N_2$: 50.6 | Permeability values for He, $H_2$, $CO_2$, and $N_2$ increased with zeolite loadings.<br>Selectivity of $H_2/N_2$ showed a slight improvement for low loadings. | [40] |
| Amine-grafted zeolite (AU/EMT intergrowth zeolite) | -Study filler properties such as surface density of grafted amine groups in zeolites.<br>-Crosslinked Matrimid membranes using APTMDS.<br>-Gas evaluation of crosslinked MMMs using modified filler. | Huntsman Advanced Materials Americas Inc. | -Permeability: $CH_4$, and $CO_2$<br>-Ideal selectivity: $CO_2/CH_4$ | • SEM<br>• TGA<br>• FTIR<br>• BET analysis<br>• DMA | Single gas permeation<br>Conditions: 150 psi, 35◦C. | At 25wt. % amine zeolite:<br>$CO_2$: 6.3 Barrer<br>$CH_4$: 0.1 Barrer | At 25wt. % amine zeolite:<br>$CO_2/CH_4$: 48.5 | MMMs, based on crosslinked Matrimid® and modified zeolite, improve considerably the $CO_2/CH_4$ selectivity compared to the pure Matrimid membrane. | [53] |

**Table 2.1.** Recent applications of Matrimid in the preparation of MMMs for gas separation (continued)

| *Filler* | *Aim of the study* | *Supplier of Matrimid ®* | *Evaluated application* | *Techniques used for Membrane characterization* | *Measurement type:* | *Permeation performance:* | *Selectivity or separation factor:* | *Remark of the study* | *Reference* |
|---|---|---|---|---|---|---|---|---|---|
| Silica | -Development of MMMs using silica nanoparticles into PSF/Matrimid® blend matrix | Huntsman Advanced Materials Americas Inc. | -Permeability: $CH_4$, and $CO_2$<br>-Separation in binary mixture: $CO_2/CH_4$<br>-Ideal selectivity: $CO_2/CH_4$ | • SEM<br>• XRD<br>• FTIR<br>• TGA<br>• TEM<br>• DSC | Single gas permeation<br>Conditions: 10 bar, 25◦C | At 20.1 wt. % filler loading:<br>$CO_2$: 90 GPU<br>$CH_4$: 1.4 GPU | At 20.1 wt. % filler loading:<br>$CO_2/CH_4$: 55 | The $CO_2$ permeability increased (up to 73.7 GPU) with the introduction of silica in PSF/PI blend membrane.<br>The MMMs showed higher mixed gas selectivity for $CO_2/CH_4$ (61.0) than unfilled membrane | [48] |
| ZIF-8 | -Synthesis of ZIF-8/Matrimid® MMMs for gas separation | Huntsman Advanced Materials | -Permeability: $H_2$, $O_2$, $N_2$, $CH_4$, and $CO_2$<br>-Ideal selectivity: $CO_2/CH_4$, $CO_2/N_2$, $O_2/N_2$, $H_2/N_2$, $H_2/CH_4$ | • SEM<br>• TEM<br>• XRD<br>• FTIR<br>• DMA<br>• PALS<br>• BET analysis of ZIF-8 | Single gas permeation<br>Conditions: 4 bar, 22◦C | At 20 wt. % filler loading:<br>$H_2$: 28.8 Barrer<br>$CO_2$: 19.7 Barrer<br>$O_2$: 3.9 Barrer<br>$N_2$: 1.7 Barrer<br>$CH_4$: 1.0 Barrer | At 20 wt. % filler loading:<br>$CO_2/N_2$: 11.1<br>$CO_2/CH_4$: 18.6<br>$O_2/N_2$: 2.2<br>$H_2/N_2$: 16.3<br>$H_2/CH_4$: 27.3 | Permeability increased substantially with the loading of ZIF-8. Ideal electivity remains constant in comparison to the pure polymeric membrane. | [37] |
| Zeolite 4A | -Development of Matrimid® /zeolite 4A MMMs using low boiling point solvent | Huntsman | -Permeability: $H_2$, $O_2$, $N_2$, and $CO_2$<br>-Ideal selectivity: $CO_2/N_2$, $O_2/N_2$, $H_2/N_2$ | • FE-SEM<br>• DSC<br>• TGA<br>• XRD | Single gas permeation<br>Conditions: 8 bar, 30◦C | At 30 wt. % filler loading:<br>$H_2$: 101.6 Barrer<br>$CO_2$: 48.3 Barrer<br>$O_2$: 11.1 Barrer<br>$N_2$: 2.0 Barrer | At 30 wt. % filler loading:<br>$CO_2/N_2$: 23.3<br>$O_2/N_2$: 5.3<br>$H_2/N_2$: 49.1 | Permeability for all gases increased: $N_2$ (632%), $O_2$ (168%), $H_2$ (162%) and $CO_2$ (62%).<br>Decrease in the selectivity $O_2/N_2$ (63 %), $H_2/N_2$ (64%) and $CO_2/N_2$ (78%) was observed. | [41] |
| SAPO-34 | -Preparation and characterization of MMMs using SAPO-34 zeolite. | Huntsman Chemical Company | -Permeability: $CH_4$, and $CO_2$<br>-Ideal selectivity: $CO_2/CH_4$ | • SEM<br>• XRD<br>• Gas adsorption for zeolitic particles<br>• DLS of particles.<br>• DSC | Single gas permeation<br>Conditions: 10 bar, 25◦C | At 20 wt. % filler loading:<br>$CO_2$: 6.9 Barrer<br>$CH_4$: 0.1 Barrer | At 20 wt. % filler loading:<br>$CO_2/CH_4$: 67 | Permeation measurement showed that $CO_2$ permeability and $CO_2/CH_4$ selectivities of the MMM with 20 wt% loading of SAPO-34 zeolite particles increased up to 6.9 Barrer and 67, respectively. | [50] |

**Table 2.1.** Recent applications of Matrimid in the preparation of MMMs for gas separation (continued)

| *Filler* | *Aim of the study* | *Supplier of Matrimid ®* | *Evaluated application* | *Techniques used for Membrane characterization* | *Measurement type:* | *Permeation performance:* | *Selectivity or separation factor:* | *Remark of the study* | *Reference* |
|---|---|---|---|---|---|---|---|---|---|
| • MIL-53 (Al)<br>• $NH_2$ -MIL-53(Al) | -Effect of amino functionalized filler in the separation performance of MMMs based on Matrimid. | Huntsman | -Separation in binary mixture: $CO_2/CH_4$ | • SEM<br>• TGA<br>• FTIR<br>• BET analysis for fillers<br>• Tensile properties | Gas binary mixture separation<br>Conditions: 150 psi, 35 ◦C, feed composition (50:50) | At 15 wt. % MIL-53 (Al):<br>$CO_2$: 6.7 Barrer<br>$CH_4$: 0.2 Barrer | At 15 wt. % MIL-53 (Al):<br>$CO_2/CH_4$: 28.5<br>At 15 wt. % $NH_2$-MIL-53 (Al):<br>$CO_2/CH_4$: 2.1 | The MMMs containing $NH_2$-MIL-53(Al) particles displayed high $CO_2$ permeability. | [56] |
| MIL-53 | -Preparation and characterization of MMMs by using MIL-53 | Huntsman | -Permeability: $CH_4$, and $CO_2$<br>-Calculation of ideal selectivity: $CO_2/CH_4$ | • SEM<br>• XRD<br>• TEM | Single gas permeation<br>Conditions: 3 bar, 35 ◦C. | At 15 wt. % filler loading:<br>$CO_2$: 12.4 Barrer<br>$CH_4$: 0.2 Barrer | At 15 wt. % filler loading:<br>$CO_2/CH_4$: 51.8 | The permeability and selectivity for $CO_2/CH_4$ increased significantly compared to pure Matrimid®. The highest selectivity was 51 at 15 wt% filler content. | [51] |
| $Cu_3(BTC)_2$ | -Preparation and characterization of MMMs using $Cu_3(BTC)_2$ | Huntsman Advanced Materials | -Permeability: $O_2$, $CH_4$, $N_2$, and $CO_2$<br>-Ideal selectivity: $CO_2/CH_4$, $O_2/N_2$ | • SEM<br>• XRD<br>• TGA<br>• FTIR-ATR<br>• BET analysis of filler | Single gas permeation<br>Conditions: 2 atm, 35 ◦C. | At 20 wt. % filler loading:<br>$CO_2$: 24.8 Barrer | At 20 wt. % filler loading:<br>$CO_2/CH_4$: 37.8 | Membranes presented good performance for $O_2/N_2$ and $CO_2/CH_4$ separations. | [42] |
| $NH_2$ -MIL-53(Al) | -Analyze the structure-performance relationship between the modified filler and Matrimid®. | Huntsman Advanced Materials | -Separation in binary mixture: $CO_2/CH_4$ | • SEM<br>• EDX<br>• TGA<br>• DRIFT<br>• FTIR<br>• Gas adsorption for nanoparticles | Gas binary mixture separation<br>Conditions: 3 bar, 35 ◦C, feed composition (50:50) | At 25 wt. % filler loading:<br>$CO_2$: 14 Barrer<br>$CH_4$: 0.2 Barrer | At 25 wt. % filler loading:<br>$CO_2/CH_4$: 35 | The incorporation of the nanoparticles enhanced $CO_2$ permeability compared to pure polymeric membranes, preserving the separation factor. | [55] |

**Table 2.1.** Recent applications of Matrimid in the preparation of MMMs for gas separation (continued)

| ***Filler*** | *Aim of the study* | *Supplier of Matrimid ®* | *Evaluated application* | *Techniques used for Membrane characterization* | *Measurement type:* | *Permeation performance:* | *Selectivity or separation factor:* | *Remark of the study* | *Reference* |
|---|---|---|---|---|---|---|---|---|---|
| • MIL-53 (Al)<br>• ZIF-8<br>• $Cu_3BTC_2$ | -Analyze the performance and plasticization phenomenon of PI membranes using different fillers. | Huntsman | -Permeability: $CH_4$, and $CO_2$<br>-Separation in binary mixture: $CO_2/CH_4$ | • SEM<br>• XRD<br>• TGA<br>• DSC<br>• Density for MOF particles | Single gas permeation<br>Conditions: 5 bar, 35 ◦C. | At 30 wt. % MIL-53 (Al):<br>$CO_2$:20 Barrer<br>$CH_4$: 0.3 Barrer<br>At 30 wt. % ZIF-8:<br>$CO_2$: 22 Barrer | At 30 wt. % MIL-53 (Al):<br>$CO_2/CH_4$: 52<br>At 30 wt. % ZIF-8:<br>$CO_2/CH_4$: 45<br>At 30 wt. % $Cu_3BTC_2$:<br>$CO_2/CH_4$: 60 | At low pressure, the MMMs showed moderate enhancement in $CO_2$ permeability and $CO_2/CH_4$ selectivity compared to neat Matrimid membrane.<br>All fillers suppressed $CO_2$ plasticization and maintained large separation factors over a wide pressure range investigated | [13] |
| Fe(BTC) | -Evaluate the effect of mesoporous material on $CO_2$ induced plasticization of Matrimid®. | Huntsman | -Permeability: $CH_4$, and $CO_2$<br>-Separation in binary mixture: $CO_2/CH_4$ | • SEM<br>• XRD<br>• TGA<br>• DSC<br>• Density | Single gas permeation<br>Conditions: 5 bar, 35 ◦C. | At 30 wt. % filler loading:<br>$CO_2$: 13 Barrer<br>$CH_4$: 0.4 Barrer | At 30 wt. % filler loading:<br>$CO_2/CH_4$: 28 | In comparison to pure Matrimid the MMMs showed an increase in mixed gas $CO_2/CH_4$ selectivity of 62%. The filler suppressed $CO_2$ plasticization. | [52] |
| • $NH_2$-MIL-53 (Al)<br>• MCM-41 | -Prepare, characterize and test and mesoporous silica and amino functionalized MIL-53 filled Matrimid membranes for $H_2/CH_4$ separations. | Huntsman Advanced Materials | -Separation in binary mixture: $H_2/CH_4$ | • SEM<br>• DSC<br>• TEM<br>• Mechanical strength measurements | Gas binary mixture separation<br>Conditions: 300 kPa, 35 ◦C, feed composition (50:50) | At 12/4 wt. % MCM-41 and $NH_2$-MIL-53 (Al): respectively:<br>$H_2$: 21.3 Barrer | At 12/4 wt. % MCM-41 and $NH_2$-MIL-53 (Al):<br>$H_2/CH_4$: 178 | The MMMs displayed superior gas separation performance than those with only one type of filler because of a synergy effect. Due to their complementary interaction, two types of particles in one membrane improved the dispersion of the filler phase. | [60] |
| • Polyzwitterion coated carbon nanotubes (SBMA@CNT) | -Enhance the $CO_2$ permeability of Matrimid by incorporating composite particles. | Alfa Aesar China Co. | -Separation in binary mixture: $CO_2/CH_4$ | • TEM<br>• FESEM<br>• DSC<br>• FTIR | Gas binary mixture separation<br>Conditions: 2 bar, 30 ◦C, feed composition (30:70) | At 5 wt. % filler loading:<br>$CO_2$: 4.8 Barrer | At 5 wt. % filler loading:<br>$CO_2/CH_4$: 73.3 | Hybrid membranes show significantly enhanced $CO_2$ permeability (103 Barrer) compared to neat Matrimid membrane at a humidified state. | [61] |

**Table 2.1.** Recent applications of Matrimid in the preparation of MMMs for gas separation (continued)

| ***Filler*** | *Aim of the study* | *Supplier of Matrimid ®* | *Evaluated application* | *Techniques used for Membrane characterization* | *Measurement type:* | *Permeation performance:* | *Selectivity or separation factor:* | *Remark of the study* | *Reference* |
|---|---|---|---|---|---|---|---|---|---|
| • ZIF-8<br>• ZIF-90 | -Develop MMMs with inorganic molecular sieving additives to improve a Matrimid® polymer membrane for the $H_2/CO_2$ separation. | Huntsman | -Permeability: $H_2$, and $CO_2$<br>-Separation in binary mixture: $H_2/CO_2$<br>-Ideal selectivity: $H_2/CO_2$ | • SEM<br>• TEM<br>• XRD | Gas binary mixture separation<br>Conditions: 0.2 bar, 25 ◦C, feed composition (50:50) | At 25 wt. % ZIF-8:<br>$H_2$: 31Barrer<br>$CO_2$: 9 Barrer<br>At 25 wt. % ZIF-90:<br>$H_2$: 30 Barrer<br>$CO_2$: 6 Barrer | At 25 wt. % ZIF-8:<br>$H_2/CO_2$: 3.5<br>At 25 wt. % ZIF-90:<br>$H_2/CO_2$: 5 | Incorporation of ZIF-8 into PI matrix improved the $H_2$ permeability, whereas the $H_2/CO_2$ mixed gas separation factor remained constant (3.5).<br>Incorporation of ZIF-90 improved the $H_2/CO_2$ separation factor (9.5), but a decrease in $H_2$ permeability was observed. | [38] |
| NaY zeolite | -Evaluate the incorporation of micro- and nano-porous NaY zeolite in Matrimid®. | Huntsman | -Permeability: $CH_4$, and $CO_2$<br>-Calculation of ideal selectivity: $CO_2/CH_4$ | • SEM<br>• TGA<br>• DTG<br>• XRD<br>• FTIR-ATR | Single gas permeation<br>Conditions: 2 bar, 35 ◦C. | At 20 wt. % filler loading:<br>$CO_2$: 22 Barrer<br>$CH_4$: 0.8 Barrer | At 20 wt. % filler loading:<br>$CO_2/CH_4$: 27.6 | The $CO_2$ permeability was increased (more than two-fold) by using the filler. At the same time, the $CO_2/CH_4$ selectivity was enhanced too (around 20%). | [62] |
| ZSM-5 | -Preparation and characterization of ternary MMMs using PEG- and zeolite. | Huntsman | -Permeability: $CH_4$, and $CO_2$<br>-Calculation of ideal selectivity: $CO_2/CH_4$ | • SEM<br>• FE-SEM<br>• FTIR-ATR<br>• XRD | Single gas permeation<br>Conditions: 10 bar, 35 ◦C. | At 5 wt. % filler loading:<br>$CO_2$: 15.7 Barrer<br>$CH_4$: 0.8 Barrer | At 5 wt. % filler loading:<br>$CO_2/CH_4$: 19.2 | The ternary MMMs showed an improvement of $CO_2$ permeability and $CO_2/CH_4$ selectivity in comparison to the neat Matrimid membrane. The permeability and selectivity increased about 50% and 72%, respectively. | [58] |
| $NH_2$-UiO-66 | -Incorporation of amino modified filler in Matrimid for $CO_2$ separation | Huntsman | -Separation in binary mixture: $CO_2/CH_4$ | • DSC<br>• Mechanical test<br>• ATR-FTIR<br>• XRD | Gas binary mixture separation<br>Conditions: 2 bar, 35 ◦C, feed composition (10:90) | At 30 wt. % filler loading:<br>$CO_2$: 37.9 Barrer | At 30 wt. % filler loading:<br>$CO_2/CH_4$: 47.7 | A significant increase in the mixed-gas selectivity and<br>Permeability compared to the unfilled Matrimid membrane (i.e., 50% more selective and 540% more permeable) was achieved. | [63] |
| Aminosilane grafted NaY zeolite | -Evaluate the effect of the chemical modification in the preparation of MMMs. | Huntsman Advanced Materials | -Separation in binary mixture: $CO_2/CH_4$ | • Contact angle<br>• SEM<br>• FTIR-ATR | Gas binary mixture separation<br>Conditions: 9 bar, 35 ◦C, feed composition (50:50) | At 15 wt. % filler loading:<br>$CO_2$: 8.3 Barrer<br>$CH_4$: 0.1 Barrer | At 15 wt. % filler loading:<br>$CO_2/CH_4$: 48.9 | Good dispersion of the silane modified NaY particles in the Matrimid membranes was achieved with defect free polymer-filler interface. | [57] |

**Table 2.1.** Recent applications of Matrimid in the preparation of MMMs for gas separation (continued)

| ***Filler*** | *Aim of the study* | *Supplier of Matrimid ®* | *Evaluated application* | *Techniques used for Membrane characterization* | *Measurement type:* | *Permeation performance:* | *Selectivity or separation factor:* | *Remark of the study* | *Reference* |
|---|---|---|---|---|---|---|---|---|---|
| POP-2 | -Evaluate the impact of the nanofiller on the gas separation performance of Matrimid. | Huntsman Advanced Materials Americas Inc | -Permeability: $O_2$, $N_2$, $CH_4$, and $CO_2$<br>-Calculation of ideal selectivity: $CO_2/CH_4$ and $CO_2/N_2$ | • SEM<br>• FFV<br>• BET sorption | Single gas permeation<br>Conditions: 2 atm, 35 ◦C. | At 20 wt. % filler loading:<br>$CO_2$: 28 Barrer | At 20 wt. % filler loading:<br>$CO_2/CH_4$: 32<br>$CO_2/N_2$:24 | The pure gas permeabilities increased with increasing particle loading with no reduction in the selectivity. | [43] |
| ZIF-11 | -Improve the $H_2/CO_2$ separation performance of Matrimid through incorporating nanoparticles. | Huntsman Advanced Materials | -Separation in binary mixture: $H_2/CO_2$ | • XRD<br>• FTIR<br>• TEM<br>• TGA<br>• Adsorption isotherms | Gas binary mixture separation<br>Conditions: 330 kPa, 35 ◦C, feed composition (50:50) | At 15 wt. % filler loading:<br>$H_2$: 95.9 Barrer | At 15 wt. % filler loading:<br>$H_2/CO_2$: 4.4 | The MMMs demonstrated an enhancement on the separation properties of the neat polymer, but a strong enhance was found at high temperatures (200◦C) | [3] |
| • Graphite oxide (GO)<br>• CNT | -Evaluate the synergistic effect of the addition of two fillers into Matrimid to improve $CO_2$ separation performance. | Alfa Aesar | -Permeability: $N_2$, $CH_4$, and $CO_2$<br>-Calculation of ideal selectivity: $CO_2/CH_4$ and $CO_2/N_2$ | • SEM<br>• FTIR<br>• AFM<br>• TEM | Single gas permeation<br>Conditions: 200 kPa, 30◦C. | At 5 wt. % of both fillers:<br>$CO_2$: 38.0 Barrer | At 5 wt. % of both fillers:<br>$CO_2/CH_4$: 86.4<br>$CO_2/N_2$: 81 | The MMMs containing 5 wt. % of CNTs and 5 wt. % GO showed the optimum performances with an enhancement of 331 % in $CO_2$ permeability. | [64] |
| $NH_2$-MIL-53(Al) | -Evaluate the impact of the filler morphology on the gas separation performance. | Huntsman Advanced Materials | -Separation in binary mixture: $CO_2/CH_4$ | • FBI-SEM<br>• DSC<br>• Gas adsorption for nanoparticles<br>• XRD<br>• TEM analysis for nanoparticles | Gas binary mixture separation<br>Conditions: 3 bar, 25 ◦C, feed composition (50:50) | At 8 wt. % filler loading:<br>$CO_2$: 9 Barrer<br>$CH_4$: 0.2 Barrer | At 8 wt. % filler loading:<br>$CO_2/CH_4$: 38 | The use of nanoparticles and nanorods tends to offer better separation performance than microneedles. The $CO_2$ permeability increased (9 Barrer) upon 8 wt% loading of nanoparticles . | [65] |

**Table 2.1.** Recent applications of Matrimid in the preparation of MMMs for gas separation (continued)

| ***Filler*** | *Aim of the study* | *Supplier of Matrimid ®* | *Evaluated application* | *Techniques used for Membrane characterization* | *Measurement type:* | *Permeation performance:* | *Selectivity or separation factor:* | *Remark of the study* | *Reference* |
|---|---|---|---|---|---|---|---|---|---|
| • Zeolite 13X,<br>• Sepiolite<br>• CMS<br>• BRITESORB D300<br>• | -Evaluate the incorporation of several types of fillers in Matrimid®. | Huntsman Advanced Materials | -Permeability: $CH_4$, and $CO_2$<br>-Calculation of ideal selectivity: $CO_2/CH_4$ | • SEM<br>• AFM<br>• FTIR<br>• XRD<br>• TGA | Single gas permeation<br>Conditions: 12 bar, 25 ◦C. | At 20 wt. % Britesorb D300:<br>$CO_2$: 13.8 Barrer<br>$CH_4$: 0.5 Barrer | At 20 wt. % Britesorb D300:<br>$CO_2/CH_4$: 26.2<br>At 20 wt. % sepolite:<br>$CO_2/CH_4$: 27.5 | Sepiolite and AEROSIL (at 30 wt%) demonstrated a slight improvement of selectivity through the $CO_2$ permeability increase. | [44] |
| MIL-96(Al) | -Evaluate the potentiality of the filler in MMMs based on Matrimid®. | Huntsman | -Separation in binary mixture: $H_2/CO_2$ | • SEM<br>• DLS | Gas binary mixture separation<br>Conditions: 5 bar, 150 ◦C, feed composition (50:50) | At 10 wt. % filler loading:<br>$H_2$: 180 Barrer<br>$CO_2$: 30Barrer | At 10 wt. % filler loading:<br>$H_2/CO_2$: 6 | The filler (at 10 %) improved the permeability of both gases but respective decrease of selectivity was obtained. | [66] |
| Ag + ion-exchanged zeolite-Y | -Preparation and characterization of novel MMM. | Huntsman Advanced Materials | -Permeability: $CH_4$, and $CO_2$<br>-Calculation of ideal selectivity: $CO_2/CH_4$ | • SEM<br>• Gas adsorption for zeolites<br>• FTIR<br>• UV–vis DRS)<br>• XRD | Single gas permeation<br>Conditions: 2 bar, 35 ◦C. | At 15 wt. % filler loading:<br>$CO_2$: 18.6 Barrer<br>$CH_4$: 0.3 Barrer | At 15 wt. % filler loading:<br>$CO_2/CH_4$: 60.1 | The gas permeation results showed that the $CO_2$ permeability increased about 123% in Matrimid/AgY (15 wt%) compared to pure Matrimid. Whereas the $CO_2/CH_4$ selectivity was improved about 66%, | [67] |
| MIL-68(Al) | -Preparation and characterization of MIL-68(Al)/Matrimid mixed matrix membranes. | VWR International GmbH | -Separation in binary mixture: $CO_2/CH_4$ | • XRD<br>• FESEM | Gas binary mixture separation<br>Conditions: 1 bar, 100 ◦C, feed composition (50:50) | At 10 wt. % filler loading:<br>$CO_2$: 284.3 Barrer<br>$CH_4$: 3.6 Barrer | At 10 wt. % filler loading:<br>$CO_2/CH_4$: 79 | The MMMs showed high $CO_2$ permeability (284.3 Barrer) and the $CO_2/CH_4$ (79.0) selectivity which far exceed the Robeson limit and those of the previously reported MMMs. | [68] |
| • TS-1<br>• ETS-10 | -Evaluate the influence of Ti on the performance of the different MMMs | Huntsman | -Separation in binary mixture: $CO_2/CH_4$ | • SEM<br>• DSC<br>• AES-ICP and XPS analyses | Gas binary mixture separation<br>Conditions: 8 bar, 35 ◦C, feed composition (50:50) | At 30 wt. % TS-1:<br>$CO_2$: 9.5 Barrer<br>$CH_4$: 0.3 Barrer | At 30 wt. % TS-1:<br>$CO_2/CH_4$: 30.8 | Using TS-1 led to increase about 89.1% and 23.9% of $CO_2$ permeability and separation factor. | [45] |

It is important to highlight that the use of unconventional particles is currently tested in MMM preparation. There is strong evidence that the incorporation of fillers can improve the performance of Matrimid, generally, the enhancement of the permeability is observed. For example, MIL-96(Al) improved the permeability for $H_2$ and $CO_2$ but a respective decrease on selectivity was reported [66]. However, some other fillers can improve the permeability and selectivity too, i.e., Ag + ion-exchanged zeolite-Y also increased $CO_2$ permeability (about 123%, from 8.34 for pure Matrimid to 18.62 Barrer for Matrimid/AgY) and $CO_2/CH_4$ selectivity (about 66%, from 36.3 for Matrimid to 60.1 for Matrimid/AgY) [67]. Dong *et al.* [68] developed MMMs using MIL-68 (Al), which present highly perm-selective properties ($CO_2$ permeability: 284.3 Barrer, separation factor: 79.0); the study demonstrated to overcome easily the Robeson trade-off. In addition, a homogeneous distribution of the MIL-68 (Al) was confirmed by FESEM images, without visible defects, exhibiting a positive interaction between filler-polymer phases [68]. The good distribution of the inorganic phase into continuous phases provides also an outlook of good mechanical properties of the MMMs. Typically; the microstructure of the filler allows a synergistic combination with the polymer leading to achieve a hybrid material with improved functional and mechanical properties [69]. Recently, Martin-Gil *et al.* [45] incorporated TS-1 and ETS-10 nanoparticles in continuous Matrimid matrix for $CO_2/CH_4$ separation. Using TS-1 led to increase about 89.1% and 23.9% of $CO_2$ permeability and separation factor, respectively, in comparison with pure polymer. Regarding ETS-10, the $CO_2$ permeability (22.5 %) and separation factor (7.8 %) increased slightly with respect to the reference polymer membrane.

Finally, the performances of several MMMs based on Matrimid prepared until now are shown by Castro-Muñoz *et al.* [6], where different gas pairs have been tested pointing out that the separation of $CO_2$ and $CH_4$ has been the most tested gas pair to evaluate the performance of Matrimid MMMs, as **Figure 2.7** shows.

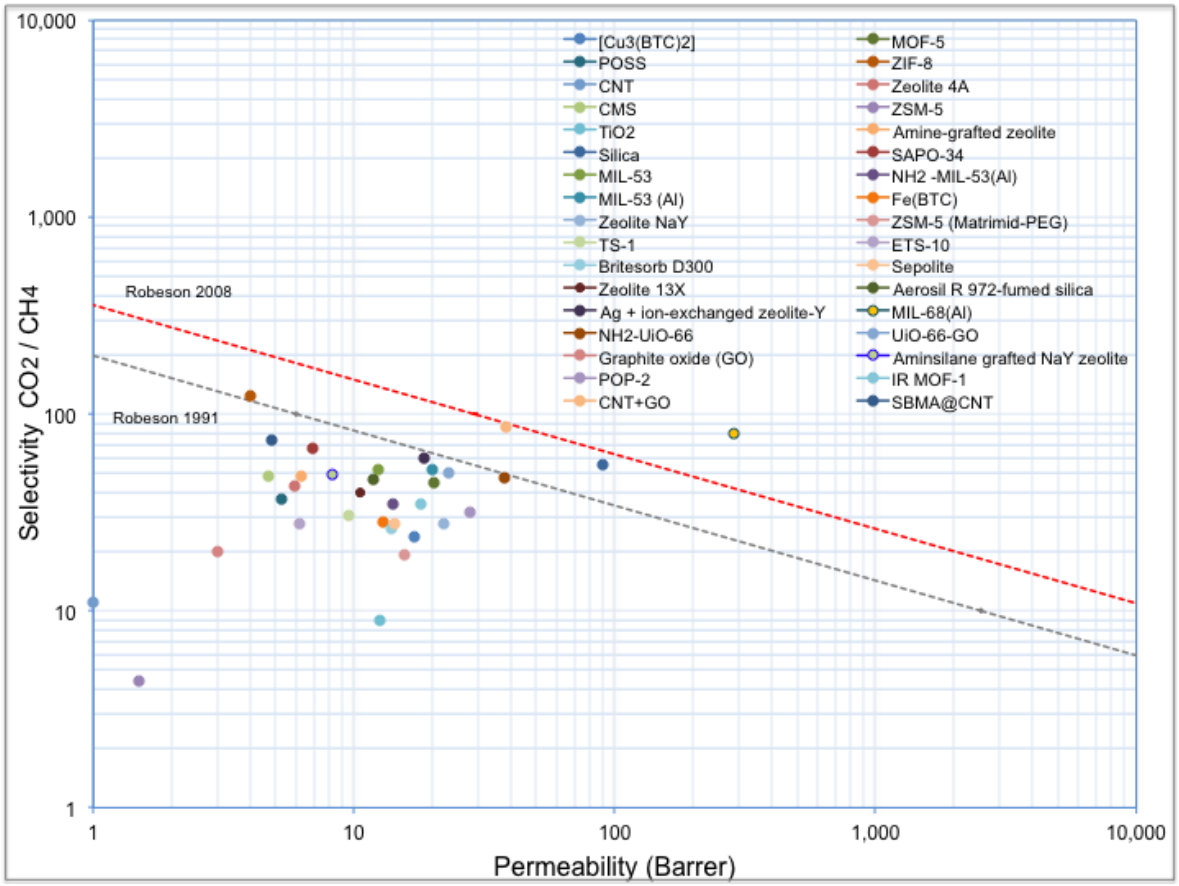


**Figure 2.7.** Status of Matrimid MMMs on Robeson trade-off 1991-2008 for $CO_2/CH_4$ [6,70,71].

## 2.6.Chapter remarks

This chapter compiled the past 20 year's research activities in preparation and testing of Matrimid® membranes in gas separation. It shows the importance of adopting a proper strategy in exploiting synergistic beneficial features of the advanced materials, processes, and modification techniques in order to achieve Matrimid membranes with desirable performance. The evolution of uses of Matrimid can be summarized in two highlighted frameworks:

*Last decade's framework (from 1998 to 2008)*

i. The $CO_2/CH_4$ separation has been the most tested binary mixture over last 20 years.
ii. The plasticization was identified as a main issue of Matrimid membranes for gas separation.
iii. The initial attempts to avoid Matrimid plasticization by $CO_2$ and propylene were: structure modification (chemical crosslinking), heat treatments (over 300 °C), blending with other glassy polymers.
iv. The enhancement of membrane separation properties through structure modification has been studied. The most used methods were the gas phase fluorination, bromination, as well as pyrolysis reaction.
v. The addition of inert gases (commonly $N_2$, $CH_4$, heptane, and toluene) in the feed gas mixture was also proposed in order to increase the gas selectivity.
vi. The preparation of dual-layer membranes by means of thin films Matrimid coatings on hollow fibers (PES, PSF, PDMS matrix) for $O_2/N_2$ separation has been widely tested.
vii. In the initial development of MMMs, $C_{60}$, CMS, zeolite beta, ZSM-5, and Cu-BPY-HFS were used as fillers

*Today's framework (from 2009 up to now)*

i. The synthesis of Mixed Matrix Membranes (MMMs) based on Matrimid is the main subject to enhance the separation properties of this polyimide. The fillers that have been tested are silica, COK-12 silica, CNT, CMS, POP-2, $TiO_2$, sepiolite, titanosilicates (e.g. TS-1, ETS-10), zeolites (e.g. ZSM-5, 4A, 13X, amine-grafted zeolite, SAPO-34, silicate-1, NaY), zeolitic imidazolate framework (ZIF-8, ZIF-90) and metal organic frameworks (e.g. $Cu_3(BTC)_2$, MOF-5, MIL-53, MIL-101, MIL-88B(Fe), IRMOF-1) and their chemical modification ($NH_2$-MIL-53(Al), $Cu_3(BTC)_2$, MIL-96(Al), MIL-68(Al), Fe(BTC)).
ii. Strategies such as structure modification by chemical crosslinking, polymers blends (with high plasticization pressures), as well as thermal annealing, have been the strategies most used against Matrimid plasticization. The blending of

Matrimid with additives and polymers has received worldwide attention due to the improving the properties of pure Matrimid.

iii. Matrimid has been used as precursor for making carbon membranes through carbonization process; demonstrating that CMS performance can overcome easily the Robeson trade-off.

iv. The most developed membrane types have been the hollow fiber due to the need of high flow processing. $CO_2/CH_4$ binary mixture separation is still the most tested due to the promising future of Matrimid in natural gas purification.

v. The first attempts of new surface modification methods, like vapor-phase modification, are starting to offer considerable enhancement of separation properties of Matrimid membranes.

vi. The first attempts to understand the physical aging of Matrimid membranes have been reported.

vii. The production of MMMs membranes is a consolidated tool for gas separation using fillers into Matrimid matrix to improve its separation performance. However, the preparation of MMMs by combination of two different approaches; *i)* chemical modification of the filler, and *ii)* chemical modification of the structure of the polymer matrix, has demonstrated to be an excellent approach for improving the membranes. According to recent studies reported above, the promising enhancement was shown at least for $CO_2/CH_4$ separation.

viii. The development of novel fillers to incorporate into Matrimid matrix has been reported.

As stated previously, Matrimid has proven excellent properties and high potential in membrane gas separation, especially $CO_2/CH_4$ separations. Moreover, we have identified the most used approaches choosing a new perspective for improving this commercial polymer. At this point, the following **Chapters 3 and 4** address the enhancement of the $CO_2$ permeability by blending the polymer with a $CO_2$-philic additive and inorganic materials (e.g. metal-organic frameworks), respectively.

# *Chapter 3*

## Matrimid® 5218-PEG 200 membranes for enhancing the $CO_2$ separation towards $CO_2/CH_4$ binary mixtures

### Chapter overview

The effect of addition of $CO_2$-philic additive into the polymeric matrix has been identified as promising approach to increase the $CO_2$ permeability and/or selectivity [72]. The PEG 200 as $CO_2$-philic additive was chosen in this work. The effect of its addition in Matrimid® 5218 on performance of prepared membranes in multicomponent gas separation is evaluated. Matrimid®-PEG 200 flat sheet blend membranes were prepared by dense film-casting method. The blend membranes were fabricated at low PEG concentrations (0-5 wt.%). Pure Matrimid® and its blend membranes were characterized by using FTIR, SEM, DSC, TGA and permeation measurements. Finally, based on the gas separation performance of the blend membranes, the best performing blend formulation was analysed at different feed compositions (25:75, 50:50, 75:25) and feed pressures (2, 4, 6, 8 bar).

### 3.1. Introduction

Membrane gas separation is an emerging technology showing consolidate commercial potential in diverse industrial applications such as carbon dioxide ($CO_2$) capture, nitrogen recovery, oxygen enrichment, natural gas processing, air purification, and hydrogen separation [28,73]. Today, the carbon dioxide removal from different gas sources like natural- and bio-gas continues to growth its importance. In this respect, particular recent attention has focused on membrane gas separation for $CO_2$ capture [74,75]. In last decades, Matrimid® 5218 was widely studied for aforementioned purpose. In addition, this polyimide (PI) has been commercially consolidated, and is still currently studied due to its advantages such as chemical and mechanical stability, thermal resistance as well as high selectivity towards $CO_2/CH_4$ [29,55]. However, Matrimid® does not show high productivity in terms of permeate flux (permeability). The recent subjects in *Research and Development (R & D)* are focusing to the enhancement of this polymer in $CO_2$ permeability, where its blending with several polymers and additives has been proposed [6]. This is the case of polyethylene glycol (PEG), which has demonstrated the enhancement of $CO_2$ permeability in polymeric membranes [76,77]. The polar ether segments (ethylene oxide units) of PEG interact positively with $CO_2$ molecules by dipole-quadrupole interactions, leading the transport through the membranes [10,11]. The PEG molecular weight as well as PEG content play an important role in gas transport properties, Xing and Ho [78] evaluated the addition of PEG with different molecular weights (200,300, 550, 775, and 1000) in polyvinylalcohol (PVA) membranes, showing addition of PEG 200 presented the highest $CO_2$ permeability. Loloei *et al.* [72] reported recently the addition of PEG 200 into Matrimid matrix, it was practically confirmed the enhancement of $CO_2$ permeability at low PEG content (5 wt.%). The study also demonstrated a remarkable improvement of $CO_2/CH_4$ selectivity; however, the study was performed testing the Matrimid-PEG membranes in single gas permeation (for $CO_2$ and $CH_4$). Nowadays, it is important to evaluate the performance of Matrimid-PEG membranes in gas binary (eventually multicomponent) mixtures, where the presence of one component influences directly the permeation of the others present components [13]. Taking into account Loloei's study, the aim of this chapter is to analyze the performance of Matrimid-PEG 200 flat sheet blend membranes prepared by dense film-casting method. The membranes were tested for separation in gas $CO_2$:$CH_4$ (50:50) binary mixture at 8 bar.

Because of the information about the progress of separation performance as a function of the operating time up to reach the steady-state is crucial parameter for potential industrial application of prepared membranes, the study evaluating the effect of PEG addition on membrane behaviour is also included in this chapter. The average steady-state permeabilities of $CO_2$ and $CH_4$ as well as the separation factor are reported. The best performing blended membrane is then tested at different feed compositions (25:75, 50:50, 75:25) and feed pressures (2, 4, 6, 8 bar). All prepared membranes were characterized by differential scanning calorimetry (DSC), thermo-gravimetric analysis (TGA), scanning electron microscopy (SEM), and Fourier transform infrared spectroscopy (FTIR). Finally, the potential of Matrimid® PEG-200 blend membranes for $CO_2$ capture is reported and discussed.

## 3.2.Materials and methodologies

### 3.2.1. Materials

Matrimid® 5218 (3, 3', 4, 4'- benzophenone tetracarboxylic dianhydride and diaminophenylindane) was kindly provided by Huntsman (Huntsman Advanced Materials, Warsaw, Poland). The solvent, NMP ($CHCl_3$, b.p. 161 ºC, >99.9 %), and the polyethylene glycol (PEG 200) were purchased from Sigma-Aldrich (Czech Republic).

## 3.3.Methodologies

### 3.3.1. Membrane preparation

In order to remove any moisture the Matrimid® 5218 was dried overnight in oven at 120 ºC. The casting solutions containing 10 wt.% of polymer were prepared by dissolving Matrimid® or Matrimid®/PEG 200 blend in NMP. The membranes were prepared in triplicate using the dense film-casting method. The labels of membranes and ratio of polymers for each formulation are shown in **Table 3.1**.

**Table 3.1.** Labels and polymer ratios of the fabricated membranes.

| Membrane label | Polymer solution (10 wt.%) |
|---|---|
| M0 | Pure Matrimid |
| M1 | Matrimid®/PEG (95:5) |
| M2 | Matrimid®/PEG (96:4) |
| M3 | Matrimid®/PEG (97:3) |
| M4 | Matrimid®/PEG (98:2) |
| M5 | Matrimid®/PEG (99:1) |

The Matrimid® solutions were prepared and mixed for 24 h. After this time, PEG polymer was added to the Matrimid® solutions. The final solution was allowed stirring for 12 h at room temperature. A glass plate was used for solution casting. Moreover, for decreasing the solvent evaporation rate, a glass cover was placed over the casted film for 24 h. The fabricated membranes were dried in an oven at 30 ºC for 24 h to remove residual solvent. The dry membrane was immersed in a large amount of water for at least 2 days to remove any solvent residual. The water was changed daily. After that the membrane was dried at 100 ºC for 48 h [10]. Finally, the membranes were stored in a desiccator before testing.

### 3.3.2. Gas binary mixture separation

The efficiency of pure Matrimid® membranes and its blends with PEG 200 in $CO_2/CH_4$ binary mixture separation was determined at 25 °C using the permeation unit depicted in **Figure 3.1**. The construction is similar one as used in work [79].

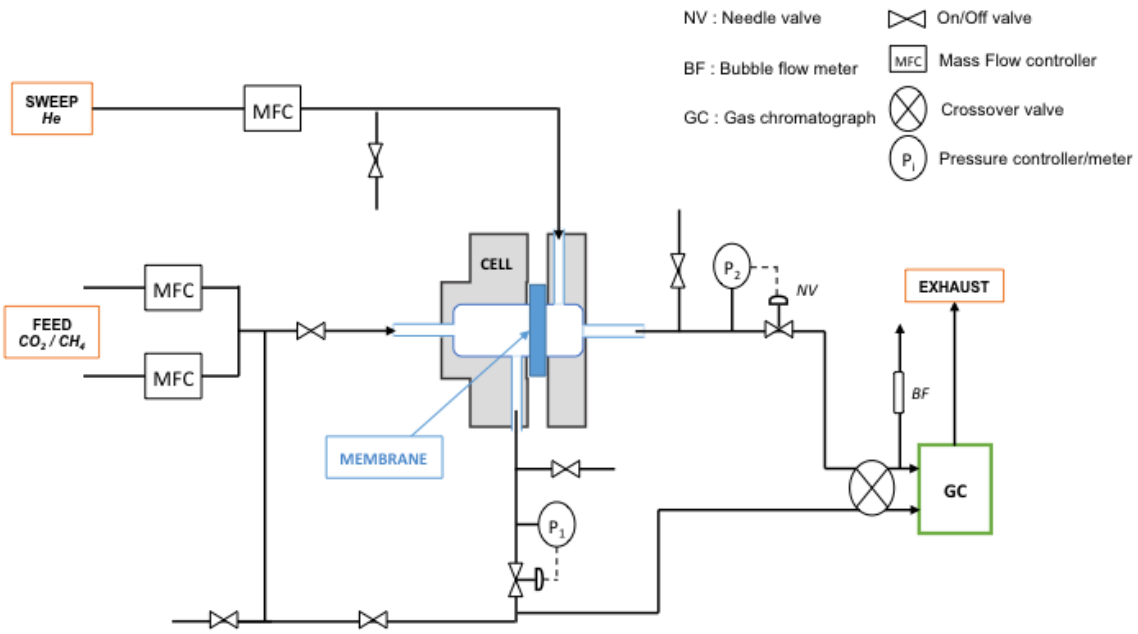


**Figure 3.1.** General scheme of the permeation unit used to carry out binary mixture tests.

The binary $CO_2/CH_4$ mixture of composition 50:50 vol/vol under constant pressure of 8 bar was fed in membrane cell at total flow 40 mL $min^{-1}$(STP). The helium, flow rate of 5 mL $min^{-1}$ (STP) and pressure 1 bar, was used as sweep gas. The gases of purity at least of 99.99 % (SIAD Czech Republic) were used. The flow and pressure were controlled using mass and pressure controllers (Bronkhorst, Netherlands). The $CO_2$ and $CH_4$ concentrations were directly measured in permeate stream by gas chromatograph (Thermo Electron Corporation, GC Focus series, Italy) equipped with methanizer and flame ionization detector (FID). The gas separation factor (α) was calculated using the following equation (1):

$$\alpha_{CO_2/CH_4} = \frac{Y_{CO_2} / Y_{CH_4}}{X_{CO_2} / X_{CH_4}} \qquad (1)$$

where $Y_{CO_2}$ and $Y_{CH_4}$ are the molar fractions of the components in the permeate stream, whereas $X_{CO_2}$ and $X_{CH_4}$ are the molar fractions in feed stream. Eq. (1) is usually used in

gas separation membranes to calculate the mixed gas separation, as in the case of gas mixture, the presence of one component influences the permeation behavior of the other components in the mixture [13]. The permeability and separation factor values are the averages of 3 membranes for each formulation to ensure the reproducibility of the results. The permeabilities (P) were calculated using modified equation of Cecopieri-Gomez *et al.* [80], as given in Eq. (2):

$$P_{gas} = \frac{Y_{gas}^{P} \cdot F^{S} \cdot l}{A\left(Y_{gas}^{R} \cdot P^{R} - Y_{gas}^{P} \cdot P^{P}\right)} \qquad (2)$$

where $Y_{gas}^{P}$ and $Y_{gas}^{R}$ are the molar fractions of any gas ($CO_2$, $CH_4$) in permeate and retentate, respectively; $F^{S}$ is the sweep gas flow rate, $l$ is the membrane thickness, $A$ is the membrane area, and $P^{R}$ and $P^{P}$ are pressures in retentate and permeate, respectively. Permeability values were expressed in the widely used non-SI unit Barrer (1 Barrer=1 x $10^{-10}$ $cm^3$ (STP) cm $cm^{-2}$ $s^{-1}$ cm $Hg^{-1}$)

Finally, the blend membrane (M2), which displayed the best performance in terms of $CO_2$ permeability and separation factor during standard binary experiments ($CO_2$, $CH_4$ 50:50, 8 bar), was tested at different feed composition (25:75 and 75:25) and pressures (2, 4, 6 bar). The total feed flow was maintained constant at 40 mL $min^{-1}$ (STP).

### 3.3.3. Membrane characterization

#### 3.3.3.1.Scanning electron microscopy (SEM)

The morphological structure of the membrane surface and cross-section was evaluated using a scanning electron microscope (Hitachi S 4700, Japan). The samples were attached to SEM aluminum stubs with a diameter of 1 inch using two-sided adhesive carbon tape. The specimens were coated through a sputtering process with gold-palladium (Au / Pd). The corresponding images were captured at suitable magnification. In case of cross-section analysis all samples were prepared by cryogenic fracture after immersion in liquid $N_2$.

#### 3.3.3.2.Differential scanning calorimetry (DSC)

Differential scanning calorimetry (DSC) for glass transition temperature ($T_g$) determination was recorded by SENSYS Evo-TG-DSC calorimeter (Setaram

Instrumentation, France). The $T_g$ measurements were performed under Argon as carrier gas (20 mL (STP) $min^{-1}$) in range of temperature between 30 and 450 ºC; with a heating rate of 20º C $min^{-1}$. The sample (weight around 10 mg) was placed in Pt crucibles. The $T_g$ determination was done in triplicate for each formulation.

3.3.3.3.Thermal gravimetric analysis (TGA)

Thermal Gravimetric Analysis (TGA) using a Linseis (STA 700LT, Germany) investigated thermal properties of membranes. The analysis was carried out by placing the sample (around 10 mg) in an alumina crucible. TGA analysis was carried out heating up the sample to 700 °C with a heating rate of 20 °C $min^{-1}$ under nitrogen flow of 20 mL (STP) $min^{-1}$. Temperature was hold at 700 °C for 30 min, and then cooled down to 50 °C at rate 20 °C $min^{-1}$.

3.3.3.4.Fourier transform infrared spectroscopy (FTIR)

The chemical structure of the polymeric membranes was characterized by Fourier Transform Infrared (FTIR) spectroscopy by using NICOLET 6700s (Thermo Electron Corporation, USA) with a DTGS detector, under the range of 4000-400 $cm^{-1}$ at a resolution 2.5 $cm^{-1}$.

## 3.4.Results and discussion

### 3.4.1. Effect of PEG 200 addition on Matrimid® membranes for $CO_2/CH_4$ separation

The separation factors as a function of the operating time for Pure Matrimid® (M0) membrane and its blends with PEG (M1-M5) at different ratios are shown in **Figure 3.2**. A similar behaviour of Matrimid® and its blends was observed until reach the steady-state. The initial separation factor values were higher and a continuous decrease was showed with time until reaching the steady-state. Pure Matrimid® membrane presented its steady-state after first 20 min approximately. All blend membranes (M1 to M5) presented their steady-state after 70 min.

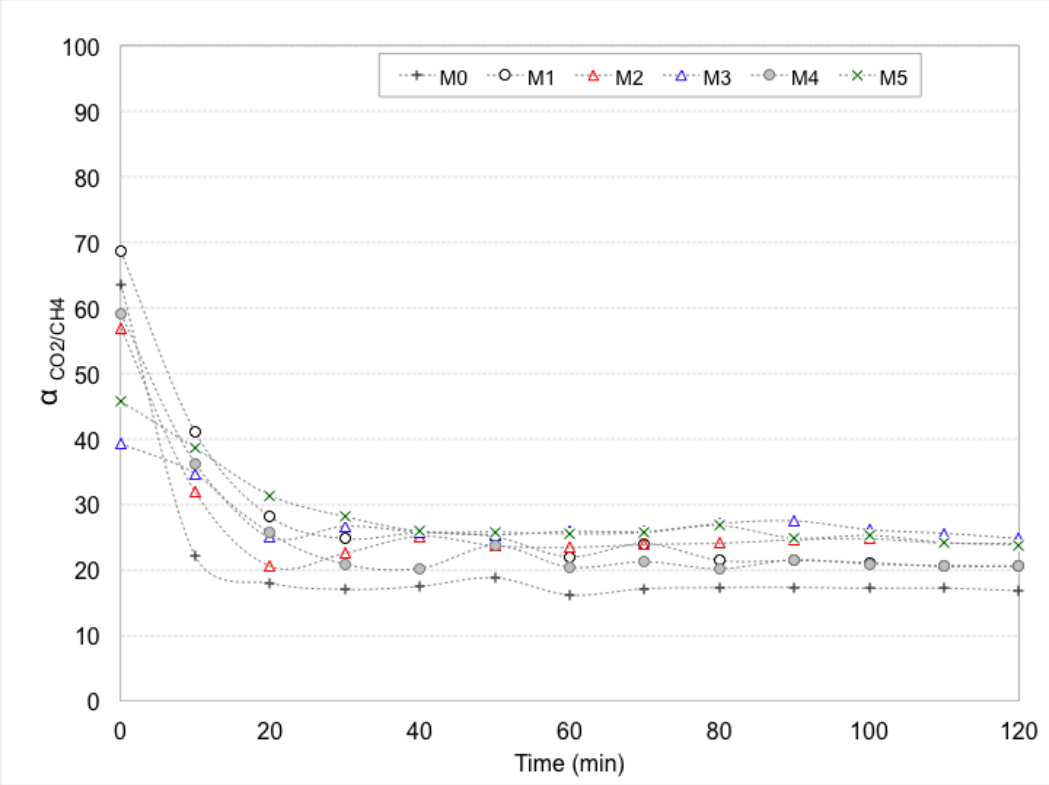


**Figure 3.2.** $CO_2/CH_4$ separation factor as a function of the operating time for pure Matrimid® membrane and its blends with PEG.

Generally, the use of PEG in Matrimid® tends to reach the steady-state after longer time. It can be seen as the amount of PEG increase (from M5 to M1), the stabilization period is longer. This can be supported because the increase of PEG contents enhanced the segmental motions of the polymer, it means, an increasing of chain mobility that results in enhanced transport of all gases [81]. As separation factor displayed, similar behaviour from the stabilization period point of view was observed in $CO_2$ permeability for all membranes (see **Figure 3.3**) but the trend in the values is opposite, the initial $CO_2$ permeability started to increase as a function of the operating time up to achieve the stable value. This tendency has been also well documented in literature for Matrimid® membranes in single $CO_2$ permeability [82,83]. The increase of the $CO_2$ permeability during operating time cannot be attributed by the presence of plasticization phenomenon [84], which is the swelling of the polymer matrix caused by condensable gases (like $CO_2$, propylene); basically, the plasticization increase the segmental mobility and free volume in the matrix membrane resulting in the increase of permeability [85]. But pure Matrimid® membrane cannot present plasticization under pressure 11-12 bar as is well documented [86].

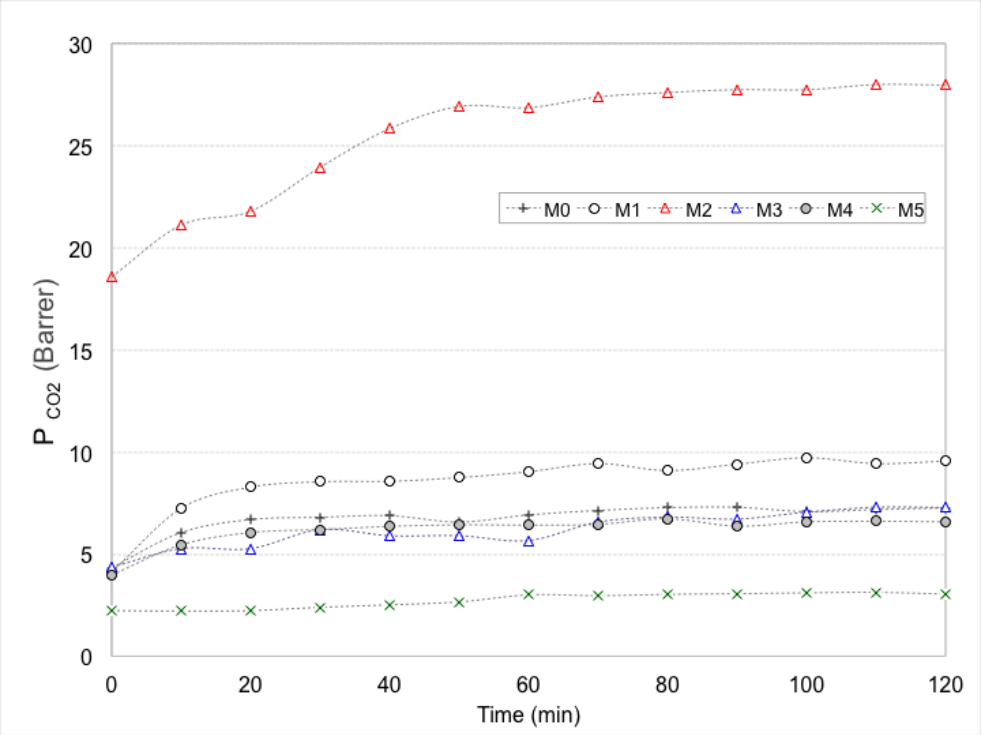


**Figure 3.3.** $CO_2$ permeability as a function of the operating time for pure Matrimid® and its PEG blend membranes.

**Table 3.2** shows the permeabilities and separation factor values of pure Matrimid® membrane and its blends with PEG at steady-state for feed $CO_2/CH_4$ (50:50) binary mixture at 8 bars. The separation factor for pure Matrimid® is lower (17.40) than reported by Loloei *et al.* [72] about 34, which was expected because our experiments were carried out in gas binary mixture where the presence of one component influences the permeation behavior of the other components in the mixture [13]. For example, Khan *et al.* [87] reported in $CO_2/CH_4$ binary mixture a separation factor of 16 for Matrimid membranes, a value close to our findings. In addition, all blend membranes showed an enhancement of separation factor.

On the other hand, our $CO_2$ permeability values for pure Matrimid® (7.16 Barrer) were closed to the one reported by Loloei 's study (about of 7.68 Barrer). The novelty of this work can be highlighted on formulation M2 which demonstrated an increase of $CO_2$ permeability (up to 27.54 Barrer) compared to pure Matrimid®, it means, an enhancement around of 284 % in $CO_2$ permeability was observed. At 5 % of PEG 200, Loloei *et al.* [72] demonstrated an improvement of 25 % in $CO_2$ permeability (from 7.68

to 9.62 Barrer). In case of our formulation M1 (5 % PEG) displayed similar increase on permeability (from 7.16 to 9.38 Barrer) but an enhancement approximately about 31% was observed. However, the formulation M2 (96:4) can be considered as the best one because it showed an enhancement on separation factor to 24.32 from 17.40 reached for pure Matrimid®. This enhancement is attributed to the high $CO_2$ solubility in PEG associated to the dipole-quadrupole interactions between the additive and $CO_2$ [76,88].

As part of the addition of PEG into Matrimid® matrix, formulation M2 also showed an increase on $CH_4$ permeability caused by increasing on chain mobility in PEG presence which results in enhanced transport all gases [81]. Finally, our contribution confirmed Loloei's hypothesis about the addition of PEG at low content (5 %) into Matrimid® membranes improve the $CO_2$ permeability and $CO_2/CH_4$ selectivity. However the highest content of PEG 200 not always guarantees the highest performance, the addition of PEG 200 at 4 % even demonstrated stronger performance in $CO_2/CH_4$ binary mixture separation highlighting the amazing $CO_2$ permeability.

**Table 3.2.** Permeabilities and $CO_2/CH_4$ separation factor for Matrimid®/PEG 200 blend membranes at steady-state (at feed composition 50:50, 8 bar).

| Membrane | $P_{CO2}$ (Barrer)* | $P_{CH4}$ (Barrer)* | α ($CO_2/CH_4$) |
|---|---|---|---|
| M0 | 7.16 ± 0.25 | 0.42 ± 0.04 | 17.40 ± 2.57 |
| M1 | 9.38 ± 2.22 | 0.43 ± 0.12 | 22.91 ± 3.30 |
| M2 | 27.54 ± 3.58 | 1.12 ± 0.06 | 24.32 ± 1.92 |
| M3 | 7.04 ± 2.24 | 0.28 ± 0.15 | 29.12 ± 3.18 |
| M4 | 6.37 ± 0.43 | 0.30 ± 0.02 | 22.06 ± 0.96 |
| M5 | 3.05 ± 0.65 | 0.12 ± 0.02 | 25.08 ± 0.48 |

*Data represents the means ± standard deviation in triplicate.
1 Barrer = 1 x $10^{-10}$ $cm^3$ (STP) cm $cm^{-2}$ $s^{-1}$ $cmHg^{-1}$

M2 was the blend membrane that displays the best performance, **Table 3.3** shows the performance of this blend membrane under different feed composition and pressures. It was noted that at feed composition 25:75 ($CO_2$:$CH_4$) the $CO_2$ permeability decreased

with the increase of pressure. This behavior was previously reported by Bos *et al.* [89] and Bos *et al.* [85]. They observed this trend at low total pressures (<12 bar). At the partial $CO_2$ pressures between 8-10 bar, Bos *et al.* [85] reported that this polyimide tends to present its $CO_2$ plasticization. Indeed, the decrease of $CO_2$ permeability as a function of pressure influences directly on the separation factor. In case of the feed composition 75:25, the major presence of the $CO_2$ in the feed mixture leads to promote high $CO_2$ permeability [90]; however, it is also clear that the $CO_2$ permeability decreased as pressure increase up to 6 bar, while at 8 bar it can be seen an abrupt increase of $CO_2$ permeability. This phenomenon has been reported in Matrimid hollow fibers by Sridhar *et al.* [90].

Finally, high concentrations of $CO_2$ in the mixtures (75:25) tend to obtain even more $CO_2$ permeability contributing to increasing the separation factors as well. Concerning to the partial $CO_2$ plasticization pressure, we guess that PEG could promote the plasticization at partial $CO_2$ pressure of 6 bar (75:25).

**Table 3.3.** Permeabilities and $CO_2/CH_4$ separation factor for M2 blend membrane at different feed composition and pressure (at steady-state).

| Feed composition ( $CO_2$:$CH_4$ ) | Pressure (bar) | $P_{CO2}$ (Barrer)* | $P_{CH4}$ (Barrer)* | α ($CO_2/CH_4$)* |
|---|---|---|---|---|
| 25:75 | 2 | 27.23 ± 0.50 | 1.66 ± 0.13 | 16.41 ± 1.43 |
| | 4 | 22.88 ± 0.36 | 1.24 ± 0.08 | 18.51 ± 1.22 |
| | 6 | 20.95 ± 0.45 | 1.31 ± 0.15 | 16.08 ± 1.96 |
| | 8 | 18.98 ± 0.94 | 1.34 ± 0.15 | 14.34 ± 2.09 |
| 75:25 | 2 | 30.84 ± 1.03 | 1.22 ± 0.11 | 25.32 ± 2.23 |
| | 4 | 25.09 ± 1.88 | 0.98 ± 0.10 | 25.57± 2.34 |
| | 6 | 22.74 ± 0.37 | 0.83 ± 0.07 | 27.34 ± 2.82 |
| | 8 | 31.82 ± 1.06 | 2.13 ± 0.26 | 15.08 ± 2.19 |

*Data represents the means ± standard deviation in triplicate.
1 Barrer = 1 x $10^{-10}$ $cm^3$ (STP) cm $cm^{-2}$ $s^{-1}$ $cmHg^{-1}$

### 3.4.2. Blending of Matrimid® with other secondary materials for improving its $CO_2$ permeability: Comparison with other works

Last decade, researchers have been focused on the enhancing of Matrimid® for increase its $CO_2$ permeability, where its blending with different agents (polymers, additives) has been widely developed. **Table 3.4** summarizes the most recent studies of Matrimid® blending aimed in aforementioned subject. According to the recent results, the blending of Matrimid® polymer with PEG, PIM-1, and S-PEEK has been demonstrated, increase of $CO_2$ permeability around 25 % [72], 118-483 [32,33], and 31 % [87] were reported, respectively. This work showed also a considerable increasing of $CO_2$ permeability using low amount (4 %) of PEG 200. On the contrary, the Matrimid® blending not always lead to improve the property, i.e., Hosseini & Chung [91] reported a reduction around 70% on $CO_2$ permeation in Matrimid®/PBI blend (1:1) compared to Pure Matrimid®. This tendency was also observed in our study in the case of samples M3, M4 and M5, which presented a decrease in $CO_2$ permeability and underline the need of optimization of additive content in the blend. Finally, it is important to note that the use of a small amount of cheap additive like PEG 200 can promote the effect better than other significantly expensive polymers such as PIM-1 or S-PEEK, this gives a promising outlook on the potential of this blend for $CO_2$ capture by membrane technology.

**Table 3.4.** Blending of Matrimid® with other secondary materials aimed to improve $CO_2$ permeability.

| Blend | Blend ratio (%) | Operating conditions: | Percent of improvement: | Reference: |
|---|---|---|---|---|
| Matrimid®/PEG 200 | 96:4 | $CO_2/CH_4$ binary mixture (1:1), 8 bar, 25 ºC | 258 % (27.54 Barrer) | This work |
| Matrimid®/PEG 200 | 95: 5 | Single gas permeation for $CO_2/CH_4$, 10 bar, 35 ºC | 25 % (9.62 Barrer) | [72] |
| Matrimid®/PIM-1 | 70:30 | $CO_2/CH_4$ binary mixture (1:1), 7 atm, 35 ºC | 483 % (56 Barrer) | [32] |
| Matrimid®/PIM-1 | 85:15 | $CO_2/CH_4$ binary mixture (1:1), 2 atm, 25 ºC | 118 % (21 Barrer) | [33] |
| Matrimid®/S-PEEK | 70:30 | $CO_2/CH_4$ binary mixture (1:1), 8 bar, 25 ºC | 31 % (10 Barrer) | [87] |
| Matrimid®/PBI | 50:50 | Single gas permeation for $CO_2/CH_4$, 10 atm, 35 ºC | -70 % (2.1 Barrer) | [91] |

### 3.4.3. Membrane characterization

The glass transition temperatures ($T_g$) for our pure Matrimid® membranes were around 310 ºC (see **Table 3.5**), similar to the values well documented until now [51,72]. During the addition of PEG into polymeric membranes there is a free volume increase; a decrease in density and $T_g$ temperature are generally observed [76]. However, all blend membranes (Matrimid®-PEG 200) presented a slight increasing on $T_g$ values (313-315 ºC). He *et al.* [92] reported the increasing $T_g$ values of Chitosan films by adding PEG. This slight increase of $T_g$ could be associated to PEG addition because during the addition of polar groups (i.e. hydroxyl groups from PEG) to a polymer can increase the polymer cohesive energy and, in turn, chain rigidity [93,94]. This shift on the property can offer a clear overview about the good miscibility of the blends [72].

**Table 3.5.** $T_g$ values determined for Matrimid® and its blend membranes

| Membrane | Tg value ( ºC) |
|---|---|
| M0 | 310.14 ± 0.22 |
| M1 | 314.76 ± 1.64 |
| M2 | 313.60 ± 2.11 |
| M3 | 315.80 ± 1.59 |
| M4 | 313.17 ± 0.27 |
| M5 | 313.02 ± 0.20 |

*Data represents the means ± standard deviation with triplicate for each membrane.

The TGA curves of pure Matrimid® and its blend membranes are shown in **Figure 3.4**, where was revealed a ~10 % weight loss starting from 50 up to 300 ºC for pure Matrimid® membrane. While, all blends showed the same behaviour up to 250 ºC but they increased the weight loss to ~15 % at 300 ºC. This typical thermal behavior of

Matrimid® membranes has been documented before [95] where the weight loss is generally attributed to the presence of residual solvent or guest molecules [28].

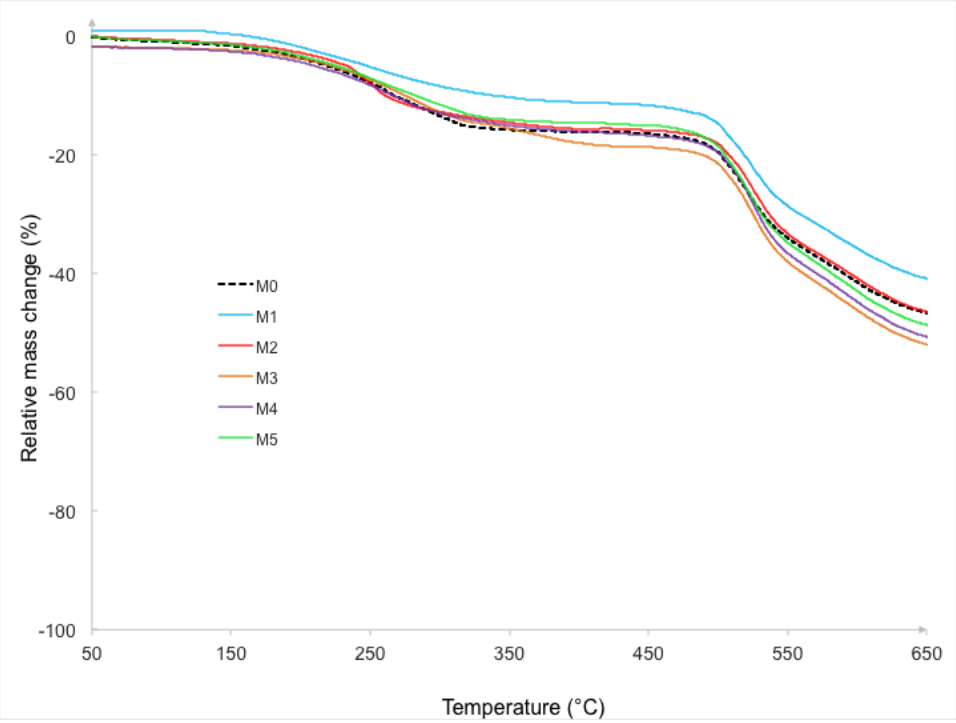


**Figure 3.4**. TGA profiles of Matrimid® and its blends with PEG 200.

The pure Matrimid® and its blend membranes presented good thermal stability. The pure Matrimid® membranes were stable up to ~470 ºC; however, blend membranes exhibit a slightly better thermal stability up to ~500 ºC. These results showed that the addition of PEG can promote the thermal stability of polymeric membranes. This was demonstrated at least at low PEG 200 concentrations in Matrimid.

**Figure 3.5** demonstrates the FTIR spectra for all the membranes, to identify any possible changes in the Matrimid's characteristic functional group peaks after addition of PEG 200. Basically, Matrimid® (M0) is characterized by the C=O carbonyl group bands at 1777 $cm^{-1}$ and 1714 $cm^{-1}$, for both symmetric and asymmetric stretching associated to the imide ring carbonyl (ketonic group), and 1671 $cm^{-1}$ and 1618 $cm^{-1}$ which define the symmetric and asymmetric stretching of benzophenonen carbonyl (imidic group) [51]. The aliphatic C-H stretching is ascribed by the peaks at 2850 and 2950 $cm^{-1}$, while C-H aromatic ring stretching can be seen at ≈3000 $cm^{-1}$. Furthermore, the typical amine stretching vibrations related to the N-H bonds are positioned at 1350 and 3500 $cm^{-1}$.

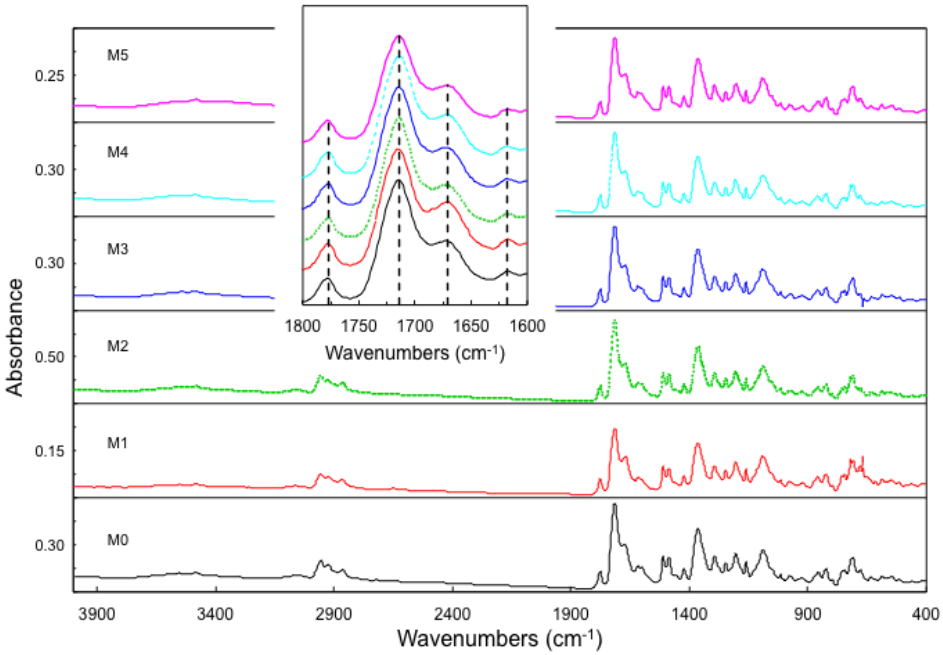


**Figure 3.5**. FTIR spectra of Matrimid® and its blends with PEG 200.

It is evident that the only possible interaction occurring between Matrimid® and PEG is hydrogen bonding between the oxygen and nitrogen atoms in Matrimid®'s carbonyl and imide groups and the hydrogen atom of terminal hydroxyl groups in the short-chain PEG [72,96]. In this framework, a slight downward shift (less than 3 $cm^{-1}$) in the imide C=O stretching bands was observed in the blended membranes as a clear indication of H-bonding presence after the PEG addition. Additionally a secondary imide C=O peaks (both symmetric and asymmetric stretching) were witnessed in the blended M1 membrane at 1683 $cm^{-1}$ and 1636 $cm^{-1}$, upward shift from 1671 $cm^{-1}$ and 1618 $cm^{-1}$ in Matrimid®. The shift may be attributed to the stronger H-bonding which may have occurred between the PEG at the highest loading and the highly electronegative nitrogen atom in Matrimid®, which is an effective electron donor and acceptor. Furthermore, the presence of this hydrogen bonding is in agreement with the discussed thermal properties enhancement.

Regarding the effect of PEG 200 on Matrimid® membrane morphology, **Figures 3.6A** and **B** show the surface and cross-section SEM images of some prepared

membranes. Pure Matrimid® membrane displayed a uniform and smooth surface characteristic without signs of plastic deformation, which is common for dense polymeric membranes [86,97]. A strong crater-like pattern, also well documented by Loloei *et al.* [72], was observed in cross-section view of pure Matrimid membrane. This pattern was dissipated by the addition of PEG 200. Except membrane M1 (highest content of PEG in our measured set) for all blend membranes the smooth and clean surface has been obtained too. The M1 membrane showed a not complete dissolution of PEG in polymer matrix. According to Loloei *et al.* [72], as the PEG content increases, the miscibility between the polymers can be reduced.

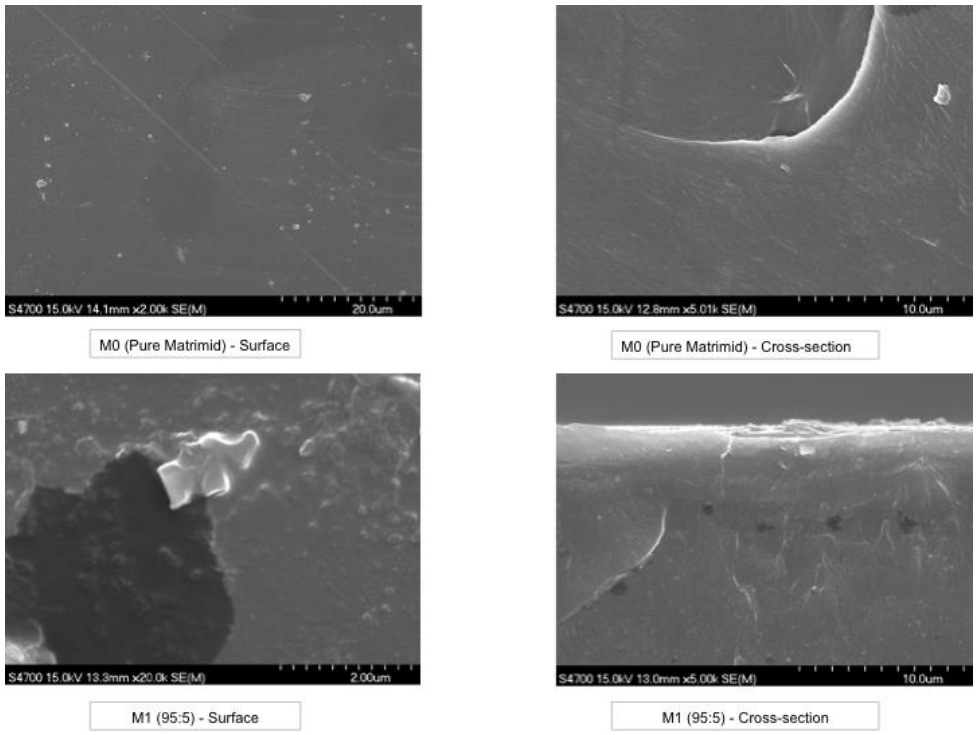


**Figure 3.6.A.** SEM images of pure Matrimid® and its blends with PEG 200.

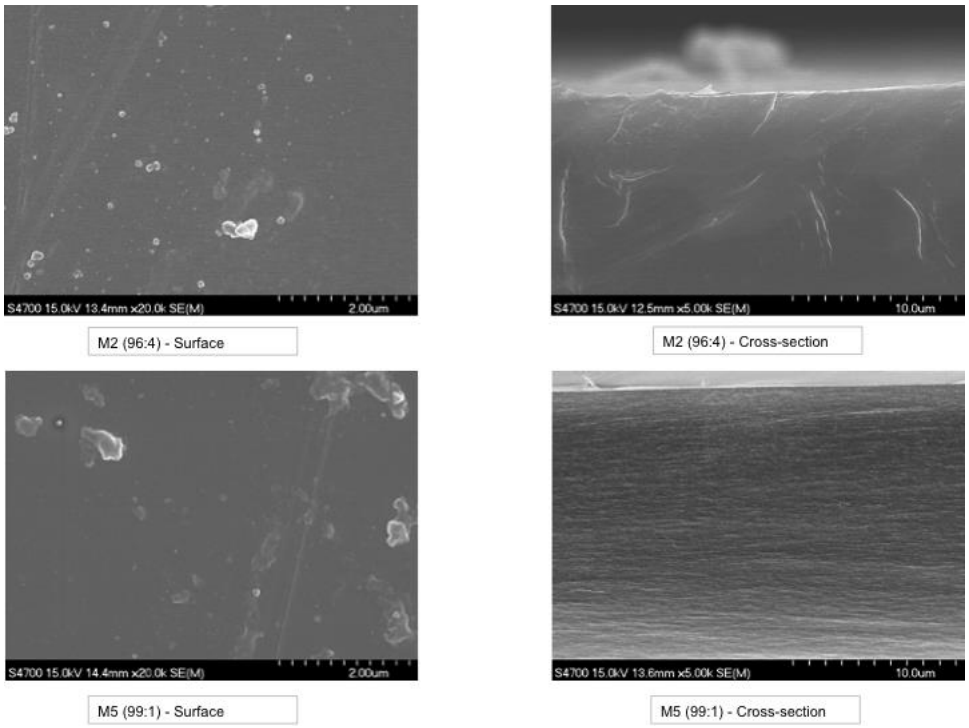


**Figure 3.6.B**. SEM images of pure Matrimid® and its blends with PEG 200.

### 3.4.4. Promising framework of the use of PEG in Matrimid® membranes to $CO_2$ capture

Today, it is well known that carbon dioxide is one of the major greenhouse gases responsible for global warming [74]. There are several sources for $CO_2$ production such as natural matter decomposition, ocean release, biochemical processes, and human production coming from industrial processes where burning of fossil fuels (oil, natural gas) is usually employed [98,99]. The latter source has been confirmed as the major source of emission of this greenhouse gas for the high electrical energy demand, i.e., in USA alone, the recent report of its current demand (May, 2016) is of around 317, 739 thousand megawatts/hour [100]. The EIA estimates that demand for electricity will increase up to 40% in the U.S. in coming 25 years.

Currently, $CO_2$ capture and utilization have attracted remarkable attention from the scientific community due to its major impacts to our environment. Attending to this task, there are different $CO_2$ capture technologies that have been employed in post-combustion gas treatment such as amine-based systems, carbonated-based systems, aqueous ammonia systems, enzyme-based system, $CO_2$ capture absorbents, ionic liquid systems, and physical separation by membrane technologies [101]. Membrane gas

separation has been recognized as an emerging technology for $CO_2$ capture, where, membrane engineering is very focusing on developing new membranes which demonstrate excellent performance for $CO_2$ sequestration. Our contribution already demonstrated the potential performance of Matrimid® $CO_2$ separation from other gases like $CH_4$; highlighting the promising and synergistic performance that PEG 200 produces in Matrimid® polymer matrix. It is important to note how a small amount of conventional additive like PEG can enhance more than 3-fold the $CO_2$ permeability of Matrimid® being as competitive as other polymer blends which are economically less feasible [32]. This work in agreement with Loloei's study shows strong evidence of this promising blend for future developments, where membrane-based technology for $CO_2$ capture is closer to be applied at industrial level with the testing of lab-scale membranes by gas binary mixtures [102].

### 3.5.Chapter summary

The Matrimid® blending with low contents of PEG 200 (0-5 %) was successfully applied for the preparation of dense membranes, and concluded with the following statements:

- Good interaction between the Matrimid®-PEG 200 has been demonstrated by using FTIR, DSC, SEM and TGA analysis. In addition, thermal properties enhancement of Matrimid® through the addition PEG 200 was confirmed.
- The addition of 4 and 5 % of PEG 200 improved the $CO_2$ permeability of pure Matrimid® membrane. Particularly, the 96 % Matrimid®, 4% PEG 200 blend membrane showed the best separation performance with the highest $CO_2$ permeability improvement (more than 3-fold) and 39 % higher $CO_2/CH_4$ separation.
- The potential of the proposed blend was discussed and confirmed by comparison with other recent studies.

# *Chapter 4*

## Matrimid®5218 mixed matrix membranes for separating binary $CO_2/CH_4$ mixtures using MOFs

### Chapter overview

In chapter 3 already the promising results in enhancement of the Matrimid® 5218 performance in $CO_2/CH_4$ separation has been reached by PEG-200 addition. As discussed in chapter 2 the synergetic effect of ternary MMMs components would be also expected. In this chapter the effect of combined additions of a $CO_2$-philic additive (PEG 200) and ZIF-8 nanoparticles in to Matrimid® 5218 on $CO_2$ permeability and membrane selectivity is studied. In this way, we used the best blend membrane containing 4% PEG as main continuous polymeric phase in the preparation of ternary MMMs. ZIF-8 nanoparticles were selected as the third phase of the ternary membranes. The synthesis procedure of this metal-organic framework, like ZIF-8, was also given. The chapter also reports the preparation procedure to obtain well-dispersed filler by solvent exchange method.

### 4.1. Introduction

Matrimid® 5218 is one of the most used polyimides (PI) applied as continuous matrix for membrane gas separation [28,55,103]. It is commercially available and has been extensively studied but it is still studied today due to many advantages such as excellent thermal and mechanical properties, high solubility in organic solvents, and good processability in membrane preparation [104,105]. This PI presents high selectivity for $CO_2/CH_4$ [28,34,35,51]; but it has poor performance in terms of $CO_2$ permeation. Different types of approaches have been tested in order to improve the $CO_2$ permeation of Matrimid® 5218, such as blending with other polymers [33,72], structure modification by cross-linking [106], pyrolysis [107], and generation of mixed matrix membranes (MMMs) [13,28]. MMMs, well-defined as the dispersion of organic-inorganic particles (filler) into a continuous polymeric matrix [9], can be found as the current development for facing the limitation of Matrimid® 5218. Different types of fillers have been incorporated into this PI matrix such as MOF-5 [34], ZIF-8 [28], $[Cu_3(BTC)_2]$ [35], ZSM-5 [46], zeolite 4A [41], MIL-53 [51], and titanosilicates (TS-1, ETS-10) [45], to mention just a few studies. In Chapter 3 of this thesis, we demonstrated that the addition of low molecular weight polyethylene glycol (PEG) at 4% into Matrimid® 5218 is able to increase considerably the $CO_2$ permeability (from 7.16 to 27.54 Barrer) coupled with slightly increasing on $CO_2/CH_4$ separation factor (from 17.40 to 24.32). We chose this promising blend to generate MMMs, with the attempt to increase the $CO_2$ permeability of the pristine polymer. Thereby, ZIF-8 nanoparticles have been chosen as the inorganic dispersed phase. The aim of this work was to prepare ternary MMMs based on Matrimid® 5218, PEG 200 and ZIF-8 nanoparticles, highlighting that there is no report until now about the preparation of these proposed formulations. The membranes were prepared by dense film-casting method at low PEG concentration (4 wt.%) and different filler loadings (10, 20, 30, and 40 wt.%). The membranes were tested for $CO_2/CH_4$ binary mixture at a fixed feed composition (50:50) and different pressures (from 2 to 8 bar). The MMMs were characterized by differential scanning calorimetry (DSC), thermo-gravimetric analysis (TGA), scanning electron microscopy (SEM) and energy dispersive X-ray spectroscopy (EDX). Finally, binary mixed matrix membranes (Matrimid® + ZIF-8) were also prepared in order to visualize clearly the influence of the addition of PEG in the MMMs.

## 4.2.Materials and methods

### 4.2.1. Materials

The used materials for the membrane synthesis are the same that the ones specified in the **Chapter 3**, section 3.2.1. For the ZIF-8 nanoparticles synthesis, methanol, $Zn(NO_3)_2.6H_2O$ and 2-methylimidazole were purchased from Sigma-Aldrich (Czech Republic).

### 4.2.2. Synthesis of ZIF-8 particles

The ZIF-8 nanoparticles were produced according to the methodology reported by Diestel *et al.* [38]. 1.03 g of $Zn(NO_3)_2.6H_2O$ was dissolved in 70 mL of methanol, then solution was added to 70 mL of a stirred 2-methylimidazole solution (70 mL of methanol with 2.07 g of 2-methylimidazole). After 1 h the nanoparticles were collected by centrifugation, washed with NMP. The nanoparticles were characterized by SEM and XRD (**Figure 4.1.A** and **B**). The images with 100k magnification were analyzed using NIS elements AR v3.00, SP6® software. The particle sizes were recorded and a mean particle size of 33.83±6.2 nm calculated.

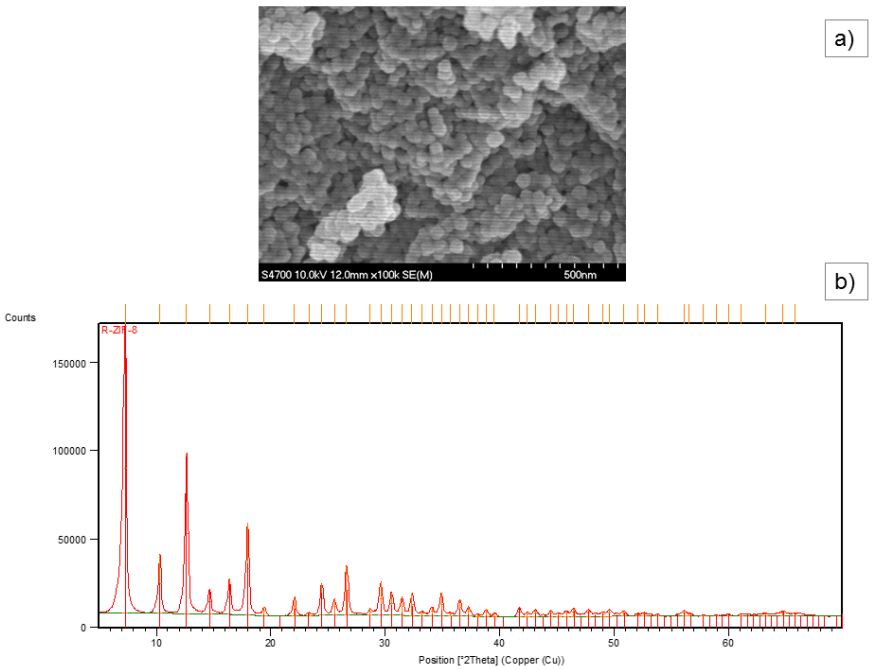


**Figure 4.1.** a) SEM images and b) XRD pattern of the synthesized ZIF-8 used in this study.

### 4.2.3. Methodologies

### 4.2.4. Membrane preparation

In order to remove any moisture the Matrimid® 5218 was dried overnight in oven at 120 ºC. The dope solutions were prepared in NMP to form a 10 wt.% solution. The pure Matrimid®, Matrimid®/PEG 200, and Matrimid®/PEG 200/ZIF-8 membranes were prepared in triplicate using the dense film-casting method. The ratio for each formulation is shown in **Table 4.1**.

**Table 4.1.** Polymer solution composition of the mixed matrix membranes

| Polymer solution (10 wt.%) |
|---|
| Pure Matrimid® |
| Matrimid®-PEG (96:4) |
| Matrimid® + 10 wt.% ZIF-8 |
| Matrimid® + 20 wt.% ZIF-8 |
| Matrimid® + 30 wt.% ZIF-8 |
| Matrimid®+ 40 wt.% ZIF-8 |
| Matrimid®-PEG (96:4)+ 10 wt.% ZIF-8 |
| Matrimid®-PEG (96:4)+ 20 wt.% ZIF-8 |
| Matrimid®-PEG (96:4)+ 30 wt.% ZIF-8 |
| Matrimid®-PEG (96:4)+ 40 wt.% ZIF-8 |

The specific amount of the filler was determined according to Eq. (1) [42]:

$$ZIF\ \ loading \quad wt\ \ \% = \left[ \frac{wt\ \ ZIF}{wt\ \ ZIF\ +\ wt\ \ polymer} \right] x\ 100 \quad (wt\ \ \%) \qquad (1)$$

The polymer solutions were mixed and stirred for 24 h, separately; the specific amount of the filler was dissolved and stirred in 5 mL of NMP for 24 h then sonicated for

90 min. After this time, 15 % of polymer solution was added to filler solution and stirred for 4 h then sonicated for 90 min; the procedure was performed up to the total incorporation of the polymeric solution into final dope solution. The final solution was allowed stirring for 12 h at room temperature. A glass plate was used for casting. The membranes were prepared by solvent evaporation in an oven at 40 ºC for 24 h. The formed membrane was immersed in a small amount of deionized water to peel the membrane away from glass. Then, membranes were dried at 40 ºC in an oven for 24 h [10].

### 4.2.5. Membrane characterization

Regarding the characterization of these MMM membranes, the carried out DSC and TGA analysis are the same as reported in **Chapter 3**. Especially, SEM was particularly used for analyzing the ZIF-8 particle size distribution, while the XRD diffraction was employed for the ZIF-8 patterns.

#### 4.2.5.1.Scanning electron microscopy (SEM)

The SEM procedure for determination of morphology of prepared membrane was similar that the one described previously, but the membranes were also characterized by energy dispersive X-ray spectroscopy (EDX), to map the zinc distribution and thus visualize the particles distribution across the membrane.

#### 4.2.5.2.X-ray diffraction (XRD)

Prepared ZIF-8 particles were characterized by XRD analysis. X-ray powder diffraction data were collected at room temperature with an X'Pert PRO θ-θ powder diffractometer with parafocusing Bragg-Brentano geometry using CoKα radiation (λ = 1.79028 Å, U = 35 kV, I = 40 mA). Data were scanned with an ultrafast detector X'Celerator over the angular range 5-60° (2θ) with a step size of 0.017° (2θ) and a counting time of 20.32 s $step^{-1}$. Data evaluation was performed in the software package HighScore Plus 4.0. [45].

### 4.2.6. Gas binary mixture separation

The efficiency of pure Matrimid® membranes and its ternary MMMs in $CO_2/CH_4$ binary mixture separation was determined at 25 °C using the permeation unit reported in the

**Chapter 3** (Figure 3.1.) [79]. Similarly, the calculation procedures in terms of $CO_2$ permeability and separation factor are the ones previously described in this chapter.

## 4.3.**Results and discussion**

### *4.3.1. Membrane characterization*

Pure Matrimid® membranes present a glass transition temperature ($T_g$) around 310 ºC (**Table 4.2**), which is in agreement with Dorosti *et al.* [51] and Loloei *et al.* [72]. ZIF-8 nanoparticles lead to provide a higher glass transition temperature of membranes based on Matrimid®; the incorporation of the MOF into Matrimid® matrix increased the $T_g$ values of the generated binary and ternary MMMs (from 310 up to 371 ºC). Zhang *et al.* [86] reported also this $T_g$ variation (from 317 up to 340 ºC ) for 30 wt.% mesoporous ZSM-5-Matrimid® MMMs. Likewise, the increase of $T_g$ suggests a good interaction between ZIF-8 particles and the polymeric matrix restricting the polymer chain mobility which leads to the rigidity and the increment of the $T_g$ [12].

The TGA graph of pure Matrimid® and MMMs are depicted in **Figure 4.3**. Matrimid® membrane showed a first weight loss ~3 % which can be attributed moisture evaporation. Lately, a second weight loss (~13 %) starting from 150 up to ~350 ºC was observed, it revealed the evaporation of rests of solvent. A third weight loss was started at 520 ºC and ended at 670 ºC, where the chains of polyimides can undergo thermal degradation and exhibit the decomposition of the polymer fractions with imide groups [108]. This typical behavior of Matrimid® membranes has been documented before [45,95].

**Table 4.2.** $T_g$ determination for Matrimid®, Matrimid®-PEG, binary and ternary MMMs.

| Membrane | Tg value ( ºC) |
|---|---|
| Pure Matrimid® | 310.14 ± 0.22 |
| Matrimid®-PEG (96:4) | 313.60 ± 2.11 |
| Matrimid® + 10 wt.% ZIF-8 | 371.57 ± 0.04 |
| Matrimid® + 20 wt.% ZIF-8 | 372.98 ± 1.11 |
| Matrimid® + 30 wt.% ZIF-8 | 371.45 ± 0.14 |
| Matrimid®+ 40 wt.% ZIF-8 | 371.43 ± 0.09 |
| Matrimid®-PEG (96:4)+ 10 wt.% ZIF-8 | 371.50 ± 0.09 |
| Matrimid®-PEG (96:4)+ 20 wt.% ZIF-8 | 372.44 ± 1.23 |
| Matrimid®-PEG (96:4)+ 30 wt.% ZIF-8 | 371.44 ± 0.09 |
| Matrimid®-PEG (96:4)+ 40 wt.% ZIF-8 | 371.50 ± 0.07 |

*Data represents the means ± standard deviation with triplicate for each membrane.

In the case of ZIF-8 revealed a ~12 % weight loss starting at 120 ºC and continuing up to 320 ºC, which is generally attributed to the presence of residual solvent or guest molecules. Between 370-560 ºC, the decomposition of ZIF-8 occurred; remaining only 35 % of the material after 560 ºC, which can be associated to ZnO [28]. For all MMMs, they presented a higher weight loss (~15 %), from 150 to 300 ºC, than pure Matrimid, which can suggest of more solvent residue is placed. The increase of mobility of the polymer chains by increasing the temperature, it promotes the desorption of the NMP kidnaped between polymer chains [45,52]. After 520 ºC, the MMMs display the highest weight loss associated with the polymer; most of the weight loss of polyimides is induced by the expelling of non-carbon atoms [109].

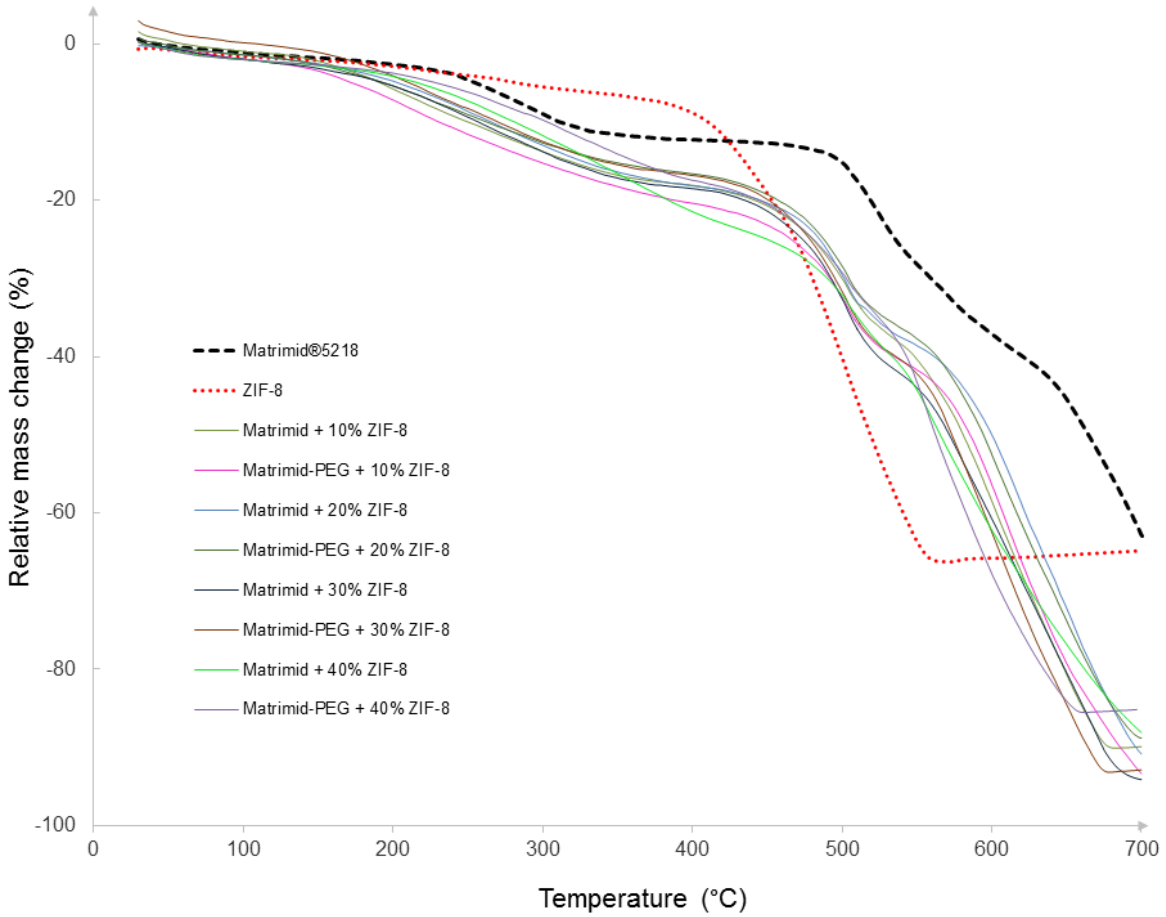


**Figure 4.3**. TGA profiles of the Matrimid®, ZIF-8, binary and ternary MMMs.

Regarding the morphology of the binary and ternary MMMs, SEM images were acquired from the cross-sections of the binary and ternary MMMs with different ZIF-8 loadings. It can be seen that from 10 up to 30 wt. %, the ZIF-8 nanoparticles are well embedded and dispersed (with non-visible agglomeration) into the polymer matrix even though their high loading, wherein there was increased ZIF-8 content. In addition, the homogeneous dispersion of the nanoparticles was also confirmed through the zinc distribution into the MMMs by EDX (**Figure 4.4**). Generally, the nanoparticles present good compatibility with the polymer due to the inorganic-organic nature of the ZIF-8, which can result in an increased interaction with the polymer [28,38].

It is important to highlight that successful incorporation up to 40 wt.% ZIF-8 with a good particle dispersion was achieved. ZIF-8 nanoparticles tend to offer better polymer-particle interfacial contact that can lead to a higher percentage loading in the polymer matrix [28].

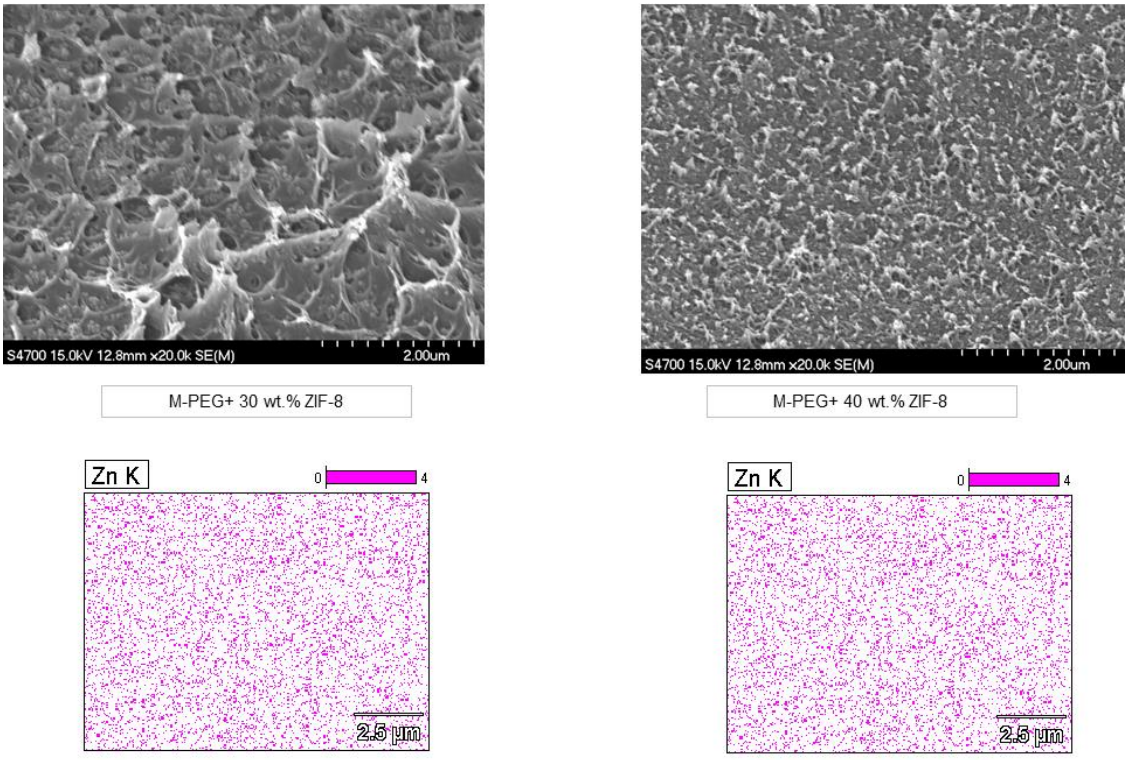


**Figure 4.4**. Cross section SEM images for the ternary mixed matrix membranes at high filler loading. EDX images indicated zinc distribution in the same membranes.

Furthermore, the increase in $T_g$ values suggests also the good dispersion of smaller particles with a good filler-polymer interaction leads to less restriction of the polymer chain mobility [12]. Finally, the PEG in the MMMs tended to form craters in Matrimid® structure but it cannot be seen any influence on particle distribution; it means that the well-dispersed particles are still visible. These characteristic craters have been observed previously in other type of ternary MMMs based on Matrimid®-PEG and ZSM-5 [58].

### *4.3.2. Performance of the binary-ternary MMMs in $CO_2/CH_4$ separation.*

#### 4.3.2.1.Effect of the addition of PEG 200 into Matrimid® and MMMs.

Based on Loloei *et al.* [72] study and our previous study [110], it is demonstrated that PEG 200 at low concentrations (4-5 wt.%) enhances the $CO_2$ permeability in Matrimid® membranes, which is fully attributed to its strong affinity for $CO_2$. The polar ether segments (ethylene oxide units) of PEG can interact positively with $CO_2$ molecules by dipole-quadrupole interactions, leading the transport through the membranes [10,72]. At feed composition 50:50 and pressure 8 bar, the Matrimid-PEG 200 membranes

displayed higher $CO_2$ permeability (27.5 Barrer) value than pure Matrimid membranes (7.1 Barrer) (see **Figure 4.5**).

On the other hand, the incorporation of ZIF-8 nanoparticles (from 10 to 30 wt.%) also enhances considerably the $CO_2$ permeability in Matrimid membranes, which was previously demonstrated by Ordoñez *et al.* [28]. Typically, ZIF-8 tends to increase the permeability in Matrimid due to the increment of the distance between polymer chains resulting in more polymer free volume. Likewise, nanoparticles can disrupt chain packing in glassy polymers leading to increases in polymer free volume and permeability [28,111]. Furthermore, the addition of a porous material increases the diffusivity of the membrane, increasing the overall permeability. For example, the highest $CO_2$ permeability for binary MMMs was observed at 30 wt.% filler loading, which showed up to 31.4 Barrer.

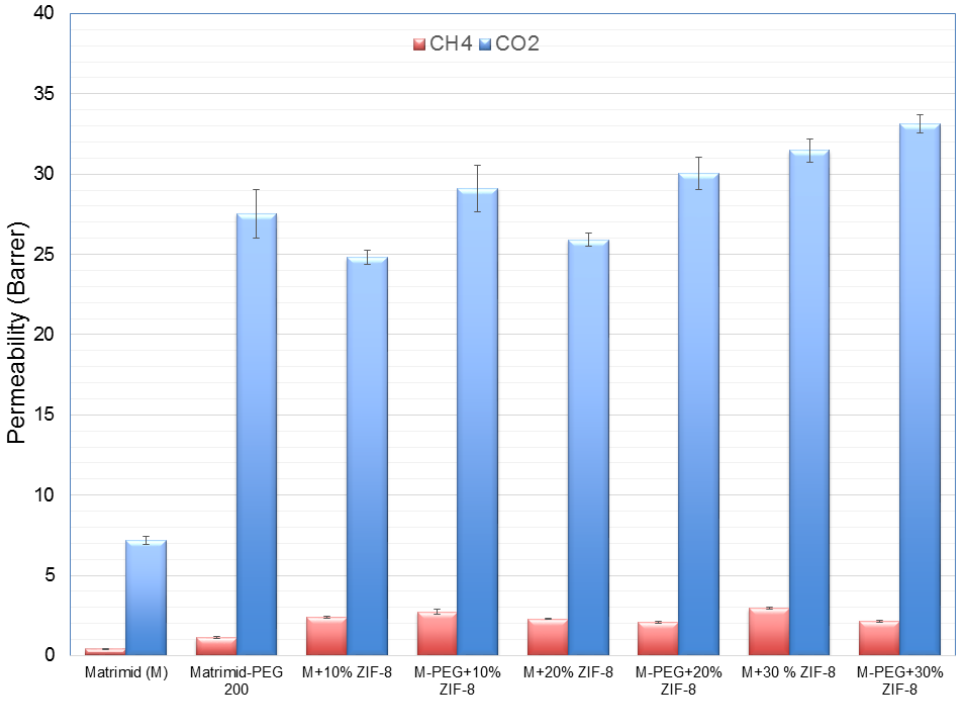


**Figure 4.5.** Permeabilities for pure Matrimid®, Matrimid-PEG, binary and ternary MMMs at steady-state (50:50 $CO_2$:$CH_4$ feed mixture, 8 bar).

The presence of PEG and ZIF-8 demonstrated also a considerable enhancement on $CO_2$ permeability compared to pure Matrimid® membranes, the permeability tended to increase with the filler loading from 10 to 30 wt.% for binary and ternary MMMs. For

the ternary MMMs, the PEG enhanced even more the $CO_2$ permeability for all formulations. In contrast to Matrimid-PEG membranes which demonstrated an enhancement not only on $CO_2$ permeability but also in separation factor (up to 24.3). Most of the binary (Matrimid/ZIF-8) and ternary (Matrimid/PEG/ZIF-8) MMMs showed a slight decrease on separation factor (**Figure 4.6**). This behaviour was noted by Nordin *et al.* [12] too, for MMMs based on polysulfone-ZIF-8. In case of the Matrimid-PEG+ 30 wt.% ZIF-8 membranes maintain the separation factor (15.4) compared to pure Matrimid® (17.4). It is important to highlight that the addition of PEG also results in enhancing local segmental motions of polymer, which significantly increase in $CH_4$ permeability based on enhanced transport of all gases [81].

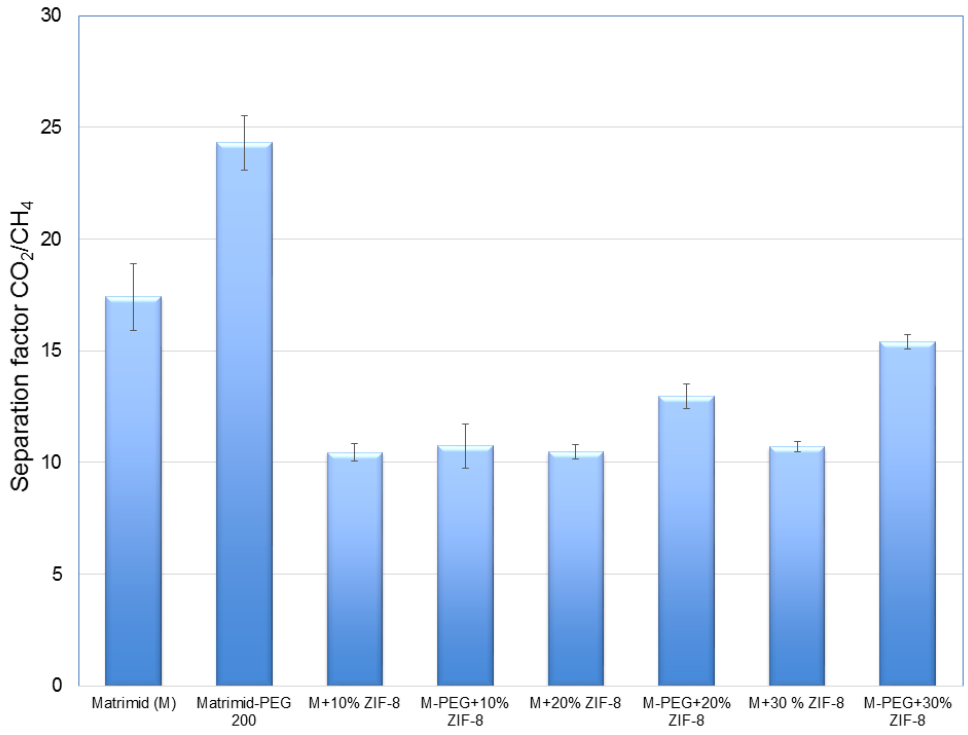


**Figure 4.6.** $CO_2/CH_4$ separation factor for pure Matrimid®, Matrimid®-PEG, binary and ternary MMMs at steady-state (50:50, 8 bar).

Finally, we achieved to incorporate up to 40 wt.% filler loading into Matrimid® matrix; however, it is important to note that we were only able to measure up to 30 wt.%, this is in agreement with Song *et al.* [37]. At higher filler loading, the membranes were fragile and unable to be tested. These amounts of particles (30-40 wt.%) in the polymeric matrix are usually excessive but often being used for gas separation [112]. Such filler loadings tend to rise the tiny defects during the membrane preparation procedure and reduce the integrity of the matrix [113].

4.3.2.2.Effect of feed pressure on gas permeation performance of binary and ternary MMMs.

The $CO_2$ permeability values of the binary and ternary MMMs as a function of feed pressure are provided by Castro-Muñoz et al. [114]. Generally, for all the binary and ternary MMMs membranes at 50:50 $CO_2/CH_4$ feed composition, the $CO_2$ permeability increases abruptly at 8 bar (See **Figure 4.7**). Loloei *et al.* [58] also reported the increase of $CO_2$ permeability by increasing the feed pressure in MMMs based on Matrimid®. In theory, the addition of MOFs tends to suppress the plasticization phenomenon in Matrimid due to restrict the mobility of polymer chain [52]. However, the increase of $CO_2$ permeability in binary and ternary MMMs can be attributed to: *i)* the addition of PEG which has demonstrated that reduces the $CO_2$ plasticization pressure of pure Matrimid® up to 8.1 bar [58], in spite that the plasticization of Matrimid® cannot be recognized up to 10 bar [84,91], *ii)* the gas transport properties can be controlled by MOF particles at high pressures [52] based on their excessive filler content [112], *iii)* the presence of "unselective voids", which clearly lead to increase the permeance and diminish selectivity [12], which is in agreement with our results.

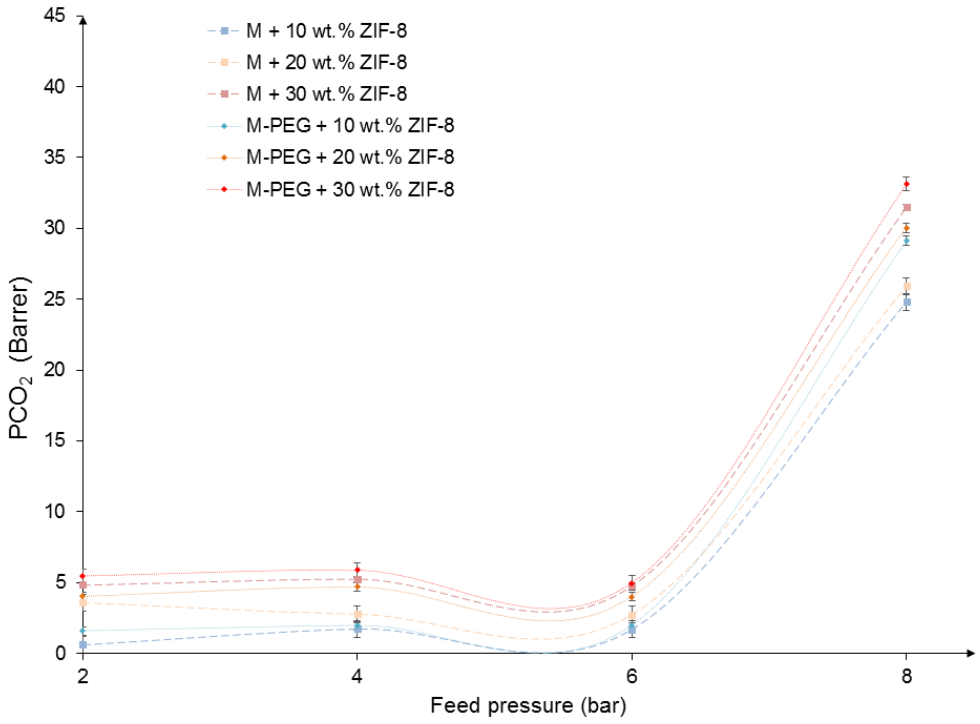


**Figure 4.7.** $CO_2$ permeabilities for binary and ternary MMMs at different feed pressures (50:50). The curves are only guides to the eye.

The $CH_4$ permeability for binary and ternary MMMs (at 50:50 mixture) by increasing the feed pressure tended to decrease slightly the permeability (**Figure 4.8**); based on Loloei *et al*. [58], this can be attributed to the chain rigidification of polymer near the bulk of the filler which remarkably reduces the penetration of gas molecules. The slow diffusion of large gases (like $CH_4$) in the filler plays also an important role [58]. On the contrary, the $CH_4$ permeability increased strongly at 8 bar, and for some membranes. Finally, at 8 bar, the separation factor was around 10-16 for all MMMs.

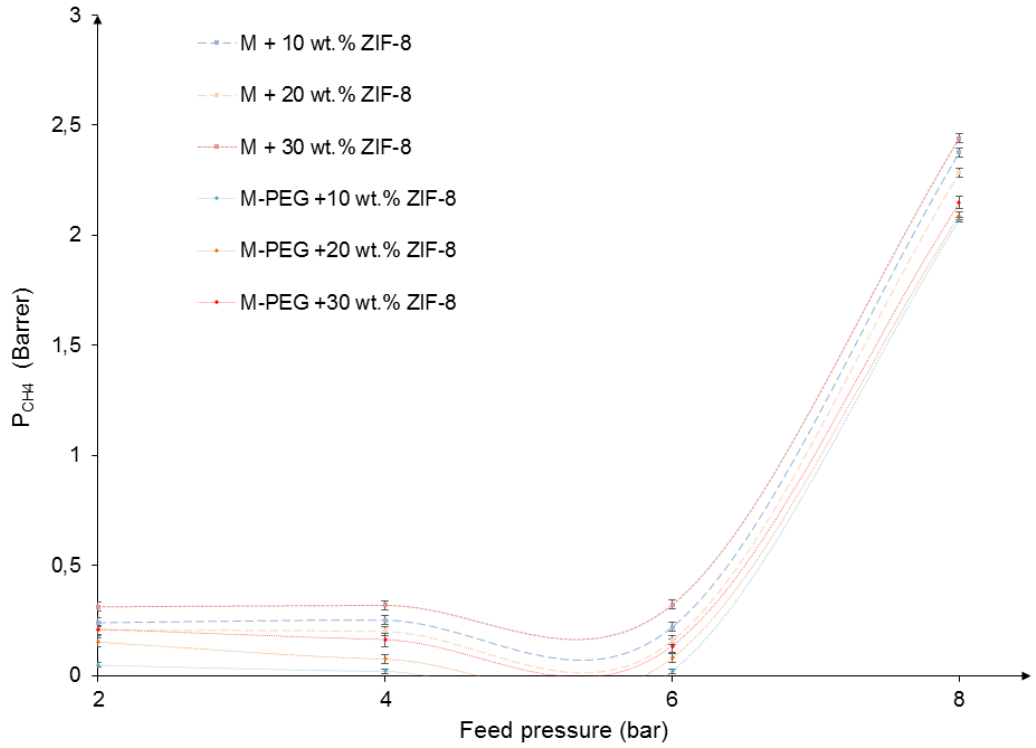


**Figure 4.8.** $CH_4$ permeabilities for binary and ternary MMMs at different feed pressures (50:50). The curves are only guides to the eye.

4.3.2.3.Status of Matrimid®-PEG, binary and ternary MMMs on Robeson trade-off.

As it is well known the correlation between the separation factor and permeability was established by the Robeson trade-off [7,8]. It is important to note that this trade-off relationship is aimed for polymeric membranes, in which for polyimides, the experimental data were taken at 10 atm, 35 °C, using $CO_2/CH_4$ mixtures [8,115]. However, many researchers are performing a comparison of their MMMs performance

data according to this Robeson relationship [23,65,68], the aim is clearly pointed out to have an overview of their status. Based on this, **Figure 4.9** depicts the status of our Matrimid®-PEG blend membranes as well as binary and ternary MMMs.

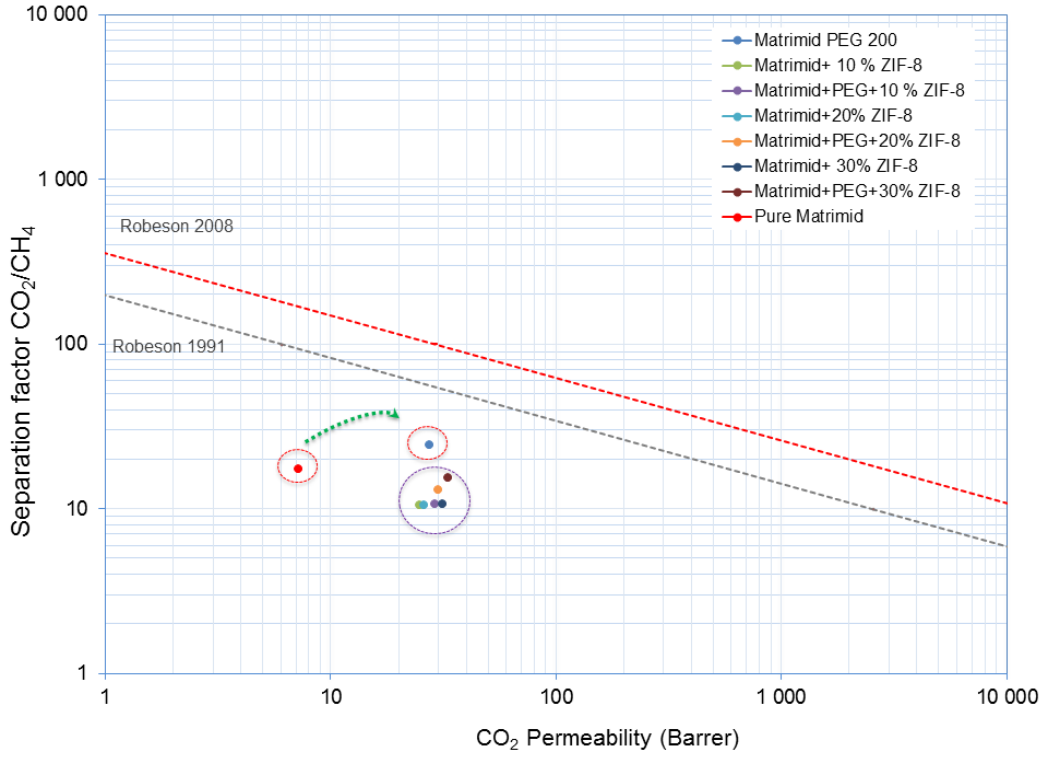


**Figure 4.9.** Status of our Matrimid®-PEG, binary and ternary MMMs on Robeson trade-off.

All binary and ternary MMMs have demonstrated to present better performance in terms of $CO_2$ permeability than the pure Matrimid® membrane (50:50, 8 bar, 25°C). The experimental data are more close to the Robeson limit established in 1991 but still far from the current upper bound 2008. Some of our binary MMMs (10 and 20 wt.%) tended to equal the $CO_2$ permeability of the Matrimid®-PEG blend membranes, with minimal changes on separation factor. In the case of Matrimid®+ 30 wt.% membranes showed a slight increase compared to the polymeric blend.

On the other hand, it was found that the ternary MMM based on Matrimid®-PEG + 30 wt.% displays the best $CO_2$ permeability overcoming even the Matrimid-PEG blend. To have an outlook of the potential of these ternary MMMs,

**Table 4.3** compares these results with other MMMs based on Matrimid already tested for $CO_2$/ $CH_4$ separation.

**Table 4.3.** Comparison of the performance of Matrimid®-PEG+ 30 wt.% ZIF-8 with other MMMs.

| Type of MMM: | Operating conditions: | $CO_2$ permeability (Barrer) | $CO_2/CH_4$ α | Reference: |
|---|---|---|---|---|
| Matrimid®-PEG+ 30 wt .% ZIF-8 | $CO_2/CH_4$ binary mixture (50:50), 8 bar, 25 ºC | 33.1 | 15.4 | This work |
| Matrimid®+ 30 wt. % TS-1-100 | $CO_2/CH_4$ binary mixture (50:50), 8 bar, 35 ºC | 9.6 | 25.0 | [45] |
| Matrimid®+ 8 wt. % $NH_2$-MIL-53(Al) | $CO_2/CH_4$ binary mixture (50:50), 3 bar, 25 ºC | ~9.0 | ~45.0 | [65] |
| Matrimid®+ 37.5 wt. % MIL-53 | $CO_2/CH_4$ single gas permeation, 2 bar, 35 ºC | 40.0 | 90.1 | [116] |
| Matrimid®+ 30 wt .% ZIF-8 | $CO_2/CH_4$ single gas permeation, 2.6 bar, 35 ºC | 14.2 | 37.4 | [28] |
| Matrimid®-PEG+ 5 wt .% ZSM-5 | $CO_2/CH_4$ single gas permeation, 10 bar, 35 ºC | 11.5 | 60.1 | [58] |

In terms of $CO_2$ permeability, our ternary MMMs tend to offer a better performance compared to other MMMs using different types of fillers such as TS-1-100 [45], $NH_2$-MIL-53(Al) [65], ZIF-8 [28], and ZSM-5 [58]; however, membranes based on Matrimid- MIL-53 [116] overcomes the permeability (40.0 Barrer) of our study. While the separation factor values of our ternary MMM could not demonstrate better performance of the aforementioned studies. It has to be taken into account because the presence of one gas component directly influences the transport of the other in mixtures [13]. Furthermore, it is important to point that the membrane preparation procedure is a critical key due to determines the membrane characteristics for the gas separation performance [117]. The gas transport behaviour through the MMMs can be influenced by the intrinsic properties of the inorganic and organic materials, the compatibility and contact between filler-polymer avoiding interfacial voids, and the filler dispersion within the polymer matrix according to its morphology [12,24,112].

## 4.4. **Chapter remarks**

In this chapter, ternary mixed matrix membranes based on Matrimid®-PEG 200 and ZIF-8 were successfully prepared. The proposed membrane preparation procedure leads to obtain a homogeneous dispersion of the ZIF-8 nanoparticles (~33 nm) without visible agglomeration into the polymer phases. The MMMs were tested in gas binary mixture at different feed pressures up to 30 wt.% filler loading (at 50:50 feed composition); however, our procedure lead to incorporate up to 40 wt.% of the MOF into Matrimid matrix. According to the gas separation performance, the incorporation of 30 wt.% of ZIF-8 nanoparticles leads to increase the $CO_2$ permeability in binary (up to 31.47 Barrer) and ternary MMMs (up to 33.12 Barrer); pointing out that the addition of PEG and ZIF-8 enhanced the $CO_2$ permeability in the neat Matrimid® membranes (7.16 Barrer). Finally, this study confirms the enhancement of $CO_2$ permeability of neat Matrimid® membranes through three scenarios: i) the addition of PEG 200 with an enhanced on the separation factor, ii) the incorporation of ZIF-8 nanoparticles but losses in separation factor are obtained, and iii) the blending with PEG and incorporation of ZIF-8 nanoparticles (30 wt.%) leads the increase of $CO_2$ permeability maintaining the separation factor close to neat Matrimid®. Finally, the prepared MMMs of this work did not overcome the Robeson trade-off but a remarkable displacement was reached in terms of permeability towards $CO_2$.

# *Chapter 5*

# Literature review: Mixed matrix membranes for pervaporation

**Chapter overview**

Over the last decades, different polymers have been employed as materials in membrane preparation for pervaporation (PV) applications, which are currently used in the preparation of mixed matrix membranes (MMMs) for ethanol recovery and ethanol dehydration. The ethanol-water and water-ethanol mixtures are, in fact, the most studied PV systems since the bioethanol production is strongly increasing its demand. The present chapter focuses on the current state-of-the-art and future trends in ethanol purification by using mixed matrix membrane (MMMs) in PV. A particular emphasis is, therefore, devoted on the enhancement of specific components transport and selectivity through the incorporation of inorganic materials into polymeric membranes, mentioning key principles on suitable filler selection for synergistic effect towards such separations. In addition, the following topics are discussed: *i)* the generalities of PV, including the theoretical aspects and its role in separation, *ii)* a general overview of the methodologies for the preparation of MMMs, and, *iii)* the most recent findings based on MMMs for both ethanol recovery and ethanol dehydration for better evaluation of progress in the field. From last decade of literature inputs, the PVA has been the most used polymeric matrix targeting ethanol dehydration, while the zeolites have been the most used embedded materials. Today, the latest developments on MMMs preparation declare that the future efforts will be directed to the chemical modification of polymeric materials as well as the incorporation of novel fillers or enhancing the existing ones through chemical modification. Finally, this chapter also convey the evidence from recent literature reports about PV-assisted esterification reactions.

## 5.1.Introduction

Pervaporation (PV) is considered as a suitable and effective membrane technology to carry out the separation of similar boiling points components contained in an ‘‘azeotropic mixture’’, where phase change from liquid to vapor takes place. Nowadays, PV is considered as a “green” process and alternative to traditional ones (e.g. simple distillation, vacuum distillation, fractional distillation and steam stripping) [118], based on its low energy consumption and non-use of solvent [119]. However, the main bridles which still limit a full exploitation of PV at industrial level are: *i)* the membranes and setup are currently relatively expensive, *ii)* low productivities (averaged mass flux for a conventional process 1 kg/m$^2$ h at temperatures of 50-100°C), *iii)* it removes the minority of a component contained in the mixture only, *iv)* it requires purified feed mixtures, *v)* the membrane material could present swelling when in contact with the mixture, and *vi)* components with high boiling points tend to make PV difficult, they may restrict selectivity and can block the membrane [120].

Different types of azeotropic mixtures, such as organic-water, organic-organic and water-organic, have been processed by PV using hydrophobic or hydrophilic membranes, depending on the species to be separated [121]. For example, e.g., mixtures of water with ethanol [122], isopropanol [123], acetone [124], butanol, acetic acid[125], N,N-dimethylformamide, N,N-dimethylsulfoxide, N,N-dimethylacetamide, hydrogen peroxide [126], ethylene glycol[127], N-methyl-2-pyrrolidone[128], and tetrahydrofuran [129]. Moreover, organic-water mixtures that have been separated to isolate the organic component from the water include butanol-water [130], furfural-water [131], pyridine-water [132], and ethylene dichloride-water [133], whereas among organic-organic mixtures, benzene-cyclohexane [134], dimethylcarbonate-methanol [135], methanol-methyl tert-butyl ether [136,137], and acetone-butanol [138] have been, for instance, considered. Among all the different mixtures studied, the present review will focus its attention on the ethanol-water and water-ethanol mixtures as main representatives, considering the commercial PV application, of the azeotropic models investigated by this technology [138–142]. The importance of the ethanol recovery lies in the fact that it can be considered as one of the main renewable and sustainable sources of green energy [143,144], where the bio-ethanol production through the fermentation from biomass resources represents an economically profitable way [145].

The global bio-ethanol production increased from 17.25 billion liters in 2000 [146] to over 100 billion liters in 2017 [147], and its demand is expected to increase promptly over coming years. Commonly, the major industrial scale production of bioethanol belongs to the first generation of biofuels (sugarcanes as the main substrate); nevertheless, the production of second generation ethanol does exist (lignocelluloses as the main substrate) [148]. Relatively, the most commercial technology for separating ethanol, "distillation", seems to satisfy the requirements for its purification. However, distillation has some disadvantages such as the high energy requirements (meaning high costs), the low separation efficiencies in mixtures formed with a close boiling point and the possible chemical reactions with impurities by heating [149,150]. Regardless of the ethanol production process, from fermentation or from direct hydration of ethylene, the product is normally a dilute aqueous solution. At industrial level, the product is processed by distillation system to concentrate ethanol. The separation of ethanol and water is complicated by the fact that ethanol and water form at atmospheric pressure an azeotrope at 95.6 weight % ethanol. It is quite difficult to produce pure ethanol from an azeotropic mixture by normal distillation: at the azeotropic composition, the composition of the vapor coming off is the same as that of the liquid. For dehydration of ethanol, there are several methods available such as azeotropic distillation (in which the carrier is added to break the azeotrope) and adsorption (the water is removed by adsorption agents which adsorb more polar water molecules) [151].

For all these reasons, the separation of ethanol requires an efficient technology to perform such recovery. Certainly, PV technology has been used since a long time ago offering several advantages in separating heat-sensitive azeotropic mixtures (e.g. water-organic, organic-water and organic-organic) [152,153] such as:

i. mild and simple operating conditions through the handling of the feed temperature, feed composition, feed flow rate and permeate vacuum pressure;
ii. no emission to the environment due to the absence of additional streams;
iii. no-use of additional chemicals to the feed stream, thus reducing the cost of disposal pollution agents;
iv. low energy requirement in comparison with distillation separation processes.

PV has some drawbacks for further implementation in industrial applications, e.g. conventional distillation provides higher productivities (in terms of flux) than PV.

However, to reach the high purification degree obtained by PV, distillation involves the installation of at least two distillation columns [154,155], which directly influence the energy consumption of the overall process, and certainly impact the economic evaluation [156]. On the contrary, the production demand in PV can be reached by handling operating parameters (such as membrane area, temperature, driving force) [154].

Polymeric membranes have been widely applied in PV over the last decades [153,157]. In principle, the ethanol purification, which represents the main challenge, occurs by using hydrophobic membranes, while the ethanol dehydration comprises the use of hydrophilic membranes. For example, polydimethylsiloxane (PDMS) and poly(1-trimethylsilyl-1-propyne) (PTMSP) were the primary hydrophobic membrane materials used in membrane preparation for the removal of low alcohols concentrations from aqueous solutions; while the polydimethylsiloxane-imide (PSI), polyoctylmethylsiloxane (POMS), polyether block amide (PEBA) and perfluoropropane (PFP) are currently proposed [157]. On the contrary, hydrophilic polymers are used for the dehydration of alcohols, including poly(vinyl alcohol) (PVA), polyimides (polyimide-6, Matrimid®5218, 6FDA-HAB/DABA polyimide) [122,158–161] and polyacrinolonitrile (PAN) [162] together with natural biodegradable ones (i.e. chitosan, cellulose) [163,164].

Over the last decades, academy and industry have worked for enhancing the performance of polymeric membranes used for ethanol dehydration and ethanol separation from diluted solutions by PV. As can be seen in **Figure 5.1**, the main polymer that has been used so far for "such separation" through PV technology is the well-known hydrophilic PVA, which is followed by other hydrophilic materials (sodium alginate and chitosan).

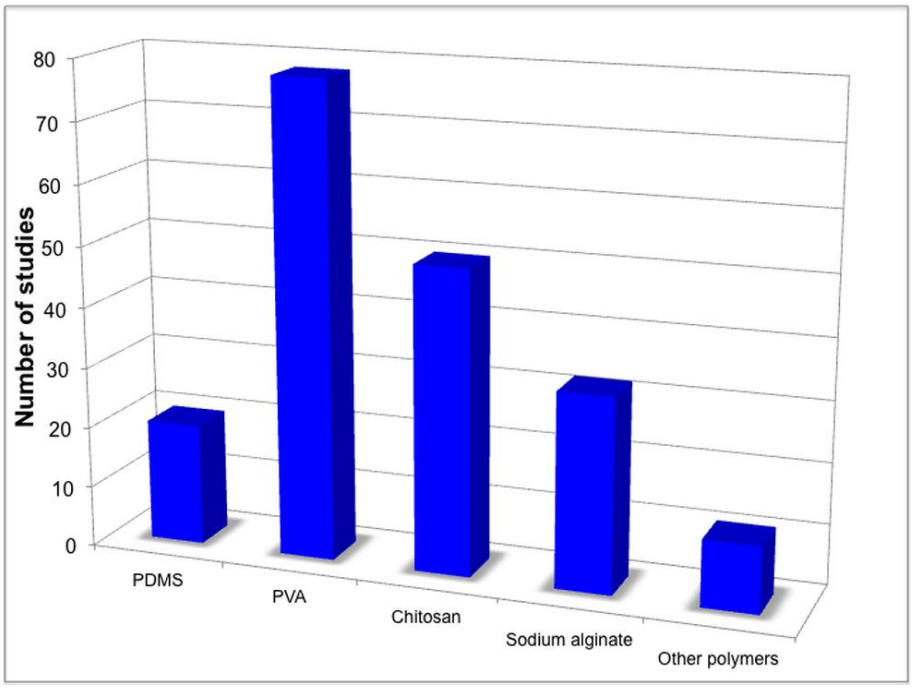


**Figure 5.1.** Overview of the main polymers used for PV.

It is important to highlight that these polymers have started to be used for the preparation of MMMs. Indeed some companies, as DeltaMem AG (previously called Sulzer Chemtech) is fabricating different types of composite membranes (Pervap®) presenting a thin selective layer based on PVA [119]. Today, DeltaMem is one of the main suppliers of pervaporation PVA membranes and PV setups for companies and research labs aiming to the dehydration of ethanol used as a fuel, or as a solvent in the pharmaceutical industry (http://www.deltamem.ch/). Finally, PV technology seems to be considered strongly as a promising and emerging tool for such aim. **Figure 5.2** provides an overview of the progress of studies concerning the use of PV in the last 10 years (for ethanol separation and ethanol dehydration). It is clear that the use of this technology is potentially growing up getting the attraction of researchers and companies. Surely, considering the data from Sulzer Chemtech, and its current commercial expansion to DeltaMem AG, the sales of membranes could motivate some other factories to invest in the research field of this membrane-based technology.

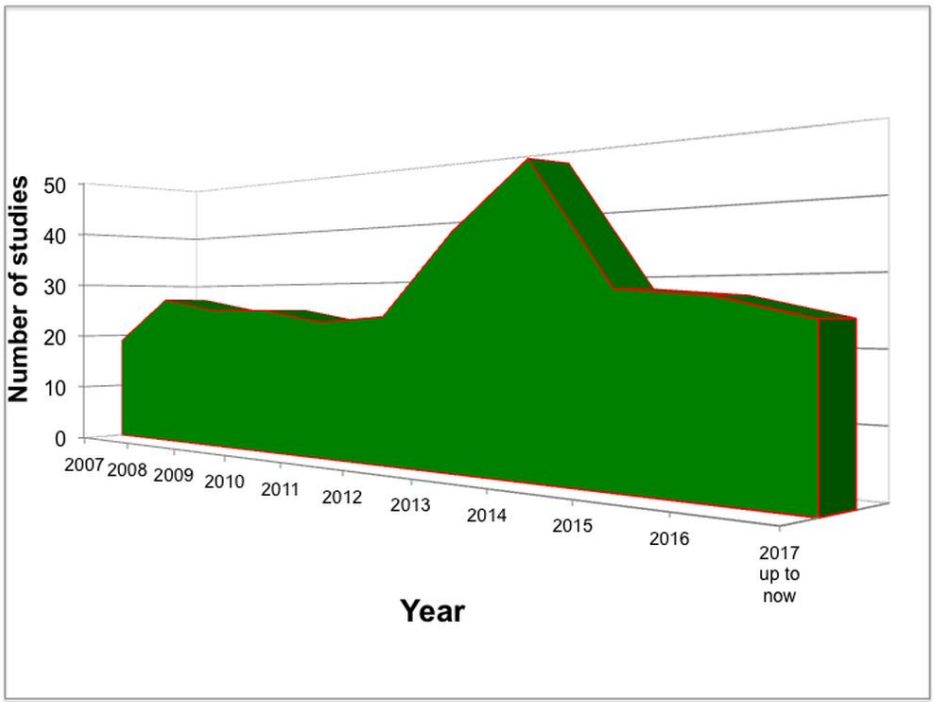


**Figure 5.2.** Evolution of the use of PV technology for ethanol separation and ethanol dehydration.

Nick Wynn (general manager of Sulzer Chemtech in 2001) reported that their sold units are primarily used to purify chemicals, and today (as DeltaMem AG, http://www.deltamem.ch/), over one hundred thirty pervaporation units are operating worldwide, most of them dehydrating solvents, such as ethanol. Furthermore, he explained that PV has been proven, and its attention is aiming to separations closer to the chemical reaction step which is more critical to production, but it could promise much greater benefits [165].

Nowadays, researchers are still looking for new membrane materials or improving the existing ones aiming at obtaining better membrane performances for both ethanol removal and dehydration. The attempts have been focused on the modification of these primary polymers (i.e. by cross-linking, chemical, etc.), blending with other polymers or additives, and incorporating a dispersed phase (fillers) into a continuous phase (polymers). The preparation of MMMs in which the organic-inorganic particles (metal-organic frameworks, zeolitic-imidazolate frameworks, etc.) are loaded in the polymeric matrix [166] is one of the new directions where researchers are more and more addressing their studies. Therefore, this chapter focuses on latest findings of using MMMs for ethanol removal and dehydration by PV, together with the theoretical background in PV, generalities of fabrication of MMMs and future perspectives.

### 5.2.Brief background on pervaporation and its role in separation

PV is a separation process in which a binary or a multi-component liquid mixture is separated by partial vaporization using a dense non-porous membrane. The liquid feed mixture (i.e. ethanol-water or water-ethanol) is in direct contact with the "selective" side of the membrane, while the permeate (collected at the other side of the membrane) is in a vapor phase, enriched by the species with higher affinity with the membrane (hydrophilic or hydrophobic type). The transport of the permeating species occurs thanks to the driving-force applied: *i*) vacuum (see **Figure 5.3**) or *ii)* sweeping gas (like nitrogen) and *iii)* temperature, and then condensed and recovered. In fact, PV is the combination of "permeation" and "evaporation" processes [162].

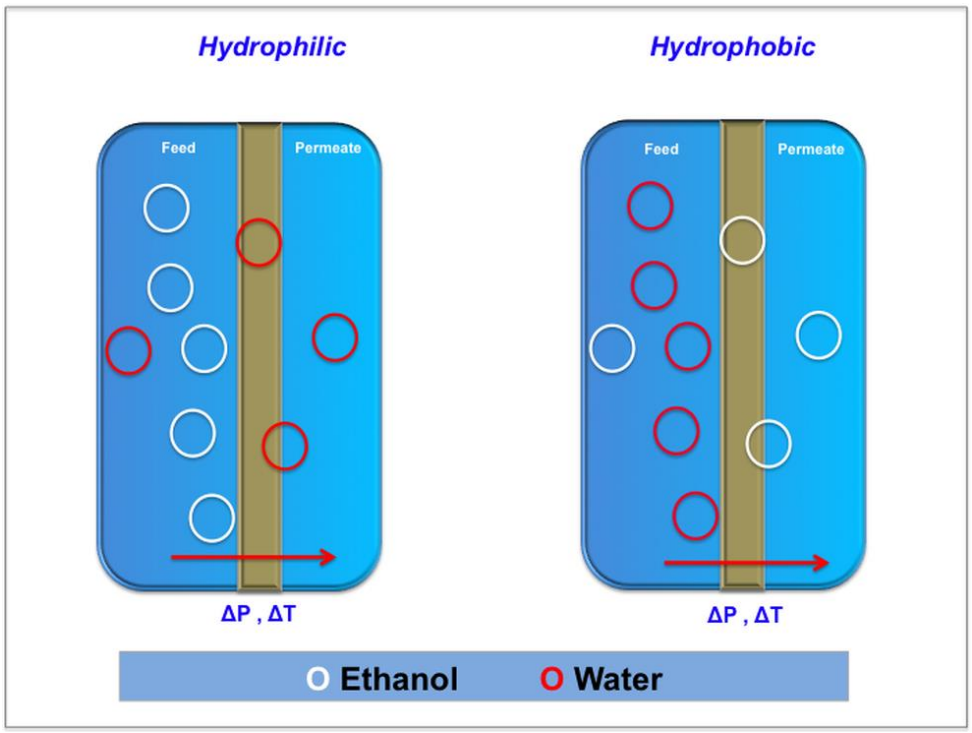


**Figure 5.3.** Schemes of the water-ethanol and ethanol-water separations by PV

The transport mechanism through dense polymeric membranes is described by the well-known solution-diffusion model [162,167]. The mass transfer across a PV membrane can be described in three main steps: *i)* adsorption of the target component from the mixture to the "selective" layer of the membrane on the basis of its chemical affinity, *ii)* diffusion of the component through the membrane as a result of the concentration gradient, iii) desorption of the component at the permeate side of the membrane [168].

The mass transport is governed by the chemical potential ($\mu_i$) gradient, the physical properties of the permeating component *(i)* and its concentration in feed and permeate side. Finally, the permeability (*P*) depends on the diffusivity (*D*) and solubility (*S*) of the target components [162,167], as **Eq. (1)** describes:

$$P = D\,S = D\,K \qquad \textbf{(1)}$$

The solubility *(S)* is a thermodynamic parameter that provides information on the amount of penetrant adsorbed by the membrane under equilibrium conditions. While, the diffusivity *(D)* is a kinetic parameter that indicates the transport rate of the penetrating component through the membrane [121]. The variables *D* and *K* represent the diffusion and sorption coefficient, respectively. However, some other phenomena can make to differ this typical solution-diffusion model, e.g. the non-uniform swelling of the membrane across its thickness, concentration and temperature polarization, the use of fillers or different support materials can be responsible for anomalous behaviors in the sorption and diffusion [121].

As in all membrane technologies, the performance of the membrane in contact with the complex mixture is usually described in terms of permeate flux and separation factor [152]. The permeate flux ($J_A$) of the component *A* (commonly denotes the faster permeating compound), where $m_A$ is the mass of the component *A* transported to the permeate stream through the membrane area $A_m$ during the time period *t* [144,152], as **Eq. (2)** describes:

$$J_A = \frac{m_A}{A_m t} \qquad (2)$$

The separation factor *(β)* is the ratio between the concentrations of components *A* ($C_A$) and *B* ($C_B$) in permeate and retentate (usually feed stream), as **Eq. (3)** describes:

$$\beta = \frac{\left(C_A / C_B\right)_{PERMEATE}}{\left(C_A / C_B\right)_{FEED}} \qquad (3)$$

The trade-off relationship between $J$ and $\beta$ is defined as "pervaporation separation index" (PSI) that is defined as a product of permeation flux and separation factor, as it is given by **Eq. (4)**. The PSI basically evaluates the overall performance of a membrane.

$$PSI = J\beta \qquad \textbf{(4)}$$

However, in this definition, the PSI can be large if the membrane has a high flux even when $\beta$ is equal to 1. Thus, the definition of PSI was later modified as a product of $J$ and $(\beta - 1)$ [169]. On the other hand, the permeability ($P_A$) of a dense membrane, defined by the solution-diffusion model (see **Eq. (1)**), can be rearranged as follows:

$$P_A = \frac{J\,l}{p^F_{A,G} - p^P_{A,G}} \qquad (5)$$

where $p^F_{A,G}$ and $p^P_{A,G}$ are the partial vapor pressure in hypothetical vapor phase at equilibrium for the feed and permeate, respectively, while $l$ is the dense selective layer thickness. The selectivity $(\alpha)$ of a membrane for components $A$ over $B$ describes how efficient the two components can be separated; the parameter is then the ratio of permeabilities or permeances for components $A$ and $B$ according to the following **Eq. (6)**:

$$\alpha = \frac{P_A}{P_B} = \frac{\bar{P}_A}{\bar{P}_B} = \frac{D_A}{D_B}\frac{K_A}{K_B} \qquad (6)$$

where $\bar{P}_i$ is the permeance of component $i$ well defined as the ratio of permeability $P_i$ and the layer thickness $(l)$. It is important to highlight that $\beta$ and the $J$ parameters depend on the operating conditions, whereas the α depends on the membrane material used and its properties [144].

## 5.3.Current state-of-the-art on ethanol purification by using MMMs in PV

### *5.3.1. Dehydration of ethanol*

#### *5.3.1.1.Zeolites*

Over last decades, the starting attempts on the preparation of MMMs concerned mainly the incorporation of zeolites [170]. **Table 5.1** shows chronologically the main fillers incorporated in different polymeric matrixes to create MMMs for the dehydration of ethanol. The zeolites are aluminosilicate solids exhibiting a negatively charged framework of micropores into which specific molecules may be adsorbed [171]. This characteristic allows to enhance the separation performance of membranes containing zeolites. For example, some zeolites, such as 3A, 4A and 13X, were added into polyacrylonitrile (PAN) membranes [172] which (at 32 wt.% zeolite loading) showed higher water permeate fluxes of about 9-fold than pattern PAN membranes. However, a considerable decrease in selectivity was observed at high filler loadings (>30 %), due to the fact that zeolite particles loosen the membrane structure causing a complete loss of selectivity.

Generally, the incorporation of fillers tends to increase the free volume in polymeric membranes, which can be produced by inefficiencies in polymer chain packing in the solid state and by the molecular motion of polymer chain segments. The free volume created definitely opens gaps in the polymer matrix on a transient basis allowing penetrant molecules to diffuse through the polymer [31]. In other words, the fillers act as a spacer for polymer chains providing an extra space for water permeation and, therefore, promoting high permeation in respect to the poor permeance of polymeric materials. Huang *et al.* [173] also demonstrated that after the incorporation of different zeolites (3A, 4A, 5A, NaX, NaY, silicate and beta at 20 wt.%) into PVA polymer, the composite membranes showed lower separation factor and higher fluxes than pure polymer membranes. Their PV performances in terms of water permeability and selectivity, for zeolite-filled membranes, were strongly related to *i)* zeolite pore dimension, *ii)* its hydrophilic/hydrophobic nature and *iii)* its crystal framework. In addition, the authors concluded that the tendency of these membranes to provide higher permeability to water was related to the fact that the water molecules require less energy than ethanol molecules to the transport, as proved by the results obtained with Arrhenius activation energies calculations [173,174].

In case of zeolite 4A with 25 wt.% of loading, a water permeate flux about of 2.5 kg $m^{-2}$ $h^{-1}$ [174] was achieved. This was in line with the results obtained by Amnuaypanich *et al.* [175,176]. However, the addition of 40 wt.% zeolite 4A in PVA membranes provided even higher water permeate fluxes (around 3.7 kg $m^{-2}$ $h^{-1}$) [175,176]. Another zeolite filler, such as KA (potassium exchanged A zeolite), was incorporated into PVA polymer too, followed by a chemical cross-linking of the polymer using fumaric acid [177], aiming at the selectivity enhancement of the MMMs. Typically, the chemical cross-linking procedure tends to decrease the free volume of the polymers, producing an increase in selectivity. For example, Guan *et al.* [177] demonstrated that at 20 wt.% KA zeolite loading, the cross-linked membrane exhibited higher selectivity than the non-cross-linked MMM (1279 versus 511) at 60 °C (a mixture of 80/20 ethanol/water). According to the authors, the membranes presented swelling even when zeolite particles counteracted the swelling of the polymer caused by water. These swollen MMMs, in fact, can also lead the ethanol permeation thanks to the enlargement of the polymeric chain segments; finally, the highest water flux was around 1.1 kg $m^{-2}$ $h^{-1}$ for this cross-linked formulation at 100 °C. A silicone rubbery polymer, like PTFPMS, was used for MMMs (zeolite 4A) to dehydrate ethanol [178]. The addition of these hydrophilic zeolite 4A particles enhanced the water permeability more than 6-fold in MMMs compared to the unfilled PTFPMS membrane. Generally, the silicone rubber PTFPMS, which is considered as the benchmark hydrophobic membrane material in PV, tends to offer good ethanol-water perm-selectivities (0.89) in comparison to other several polymers. However, PTFPMS/zeolite 4A mixed matrix membranes displayed selectivities of about 11.5, resulting in a performance 6 times higher than for the unfilled PTFPMS membrane [178].

**Table 5.1.** Chronological applications of MMMs based on polymeric materials for the dehydration of ethanol through PV

| ***Concentration of mixture:*** | ***Type of filler:*** | ***Loading (wt. %):*** | ***Filler characteristics:*** | ***Polymeric matrix:*** | ***Operating conditions:*** | ***Permeability or flux values*** | ***Selectivity or SF of MMMs:*** | ***Techniques used for membrane characterization:*** | ***Remark of the study:*** | ***Reference:*** |
|---|---|---|---|---|---|---|---|---|---|---|
| 50, 72, 92 % EtOH | Zeolites (3A, 4A and 13X) | 0, 25, 32, 40, and 50 % | Particle size: 3A (2–5 µm) 4A (3–5 µm) and 13 (600 Mesh) | PAN | 50 °C 0.9 mmHg | *Highest $H_2O$ flux (34.47 g $m^{-2}$ $h^{-1}$) at 50% EtOH feed composition.* | *Maximum selectivity around 50 at 32 % zeolite loading.* | -Pervaporation performance -SEM | -At 32 wt.% zeolite, the flux increased around 9-fold with a loss of selectivity about 7-fold relative to homogeneous PAN membranes. | [172] |
| 90 % EtOH | silica nanoparticles | 5 % | Particle size: 10-20 nm | Chitosan | 70 °C 5-8 Torr | *$H_2O$ permeation flux of 410 g $m^{-2}$ $h^{-1}$.* | *SF was around of 919.0* | -Pervaporation performance -SEM -DSC -TGA -Degree of swelling | -The membranes showed a SF and permeate flux around 919 and 410 g $m^{-2}$ $h^{-1}$, respectively, better performance than pure chitosan. | [179] |
| 80 % EtOH | Zeolites (3A, 4A, 5A, NaX, NaY, silicate and beta) | 20% | Particle size: 3A: < 4 A° 4A: < 4 A° 5A: > 4 A° NaX: 7.4 A° NaY: 7.4 A° Beta: 7.1 A° Silicate-1: 5.2 A° | PVA | 70, 80, 100 °C Vacuum pressure at permeate side 0 mbar | *Maximum $H_2O$ permeate flux about of 3200 g $m^{-2}$ $h^{-1}$ for 5A zeolite at 100°C.* | *Highest SF was around of 1600 for 3A zeolite at 60 °C.* | -Pervaporation performance -FESEM | -The zeolite filled-membranes presented an increase in permeate flux as a function of temperature, whereas SF decreased inversely. The separation performance of the MMMs was better than the pure PVA membranes. | [173] |
| 80 % EtOH | Zeolite (4A) | 5- 35% | Particle size: 4A: < 4 A° | PVA | 70, 80, 100 °C Vacuum pressure at permeate side 0.4 mbar | *Maximum $H_2O$ permeate flux about of 2500 g $m^{-2}$ $h^{-1}$at 25 % filler loading and 80°C.* | *Highest SF was around of 600 at 20 % filler loading, 80°C.* | -Pervaporation performance -FESEM -FTIR | -Zeolite addition has increased the SF and significantly increased the water flux, indicating that incorporated zeolite 4A can promote water transport and at the same time restricting ethanol permeation. | [174] |

**Table 5.1.** Chronological applications of MMMs based on polymeric materials for the dehydration of ethanol through PV (continued)

| ***Concentration of mixture:*** | *Type of filler:* | *Loading (wt. %):* | *Filler characteristics:* | *Polymeric matrix:* | *Operating conditions:* | *Permeability or flux values:* | *Selectivity or SF of MMMs:* | *Techniques used for membrane characterization:* | *Remark of the study:* | ***Reference:*** |
|---|---|---|---|---|---|---|---|---|---|---|
| 80 % EtOH | Zeolites (KA) | 20 % | Particle size: KA: 1–3 µm | cross-linked PVA | 60, 80, 100 °C Vacuum pressure at permeate side 1 mbar | *Highest $H_2O$ flux (around 1100 g $m^{-2}$ $h^{-1}$) at 100* °C | *Highest selectivity was around of 1279 at 20 % filler loading and 60*°C. | -Pervaporation performance<br>-DSC<br>-FTIR<br>-TGA<br>-FESEM | -An improvement on selectivity was obtained (1279 from 511 in non-cross-linked one) by using chemical cross-linking in KA-filled PVA membrane. | [177] |
| 5 % EtOH | ZSM-5 | 0-65 % | Particle size: ZSM-5: 2.4 µm | PDMS | 50 °C, Vacuum pressure at permeate side <4 Torr | *Highest EtOH flux around 0.144 kg $m^{-2}$ $h^{-1}$ at 50* °C, 50 % filler loading. | *The highest selectivity of 3.0 was observed with 65 wt% zeolite loading* | -Pervaporation performance<br>-SEM | -These MMMs resulted to offer better permeability for ethanol than water. The selectivity was lost directly by increasing the filler loading. | [180,181] |
| 90 % EtOH | ZSM-5 | 2, 4, 6, 8, 10 % | Particle size: ZSM-5: 0.5 µm | Chitosan | 80 °C, Vacuum pressure at permeate side 1 kPa | *Highest $H_2O$ flux around 230 g $m^{-2}$ $h^{-1}$ at 80* °C, 8 % filler loading. | *The highest SF was around 150 at 8 wt.% zeolite loading.* | -Pervaporation performance<br>-SEM<br>-TGA<br>-FTIR<br>-Tg determination<br>-Swelling and sorption properties<br>-XRD<br>-Contact angle | -An enhancement in permeate flux was achieved by using small amount of filler loading. In case of SF, it remained constant compared with patter polymer membranes. | [182] |
| 90 % EtOH | Zeolite beta | 2.5, 5, 7.5, 10 % | Particle size: Zeolite beta : 500 nm | Sodium alginate | 30-60 °C | *Highest $H_2O$ flux around 0.178 kg $m^{-2}$ $h^{-1}$ at 60* °C, 10 % filler loading. | *The highest SF was around 1600 at 10 wt% filler loading.* | -Pervaporation performance<br>-SEM<br>-Tensile strength<br>-FTIR<br>-Sorption measurements | -The addition of the filler into sodium alginate membranes improved considerably the separation properties of the polymer. | [183] |
| 10 % $H_2O$ | MWCNT | 1-5 % | Filler size: MWCNT: average diameter (10-20 µm) and length (10-50 µm) | PVA | 30-60 °C, Vacuum pressure at permeate side $1x10^{-1}$ Torr. | *Highest $H_2O$ flux around 170 g $m^{-2}$ $h^{-1}$ at* 5 % filler loading, 60 °C. | *The highest SF was around 1300 at 1 wt. % filler loading, 30* °C. | -Pervaporation performance<br>-TEM<br>-DSC<br>-XRD | - The incorporation of 1 wt. % of MWCNT showed a slight increase in permeate fluxes, maintaining the SF for all temperatures tested. | [185] |

**Table 5.1.** Chronological applications of MMMs based on polymeric materials for the dehydration of ethanol through PV (continued)

| ***Concentration of mixture:*** | *Type of filler:* | *Loading (wt. %):* | *Filler characteristics:* | *Polymeric matrix:* | *Operating conditions:* | *Permeability or flux values* | *Selectivity or SF of MMMs:* | *Techniques used for membrane characterization:* | *Remark of the study:* | ***Reference:*** |
|---|---|---|---|---|---|---|---|---|---|---|
| 10 % $H_2O$ | Zeolite (4A) | 3, 5, 7, 10 % | Particle size: Zeolite 4A: 500 nm | Sodium alginate | 30 °C, Vacuum pressure at permeate side 6.66 Pa. | *Highest $H_2O$ flux around 0.137 kg $m^{-2}$ $h^{-1}$ at* 10 % filler loading. | *The highest selectivity was around 1334 at 10 wt. % filler loading.* | -Pervaporation performance<br>-SEM<br>-Sorption measurements. | -The zeolite 4A loading of into alginate increased the efficiency of the membranes due to the available free channels. | [184] |
| 2-15 % $H_2O$ | $TiO_2$ | 0-10 % | Particle size: $TiO_2$: 10 nm | Chitosan | 50-80 °C, pressure at permeate side 0.5 kPa. | *Highest $H_2O$ flux around 0.340 kg $m^{-2}$ $h^{-1}$ at* 90 % EtOH feed composition, 80°C, 6 % filler loading. | *The highest SF was around 196 at* 90 % EtOH feed composition, 80°C, 6 % filler loading | -Pervaporation performance<br>-SEM<br>-FTIR<br>-XRD<br>-TGA<br>-Sorption determination<br>- Swelling degree | - The permeability and SF increased from 2 to 6 % filler loading, however, the separation properties decreased after 6 % of filler. | [186] |
| 9 % $H_2O$<br>8.4 % EtOH | VTES | 4.32, 11.94, 18.43, 24.04 % | Particle size: N.D. | PVA | Vacuum pressure 650 Pa. | *Highest $H_2O$ flux around 540g $m^{-2}$ $h^{-1}$, at 4.43 wt. % filler loading* | *Highest SF for $H_2O$/EtOH was around 1079, at 4.43 wt. % filler loading* | -Pervaporation performance<br>-SEM<br>-FTIR<br>-AFM<br>-XRD<br>-DTG<br>-Contact angle<br>-Swelling degree | -The dehydration of a complex feed mixture was well done by these MMMs. The filler used helped to reduce the swelling degree of the pattern polymer. | [187] |
| 2.5 % $H_2O$ | Zeolite (4A)<br><br>Clinoptiloli te-CL | 10 % | Particle size: Zeolite (4A) : 10 µm Clinoptilolite-CL: 13 µm | Sodium alginate | 25 °C, Vacuum pressure 40 mbar. | *Total flux around 0.107 and 0.123 g $m^{-2}$ $h^{-1}$, at 10 wt. % filler loading for 4A and CL zeolites, respectively.* | *Selectivity around 45.6 and 43.5, at 10 wt. % filler loading for 4A and CL zeolites, respectively.* | -Pervaporation performance<br>-SEM | - The filler 4A was a bit more effective than CL zeolite for the dehydration of EtOH–water mixtures. In addition, as zeolite loading in membrane increased, both flux and selectivity increased. | [188] |
| 15 % $H_2O$ | ZIF-8 | 34 and 58 % | Particle size: ZIF-8 : 40 nm | PBI | 60 °C | *Highest $H_2O$ permeability around 22,000 Barrer, at 58 wt. % filler loading* | *The highest SF was around 80, at 34 wt. % filler loading.* | -Pervaporation performance<br>-FESEM<br>-XRD<br>-Sorption measurements<br>-DSC | -The MMMs tested for dehydration of EtOH showed a water permeability about one order higher than the pure PBI membrane. | [189] |

The zeolite ZSM-5 was also incorporated into an unconventional polymer, like chitosan, in order to dehydrate ethanol by PV [182]. The MMMs with just 8 wt.% filler loading exhibited a remarkable enhancement in PV performances regarding the permeation flux (0.230 kg $m^{-2}$ $h^{-1}$) keeping, at the same time, a good separation factor (152.82) in comparison with pattern chitosan membranes (0.054 kg $m^{-2}$ $h^{-1}$ and 158.02, respectively).

Another non-common polymer like sodium alginate was used to generate MMMs [183]. The incorporation of zeolite beta improved considerably the water permeability (from 0.039 up to 0.178 kg $m^{-2}$ $h^{-1}$) and separation factor of the polymer (from 23 up to 1600) by using low filler loading (10 wt.%). The authors concluded that the enhancement was totally attributed to the hydrophilic nature of the zeolite as well as its molecular sieving effect. The incorporation of zeolite 4A in sodium alginate has been also studied [184], where the addition of 10 wt.% filler loading, led to a considerable improvement in selectivity (1334) and good water flux (0.137 kg $m^{-2}$ $h^{-1}$). The performances of a synthetic zeolite membrane (4A) and a natural one (clinoptilolite (CL)) in sodium alginate, was evaluated by Nigiz, Dogan, & Hilmioglu (2012). The synthetic 4A zeolite membrane was more suitable to remove water from ethanol than the natural CL zeolite at the same filler loading concentration (wt.%), displaying total flux and separation factor values of about 0.107 kg $m^{-2}$ $h^{-1}$, 45.6 and 0.123 kg $m^{-2}$ $h^{-1}$, 43.45, respectively. The high water fluxes can be related to the presence of hydrophilic functional groups that sodium alginate presents; establishing a strong affinity between sodium alginate membrane and water molecules [190]. This demonstrates that the nature of the membrane material is one of the main factors affecting PV processes; while, in the case of MMMs, the key factors playing the major role are the nature of the polymeric material, the degree of crystallinity, the presence of fillers (and type of filler) as well as presence of functional groups [121].

#### *5.3.1.2.Carbon nanotubes (CNTs)*

Carbon nanotubes have recently attracted the attention of researchers due to their extraordinary electrical and mechanical properties. Indeed, they show multifunctional properties encouraging their potentiality for several applications [191], e.g. in the preparation of MMMs. In case of multiwalled carbon nanotubes (MWCNT), they are typically recognized as microtubules of graphitic carbon with concentrically arranged cylinders [192], which have been incorporated into polymeric membranes for the

dehydration of ethanol. For example, the addition of MWCNT (1 wt.%) in PVA membranes also showed a slight improvement of permeate flux (~0.030 kg $m^{-2}$ $h^{-1}$), with a high separation factor (1300), respect to the pristine membrane [185]. Lower amounts of filler loading (2-5 wt.%) increased the permeate flux with the subsequent loss of separation factor. It is important to highlight that the membrane performance in PV technology is also influenced by the temperature of the feed mixture. Generally, the increase in temperature tends to increase the permeate fluxes; however, separation efficiency commonly decreases. This can be attributed to the expansion of the free volume in the polymeric matrix producing a major mobility of the penetrants [174,177,185].

*5.3.1.3.Silicas*

Silica is another material that has also been incorporated into hydrophilic membranes for the dehydration of ethanol. This material is abundant and versatile, it can be naturally found as sand, flint, clay, and volcanic ash. Certainly, the silica was firstly used for the production of nanocomposite membranes due to the fact that strongly improve the mechanical, thermal and rheological properties of the polymer matrix. However, the surface hydroxyl groups of silica influence also the separation performance of the membranes where they are dispersed [193]. Indeed, the enhancement of separation properties in chitosan membranes was also obtained through the addition of silica nanoparticles [179]. The incorporation of 5 parts per hundred of the filler produced a MMM which exhibited a separation factor of 919 and a permeation flux of 0.410 kg $m^{-2}$ $h^{-1}$ in the PV of 90 wt.% ethanol solution. It is important to highlight that both performance properties were improved in comparison with the unfilled chitosan membranes ($\beta \sim 554$, and permeate flux 0.232 kg $m^{-2}$ $h^{-1}$), leading to obtain a permeate with 99% of water concentration.

*5.3.1.4.Metal-organic frameworks (MOFs)*

Metal-organic frameworks (MOFs) are the new class of crystalline nanoporous materials formed of metal ions or clusters bridged by organic linker through strong chemical bonds. These relatively new materials have been successfully incorporated into polymer matrixes based on the functional groups of the organic ligands and on the metal ions associated with the secondary building units which facilitate interactions with the polymer. Their unique properties have been, therefore, explored and

investigated for water-ethanol separation in PV. Shi *et al.* [189], for instance, proposed the addition of ZIF-8 (at 58 wt.%) into PBI polymer for the dehydration of ethanol. The MMMs presented a water permeability of about one order higher than the pure PBI membrane (22,000 and 2300 Barrer, respectively). In addition, the authors highlighted that the MMMs showed effectiveness in suppressing ethanol-induced swelling in the polymeric matrix owing to their inorganic properties. The PV of water-ethanol mixtures through commercial polyimide (Matrimid®5218) based MMMs containing ZIF-8 was reported by Kudasheva *et al.* [122]. The performance of Matrimid® was enhanced by adding this MOF, where separation factor increased (up to 300 from 260 in neat polyimide); in case of total flux, it showed a slight increase (0.26 from 0.24 kg $m^{-2}$ $h^{-1}$).

*5.3.1.5.Other type of fillers*

Novel chitosan-$TiO_2$ nanocomposite membranes were tested by Yang *et al.* [186] for ethanol dehydration. The addition of 6 wt.% in chitosan, produced membranes that exhibited acceptable permeate flux and separation factor, of about 0.340 kg $m^{-2}$ $h^{-1}$ and 196, respectively (for 90% aqueous solution of ethanol). For increasing the selectivity of chitosan membranes, the cross-linking procedure has to be also taken into account [194]. The use of PVA–polyvinylpyrrolidone (PVP) blend membranes loaded with phosphomolybdic acid (PMA) presented a good separation performance (i.e., with 4 wt.%, it showed selectivity and permeability values about of 8206 and 0.00375 kg $m^{-2}$ $h^{-1}$ $kPa^{-1}$, respectively). The selective sorption exhibited by the particles increased the permeation of water molecules from ethanol-containing mixtures [195]. The main purpose of polymer blending is to improve the polymer properties by exploiting a synergistic effect. For example, PVA presents excessive swelling degree in aqueous solution, which restricts the selectivity to water; whereas PVP seems to present less swelling degree. In addition, the polymers have to show a good compatibility, in case of PVA and PVP, they are totally miscible due to hydrogen bonds formed between donor groups of PVA and acceptor groups of PVP [195]. Therefore, the blend of PVA and PVP is ideal since each polymer compensates the deficiencies of the other one, leading to a final membrane with an acceptable swelling degree and good mechanical properties. Nowadays, a current approach aiming to the improvement of MMMs, refers to the chemical modification of the fillers incorporated into a polymer matrix. **Table 5.2** shows the fillers, which have been modified and used, up to now, for the production of MMMs in PV. Generally, the chemical modification of the fillers is performed in order

to improve specific characteristics of its structure. Wei *et al.* [196], for instance, studied silane-modified NaA zeolite-PAAS membranes, which displayed higher separation factor (435) and total flux (0.533 kg $m^{-2}$ $h^{-1}$) than the original MMMs (313 and 0.440 kg $m^{-2}$ $h^{-1}$, respectively) when operated under the same conditions. Additionally, the modified zeolites improved the compatibility between polymer-filler, generating fewer voids and a more homogeneous membrane structure.

Graphene is another interesting material which has received great attention over last years due its potentiality for enhancing the performance of polymeric membranes [197]. In PV, functionalized graphene sheets were embedded in chitosan by Dharupaneedi *et al.* [198]. Their incorporation led to an increase of the chitosan surface hydrophilicity accompanied with an increase in membrane tortuosity, which favored the selective permeation of water molecules. Chitosan membranes, in fact, loaded with 2.5 wt.% of modified fillers showed the highest selectivity (around 1093). The modification of carbon nanotubes through the attachment of OH- and COOH- groups was performed by Panahian *et al.* [199]. These modified-MWCNTs were incorporated into PVA membranes which displayed lower total flux compared (0.388 kg $m^{-2}$ $h^{-1}$) to the neat membrane. The addition of the modified filler increased, in fact, the resistance of the membrane due to the crosslinking esterification reaction between hydroxyl groups of the PVA molecules and carboxyl groups of the modified MWCNT. This aspect caused a decrease of polymer chain mobility, lowering the diffusion of permeating molecules through the membrane with a consequent flux decline. On the contrary, the addition of the modified fillers improved the water separation factor (up to 805) in the MMMs from a value of 100 in pristine polymeric membrane.

**Table 5.2.** Chemical modification of fillers for MMMs in dehydration of ethanol through PV.

| *Concentration of mixture:* | *Modified filler:* | *Loading (wt. %):* | *Characteristics of filler:* | *Polymeric matrix:* | *Operating conditions:* | *Permeability of flux values* | *Selectivity or SF of MMMs:* | *Techniques used for membrane characterization:* | *Remark of the study:* | *Reference:* |
|---|---|---|---|---|---|---|---|---|---|---|
| 10 % $H_2O$ | Silane modified Na zeolite | 0-20 % | Particle size: Modified zeolite: 289-452 nm | PAAS | 30-100°C, pressure at permeate side 135 Pa | *Highest total flux (533 g $m^{-2}$ $h^{-1}$) at 20 wt. % filler loading, 30°C.* | *Highest SF was around 435 at 20 wt. % filler loading, 30°C.* | -Pervaporation performance<br>-SEM<br>-TEM<br>-XPS<br>-FTIR | -The MMMs with modified filler displayed much better performance than normal MMMs. | [196] |
| 10-40 % $H_2O$ | Functionalized graphene sheets | 1-3 % | N.R. | Chitosan | 30-50°C. | *Highest total permeability (107 barrier) at 20 wt. % filler loading, 10 % $H_2O$ feed concentration 50°C.* | *Highest selectivity was around 1093 at 2.5 wt. % filler loading, 10 % water feed concentration, 30°C.* | -Pervaporation performance<br>-SEM<br>-XRD<br>-Contact angle<br>-Optical profilometry techniques<br>-Swelling degree<br>-TGA | - The incorporation of the modified filler showed an enhancement in the surface hydrophilicity of chitosan membranes, producing a more selective permeation of water. | [198] |
| 90 % EtOH | Modified MWCNT | 0.5-4 % | Filler size: MWCNT: diameter (5-10 mm) and inner (20-30 nm) | PVA | 30°C, permeate-side pressure 1 mmHg. | *Highest total flux (395 g $m^{-2}$ $h^{-1}$) at 4 wt. % filler loading.* | *Highest selectivity was around 662 at 4 wt. % filler loading.* | -Pervaporation performance<br>-FESEM<br>-TGA<br>-XRD<br>-ATR-FTIR<br>-AFM<br>-Swelling degree | -Whole MMMs had lower total flux than the neat PVA membranes. On the contrary, the modified filler improved the separation performance. | [199] |
| 85 % EtOH | ZIF-8-$NH_2$ | 2.5-10 % | Filler size: ZIF-8: 200 nm | PVA | 40°C, permeate-side pressure <1mbar. | *Highest total flux (250 g $m^{-2}$ $h^{-1}$) at 10 wt. % filler loading.* | *Highest SF was around 200 at 7.5 wt. % filler loading.* | -Pervaporation performance<br>-SEM<br>-XRD<br>-Mechanical test<br>-FTIR<br>-Contact angle<br>-Sorption test | -MMMs exhibited enhanced separation performance based on the chemical modification. Furthermore, the amino functionalization restricted agglomeration of the particles | [200] |

Recently, the amino functionalization of ZIF-8 added into PVA membranes for ethanol dehydration was carried out by Zhang *et al.* [200]. The chemical modification enhanced the hydrophilicity and affinity with the PVA material through the hydrogen bonding between ZIF-8-$NH_2$ molecules and PVA chains. The highest total flux and separation factor were around 0.250 kg $m^{-2}$ $h^{-1}$ and 200, respectively. The enhancement of separation performance was attributed to the higher hydrophilicity and restricted clustering of the modified particles in MMMs compared to the unmodified filler loaded in PVA [200].

### 5.4.Pervaporation-assisted esterification reactions by means of mixed matrix membranes

The versatility of PV technology has allowed its coupling to other processes, for example, to reaction processes. PV has been successfully applied to the esterification of carboxylic acids (acetic acid, lactic acid, etc.), i.e., the reaction of carboxylic acids with alcohols (methanol, ethanol, etc.) to produce esters [201,202], as shown in **Figure 5.4**.

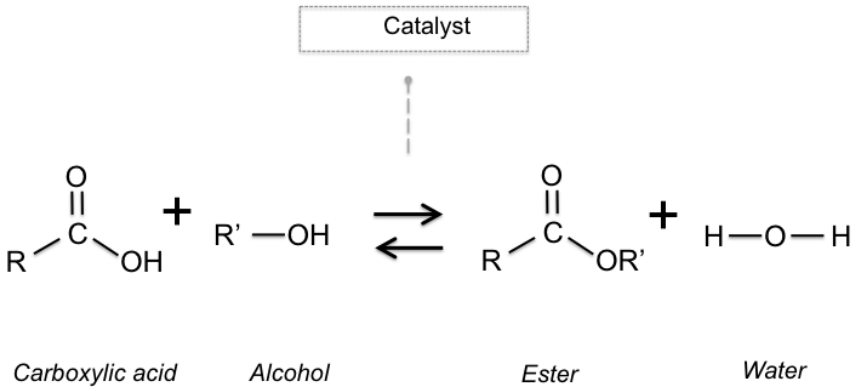


**Figure 5.4.** Typical esterification reaction of carboxylic acids and alcohols for ester synthesis.

As esterification occurs, water is produced as a byproduct, representing an issue due to the simultaneous hydrolysis of the ester up to a point at which thermodynamic equilibrium is reached. To overcome equilibrium conversion, the addition of excess alcohol has been previously used, as the limiting step of the reaction is the attack of the carboxylic group by the alcohol. However, this strategy requires additional separation of

the alcohol. Recently, PV with MMMs comprising the metal-organic framework (MOF) MIL-101(Cr) and the polyimide Matrimid® has been used for the removal of water from the reaction environment [203]. The use of PV in such reactions is practically *in situ*; i.e., the membrane constitutes one of the reactor walls, as **Figure 5.5** depicts. For many years, water has been removed using hydrophilic polymeric membranes, and PV has been employed to promote esterification reactions for the synthesis of ethyl lactate [204,205], n-butyl acrylate [206], butyl acetate [207,208], diethyl succinate [209], and isobutyl propionate [210] through the use of chitosan/carbomer/polyacrylonitrile (PAN) composite, Pervap 2201, PervaTech, polyvinyl alcohol (PVA), PVA-polyethersulfone (PES) and polyvinyl acetate membranes.

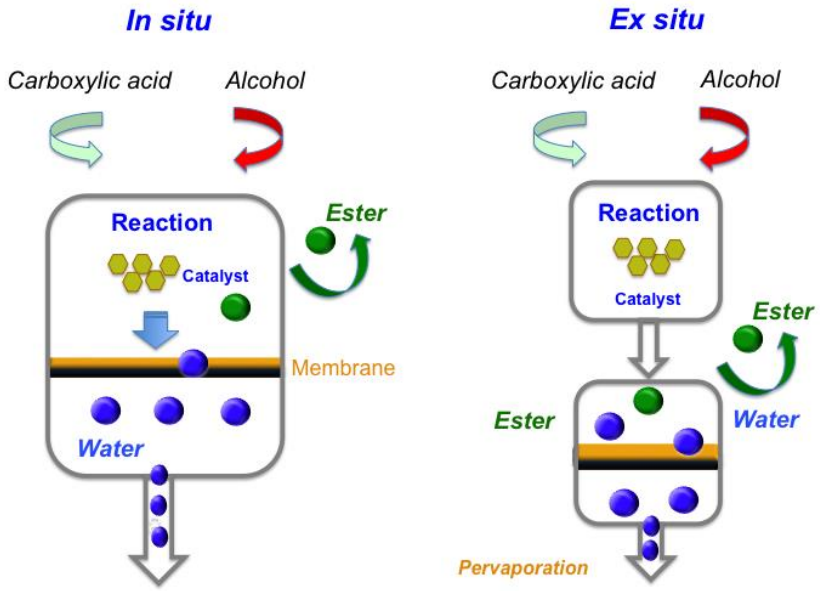


**Figure 5.5.** Pervaporation (PV)-assisted esterification reactions (*in situ* and *ex situ* modes).

PV has been mainly used for the removal of the water from esterification reactions to displace the chemical reaction equilibrium. Certainly, the esterification of lactic acid was the first PV-assisted reaction [211–213].The interest in this reaction stems from the production of ethyl lactate (also known as ethyl 2-hydroxypropanoate) by reacting lactic acid and ethanol. To the best of our knowledge, the first study using an MMM to assist the esterification of lactic acid was reported by Ma *et al.* [214] They proposed the use of hybrid membranes based on tetraethoxysilane (TEOS)-filled chitosan. This MMM could

remove water from the reaction mixture and could substantially enhance the ethyl lactate yield from 66 to 80% (at 80 °C). TEOS allowed the adjustment of the hydrophilicity of the membrane material, thereby enhancing the water removal efficiency.

Sorribas *et al.* [215] incorporated this MOF into a commercial hydrophilic polyimide (Matrimid® 5218), achieving a 63% reactant conversion (at 50 °C), higher than that of the batch reaction (47% for the non-PV-assisted reaction). These MMMs were able to remove water (0.35 $kg \cdot m^{-2} \cdot h^{-1}$), shifting the reaction towards the esterification products and increasing the total conversion; in fact, the permeate was nearly 90% water. Even though HKUST-1 is highly selective for water, higher permeation fluxes could be obtained by using other types of MOFs with a higher porosity (pore/cavities of 1.2/2.9 nm), such as MIL-101(Cr). For instance, de la Iglesia *et al.* [203] evaluated the performance of MIL-101(Cr) filled into Matrimid® 5218, demonstrating that these MMMs exhibited higher water stability in the reaction medium than HKUST-1-based MMMs (as shown in **Figure 5.6**).

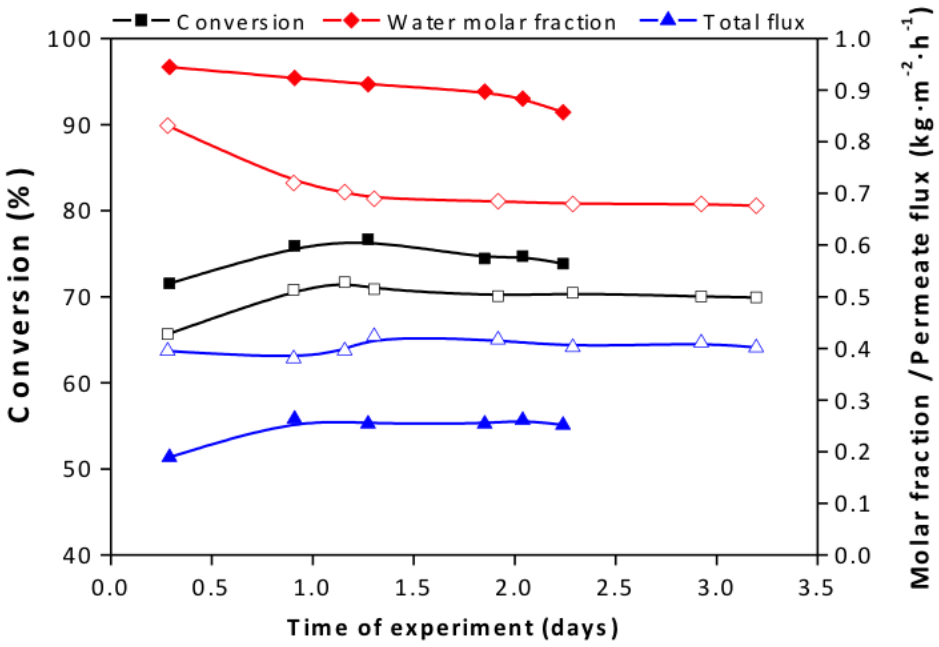


**Figure 5.6**. Effect of water removal on ethyl acetate conversion in a membrane reactor at 70 ° C (Data taken from de la Iglesia *et al.* [203]. Solid and hollow symbols correspond to the HKUST-1 and MIL-101(Cr) containing polyimide Matrimid® 5218 MMMs, respectively. The curves are only guides to the eye.

There was also no significant reduction in particle size arising from partial dissolution; however, their conversions were relatively similar, i.e., approximately 70.5 and 71.8% (at 70 °C) for the MIL-101(Cr) and HKUST-1 MMMs, respectively. Nevertheless, both MOF-based MMMs afforded better conversions than the pristine polyimide membrane (63.5%) and better water permeation fluxes (0.15-0.18 $kg \cdot m^{-2} \cdot h^{-1}$), more than two-fold higher than that of the pristine polymer (0.07 $kg \cdot m^{-2} \cdot h^{-1}$).

The enhancement was due to the large pore size of the filled MOF MIL-101(Cr): compared to HKUST-1 (smaller pore size), MIL-101(Cr) allows high water uptake at the hydrophilic sites near the metal centers and then enables the water molecules to propagate to the hydrophobic organic linkers [216,217]. In fact, the MIL-101(Cr) MMMs presented a water uptake of 15.8 wt.%, while that of the bare polyimide was approximately 2.5 wt.% [203].

### 5.5.Chapter remarks

Over the course of this chapter, it has been shown that a great number of azeotropic models are based on ethanol-water and water-ethanol mixtures. Indeed, it was also confirmed that technology-using MMMs seems to be one of the most attempted approaches to perform the task. Finally, based on the literature survey obtained, it is possible to summarize and address the following points:

- The polymers most used in membrane preparation are PVA, sodium alginate, chitosan PDMS, while in some cases their blending has been carried out in order to provide the possibility of modifying the membrane properties [138,218]. Furthermore, some other commercial polymers employed in other membrane fields, i.e. gas separation, have started to be implemented such as Pebax, PBI, PAAS, PBZ and Matrimid®5218. They could be another alternative in the way of looking for new membrane materials which can provide better characteristics in terms of ethanol dehydration [186,188]; where the chemical modification of these membrane materials is potentially carried out [128]. Finally, the synthesis of other polymeric materials has also been studied; for example, membrane materials based on pure copolymers such as butyl acrylate-styrene [144] which have shown their potentiality in PV even if, in case of styrene-butadiene-styrene, has not been used in MMMs until now.
- The most used fillers for the preparation of MMMs are zeolites (ZSM-5, KA, 3A, 13X, 4A, 5A, NaX, NaY, silicalites), but additionally some other new types

of fillers have been used, such as silicas, PZSN, MWCNT, POSS, MOFs (ZIF-8, ZIF-71, MIL-53), Cloisite 15A and PSS-2. Based on our literature study, the production of MMMs using different types of dispersed phases is a consolidated approach in ethanol separation and ethanol dehydration at lab scale.

- Different types of chemically modified fillers have been incorporated in polymeric membranes, such as Cl-, $NH_2$- and N- modified silicalite-1, VTES modified silicalite-1, silane-NaA zeolite, silane-modified ZSM-5, functionalized graphene sheets, and ZIF-8-$NH_2$. Thus, the chemical modification of the fillers is a current approach and a challenge in order to improve some properties such as hydrophobicity [140], hydrophilicity [198], affinity between filler-polymer [219,220], or trying to reduce the swelling degree of the polymeric membranes [187].
- Starting attempts of chemical cross-linking (using fumaric acid, glutaraldehyde) in polymers, aiming to enhance the selectivity of PV membranes, have been proposed [177,221]. The procedure is able to improve the chemical and mechanical resistance of most of the polymers; therefore, it improves their separation properties. But additionally, this procedure contributes to reduce the swelling in polymers, which has been identified as a limiting point of PV technology for ethanol-water and water-ethanol mixtures.
- Only a few works on MMMs deal with the use of multicomponent feed mixtures in PV, therefore, more efforts should be oriented in this direction for tests closer to reality [187,222,223]. In fact, real bulk solutions contain large different types of components, e.g. bioethanol separated from biomass, fermentation broth [138], which could also reduce the performance of the existing membranes.

Overall, the application of PV technology will continue for the dehydration of many chemical compounds, on the basis of the great success obtained with ethanol. Moreover, the flexibility of PV to be combined with other technologies in hybrid processes can easily allow its establishment in industries. It is also worth to mention that the dehydration process using MMMs in PV during the synthesis of organic compounds has started to be developed, e.g. esterification reaction between carboxylic acids and alcohols [203,215], since the water produced as a by-product affects the reaction efficiency. In the future, it is also expected that hybrid processes based on PV and distillation will find new opportunities, especially in water removal applications.

Therefore, it has been identified that Matrimid polyimide, as a hydrophilic polymer, has not been used for any PV application. In this regard, it is a potential candidate for an organic-organic separation. In **Chapter 6**, we proposed, for the first time, the separation of azeotropic methanol (MeOH)- methyl *tert*-butyl ether (MTBE) mixtures. On the other hand, in **Chapter 7**, we investigated the enhancement of the most used commercial polymer in pervaporation (polyvinyl alcohol) by the addition of a highly hydrophilic material, like graphene oxide (GO), for the dehydration of ethanol, where PV finds its main application at large scale processes.

# *Chapter 6*

## Matrimid®5218 dense membrane for the separation of azeotropic MeOH-MTBE mixtures by pervaporation

### Chapter overview

In this chapter, Matrimid®5218 dense membranes were produced using NMP by solvent evaporation. The membranes have been used, for the first time, in pervaporation (PV) separation of azeotropic methanol (MeOH)- methyl *tert*-butyl ether (MTBE) mixtures (14.3 and 85.7%, respectively). The membranes were characterized by TGA, SEM, DSC, contact angle and swelling tests. The PV experiments were carried out at different feed temperatures (25-45ºC) and vacuum pressures (0.0538, 0.2400, 2.1000 mbar). Moreover, an analysis of the PV process through the Arrhenius relationship has been provided. Finally, the Matrimid PV performance was compared with other polymeric membranes at the azeotropic conditions.

### 6.1.Introduction

Pervaporation (PV) technology, as the combination of permeation and evaporation processes, is efficiently able to separate organic-organic mixtures formed by close-boiling compounds [121,162,224,225]. Methanol (MeOH)- methyl *tert*-butyl ether (MTBE) is one of the most studied organic/organic mixture. The importance of this separation lies in the fact that MTBE is an octane enhancer which is used to produce lead-free gasoline aiming the reduction of air pollution. Even though its use has been limited in some countries (e.g. USA) due to the groundwater contamination, it is still used in European and Asian countries in order to satisfy the growing demand of fuel worldwide production [226]. On the other hand, the primary applications for MeOH are the production of chemicals and the use as a fuel. The reacting MeOH with isobutylene produces MTBE forming a minimum boiling azeotrope at a composition of 14.3% MeOH and 85.7% MTBE [227]. In MTBE production, the excess of MeOH is commonly removed from the final product by using distillation; however, this process is not energy efficient due to the formation of the azeotropic organic-organic mixture [228].

Today, PV technology represents a valid candidate for the replacement of conventional separation processes, such as distillation, for the separation of azeotropic mixtures [136]. Taking into account the similar nature of MeOH and water, many hydrophilic polymers have been proposed in the preparation of polymeric membranes for MeOH-MTBE separation, including cellulose acetate (CA) [229], CA-poly(N-vinyl-2-pyrrolidone) (PVP) blend [230], poly(vinyl alcohol) (PVA) [228,231,232], poly(lactic acid) (PLA) [233], polyarylethersulfone with cardo (PES-C) [234], poly(ethylene-co-vinyl acetate) (EVAc) [235], modified poly(ether ether ketone) (PEEKWC) [136], PVA-CA blend [236], acrylic acid plasma polymerized poly(3-hydroxybutyrate) [237], cross-linked 2-hydroxyethyl methacrylate (PAMHEMA) [238]. To the best of our knowledge, there is no report on the use of Matrimid® 5218 membranes for the separation of MeOH-MTBE azeotropic mixtures. Matrimid® 5218 has been used just for the dehydration of alcohols (ethanol,1-butanol, t-butanol, isopropanol), MTBE, and acetic acid [122,169,239,240] and never for the separation of organic-organic mixtures. Generally, this polymer has been widely studied for gas separation [105], and minimally for other membrane processes e.g.

hyperfiltration of methyl ethyl ketone-toluene mixture [241] and organic solvent nanofiltration [242]. Matrimid® 5218 is a commercial polyimide which presents excellent thermal stability and mechanical performances, e.g. high tensile strength (72.2 MPa), elongation at break (19.40 %) and Young's module (1410.4 MPa) [10,28,35]. As most of the polyimides, is stable in most organic solvents (hexane, MeOH, benzene, toluene, MTBE, acetone, to mention just a few) and weak acids [243]. It has also high affinity to water molecules based on its hydrophilic nature.

Based on the evidence that hydrophilic polymeric membranes are potential candidates for MeOH-organic separation by means of PV, in the present study, we propose Matrimid® 5218 dense membranes, thanks to its chemical resistance and hydrophilic nature, for the separation of the MeOH-MTBE azeotropic mixture. The effect of operating conditions, such as feed temperature and vacuum pressure in permeate side, on total permeate flux and separation factor was investigated. In addition, the Matrimid® membranes were characterized by thermo-gravimetric analysis (TGA), differential scanning calorimetry (DSC), scanning electron microscopy (SEM), degree of swelling (DS), and water contact angle.

## 6.2.Materials and methods

### 6.3.1. Materials

The polymer specifications are the ones specified in the **Chapter 3** (section 3.2.1). Regarding the solvent for the preparation of the azeotropic mixture, methanol (99.8%), methyl *tert*-butyl ether (MTBE) (99.7%), were purchased from Sigma-Aldrich (St. Louis, USA) and used without further purification.

### 6.3.2. Methodologies

#### 6.3.2.1.Membrane preparation

The pure Matrimid® 5218 dense membranes were prepared following the fabrication procedure described in the **Chapter 3** (section 3.3.1). Finally, the membranes were stored in a desiccator up to be characterized and tested. The final thickness of the membranes was 64±3.6 μm.

#### 6.3.2.2.Membrane characterization

Similarly, the characterization techniques, such as SEM, TGA, DSC, have been also described in the **Chapter 3** (from section 3.3.1). The additional characterization for the PV application is detailed as follows:

#### *6.3.2.2.1. Degree of swelling (DS)*

The degree of swelling (DS) of the Matrimid membrane was investigated for pure feed components (MeOH, MTBE), different MeOH-MTBE mixtures (25, 50, 75 wt.% MeOH) as well as azeotropic mixture (14.3% MeOH and 85.7% MTBE). The procedure previously reported by Zereshki *et al.* [233] was followed: three small pieces of membranes (1x5 cm) were weighed and immersed in the mixtures at 30ºC for 48 h. The wet membranes were quickly wiped with tissue paper to remove the excess free liquid on their surface and weighed with a digital balance (Gibertini, Crystal 500, Italy, Crystal 500, Gibertini Elettronica srl, Milan, Italy) with an accuracy of 0.001 g. Basically, the DS was calculated as follows [136]:

$$DS(\%) = 100\,\frac{W_w - W_d}{W_d} \qquad \textbf{(1)}$$

where $W_w$ and $W_d$ were the weights of the membranes in wet and dry states, respectively.

#### *6.3.2.2.2. Water contact angle*

The water contact angle measurements were performed using ultrapure water by the method of the sessile drop using a CAM200 instrument (KSV Instrument LTD, Finland). The average and standard deviation values were determined for five measurements.

#### *6.3.2.2.3. Mechanical tests*

Mechanical properties were evaluated before and after soaking the Matrimid membranes in a MeOH/MTBE solution (at the azeotropic point) for 24 h in order to measure its mechanical stability even after treatment in the PV process. Measurements were carried out with a Zwick/Roell testing machine, single column model Z2.5, equipped with a 50 N maximum load cell (BTC-FR2.5TN-D09, Germany).

### 6.3.4. Pervaporation tests

The PV experiments were performed in a laboratory-scale setup shown in detail on **Figure 6.1**.

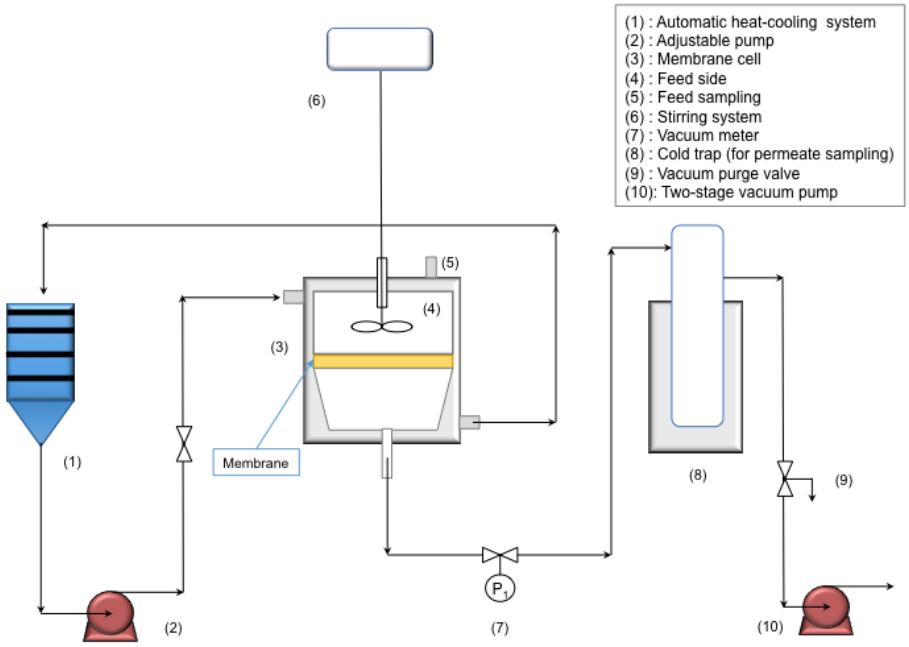


**Figure 6.1.** Scheme of the PV setup used for the experiments.

An azeotropic MeOH-MTBE (14.3% -85.7%, respectively) feed solution (250 mL) was poured in the feed tank. The feed temperature (at 25, 35, 45 ºC) was controlled with an accuracy of 0.01 ºC using a thermo digital circulating bath (Neslab RTE-201, USA). The vacuum on permeate side (at 0.0538, 0.2400, 2.1000 mbar) was controlled by using a RV5 two-stage vacuum pump (Edwards, UK).

The membrane, with a membrane area of 9.6 $cm^2$, was located on a porous support within the membrane cell. The permeated vapor was condensed and collected in a glass trap located in a liquid nitrogen condenser. Up to reach the steady-state, the permeates were collected for 5 h and weighted in order to calculate the total permeate flux. The total permeate flux (J) was calculated as follows:

$$J = \frac{Q}{A\ t} \qquad (2)$$

where $Q$ is the weight of the permeate (kg), $A$ is the membrane area ($m^2$) and $t$ is the operating time (h). The partial flux ($J_i$) for component $i$ was determined by multiplying

its weight fraction ($y_i$) in the collected permeate by the total permeate flux ($J$), as given in following Eq. (3):

$$J_i = y_i J \tag{3}$$

The separation factor (α) or MeOH selectivity was calculated based on Eq. 4:

$$\alpha = \frac{y_{MeOH} / y_{MTBE}}{x_{MeOH} / x_{MTBE}} \tag{4}$$

where $y$ and $x$ are the weight fractions of the components in the permeate and feed, respectively. The permeate composition was determined by an Abbe 60 type direct reading refractometer (Bellingham+Stanley Ltd., UK) at 25 ºC. The $J$ and $\alpha$ values are the averages of more than two runs to ensure the accuracy of the results.

## 6.3.Results and discussion

### 6.3.1. Membrane characterization

6.3.1.1.DSC ($T_g$), TGA, SEM and water contact angle determination

The glass transition ($T_g$) temperature for Matrimid® membranes was around 310.14 ± 0.22 ºC, which is in agreement with previous reports [51,72]. Concerning the TGA curve for Matrimid® which can be seen in **Figure 6.2**, a ~10% weight loss starting from 50 up to 300 ºC was revealed. This typical thermal behaviour of Matrimid® membranes has been documented before [95], where the weight loss is generally attributed to the presence of residual solvent or guest molecules [28]. Lately, Matrimid® membrane presented good thermal stability from 300 up to reach ~470 ºC. After this, a decomposition temperature was observed at ~520 ºC [45], followed by a degradation step up to 650ºC with a ~46% weight loss.

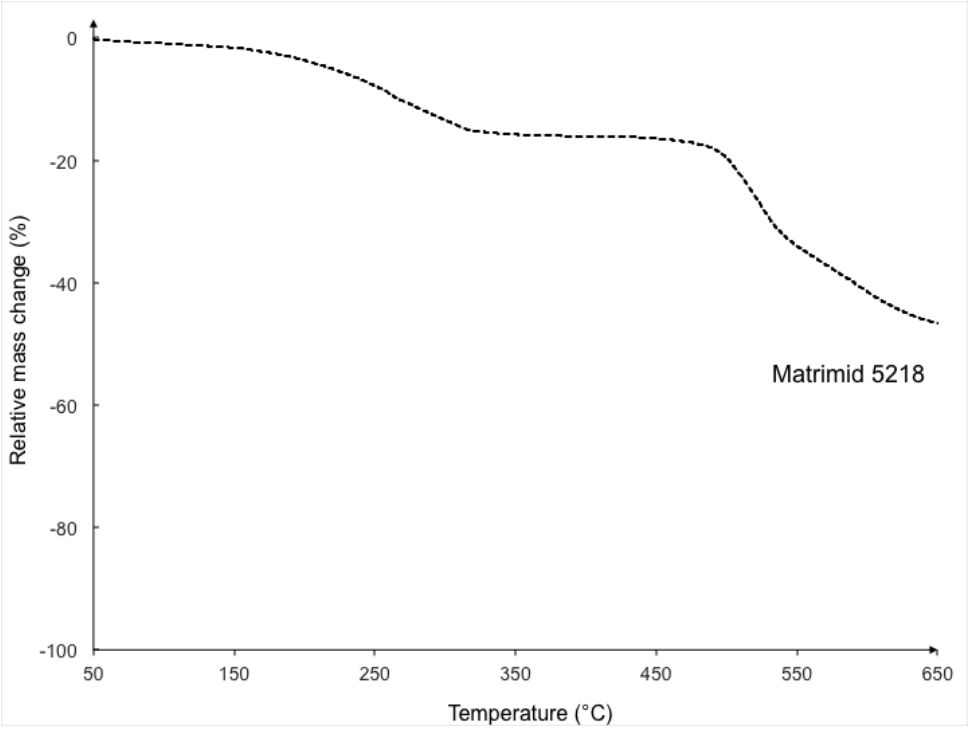


**Figure 6.2**. TGA profile of Matrimid®.

Regarding the morphological structure, **Figure 6.3** shows the surface and cross-section SEM images. In case of surface view, Matrimid® membrane showed a uniform and smooth surface characteristic without signs of plastic deformation, which is common for dense polymeric membranes [86,244]. On the other hand, a crater-like pattern was observed in cross-section view which has been already reported by Loloei *et al.* [72]. Typically, this crater-like pattern is generated during deformation by the freeze fracture [51].

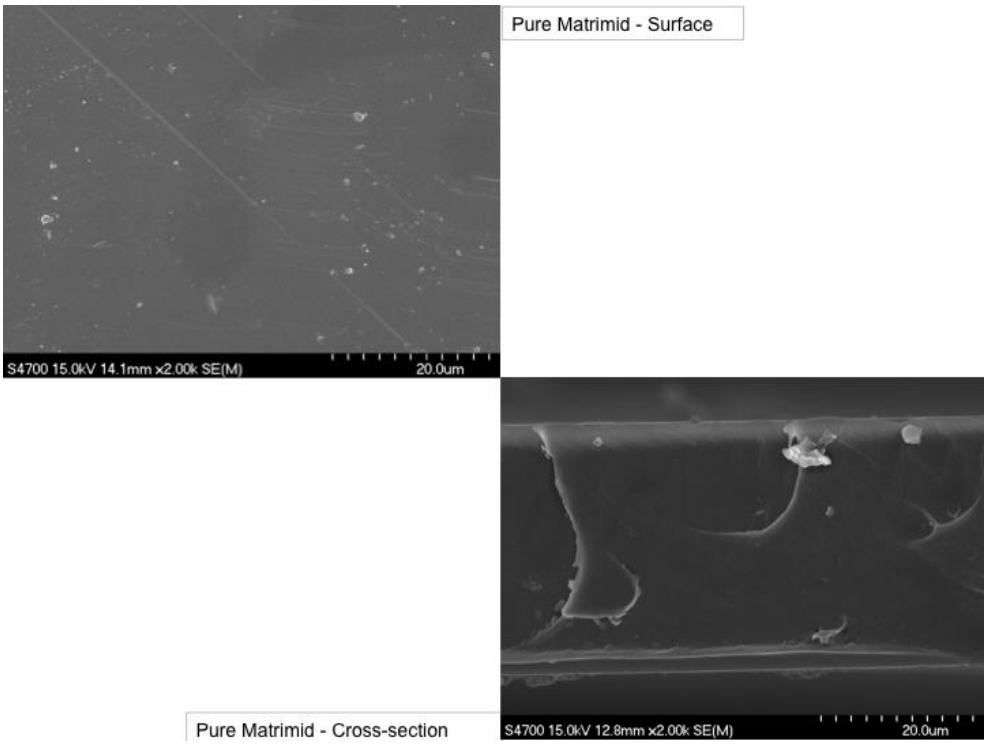


**Figure 6.3**. Membrane surface and cross-section SEM images of Matrimid®.

The measured water contact angle value for Matrimid® membrane was around 74.36º±4.72, which is in agreement with the value reported by Fatyeyeva *et al.* [245], around 75 and confirms the hydrophilic nature of the membrane (as also showed in **Figure 6.4**). This behaviour is at the basis of the Matrimid® higher affinity for water and polar molecules such as methanol. Typically, the hydrophilicity of this polymer is attributed to the preferential interaction between the water molecules and its imide groups. Therefore, Matrimid® membranes can be considered as promising candidates for the PV separation of polar/non-polar mixtures.

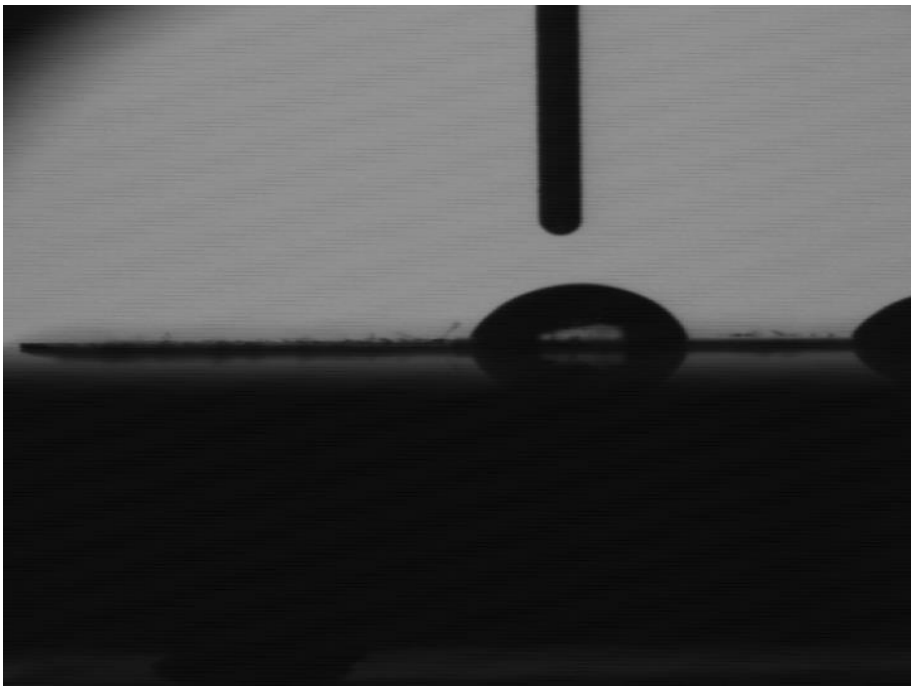

**Figure 6.4**. Image of water contact angle for Matrimid®5218 membrane.

6.3.1.2.Degree of swelling (DS) test

The calculated swelling results are represented in **Figure 6.5.** Basically, an increasing trend of swelling was noted as the MeOH concentration increased, displaying the highest swelling degree with pure MeOH around ≈ 9.6%. The results obtained by DS measurements can be used for the prediction of membrane chemical stability once in contact with the organic feed solution during the PV tests. The relative low values of DS prove the solvent resistance of the membrane and its dependence on MeOH concentration. The higher DS for MeOH (about 9.6%) than MTBE (about 3%) indicates the higher affinity of the membrane material for the more polar alcohol respect to the ether. In case of the azeotropic mixture, Matrimid® presents a DS lower than 5%. For the different MeOH concentrations, Matrimid® tends to suffer relatively higher DS values in comparison with PEEKWC (2-7%) [136] and PLA (5-12%) [233] membranes but it can still be considered resistant for those solvents.

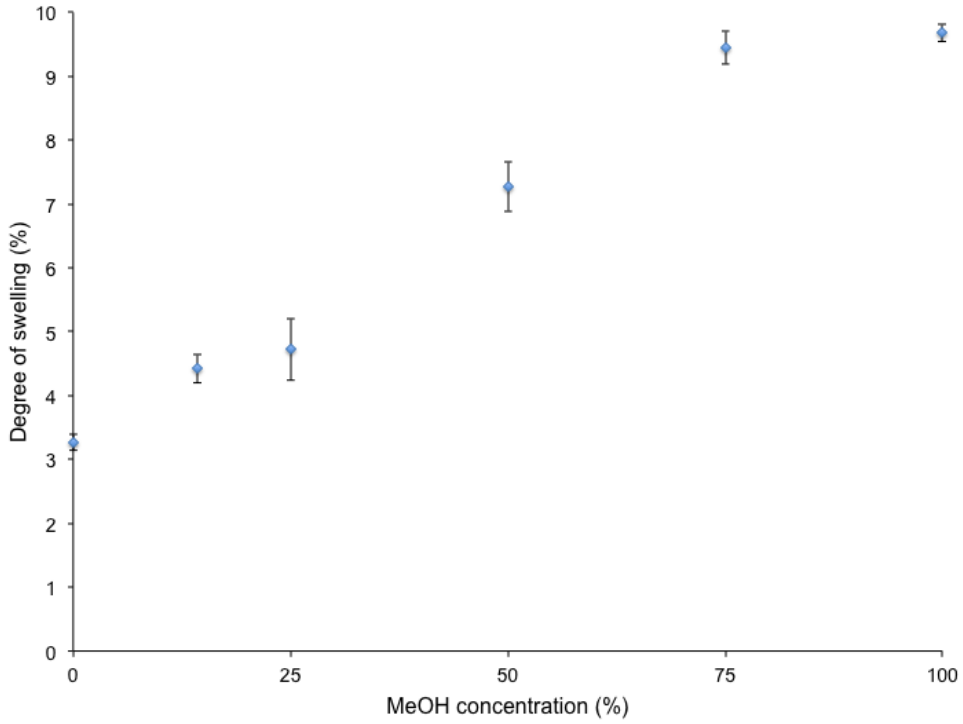


**Figure 6.5.** Degree of swelling of Matrimid® membrane at different MeOH concentrations (at 30ºC)

Since Matrimid® dense membranes were proposed for such PV separation, and the solution-diffusion mechanism governs the transport of species in dense membranes, the analysis of the solubility parameters takes an important relevancy. For instance, **Table 6.1** contains the Hansen solubility parameters of the dispersive ($\delta_d$), polar ($\delta_p$) and hydrogen bonding ($\delta_h$) contributions for MeOH, MTBE, and Matrimid®. While the total solubility ($\delta_T$) is listed as well, the calculated value was obtained by using the contributions of those three imposing concepts as describes Eq. 5

$$\delta_T = \sqrt{\delta_d^2 + \delta_p^2 + \delta_h^2} \qquad (5)$$

Typically, closer values of the solubility parameters indicate higher compatibility and hence solubility of a polymer-solvent pair [136,246], being the hydrogen bonding ($\delta_h$) and polar ($\delta_p$) contributions the ones that indicate strong affinity or compatibility between solvent and polymer [136,247,248]. In fact, the $\delta_h$ and $\delta_p$ contributions of MeOH-Matrimid present closer values each other. Moreover, the hydrophilic nature of the polymer and the polarity of the solvent molecule are also crucial for a polar/non-polar separation; it means, for the polarity of MeOH molecule, hydrophilic membranes are favored for separating MeOH from MTBE (as non-polar solvent). It worth to remind that water (H-O-H) and alcohols (R-O-H) are able to form hydrogen bonds with

polyimides displaying proton acceptor groups on their backbone, and such interaction strongly plays an important role in the transport properties and separation performance of those compounds [249]. Indeed, this is in agreement with the higher degrees of swelling in MeOH enriched solutions confirming the preferential MeOH absorption in membrane polymeric structure. On the other hand, this phenomenon could not occur in ethers (R-O-R), like MTBE, because alkyl or aryl groups replace the hydrogen atoms. This particular interaction supports the success of polyimides during the separation of this organic-organic mixture [250,251].

**Table 6.1.** Solubility parameters of the feed components and Matrimid® [136,169].

| Membrane material | Solubility parameter ($MPa^{1/2}$) | | | |
|---|---|---|---|---|
| | $\delta_d$ | $\delta_p$ | $\delta_h$ | $\delta_T$ |
| MeOH | 15.1 | 12.3 | 22.3 | 29.6 |
| MTBE | 15.5 | 3.6 | 5.2 | 16.7 |
| Matrimid® | 18.7 | 9.5 | 6.7 | 22.0 |

From the mechanical tests carried out on the Matrimid® membrane before and after soaking in the MeOH/MTBE solution, as can be seen from **Table 6.2**, no appreciable variations in its mechanical properties (Young's modulus and elongation at break) were observed. This result was an indication of the stability of the membrane material towards the organic/organic solution used.

**Table 6.2.** Mechanical properties of Matrimid® membrane before and after exposure to MeOH/ MTBE solution.

| | **Young's modulus ($N/mm^2$)** | **Elongation at break (%)** |
|---|---|---|
| **Matrimid® membrane before treatment** | 1100 ± 137 | 24 ± 3 |
| **Matrimid® membrane after exposure to MeOH/MTBE solution** | 1024 ± 159 | 22 ± 4 |

### 6.3.2. Pervaporation tests

*6.3.2.1.Effect of feed temperature*

**Figure 6.6** displays the effect of feed temperature on total permeate flux and separation factor at specific vacuum pressure. Basically, an increase on total permeation was observed with temperature increase. Typically, the polymer chains tend to be more flexible at higher temperatures promoting the sorption ability of the components, leading to the increase of permeating compounds through the intermolecular distances of the polymeric membrane. Regarding the separation factor (MeOH selectivity), it increases as a function of the feed temperature as well. This atypical tendency has not reported with other hydrophilic membranes based on PLA [233], PEEKWC [136], PVA [232], EVAc [235] CA-(PVP) blend [230] used for the MeOH-MTBE separation, where the decrease in separation factor was observed when the feed temperature was increased.

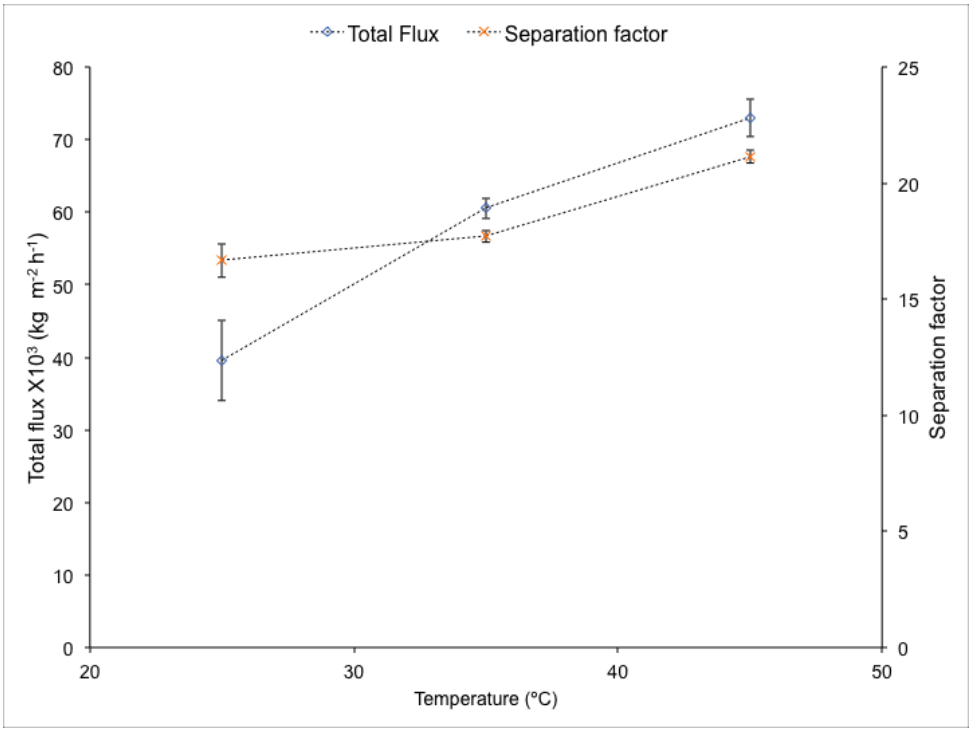


**Figure 6.6.** Effect of feed temperature on total flux and separation factor (feed composition: 14.3 wt.% MeOH; 85.7 wt.% MTBE, pressure: $5.4x10^{-2}$ mbar).

Generally, in fact, the thermal motion of the polymeric chains facilitates the diffusion of larger molecules (like MTBE) through the membrane causing a decrease in membrane separation factor.

The analysis of the temperature dependence on permeate fluxes by using the well-known Arrhenius model (Eq. 6) [136], can also be useful for the analysis of the temperature effect on the separation factor:

$$J = J_0 \exp\left(-\frac{E_P}{RT}\right) \quad (6)$$

Where $J_o$ is the pre-exponential factor, $E_P$ is the apparent activation energy for permeation (in this case for each component and total), R is universal gas constant and $T$ is the temperature. The linearization of the Eq. (6) leads the plotting of **Figure 6.7**, which displays the total and partial fluxes as a function of the reciprocal temperature at azeotropic conditions. The figure confirms that an Arrhenius relationship exists between fluxes and feed temperature, e.g. the total flux tends to increase with the increase of the temperature. Furthermore, the apparent activation energy ($E_P$), which can be calculated as the slope of the curve, can provide an outlook of the relationship between the total flux and the flux of specific permeating compound. At azeotropic conditions, it can be seen that the $E_P$ values for total and MeOH fluxes were around 10.6 kJ $mol^{-1}$, while for MTBE was 5.49 kJ $mol^{-1}$. The similarity of $E_P$ values for total and MeOH flux let conclude that temperature (in the range of 25-45 ºC) affects mainly the permeation of MeOH, and does not influence strongly the MTBE permeation. Therefore, this affects the separation factor significantly as well.

Furthermore, the partial flux for each component increases also as a function of the feed temperature (see **Table 6.3**); however; it can be noted that the MeOH permeation is more pronounced than the MTBE one as the feed temperature increases. This is in agreement with the increase of the separation factor.

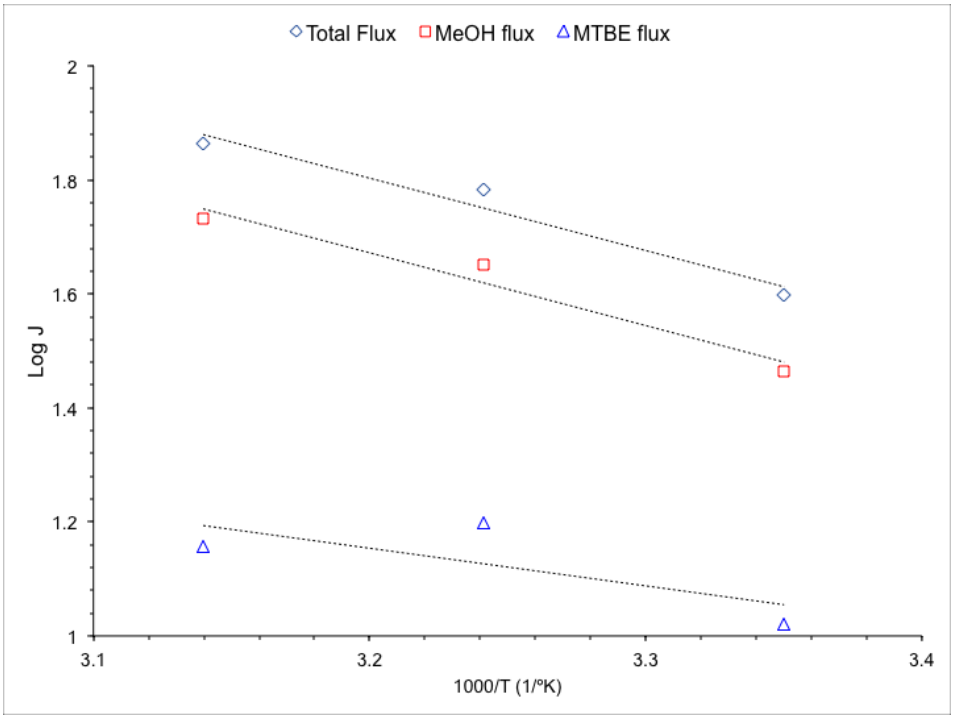


**Figure 6.7.** Temperature dependence of permeate fluxes by Arrhenius plot (feed composition: 14.3 wt.% MeOH; 85.7 wt.% MTBE, pressure: 5.4x10$^{-2}$ mbar).

Generally, an enhancement of the diffusion coefficients of the components at high temperatures could also increase the mass transfer [136]; in this case, the temperature is influencing more on MeOH than MTBE, this possible enhance on MeOH diffusion coefficient can explain the higher MeOH permeation rate observed in comparison with MTBE. While the thermodynamic and physicochemical properties of the organic compounds play an important role in their transport through polymeric materials [232], i.e. the solubility parameters, that for MeOH tend to be higher than MTBE for several hydrophilic polymers [236].

**Table 6.3.** Performance of Matrimid membrane as a function of feed temperature (feed composition: 14.3 wt.% MeOH; 85.7 wt.% MTBE, pressure: 5.4x10$^{-2}$ mbar)

| Temperature (ºC) | Total flux (kg m$^{-2}$ h$^{-1}$) x10 $^{3}$ | MeOH partial flux (kg m$^{-2}$ h$^{-1}$) x10$^{3}$ | MTBE partial flux (kg m$^{-2}$ h$^{-1}$) x10$^{3}$ | Separation factor (α) |
|---|---|---|---|---|
| **25** | 39.57±5.53 | 29.20±5.15 | 10.47±0.37 | 16.66±0.71 |
| **35** | 60.53±1.39 | 44.73±1.02 | 15.79±0.36 | 17.71±0.25 |
| **45** | 73.03±2.60 | 54.09±6.78 | 14.34±2.31 | 21.16±0.29 |

*Data represents the means ± standard deviation with 3-4 replicates for each test.*

In addition, from solubility parameters (δ) of the feed components, it can be determined some thermodynamical properties, as energy of vaporization (ΔE, kJ $kg^{-1}$), through the following Eq. (7):

$$\delta = \sqrt{\frac{\Delta E}{V_m}} \qquad (7)$$

where the relation $\Delta E / V_m$ is called "cohesive energy density" which is defined as the energy needed to remove a molecule from its nearest neighbours per molar volume ($V_m$) of a volatile compound. The $V_m$ of each compound is defined as ratio of its molecular weight and density [247]. The calculated ΔE values for MeOH and MTBE are $1.19 \times 10^{-3}$ and $1.98 \times 10^{-3}$ kJ $kg^{-1}$, respectively. This means that MeOH needs less energy than MTBE to be removed from the azeotropic mixture and its permeation through the membrane is thus favored.

*6.3.2.2.Effect of vacuum permeate pressure*

Based on the evidence that best performance of Matrimid® membrane was found at 45 ºC, the influence of vacuum pressure on total flux and separation factor at such temperature was investigated, as showed in **Figure 6.8**. It can be seen that the increase of vacuum pressure (from 2.1 to 0.05 mbar) increases the total permeate flux. In PV process, in fact, the driving force is represented by the difference in vapor pressure at the two sides of the membrane. Increasing the vacuum pressure leads to an increase in the driving force and, therefore, to an improvement of the total flux. This was also mathematically studied and confirmed [252].

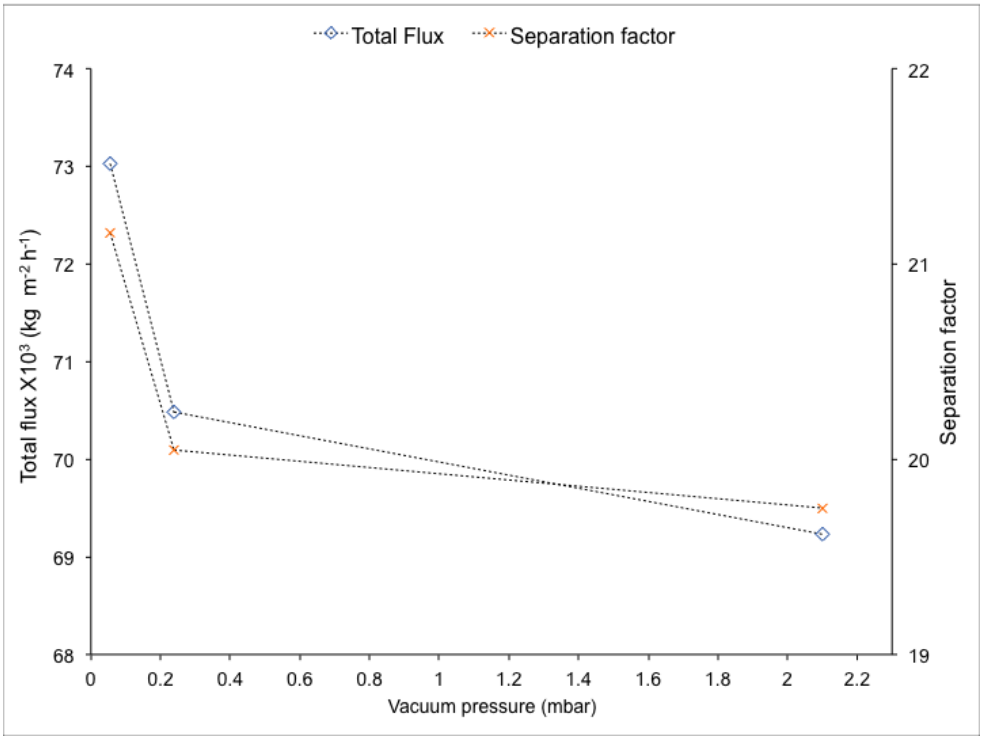


**Figure 6.8.** Effect of vacuum pressure on total flux and separation factor (feed composition: 14.3 wt.% MeOH; 85.7 wt.% MTBE, temperature: 45 ºC).

In addition, it can be noticed that the increase of vacuum pressure promotes the MeOH permeation (see **Table 6.4)**, while a decrease on MTBE permeation is observed. This behavior has been already observed by Peivasti *et al.* [232] for PVA membranes. They reported, in fact, that the MTBE permeation rate decreases due to the driving force enhancement which tends to decrease the membrane plasticizing effect which reduces the motion of the polymer chains. This behavior leads to the preferential permeation of the smaller MeOH molecules, restricting the permeation of the bigger MTBE ones. An improvement in the separation factor is, thus, observed.

**Table 6.4.** Performance of Matrimid membrane as a function of vacuum pressure (feed composition: 14.3 wt.% MeOH; 85.7 wt.% MTBE, temperature: 45ºC)

| Pressure (mbar) | Total flux (kg $m^{-2}$ $h^{-1}$) x$10^3$ | MeOH partial flux (kg $m^{-2}$ $h^{-1}$) x$10^3$ | MTBE partial flux (kg $m^{-2}$ $h^{-1}$) x$10^3$ | Separation factor (α) |
|---|---|---|---|---|
| **5.4x$10^{-2}$** | 73.03±2.60 | 54.09±6.78 | 14.34±2.31 | 21.16±0.29 |
| **2.4x$10^{-1}$** | 70.49±0.13 | 53.87±0.18 | 16.62±0.05 | 20.05±1.56 |
| **2.1x$10^{0}$** | 69.23±3.35 | 52.93±5.90 | 16.29±2.55 | 19.75±3.52 |

*Data represents the means ± standard deviation with 3-4 replicates for each test.*

### *6.3.2.3. Comparison of Matrimid® pervaporation performance with other polymeric membranes*

The PV performance of polymeric membranes for any organic-organic separation, like MeOH-MTBE, depends directly on their properties (such as materials, nature, structure, thickness), physicochemical properties and concentration of the compounds contained in the mixture, as well as the operating conditions (temperature, vacuum pressure, feed flow rate and so on) [121]. This makes difficult to make a fair comparison of PV data with works where different conditions have been applied [253], bearing also in mind that this work is the first one dealing with the use of Matrimid® membranes for MeOH/MTBE separation. However, a comparison of the performance of Matrimid® membranes with other polymeric membranes used for the same separation at close azeotropic conditions, is showed in **Table 6.5**.

The best performance of Matrimid® membrane in terms of permeate flux and separation factor was at 45 ºC and 0.054 mbar, with values of about 0.073 kg $m^{-2}$ $h^{-1}$ and 21.1, respectively. In the case of permeate fluxes, the hydrophilic polyimide Matrimid® membrane displayed relatively better performance than other reported membranes, as PEEKWC (0.068 kg $m^{-2}$ $h^{-1}$) and cross-linked PVA (0.036 kg $m^{-2}$ $h^{-1}$), but lower performance than other polymers which have high permeability values such as

PVA-CA blend, PLA, PVA, PVA-CA blend, acrylic acid plasma polymerized poly(3-hydroxybutyrate), and cross-linked PAMHEMA. However, some of these highly permeable polymers do not offer high separation factor values, i.e. PLA (α=5), acrylic acid plasma polymerized poly(3-hydroxybutyrate) (α=3); where Matrimid® tends to offer better MeOH separation factor than those polymeric materials. Additionally, the polyimide membrane presents comparable separation factor with PVA membrane (α=25). On the contrary, Matrimid does not overcome the MeOH selectivity for chemically modified membranes including such as cross-linked PVA, cross-linked PAMHEMA, or blended materials such as PVA-CA, CA-PVP.

**Table 6.5.** Comparison of Matrimid® membrane performance with other studies at close azeotropic conditions.

| Membrane material | Concentration of MeOH-MTBE mixture | Operating conditions | J (kg $m^{-2}$ $h^{-1}$) | Separation factor (α) | Reference: |
|---|---|---|---|---|---|
| Matrimid® | 14.3 wt.% MeOH<br>85.7 wt.% MTBE | 45 ºC, 0.0538 mbar | 0.073 | 21.16 | This work |
| PEEKWC | 15 wt.% MeOH<br>85 wt.% MTBE | 40 ºC, 6.1 mbar | 0.068 | 10 | [136] |
| PVA | 30 wt.% MeOH<br>70 wt.% MTBE | 45 ºC, 15 mbar | 0.900 | 25 | [232] |
| PLA | 15 wt.% MeOH<br>85 wt.% MTBE | 30 ºC, 6 mbar | 0.620 | 5 | [233] |
| CA-PVP blend | 20 wt.% MeOH<br>80 wt.% MTBE | 45 ºC, 3 mbar | 0.225 | 340 | [230] |
| PVA-CA blend | 15 wt.% MeOH<br>85 wt.% MTBE | 45 ºC, 17 mbar | 796* | 1427 | [236] |
| Acrylic acid plasma polymerized poly(3-hydroxybutyrate) | 20 wt.% MeOH<br>80 wt.% MTBE | 45 ºC, 1.3 mbar | 11* | 3 | [237] |
| Cross-linked PVA | 20 wt.% MeOH<br>80 wt.% MTBE | 50 ºC, 0.4 mbar | 0.036 | 1230 | [231] |
| Cross-linked PAMHEMA | 11 wt.% MeOH<br>89 wt.% MTBE | 50 ºC, 1.33 mbar | 0.140 | 150 | [235] |
| Polyamide filled with $Al_2O_3$ | 50 wt.% MeOH<br>50 wt.% MTBE | 30 ºC | 15* | 20 | [254] |
| CA filled with HZSM5 | 20 wt.% MeOH<br>80 wt.% MTBE | 40 ºC, 3.3 mbar | 4.2* | 150 | [255] |
| Sulfonated polyarylethersulfone with cardo filled with $[Cu_2(bdc)_2(bpy)]_n$ | 15 wt.% MeOH<br>85 wt.% MTBE | 40 ºC, 6 mbar | 0.28 | 2300 | [256] |
| CA filled with ZnO | 31 wt.% MeOH<br>69 wt.% MTBE | 40 ºC, 5 mbar | 2* | 400 | [257] |

One of the current approaches in PV technology is the incorporation of organic-inorganic materials into polymeric membranes well known as mixed matrix membranes (MMMs), which leads the enhancement of separation performance. Some MMMs have been tested for such separation, e.g. polyamide filled with $Al_2O_3$ [254], cellulose acetate (CA) filled with HZSM5 [255], sulfonated polyarylethersufone filled with $[Cu_2(bdc)_2(bpy)]_n$ [256], and CA filled with ZnO [257], which have easily overcome the separation performance of Matrimid. While, the separation factor value of Matrimid (21.16) can be comparable just with MMMs based on polyamide filled with $Al_2O_3$ (separation factor around 20).

### 6.4.Chapter remarks

In this study, Matrimid® membranes have been successfully tested for the PV separation of MeOH-MTBE azeotropic mixture. The effect of some process parameters, such as feed temperature and vacuum pressure, has been evaluated. The best performance of Matrimid® membrane in terms of separation factor ($\alpha$=21.2) and permeate flux (0.073 kg $m^{-2}$ $h^{-1}$) for such azeotropic separation was found at 45 ºC and 0.054 mbar where the permeation of MeOH was favoured. Through the analysis of the PV process by Arrhenius relationship, it was found that the increase of feed temperature (from 25 to 45 ºC), determined not only the higher MeOH permeation with respect to MTBE, but also improved the separation factor, which is not commonly observed. The results showed that the Matrimid® performance, related to the PV separation of MeOH-MTBE mixture, are comparable with the ones observed for other polymers, considering also that the tested pure polyimide does not present any additional treatment (chemical modification, or blending). Based on the results obtained, it is possible to conclude that Matrimid® membranes have the potentiality to be used in PV for the separation of MeOH-MTBE azeotropic mixture. Moreover, this study can be considered as starting point for using of Matrimid® in the separation of other organic-organic mixtures.

# *Chapter 7*

## Towards the dehydration of ethanol using pervaporation cross-linked poly(vinyl alcohol)/graphene oxide membranes

### Chapter overview

In this chapter, a highly hydrophilic inorganic material, like graphene oxide (GO), was successfully prepared and incorporated into a cross-linked poly(vinyl alcohol) (PVA) matrix. The obtained mixed matrix membranes (MMMs) have been used for the dehydration of ethanol (10:90% water-ethanol) by pervaporation (PV), monitoring their performance in terms of total permeate flux, partial components fluxes, as well as their separation factor. The effect of filler was analyzed by doubling the GO content (at 0.5, 1.0, and 2.0 wt.%) in the MMMs. A complete analysis of the operating temperature (between 40-70 ºC) was carried out by the Arrhenius relationship.

## 7.1.Introduction

Pervaporation (PV), as the merging of evaporation and permeation processes, has been consistently proposed for separating different types of azeotropic and close-boiling compounds mixtures. The benefit of using this particular membrane process for such purposes is due to the fact that it displays high selectivity, efficiency and low-energy requirements [162,225]; this latest being the main feature of PV that indeed makes it attractive to be considered as a "Green" process. These processes are currently encouraged to meet the "*Twelve Principles of Green Chemistry*". Such principles, well-established by Anastas and Warner [258], are aimed to preserve the environment through implementing green chemistry methods. Moreover, PV is a good candidate for the replacement of the conventional distillation, which, for instance, carries out the separation of azeotropic mixtures at large-scale in petrochemical industry. PV has demonstrated the ability for separating different types of azeotropic mixtures, including organic-water, organic-organic and water-organic [126,259]. In particular, at industrial level, PV has found its growing use in industry towards water-organic mixtures, which implies the dehydration of organics to reach higher purification degrees, e.g. in ethanol [122], isopropanol [260] and acetonitrile [261].

To date, the dehydration of ethanol is the most sought application due to its direct impact on commercial value. According to the IEA (Industrial Ethanol Association, http://www.industrial-ethanol.org), the main market uses of ethanol concerns the manufacture of beverages, fuels and a multiple of industrial applications related to pharmaceuticals, cosmetics, detergents, printing inks, paints, coatings, medical uses, production of polymers and chemicals, to mention just a few. This makes the ethanol production continuously growing up, e.g. over 100 billion liters demand was reported by 2017 [147], and its demands is expected to increase in coming years. Typically, ethanol can be produced by fermentation or from direct hydration of ethylene. Regardless of the ethanol production process, the product is usually a diluted aqueous solution. At large-scale level, the product is processed by a distillation system to concentrate ethanol. The separation of ethanol and water is complicated due to the fact that ethanol and water form an azeotrope at 95.6 wt.% ethanol [151]. Thereby, it is a difficult task to produce pure ethanol from an azeotropic mixture by conventional distillation. Herein, the PV has been introduced as an alternative towards such purpose.

When dealing with the dehydration of any organic (e.g. ethanol), it is inevitable to address the use of hydrophilic membranes. At this point, several types of hydrophilic polymers have been proposed and investigated as membrane materials, such as polyimides [122], sodium alginate [183], polybenzimidazole (PBI) [189], chitosan [182], polyacrylonitrile (PAN) [172] and poly(vinyl alcohol) (PVA) [260]. Among all these polymers, PVA has been the only one to be consolidated at industrial level, for instance by DeltaMem AG. Today, one of the most successful trends in enhancing the performance of polymeric membranes implies the embedding of inorganic materials, generating the so-called mixed matrix membranes (MMMs). These combine the strengths of inorganic and polymeric membranes to ideally reach an enhanced synergistic performance. In this work, the possibility of incorporating a highly hydrophilic material, like graphene oxide (GO), into cross-linked PVA membranes, for achieving better performance, was studied. GO is a layered material produced by the oxidation of graphite. GO sheets are highly oxygenated having hydroxyl and epoxy functional groups on their basal planes, in addition to carbonyl and carboxyl groups located at the sheet edges. These functional groups provide a high hydrophilic profile to the material [17], which has been noted in PVA during organic-organic separations [262,263] .

Thereby, the aim of this work is to analyze the effect of GO on the preparation of cross-linked PVA MMMs used in ethanol dehydration. To the best of our knowledge, there is no report about this [259]. The effect of operating temperature on total permeates flux and separation factor was investigated by doubling the GO content (at 0.5, 1.0, and 2.0 wt.%) in the MMMs. Moreover, the pristine and MMMs were characterized by thermogravimetric analysis (TGA), differential scanning calorimetry (DSC), field emission scanning electron microscopy (FESEM), degree of swelling (uptake), X-ray diffraction (XRD) and measurements of water contact angle and mechanical properties.

## 7.2.Materials and methods

### *7.2.1. Materials*

Poly (vinyl alcohol) (PVA, MW:130,000), glutaraldehyde (grade II, 25 wt.%) and hydrochloric acid (HCl) were acquired from Sigma-Aldrich and used without further purification.

### *7.2.2. Synthesis of graphene oxide*

Graphene oxide (GO) was synthesized following the procedure described by Castarlenas *et al.* [2], according to the Hummers' method [264]. Basically, the graphite is oxidized by treatment with $KMnO_4$ and $NaNO_3$ in concentrated $H_2SO_4$. In a round bottom flask, sodium nitrate (1.5 g) was dissolved in 70 mL of concentrated sulfuric acid. The dispersion was put under stirring at room temperature until the $NaNO_3$ was dissolved (about 5-10 min). Therefore, graphite (3.0 g) (natural flake with a diameter of 5 μm, supplied by Richard Anton KG) was added to the solution under gently stirring for about 30 min to facilitate a homogeneous suspension. Later, $KMnO_4$ (9.0 g) was gradually added to the suspension to avoid the increase of the flask temperature due to the heat generated during redox reaction. Once the addition of $KMnO_4$ was completed, the temperature of the solution was slowly raised to 35 ºC and maintained for 30 min under stirring. To facilitate the control of the exothermic reaction an ice bath was put under the glass balloon. A brownish gray paste was formed. Then, by means of a Pasteur pipette, 140 mL of deionized water was slowly added to the slurry because of the smoke production was very fast. Once the deionized water was added, the suspension was kept stirring overnight at 95 ºC and then, 500 mL of deionized water was added followed by 20 mL $H_2O_2$ that reduced the residual permanganate. The round bottom flask was kept under stirring at 95 ºC for 3 h. The resulting mixture was filtered and washed using a 10 wt.% aqueous HCl solution. Finally, GO was centrifuged and washed with water 4 times at 10000 rpm for 15 min (Beckman Coulter, Allegra x-15 R), reaching the neutral pH, and dried at 80 ºC overnight obtaining 4.2 g of a light brown solid.

### *7.2.3. Mixed matrix membrane preparation*

PVA/GO MMMs were prepared by the dense-film casting method and solvent evaporation. PVA powder (3 g) was dissolved under stirring in 100 mL of distilled water at 90 ºC. The obtained solution was filtered to remove any insoluble impurities. GO was added to the PVA solution to produce the dope suspension that was stirred during 12 h and processed by sonication twice for 30 min each one. Afterwards, the in situ cross-linking procedure was performed by adding 0.1 mL of glutaraldehyde and 0.1 mL of HCl to the dope. This was stirred during 15 min, cast on a clean glass plate and then dried in an oven at 40 ºC during 2 days. After this, the MMMs were peeled from the glass plate. The GO loading for the MMMs was varied at 0.5, 1, and 2 wt.%.

**Figure 7.1** shows typical examples of the prepared membranes for this study, with a membrane thickness of 40±2 μm (measured with digital micrometer Mitutoyo with an accuracy of 1 μm).


**Figure 7.1**. Pure cross-linked PVA membrane and its MMMs-GO at different filler loadings.

### 7.3.Membrane characterization

#### *7.3.1. Field emission scanning electron microscopy (FESEM)*

The morphological structure of the membrane surface and cross-section of the cross-linked-PVA and its MMM membranes was evaluated using a field emission scanning electron microscope (FEI-Inspect, F20, USA). The cross-sections were obtained by cryogenic fracture of the samples immersing in liquid $N_2$. The samples were attached to SEM carbon stubs with a diameter of 2.54 cm using two-sided adhesive tape. The samples were coated through a sputtering process with gold-palladium (Au/Pd). The corresponding images were captured at suitable magnification.

#### *7.3.2. Differential scanning calorimetry (DSC)*

Differential scanning calorimetry (DSC) was conducted on a ca. 10 mg sample using a Mettler Toledo DSC822e system. The $T_g$ routine was performed in two cycles from

room temperature up to 450 °C at the temperature ramping of 20 °C·min$^{-1}$. The $T_g$ determination was done in triplicate.

### *7.3.3. Thermo-gravimetric analysis (TGA)*

Thermogravimetric analysis (TGA) was performed by using a Mettler Toledo TGA/SDTA 851$^e$. The analysis was carried out by placing the sample (around 10 mg) in an alumina crucible and heating up the samples to 750 °C at a ramping of 10 °C·min$^{-1}$ under air flow of 40 mL(STP)·min$^{-1}$ .

### *7.3.4. X-ray diffraction (XRD)*

X-ray diffraction (XRD) patterns of the GO and membranes were obtained by using a PANalytical Empyrean multipurpose diffractometer (40 kV, 20 mA) with a Cu-Kα (λ = 0.1542 nm) anode, from 2θ of 2.5° to 40° with a 0.03° step·s$^{-1}$.

### *7.3.5. Uptake*

The uptake of the cross-linked PVA and MMM membranes was investigated for the 10:90 wt.% water-ethanol mixture following the procedure previously reported by Choi *et al.* [185] Three small pieces of membranes (1x5 cm) were weighed and immersed in the mixture at 40 ºC for 48 h. The wet membranes were quickly wiped with tissue paper to remove the excess of free liquid on their surface and weighed with a digital balance (Kern, ABJ220-4NM, Germany) with an accuracy of 0.001 g. The uptake was, then, calculated as follows:

$$Uptake(\%) = 100\,\frac{W_w - W_d}{W_d} \qquad \textbf{(1)}$$

where $W_w$ and $W_d$ are the weights of the wet and dry membranes, respectively.

### *7.3.6. Water contact angle (CA)*

The water contact angle measurements were performed using ultrapure water by the method of the sessile drop using the Krüss DSA 10 MK2 instrument (Germany). The average and standard deviation values were determined for three measurements.

### *7.3.7. Mechanical properties*

Mechanical properties of pristine cross-linked PVA membranes and PVA MMMs were determined by following the same procedure in **Chapter 6** (section 6.3.2.2.3). At this

point, the mechanical tests were carried out on all the investigated membranes before and after soaking them in a water-ethanol solution (10:90 wt.%) at 25 ºC for 24 h.

### 7.4.Pervaporation performance test

The PV tests were performed in a semi-continuous laboratory-scale setup. A 10:90 wt.% water-ethanol feed solution (1000 mL) was poured in the feed tank. The operating temperature (at 40, 50, 60 and 70 ºC) was controlled with an accuracy of 0.01 ºC using a thermostat. The vacuum on permeate side was set at 3-4 mbar by using a RV3 two-stage vacuum pump (Edwards, UK).

The membranes, with a membrane area of 11.7 $cm^2$, were located on a porous support within the membrane cell. The permeated vapor was condensed and collected in a glass trap located in a liquid nitrogen condenser. Up to reach the steady-state, the permeates were collected for 8 h and weighted to calculate the total permeate flux *(J)* as described previously in **Chapter 6** (section 6.3.3). Similarly, the calculation for the determination of the separation factor is described in such section. In this case, The permeate concentration in samples was determined by means of gas chromatograph (Agilent Technologies, 7820A) equipped with a PORAPAK Q80/100 column using TCD and FID detectors. The *J* and $\alpha$ values are the averages of more than two 8 h runs to ensure the accuracy of the results.

### 7.5.Results and discussion

#### 7.5.1. Membrane characterization

##### 7.5.1.1.DSC, TGA, FESEM, XRD, mechanical properties, uptake and water contact angle measurements

The glass transition temperature ($T_g$) for cross-linked PVA membranes was around 95.6±2.8 ºC, as **Table 7.1** displays. This value is in agreement with the range (69-110 ºC) reported by previous studies [185,260,265]; while the MMMs exhibited higher $T_g$ values (around 104-110 ºC) than the pristine PVA membranes. It is well documented that the incorporation of inorganic fillers into a polymer may cause an increase in $T_g$ if there are strong attractive forces working between the filler surface and the polymer. Particularly, this change could be attributed to the hydrogen bonding between multiple oxygen containing functional groups of the GO laminates and the PVA chains rich in

alcohol groups [265]. **Figure 7.2** shows the TGA curves that can be related to the thermal degradation and stability of the GO and the cross-linked PVA-GO membranes.

The GO presented a first weight loss starting at around 55 °C, which is attributed to the loss of the water molecules that were retained in its structure. This loss accounted for 17.7% by weight of the total sample analyzed. The second weight loss that took place at 200 ºC, presumably due to pyrolysis of the labile oxygen-containing functional groups yielding CO, $CO_2$ and steam [266]. Therefore, the decomposition of GO can be accompanied by a vigorous expansion of the gas resulting from the rapid thermal expansion of the material [267] in agreement with the abrupt step observed. This weight loss corresponds to 72.4% by weight of the total material. The last weight loss took place at 550 ºC and it is due to the combustion process. As observed, once dehydrated at ca. 100 ºC, the pristine cross-linked PVA membrane has its degradation step between 300-510ºC, which corresponds to the complete decomposition of the PVA (weight loss around 85%). Similarly, its MMM-GO membranes presented a first gradual weight-loss (15-19%) starting at 55 ºC, which is more remarkable at the high GO loading.

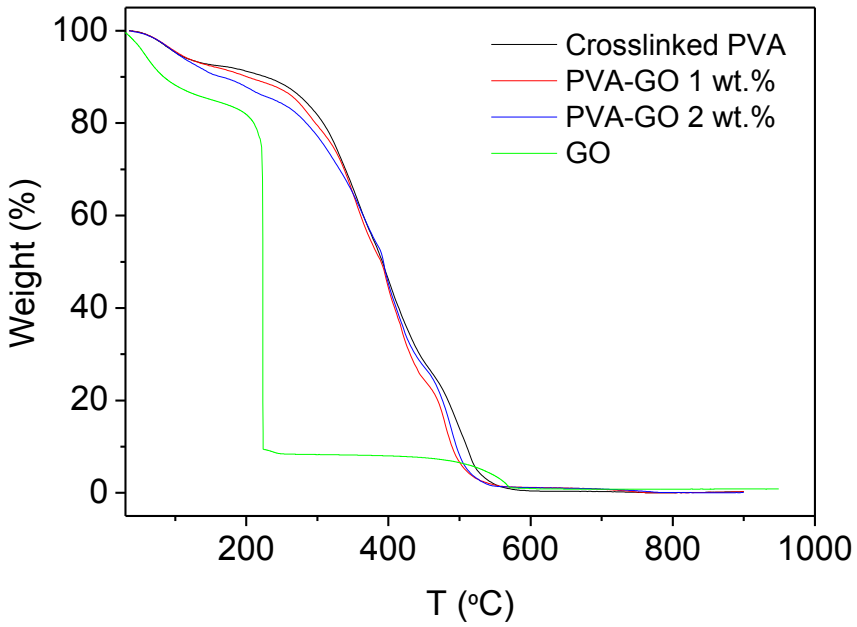


**Figure 7.2.** TGA curves of the cross-linked PVA membranes and its MMMs.

This is probably attributed to the loss of the water molecules that could be retained in the GO structure, as well as the water retained in the possible interfacial voids between the GO and PVA matrix. In particular, there was a weight-loss (between 175-275 ºC)

for the MMMs, which was increased as filler loading increase. This can be related to the GO decomposition. Moreover, the MMMs also presented their degradation step starting at 300 ºC up to 500. This represents a weight-loss of about 80-85%.

**Figure 7.3** shows the surface and cross-section FESEM images of the membranes. In case of surface view, the pure cross-linked PVA membrane (see **Figure 7.3a**) showed a uniform and smooth surface characteristic without signs of plastic deformation, which is common for cross-linked PVA dense membranes [268]. Whereas the MMMs-GO containing 1 and 2 wt.% of GO slightly lost the uniform surface by increasing the GO content (see **Figure 7.3c** and **7.3 e**), which could be attributable to the exposure of flaky GO on membrane surface.

**Table 7.1**. $T_g$ and contact angle (CA) values of the pure cross-linked PVA membranes and its MMMs-GO.

| *Membrane* | $T_g$ *(ºC)* | *CA (º)* |
|---|---|---|
| Pure cross-linked PVA | 95.6±2.8 | 69.6±0.5 |
| Cross-linked PVA + 1 wt.% GO | 104.3±0.9 | 59.9±1.2 |
| Cross-linked PVA + 2 wt.% GO | 109.6±1.4 | 58.4±0.5 |

In cross-section view, pure cross-linked PVA membrane presents a typical crater-like pattern which has been already reported by Amirilargani & Sadatnia [260]. Typically, this crater-like pattern is generated during deformation by the freeze fracture of polymeric membranes [51]. Moreover, this pure PVA membrane exhibits a skin layer, or better-known “top layer”, of about 2.6 μm in thickness. This dense surface layer commonly appears by an extremely short-term reduction of solvent concentration on the surface contacting the air. Such layer tended to be dissipated by incorporating the GO in MMMs, the cross-sectional view also displayed an increase in roughness with increasing GO loading, and when this reached 2 wt.% the flaky structure shows a tendency of assembling to the membrane surface like a segregation phenomenon (see **Figure 7.3f**), which has been reported during the GO filling into chitosan [269].

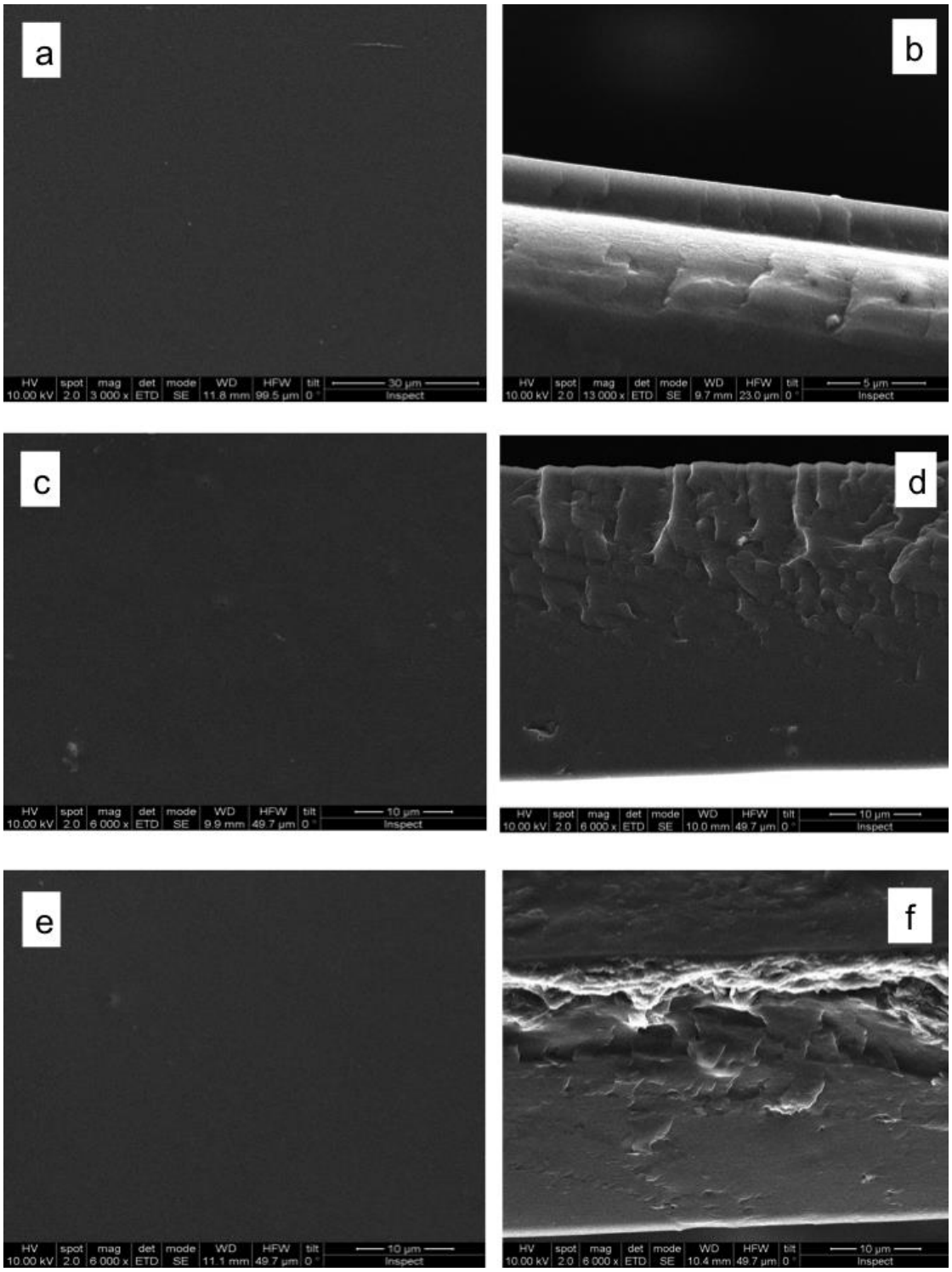


**Figure 7.3**. Surface and cross-section FESEM images of pure cross-linked PVA (a, b) and MMMs at 1 wt.% (c, d) and 2 wt.% (e, f) GO content, respectively.

In fact, in the case of cross-linked PVA- GO 2 wt.% membrane, the XRD patterns obtained from its top and bottom layers, where it can be seen that the GO shifted slightly the PVA signal, which is more remarkable at the top layer. This, more evident

at the highest GO loading, is in agreement with the floating suffered by the GO particles during MMM preparation that tend to accumulate them on the top of the MMM. Furthermore, the GO seems to be parallel deposited to the membrane surface, this pattern has been observed when embedding into polyimide [64] and PVDF [270]. This particular orientation can be related to the remaining functional groups on the edges of GO on every side. Therefore it is quite probable that GO sheets would have this preferred alignment over the membrane [265,270].

The X-ray diffractogram of the GO exhibited a sharp diffraction peak at about $2 \cdot \theta = 12^{\circ}$, as **Figure 7.4** shows, that agrees with the reported values [271], corresponding to d-spacing of 0.78 nm.

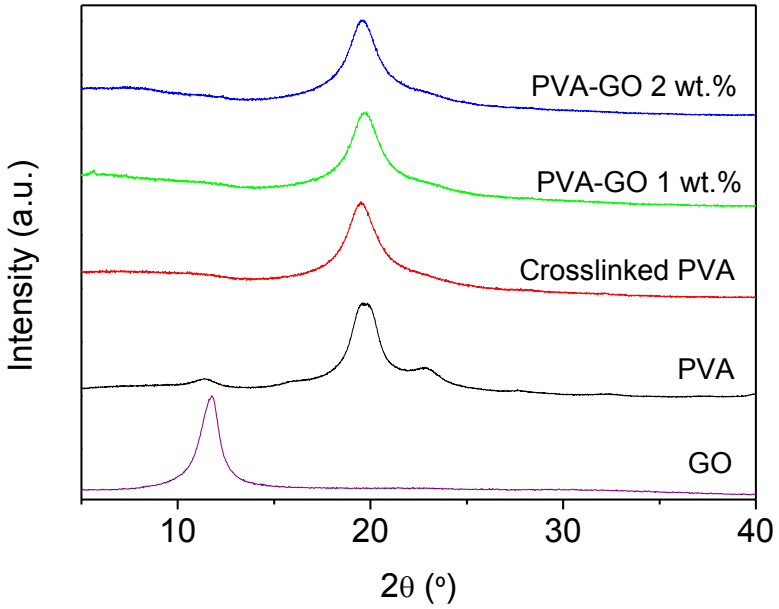


**Figure 7.4**. XRD patterns of the pure PVA, pure GO, cross-linked PVA and its MMMs-GO.

The shift of the GO peak position from its primary material (graphite) is due to the presence of oxygen-containing functional groups that intercalate into the space between individual graphene sheets provoking and increase of the d-spacing [272]. Moreover, the pure PVA displays a strong diffraction peak at $2 \cdot \theta = 19.6^{\circ}$, which was less intense after the cross-linking procedure. Some peaks at 12º and 22º in PVA were identified, the ones that were disappeared later. This is normally attributed to the reduction of crystallinity of PVA membranes by the cross-linking [260]. The cross-linked

PVA-GO MMMs also exhibited similar features with a slight change compared to the pure one. No peak corresponding to graphene layers was discernible, which can be due to the low volume loading of the material in the MMMs [265]. However, the GO loading could be enough to modify the spacing of polymer chains [260].

The measured water contact angle value for cross-linked PVA membrane was around 69.6º±0.5º, as **Table 7.1** reports. This value which is within the range 57º-77º in agreement with the one reported by several authors [268,273]. The hydrophilicity depends on the type of cross-linker used and the consumption of –OH groups during the cross-linking [268,273]. However, the hydrophilic nature was still confirmed in the cross-linked membranes. On the other hand, the cross-linked PVA displayed an enhanced hydrophilicity by embedding GO into its matrix, e.g. up to 58.4º±0.5º for the MMMs-GO 2 wt.%. Generally, the water contact angle decreased with the increase of GO content. This is related to the abundant oxygen-containing functional groups on the wrinkled GO sheets [269]. In addition, the enhancement of water contact angle of MMMs was leveled off when GO content was higher than 1 wt.%, where the contact angle did not show strong change compared to 2 wt.%. GO caused a decrease of water contact angle also in other MMMs based on chitosan [269,274] and polyimides [275]. In theory, the wettability of a membrane is directly associated with the water adsorption rate on the membrane surface, which is highly important in PV since it is regarded as the first step of water transport through the membrane based on the solution-diffusion mass transfer.

The uptake of membranes was evaluated from their contact with 10/90 wt.% water-ethanol solution (the same concentration used in the PV experiments). The calculated uptake results are depicted in **Figure 7.5.**

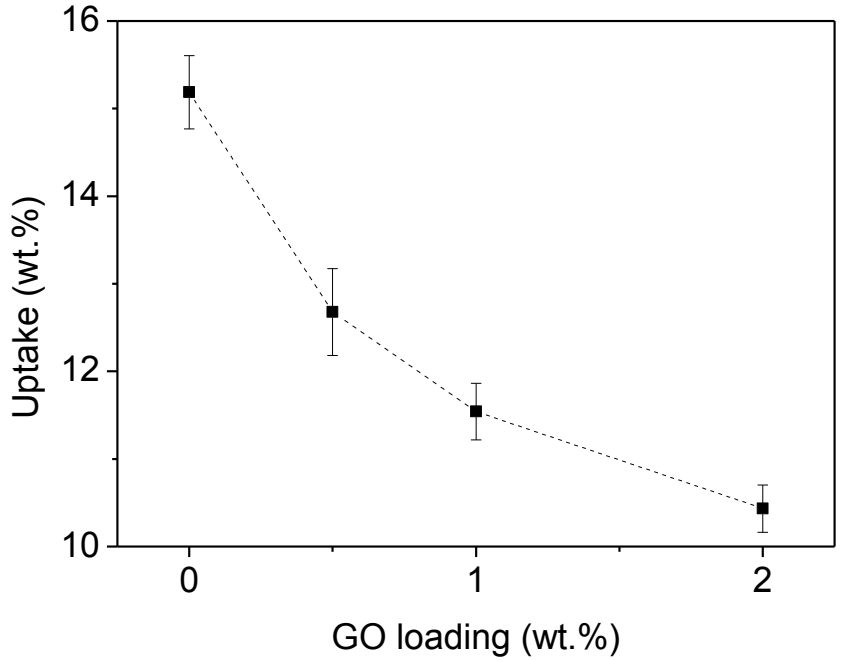


**Figure 7.5.** Uptake of the cross-linked PVA and MMMs-GO membranes at 10:90 wt.% water-ethanol (at 40ºC).

It can be seen that the uptake decreased with the increasing of the GO content. This tendency has been reported during the incorporation of GO into hydrophilic chitosan membranes [269]. Basically, the decrease in uptake is related to the strong GO-polymer interactions which, besides reducing the availability of hydrophilic groups, could restrict the mobility of PVA chains and decrease even more the free volume of the cross-linked PVA. GO has demonstrated, as multi-walled carbon nanotubes [185], to suppress the swelling degree of these PVA membranes. Therefore, GO provides a better stability to the cross-linked PVA against the swelling phenomenon. Finally, it is worth mentioning that the cross-linking made the membrane more resistant to the ethanol-water mixture that would otherwise dissolve.

As can be seen from **Figure 7.6**, the addition of GO has a relevant effect on the mechanical properties of the pristine cross-linked PVA membranes. The incorporation of GO, in particular, led to a general improvement of the mechanical behaviour of the pristine membranes in terms of Young's modulus, tensile strength and elongation at break. The tensile strength value, for instance, displayed in **Figure 7.6c**, increased from 27 $N \cdot mm^{-2}$ for the pristine PVA membrane up to 43 $N \cdot mm^{-2}$ for the membrane loaded with 0.5 wt.% GO with an increase of tensile strength of about 60%. The increase was

particularly pronounced for lower GO loadings (0.5 and 1 wt.%). An improvement of Young's modulus was also observed for all the MMMs by adding GO (**Figure 7.6a**) in particular at the lowest filler content, e.g. a 134% increase was observed in comparison to the pristine one. The elongation at break, after an initial increase at 0.5 wt.% GO (from 103% to 154 %) tended to decrease at the highest GO concentration (up to 32%) (**Figure 7. 6b**). This could be due to the interaction of GO with the membrane matrix that hinders the movement of the polymer chains at high filler concentrations [276], in line with the above discussed increases of $T_g$ values (See **Table 7.1**). This trend in the change of mechanical properties is similar to that observed by Zhao *et al.* [276], where PVA membranes were loaded with different concentrations of graphene nanosheets. They observed an increase in the tensile strength from 17 $N \cdot mm^{-2}$ for the pristine PVA membrane to 42 $N \cdot mm^{-2}$ for the membranes loaded with 1.8 vol% of graphene nanosheets.

The Young's modulus also increased from 1000 $N \cdot mm^{-2}$ to about 10000 $N \cdot mm^{-2}$ when graphene (1.8 vol%) was added to the PVA. The authors explained these results stating that exists a critical point of graphene nanosheets loading (called mechanical percolation) [265], where beyond this concentration there is no improvement in the membrane mechanical properties due to the stacking of nanosheets. Lower than this concentration (which they found at 1.8 vol% for graphene sheets), however, an improvement in the membrane mechanical properties can be obtained due to the better dispersion of the filler in the polymer matrix. In this work, the critical point can be identified at the 1 wt.% GO content. As can be observed in **Figure 7.6a&c**, the membrane mechanical properties were greatly improved below this value. A similar trend was also observed and reported by Kashyap *et al.* [265] during the reinforcement of PVA polymer matrices, where at low GO concentrations (0.3 wt.% only) the mechanical properties of PVA membranes were enhanced. This improvement was attributed to the uniform dispersion of the GO in the membrane and to the strong hydrogen bonding interfacial interaction between the filler and membrane matrix.

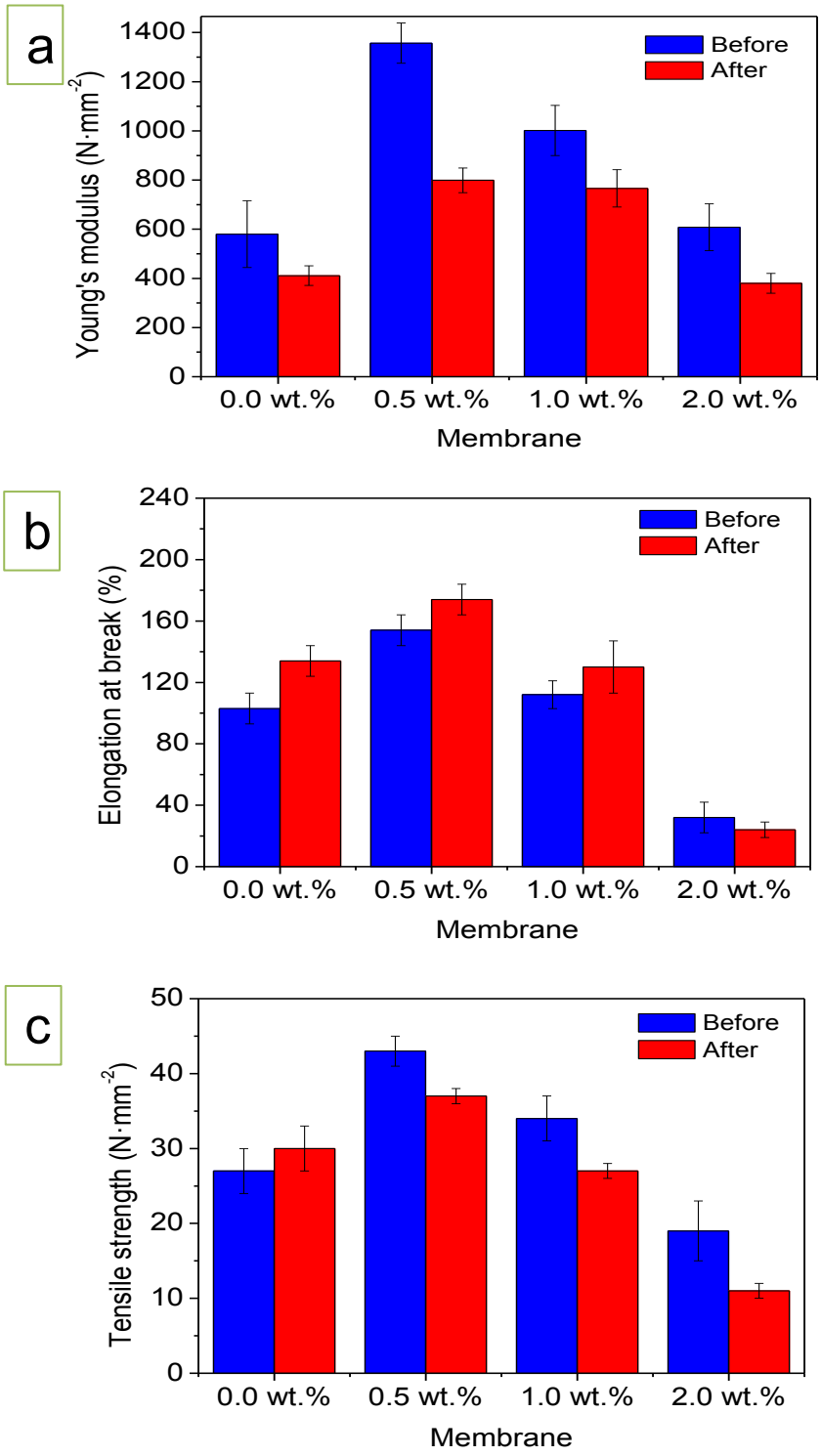


**Figure 7.6**. Mechanical properties of cross-linked PVA membrane and MMMs-GO before and after exposure to water-ethanol (10:90 wt.%) mixture.

Moreover, the mechanical properties were also measured for the pristine PVA membrane and its MMMs after soaking them in a water-ethanol solution (10:90 wt.%)

during 24 h. A general decrease of the mechanical properties in terms of Young's modulus and tensile strength was observed after exposure of the membranes to the solution. The mechanical properties of the membranes, therefore, may be subjected to a plasticization effect due to hydrogen bonds formation between polar molecules (i.e. from ethanol and water) and PVA polymer. As a consequence, in the swollen state, the chain-chain polymer interactions decreased resulting in a contraction of the mechanical properties of the membranes. Commonly, the exposure to the water-ethanol solution led to a swelling phenomenon in membranes of poly(lactic acid)/poly(vinyl pyrrolidone) [277]. On the contrary, the elongation at break of the MMMs containing 0.5 and 1 wt.% GO was slightly enhanced after soaking (**Figure 6b**).

### 7.5.2. Pervaporation tests

#### *7.5.2.1.Effect of GO loading and temperature on PV performance*

**Figure 7.7** displays the effect of GO content on the total permeate flux during the PV performance as a function of the operating temperature. Basically, an increase in the total permeation rate was observed with double increasing the GO loading. This tendency is commonly observed during the incorporation of the inorganic materials into polymer membranes, which may be a result of the free volume increase as well as the possible interfacial selective gaps between GO laminates and PVA matrix, while the highly hydrophilic nature of the filler can also produce an increase in the permeation rates by preferential adsorption of the more polar compound (water). Moreover, an increase on the total permeation was observed with temperature increase (40-60 ºC). In theory, the polymer chains tend to be more flexible at higher temperatures promoting the sorption ability of the components, leading to the increase of permeating compounds through the intermolecular distances of the polymeric membrane. Also, the viscosity of the liquid feed diminishes with temperature favoring their transport through the membrane.

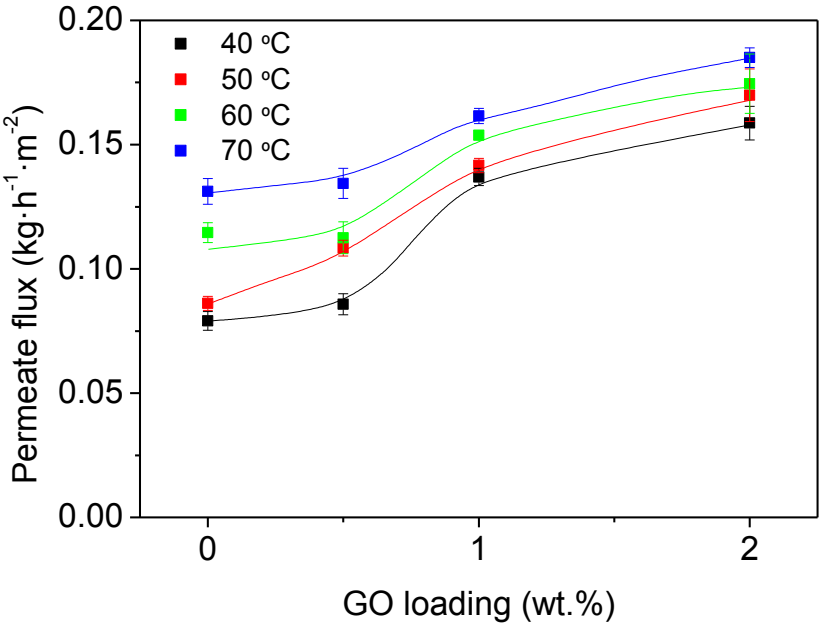


**Figure 7.7**. Total permeate flux as a function of the GO loading at different operating temperatures (10:90 wt.% water-ethanol). The curves are only guides to the eye.

The effect of the temperature on total permeate flux has been analyzed similarly as given in (section **6.3.2.**) by using the linearized form of Arrhenius relationship (eq.6). As can be seen from **Figure 7.7**, the temperature dependencies of fluxes of individual components and total flux can be well described by this equation. The apparent activation energies for water, ethanol and total flux, summarized in **Table 7.2**, were calculated for different content of GO.

**Table 7.2**. Apparent activation energy for total permeate, water and ethanol fluxes of the PVA membranes and its MMMs at different GO loadings.

| | **Activation energy values (kJ/mol)** | | |
|---|---|---|---|
| ***GO loading (wt.%)*** | *Total* | *Water* | *Ethanol* |
| **0** | 7.0 | 6.5 | 22.0 |
| **0.5** | 5.3 | 5.3 | 17.3 |
| **1** | 2.2 | 1.6 | 15.2 |
| **2** | 1.9 | 0.82 | 14.1 |

From **Table 7.2**, it can be seen that the $E_a$ values for total flux gradually decrease with the increase of filler loading, e.g. 7.0 in the pristine PVA membranes to 1.9 kJ/mol in the MMMs-2 wt.% GO. At this point, $E_a$ decrease towards water was more influenced than the one for ethanol in the range of handled temperature. This means that the presence of GO contributes to reduce the energy needed for the components to permeate across the membranes [278]; similar behavior was recently reported by Qian *et al.* [269] during the PV desalination of water through chitosan-GO membranes. Regarding the separation factor (water selectivity), see **Figure 7.8**, it has been observed a decrease as a function of the temperature for the pure cross-linked PVA membrane as well as its MMMs.

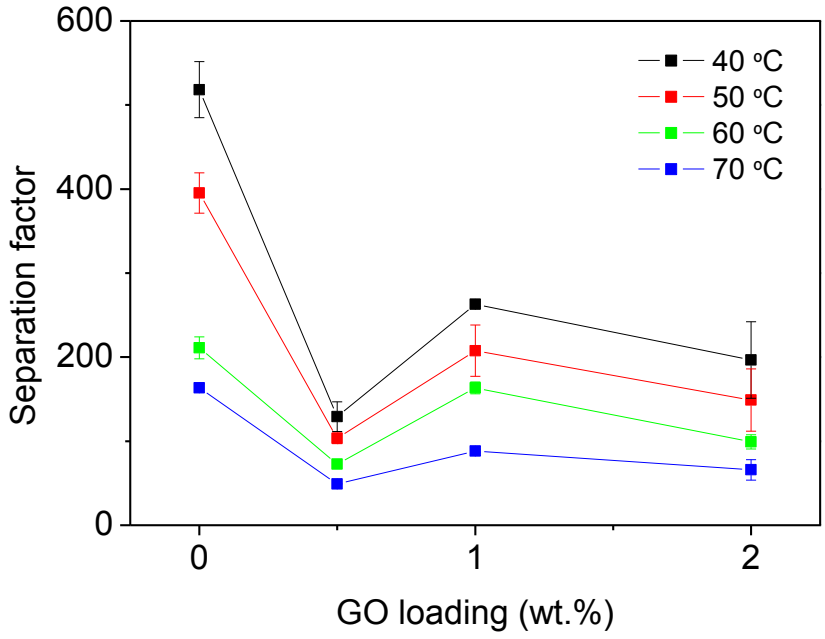


**Figure 7.8**. Separation factor as a function of the GO loading at different operating temperatures (10: 90 wt.% water-ethanol). The lines are only guides to the eye.

The thermal motion of the polymeric chains may facilitate the diffusion of larger molecules (like ethanol) through the membrane causing a decrease in separation factor, in agreement with the fact that activation energy values for ethanol are always larger than for water (see **Table 7.2**). The absence of negative values for the activation energy data reveals that the permeation of the species presented in these MMMs is less governed by the adsorption [278]; indeed, polymer cross-linking strongly tends to affect the membrane adsorption, e.g. in PVA [279].

It is worth mentioning, as **Figure 7.8** displays, that the separation factor at any of the temperatures did not follow a continuous decreasing trend. From the strict point of view of the separation factor values (**Figure 7.8**), the first addition of GO (0.5 wt.%) was not enough to compensate the distortion in the PVA chains that it caused creating non selective pores (but hydrophilic), and it was necessary doubling the filler value (1 wt.%) to compensate in part the loss of selectivity. In other words, at 1 wt.% GO, the concentration of sheets in the MMMs is high enough as to exert an additional barrier effect to bulkier ethanol molecules (decreasing the ethanol PV flux through the membrane, see **Figure 7.9**) and thus recover part of the separation factor of the bare cross-linked PVA membrane Nevertheless, the MMMs-2 wt.% GO had an excess of filler and the separation factor worsened in agreement with the loss of mechanical properties seen above.

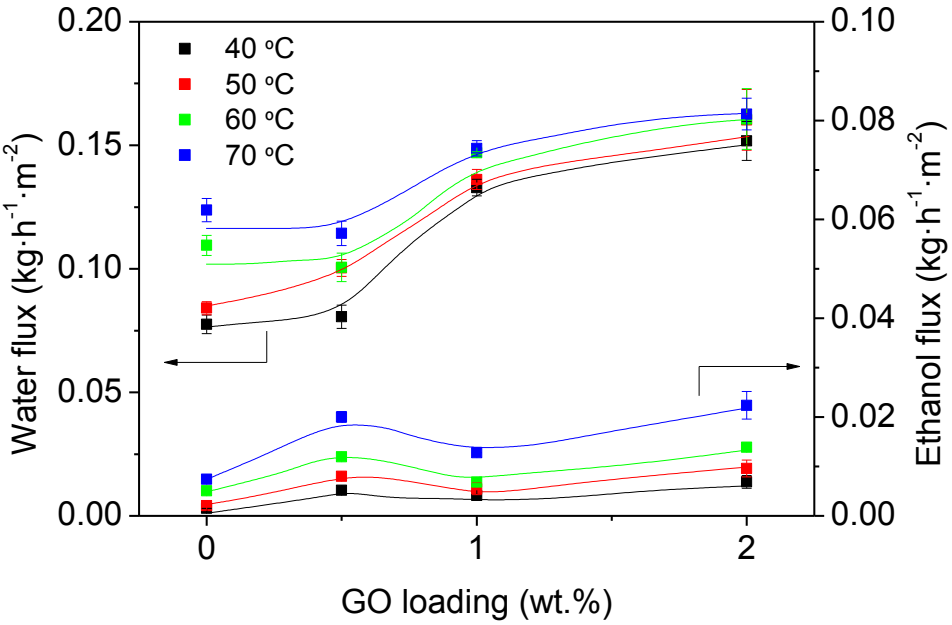


**Figure 7.9**. Water and ethanol partial fluxes as a function of the GO loading at different operating temperatures (10:90 wt.% water-ethanol). The curves are only guides to the eye.

Definitely, the modification of PVA with GO filler favors the preferential transport of water. This is due to the fact that GO laminates simultaneously have oxidized (proper GO, hydrophilic) and non-oxidized (graphene, hydrophobic) regions. The non-oxidized

regions of graphene sheets possess a d-spacing of ca. 5 Å [280], which is enough to host a monolayer of water. It has been speculated that these empty spaces form a network of pristine-graphene capillaries within GO laminates [281], which would facilitate the water transport. **Figure 7.10** depicts a schematic view of the possible water permeation mechanism involving GO species. In this study, even when the mixture of water and other compounds (e.g. gases and liquids) was fed, the water permeation rate was at least five orders of magnitude higher than that of the others components [281,282]. In fact, using equilibrium molecular dynamics simulations, it has been stated that water can easily flow through graphene nano-channels (e.g., the non-oxidized region of GO) [283].

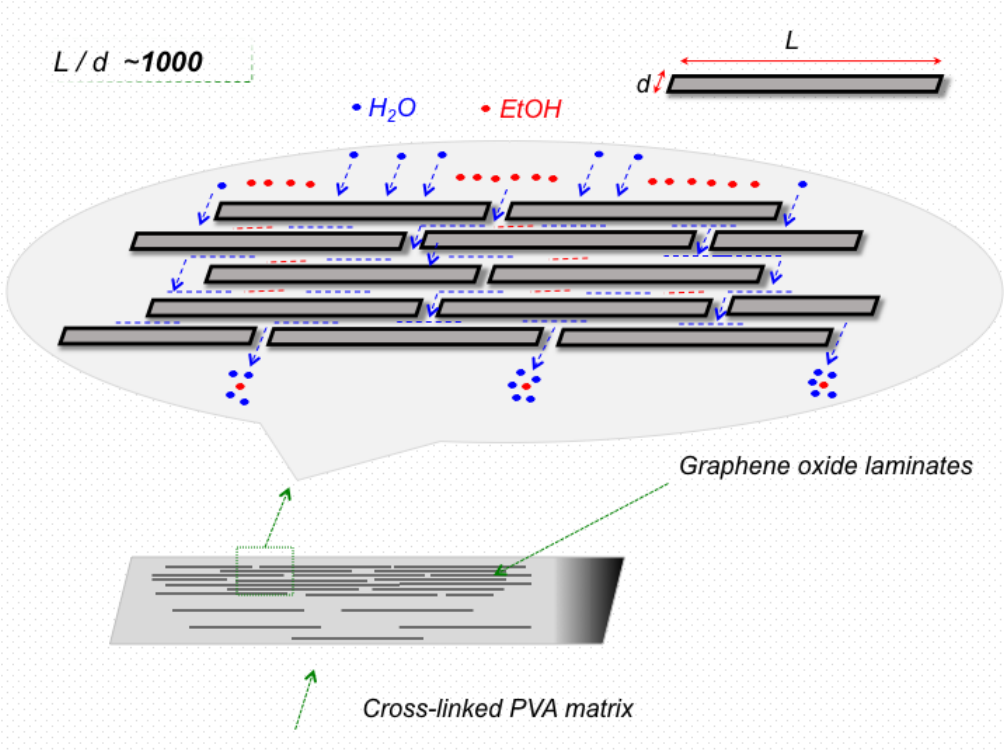


**Figure 7.10.** Schematic drawing of the possible water permeation mechanism through GO laminates. Inspired by Nair *et al.* [281]

The decrease in separation efficiency can also be affected by the GO synthesis. According to Hung *et al.* [284], it is extremely challenging to form highly ordered and precise GO laminates. It has been reported that repulsive electrostatic interactions produced by negatively charged carboxyl groups might usually create some out-of-order accumulation (i.e. wrinkles). Also, a large number of nonselective defects (basic plane

holes) derived from the strong oxidization of Hummers method may penalize the membrane separation performance [282].

*7.5.2.2.Comparison of cross-linked PVA-GO MMMs with other studies*

The PV performance of polymeric and MMMs for any water-organic separation, like water-ethanol, through PV technology, depends directly on: i) the polymer features (e.g. material type, nature, structure, thickness); the filler features (e.g. shape, size, hydrophilicity/hydrophobicity, structure, pore size and volume); iii) the physic-chemical properties and concentration of the compounds contained in the mixture to be separated; and iv) the operating conditions (e.g. temperature, vacuum pressure, feed flow rate) [5,121]. This makes difficult to provide a fair comparison of PV data with works where different conditions have been applied, bearing also in mind that this work is the first one dealing with the use of cross-linked PVA-GO membranes for water-ethanol separation by PV. **Table 7.3** compares water-ethanol PV performances of a number of MMMs filled with carbonaceous materials, zeolites, MOFs and several porous and non-porous oxides.

It is a difficult task choosing the best performance of cross-linked PVA- GO MMMs achieved in the current work in terms of permeate flux and separation factor, due to the fact that cross-linked PVA membrane itself displays high separation efficiencies ($\alpha$ =163-518 with total PV fluxes= 0.079-0.131 $kg \cdot m^{-2} \cdot h^{-1}$, see **Figures 7.7** and **7.8**) depending on handled temperature.

**Table 7.3**. Comparison of the cross-linked PVA-GO MMMs performance with other studies for the dehydration of ethanol.

| Mixed matrix membrane | Filler loading: | Mixture concentration: | Operating conditions: | J ($kg\ m^{-2}\ h^{-1}$) | Separation factor ($\alpha$) | Reference: |
|---|---|---|---|---|---|---|
| Cross-linked PVA-filled GO | 1 wt.% | 10 wt.% $H_2O$<br>90 wt.% EtOH | 40 ºC, 3 mbar | 0.137 | 263 | This work |
| Cross-linked PVA-filled GO | 2 wt.% | 10 wt.% $H_2O$<br>90 wt.% EtOH | 70 ºC, 3 mbar | 0.185 | 65.9 | This work |
| Chitosan-filled H-ZSM-5 | 8 wt.% | 10 wt.% $H_2O$<br>90 wt.% EtOH | 80 ºC, 10 mbar | 0.230 | 152 | [182] |
| Cross-linked sodium alginate-filled beta zeolite | 10 wt.% | 10 wt.% $H_2O$<br>90 wt.% EtOH | 30 ºC, 0.6 mbar | 0.130 | 1600 | [183] |
| Polyimide-filled ZIF-8 | 12 wt.% | 10 wt.% $H_2O$<br>90 wt.% EtOH | 42 ºC, 44 mbar | 0.260 | 300 | [122] |
| Cross-linked sodium alginate-filled beta zeolite | 10 wt.% | 10 wt.% $H_2O$<br>90 wt.% EtOH | 30 ºC, 0.6 mbar | 0.138 | 1334 | [184] |
| PVA-filled MWCNT | 5 wt.% | 10 wt.% $H_2O$<br>90 wt.% EtOH | 40 ºC, 1.3 mbar | 0.080 | 500 | [185] |
| Chitosan-filled $TiO_2$ | 6 wt.% | 10 wt.% $H_2O$<br>90 wt.% EtOH | 80 ºC, 50 mbar | 0.340 | 196 | [186] |
| Polyimide-filled MSS-1 | 12 wt.% | 10 wt.% $H_2O$<br>90 wt.% EtOH | 42 ºC, 44 mbar | 0.310 | 190 | [122] |
| Cross-linked chitosan-filled silica | 5 wt.% | 10 wt.% $H_2O$<br>90 wt.% EtOH | 70 ºC, 10 mbar | 0.410 | 919 | [179] |
| Cross-linked PVA-filled ZIF-8-$NH_2$ | 7.5 wt.% | 15 wt.% $H_2O$<br>85 wt.% EtOH | 40 ºC, 1 mbar | 0.120 | 200 | [200] |

Considering the MMMs containing 1 wt.% GO as the optimum (α =88.2-263 with total PV fluxes= 0.137-0.162 $kg \cdot m^{-2} \cdot h^{-1}$, see **Figures 7.7** and **7.8**), their separation factors are higher than those of other membranes based on chitosan-H-ZSM-5 [182], chitosan-$TiO_2$ [186], cross-linked PVA-ZIF-8-$NH_2$ [200] and polyimide-MSS-1 [122]; but lower than those corresponding to membranes of cross-linked sodium alginate-beta zeolite [183], polyimide-ZIF-8 [122], cross-linked sodium alginate-zeolite [184], PVA-MWCNT [185], and cross-linked chitosan-silica [179].

Moreover, the pristine cross-linked PVA displays relatively acceptable total permeate flux (J=0.079-0.131 $kg \cdot m^{-2} \cdot h^{-1}$), while its MMMs containing 2 wt.% GO have shown the highest permeate flux values of about 0.185 $kg \cdot m^{-2} \cdot h^{-1}$ (at 70 ºC). Such fluxes are higher than the reported using cross-linked sodium alginate-beta zeolite [183], PVA-MWCNT [185], and cross-linked sodium alginate-zeolite [184]; however, other MMMs provided even higher permeation fluxes than the presented in this study, such as chitosan-H-ZSM-5 [182], polyimide-ZIF-8 [122], chitosan- $TiO_2$ [186], polyimide-MSS-1 [122] and cross-linked chitosan-silica [179]. It is important to highlight that the current PV flux enhancements obtained with the cross-linked PVA-GO MMMs enhances on permeate flux (mainly towards water) were obtained by incorporating a small amount of GO filler, which is much lower than other previous studies. Finally, regardless of the amount of GO used for the preparation of these membranes, the right choice of the MMM will depend on the final purpose (high productivity or high separation efficiency), as well as the feasibility of the process considering primordially its operating conditions, e.g. temperature, that indeed influences on the PV performance.

### 7.6.Chapter remarks

Cross-linked-PVA membranes containing GO have been successfully tested for the PV separation of the water-ethanol azeotropic mixture. The effect of operating temperature has been evaluated. The best performance of cross-linked PVA-GO membranes has been provided by that containing 1 wt.% filler, displaying an acceptable separation factor (263, at 40 ºC) with a high permeate total flux of about 0.137 $kg \cdot m^{-2} \cdot h^{-1}$ (in which 0.133 $kg \cdot m^{-2} \cdot h^{-1}$ corresponds to water). At this point, these MMMs, having only 1 wt.% GO, have demonstrated to enhance the permeation performance of pristine

cross-linked PVA membranes, improving over 75 % their original permeation rates. Of course, higher permeate fluxes can be obtained by increasing *i)* the temperature, since the total, water and ethanol fluxes have shown a positive temperature dependence; and *ii)* filler loading, e.g. 2 wt.% GO. Based on the obtained results, it is possible to conclude that these PVA MMMs membranes have a promising potential to be used in PV for the dehydration of ethanol. Moreover, regarding the use of these MMMs in a "green" process, as PV, the incorporation of GO has satisfactorily enhanced the water transport of cross-linked PVA membranes, displaying losses on selectivity. However, the high water permeation fluxes could contribute to use less energy-requirement due to the fact that less operating time may be needed to reach pure ethanol in a continuous mode.

Finally, MMMs containing 1 wt.% GO have been considered as optimum membranes with an acceptable PV flux-separation factor balance in good agreement with the better thermal ($T_g$) and mechanical properties (Young' modulus, elongation at break and tensile strength) than these composites exhibited as compared to MMMs at 0.5 and 2 wt.% GO.

# *Chapter 8*

## Conclusions and recommendations

### 8.1. Conclusions

Throughout this research, we were looking for the main commercial polymers that have been used in gas separation and pervaporation processes. In this sense, Matrimid®5218 and poly(polyvinyl alcohol) were the found as the most sought polymers used for gas separation and pervaporation applications, respectively. In the case of Matrimid, we were successfully able to prepare compatible blends with PEG 200. Afterwards, we selected the best performing blend for the preparation of ternary mixed matrix membranes. Thereby, ZIF-8 nanoparticles, based on their well $CO_2$ adsorption capacity, were used as filling material. Firstly, we developed a suitable preparation procedure for excellent dispersion of the MOF over the membranes (i.e. solvent exchange procedure). Such novel ternary MMMs were tested for their capability to separate $CO_2$ from $CH_4$. Moreover, the use of Matrimid® was extended to another application, like organic-organic separations by pervaporation. Herein, we studied for the first time the ability of Matrimid to separate MeOH-MTBE mixtures. Finally, we proposed the enhancement the pervaporation performance of the polyvinyl alcohol by embedding a highly hydrophilic material (i.e. graphene oxide nanosheets). At this point, the ethanol dehydration was used as case of study for evaluating the performance of GO-PVA membranes. Base on the set goals and the studies conducted within this thesis, the contribution of this work to the research community can be summarized by the following highlighted frameworks:

- The blending of Matrimid®-PEG 200 blend membranes (at 96:4 ratio) has demonstrated the improvement (more than 3-fold) of $CO_2$ permeability compared to the pristine polymer. While the membranes also showed an increase in separation factor by 39 % in $CO_2/CH_4$ binary mixture separation
- The blend Matrimid®-PEG 200(at 96:4 ratio) membranes were also compatible with ZIF-8 in order to fabricate ternary MMMs. Such membranes (containing 30

wt.% ZIF-8) displayed up to 22% enhancement in $CO_2$ permeability compared to the blend membranes; however, a slight decrease on separation factor was observed.

- Pristine Matrimid® membranes were, for the first time, tested for an organic-organic (e.g. MeOH-MTBE) azeotropic separation by means of pervaporation. In particular, through the analysis of the PV process by the Arrhenius relationship, it was found that the increase of feed temperature (from 25 to 45 ºC), determined not only the higher MeOH permeation with respect to MTBE, but also improved the separation factor, which is not commonly observed.
- Cross-linked-PVA membranes containing GO have been successfully tested for the PV separation in ethanol dehydration. At this point, these MMMs, containing only 1 wt.% GO, have demonstrated to enhance the permeation performance of pristine cross-linked PVA membranes, improving over 75 % their original permeation rates.

As a final remark of this thesis, the current thesis provide enough insights about the improvement of commercial polymeric materials by incorporating inorganic materials. This research may be useful as starting point for future developments in gas separation and pervaporation technologies.

### 8.2. Recommendations

As future developments in the field of synthesis and preparation of mixed matrix membranes for gas separation and pervaporation applications, the following recommendations can be denoted based on the research performed:

- A possible chemical modification of the ZIF-8 may contribute to have a better interaction between the inorganic and organic phases in the MMMs; and therefore, this could increase the selectivity of the Matrimid MMMs.
- The performance of the Matrimid MMMs into real complex mixtures (at high pressure) is needed to be evaluated.
- The extension of pure Matrimid membranes, based on their hydrophilicity and solvent resistance, to another organic-organic separation could be evaluated.

- Based on the good performance of the GO-PVA MMMs for ethanol dehydration, the use of such membranes can be extended to other type of separation of industrial interest (e.g. MeOH-MTBE).
- The incorporation of other type of hydrophilic inorganic materials (e.g. Zr-based MOFs) into such commercial polymers may contribute to extend the application of those polymers for PV applications.

# References


[1] R.W.R.W. Baker, Membrane Technology and Applications, John Wiley & Sons, Ltd, Chichester, UK, 2012. doi:10.1002/9781118359686.

[2] S. Castarlenas, C. Téllez, J. Coronas, Gas separation with mixed matrix membranes obtained from MOF UiO-66-graphite oxide hybrids, J. Memb. Sci. 526 (2017) 205–211. doi:10.1016/j.memsci.2016.12.041.

[3] J. Sánchez-Laínez, B. Zornoza, Á. Mayoral, Á. Berenguer-Murcia, D. Cazorla-Amorós, C. Téllez, J. Coronas, Beyond the H2/CO2upper bound: One-step crystallization and separation of nano-sized ZIF-11 by centrifugation and its application in mixed matrix membranes, J. Mater. Chem. A. 3 (2015) 6549–6556. doi:10.1039/c4ta06820c.

[4] B. Seoane, J. Coronas, I. Gascon, M.E. Benavides, O. Karvan, J. Caro, F. Kapteijn, J. Gascon, Metal–organic framework based mixed matrix membranes: a solution for highly efficient $CO_2$ capture?, Chem. Soc. Rev. 44 (2015) 2421–2454. doi:10.1039/C4CS00437J.

[5] R.W. Baker, J.G. Wijmans, Y. Huang, Permeability, permeance and selectivity: A preferred way of reporting pervaporation performance data, J. Memb. Sci. 348 (2010) 346–352. doi:10.1016/j.memsci.2009.11.022.

[6] R. Castro-Muñoz, V. Martin-Gil, M.Z. Ahmad, V. Fíla, Matrimid® 5218 in preparation of membranes for gas separation: Current state-of-the-art, Chem. Eng. Commun. 205 (2018) 161–196. doi:10.1080/00986445.2017.1378647.

[7] L.M. Robeson, The upper bound revisited, J. Memb. Sci. 320 (2008) 390–400. doi:10.1016/j.memsci.2008.04.030.

[8] L.M. Robeson, Correlation of separation factor versus permeability for polymeric membranes, J. Memb. Sci. 62 (1991) 165–185. doi:10.1016/0376-7388(91)80060-J.

[9] M.G. Buonomenna, W. Yave, G. Golemme, Some approaches for high performance polymer based membranes for gas separation: block copolymers, carbon molecular sieves and mixed matrix membranes, RSC Adv. 2 (2012) 10745. doi:10.1039/c2ra20748f.

[10] H.Y. Zhao, Y.M. Cao, X.L. Ding, M.Q. Zhou, J.H. Liu, Q. Yuan, Poly(ethylene oxide) induced cross-linking modification of Matrimid membranes for selective separation of CO2, J. Memb. Sci. 320 (2008) 179–184. doi:10.1016/j.memsci.2008.03.070.

[11] A. Brunetti, F. Scura, G. Barbieri, E. Drioli, Membrane technologies for $CO_2$ separation, J. Memb. Sci. 359 (2010) 115–125. doi:10.1016/j.memsci.2009.11.040.

[12] N.A.H.M. Nordin, A.F. Ismail, A. Mustafa, R.S. Murali, T. Matsuura, The impact of ZIF-8 particle size and heat treatment on CO 2 /CH 4 separation using asymmetric mixed matrix membrane, RSC Adv. 4 (2014) 52530–52541. doi:10.1039/C4RA08460H.

[13] S. Shahid, K. Nijmeijer, Performance and plasticization behavior of polymer-MOF membranes for gas separation at elevated pressures, J. Memb. Sci. 470 (2014) 166–177. doi:10.1016/j.memsci.2014.07.034.

[14] J. Gascon, F. Kapteijn, B. Zornoza, V. Sebastián, C. Casado, J. Coronas, Practical approach to zeolitic membranes and coatings: State of the art, opportunities, barriers, and future perspectives, Chem. Mater. 24 (2012) 2829–2844. doi:10.1021/cm301435j.

[15] B. Ohlemann, Chemicals: Pervaporation and vapour permeation processes meet specialist needs, Filtr. Sep. 49 (2012) 18–22. doi:10.1016/S0015-1882(12)70285-9.

[16] A. Jonquières, R. Clément, P. Lochon, J. Néel, M. Dresch, B. Chrétien, Industrial state-of-the-art of pervaporation and vapour permeation in the western countries, J. Memb. Sci. 206 (2002) 87–117.

[17] V. Singh, D. Joung, L. Zhai, S. Das, S.I. Khondaker, S. Seal, Graphene based materials: Past, present and future, Prog. Mater. Sci. 56 (2011) 1178–1271. doi:10.1016/j.pmatsci.2011.03.003.

[18] M. Rezakazemi, A. Ebadi Amooghin, M.M. Montazer-Rahmati, A.F. Ismail, T. Matsuura, State-of-the-art membrane based CO2 separation using mixed matrix membranes (MMMs): An overview on current status and future directions, Prog. Polym. Sci. 39 (2014) 817–861. doi:10.1016/j.progpolymsci.2014.01.003.

[19] R. Nasir, H. Mukhtar, Z. Man, D.F. Mohshim, Material Advancements in Fabrication of Mixed-Matrix Membranes, Chem. Eng. Technol. 36 (2013) 717–727. doi:10.1002/ceat.201200734.

[20] M.A. Aroon, A.F. Ismail, T. Matsuura, M.M. Montazer-Rahmati, Performance studies of mixed matrix membranes for gas separation: A review, Sep. Purif. Technol. 75 (2010) 229–242. doi:10.1016/j.seppur.2010.08.023.

[21] P. Bernardo, E. Drioli, G. Golemme, Membrane Gas Separation : A Review / State of the Art, (2009) 4638–4663.

[22] D. Bastani, N. Esmaeili, M. Asadollahi, Polymeric mixed matrix membranes containing zeolites as a filler for gas separation applications: A review, J. Ind. Eng. Chem. 19 (2013) 375–393. doi:10.1016/j.jiec.2012.09.019.

[23] P. Bernardo, E. Drioli, G. Golemme, Membrane gas separation: A review/state of the art, Ind. Eng. Chem. Res. 48 (2009) 4638–4663. doi:10.1021/ie8019032.

[24] J. Ahn, W.J. Chung, I. Pinnau, M.D. Guiver, Polysulfone/silica nanoparticle mixed-matrix membranes for gas separation, J. Memb. Sci. 314 (2008) 123–133. doi:10.1016/j.memsci.2008.01.031.

[25] H.B. Tanh Jeazet, C. Staudt, C. Janiak, Metal–organic frameworks in mixed-matrix membranes for gas separation, Dalt. Trans. 41 (2012) 14003. doi:10.1039/c2dt31550e.

[26] G. Dong, H. Li, V. Chen, Challenges and opportunities for mixed-matrix membranes for gas separation, J. Mater. Chem. A. 1 (2013) 4610–4630. doi:10.1039/c3ta00927k.

[27] H. Dong, K. Xiao, X. Li, Y. Ren, S. Guo, Preparation of PVDF/Al $_2$ O $_3$ hybrid membrane via the sol–gel process and characterization of the hybrid membrane, Desalin. Water Treat. 51 (2013) 3685–3690. doi:10.1080/19443994.2013.781986.

[28] M.J.C. Ordoñez, K.J. Balkus, J.P. Ferraris, I.H. Musselman, Molecular sieving realized with ZIF-8/Matrimid?? mixed-matrix membranes, J. Memb. Sci. 361 (2010) 28–37. doi:10.1016/j.memsci.2010.06.017.

[29] A.C. Comer, D.S. Kalika, B.W. Rowe, B.D. Freeman, D.R. Paul, Dynamic relaxation characteristics of Matrimid?? polyimide, Polymer (Guildf). 50 (2009) 891–897. doi:10.1016/j.polymer.2008.12.013.

[30] P.S. Tin, T.S. Chung, Y. Liu, R. Wang, S.L. Liu, K.P. Pramoda, Effects of cross-linking modification on gas separation performance of Matrimid membranes, J. Memb. Sci. 225 (2003) 77–90. doi:10.1016/j.memsci.2003.08.005.

[31] D.F. Sanders, Z.P. Smith, R. Guo, L.M. Robeson, J.E. McGrath, D.R. Paul, B.D. Freeman, Energy-efficient polymeric gas separation membranes for a sustainable future: A review, Polym. (United Kingdom). 54 (2013) 4729–4761. doi:10.1016/j.polymer.2013.05.075.

[32] W.F. Yong, F.Y. Li, Y.C. Xiao, P. Li, K.P. Pramoda, Y.W. Tong, T.S. Chung, Molecular engineering of PIM-1/Matrimid blend membranes for gas separation, J. Memb. Sci. 407–408 (2012) 47–57. doi:10.1016/j.memsci.2012.03.038.

[33] W.F. Yong, F.Y. Li, Y.C. Xiao, T.S. Chung, Y.W. Tong, High performance PIM-1/Matrimid hollow fiber membranes for CO2/CH4, O2/N2 and CO2/N2 separation, J. Memb. Sci. 443 (2013) 156–169. doi:10.1016/j.memsci.2013.04.037.

[34] E. V. Perez, K.J. Balkus, J.P. Ferraris, I.H. Musselman, Mixed-matrix membranes containing MOF-5 for gas separations, J. Memb. Sci. 328 (2009) 165–173. doi:10.1016/j.memsci.2008.12.006.

[35] S. Basu, A. Cano-Odena, I.F.J. Vankelecom, Asymmetric Matrimid??/[Cu3(BTC)2] mixed-matrix membranes for gas separations, J. Memb. Sci. 362 (2010) 478–487. doi:10.1016/j.memsci.2010.07.005.

[36] F. Li, Y. Li, T.S. Chung, S. Kawi, Facilitated transport by hybrid POSS??-Matrimid??-Zn2+ nanocomposite membranes for the separation of natural gas, J. Memb. Sci. 356 (2010) 14–21. doi:10.1016/j.memsci.2010.03.021.

[37] Q. Song, S.K. Nataraj, M. V. Roussenova, J.C. Tan, D.J. Hughes, W. Li, P. Bourgoin, M.A. Alam, A.K. Cheetham, S.A. Al-Muhtaseb, E. Sivaniah, Zeolitic imidazolate framework (ZIF-8) based polymer nanocomposite membranes for gas separation, Energy Environ. Sci. 5 (2012) 8359. doi:10.1039/c2ee21996d.

[38] L. Diestel, N. Wang, A. Schulz, F. Steinbach, J. Caro, Matrimid-based mixed matrix membranes: Interpretation and correlation of experimental findings for zeolitic imidazolate frameworks as fillers in H2/CO2 separation, Ind. Eng. Chem. Res. 54 (2015) 1103–1112. doi:10.1021/ie504096j.

[39] O. Bakhtiari, S. Mosleh, T. Khosravi, T. Mohammadi, Preparation, Characterization and Gas Permeation of Polyimide Mixed Matrix Membranes, J. Membr. Sci. Technol. 1 (2011) 1–6. doi:10.4172/2155-9589.1000102.

[40] C.I. Chaidou, G. Pantoleontos, D.E. Koutsonikolas, S.P. Kaldis, G.P. Sakellaropoulos, Gas Separation Properties of Polyimide-Zeolite Mixed Matrix Membranes, Sep. Sci. Technol. 47 (2012) 950–962. doi:10.1080/01496395.2011.645263.

[41] J. Ahmad, M.B. Hägg, Development of matrimid/zeolite 4A mixed matrix membranes using low boiling point solvent, Sep. Purif. Technol. 115 (2013) 190–197. doi:10.1016/j.seppur.2013.04.049.

[42] C. Duan, X. Jie, D. Liu, Y. Cao, Q. Yuan, Post-treatment effect on gas separation property of mixed matrix membranes containing metal organic frameworks, J. Memb. Sci. 466 (2014) 92–102. doi:10.1016/j.memsci.2014.04.024.

[43] S. Kanehashi, G.Q. Chen, C.A. Scholes, B. Ozcelik, C. Hua, L. Ciddor, P.D. Southon, D.M. D'Alessandro, S.E. Kentish, Enhancing gas permeability in mixed matrix membranes through tuning the nanoparticle properties, J. Memb. Sci. 482 (2015) 49–55. doi:10.1016/j.memsci.2015.01.046.

[44] M. Rahmani, A. Kazemi, F. Talebnia, Matrimid mixed matrix membranes for enhanced CO2/CH4 separation, J. Polym. Eng. 36 (2016) 499–511. doi:10.1515/polyeng-2015-0176.

[45] V. Martin-Gil, A. L??pez, P. Hrabanek, R. Mallada, I.F.J. Vankelecom, V. Fila, Study of different titanosilicate (TS-1 and ETS-10) as fillers for Mixed Matrix Membranes for CO2/CH4 gas separation applications, J. Memb. Sci. 523 (2017) 24–35. doi:10.1016/j.memsci.2016.09.041.

[46] F. Dorosti, M.R. Omidkhah, M.Z. Pedram, F. Moghadam, Fabrication and characterization of polysulfone/polyimide-zeolite mixed matrix membrane for gas separation, Chem. Eng. J. 171 (2011) 1469–1476. doi:10.1016/j.cej.2011.05.081.

[47] B. Zornoza, O. Esekhile, W.J. Koros, C. Téllez, J. Coronas, Hollow silicalite-1 sphere-polymer mixed matrix membranes for gas separation, Sep. Purif. Technol. 77 (2011) 137–145. doi:10.1016/j.seppur.2010.11.033.

[48] S. Rafiq, Z. Man, A. Maulud, N. Muhammad, S. Maitra, Separation of CO 2 from CH 4 using polysulfone/ polyimide silica nanocomposite membranes, Sep. Purif. Technol. 90 (2012) 162–172. doi:10.1016/j.seppur.2012.02.031.

[49] F. Moghadam, M.R. Omidkhah, E. Vasheghani-Farahani, M.Z. Pedram, F. Dorosti, The effect of TiO2 nanoparticles on gas transport properties of Matrimid5218-based mixed matrix membranes, Sep. Purif. Technol. 77 (2011) 128–136. doi:10.1016/j.seppur.2010.11.032.

[50] M. Peydayesh, S. Asarehpour, T. Mohammadi, O. Bakhtiari, Preparation and characterization of SAPO-34 - Matrimid?? 5218 mixed matrix membranes for CO2/CH4 separation, Chem. Eng. Res. Des. 91 (2013) 1335–1342. doi:10.1016/j.cherd.2013.01.022.

[51] F. Dorosti, M. Omidkhah, R. Abedini, Fabrication and characterization of Matrimid/MIL-53 mixed matrix membrane for CO2/CH4 separation, Chem. Eng. Res. Des. 92 (2014) 2439–2448. doi:10.1016/j.cherd.2014.02.018.

[52] S. Shahid, K. Nijmeijer, High pressure gas separation performance of mixed-matrix polymer membranes containing mesoporous Fe(BTC), J. Memb. Sci. 459 (2014) 33–44. doi:10.1016/j.memsci.2014.02.009.

[53] X.Y. Chen, O.G. Nik, D. Rodrigue, S. Kaliaguine, Mixed matrix membranes of aminosilanes grafted FAU/EMT zeolite and cross-linked polyimide for CO 2/CH 4 separation, Polym. (United Kingdom). 53 (2012) 3269–3280. doi:10.1016/j.polymer.2012.03.017.

[54] A.L. Khan, C. Klaysom, A. Gahlaut, A.U. Khan, I.F.J. Vankelecom, Mixed matrix membranes comprising of Matrimid and -SO3H functionalized mesoporous MCM-41 for gas separation, J. Memb. Sci. 447 (2013) 73–79. doi:10.1016/j.memsci.2013.07.011.

[55] T. Rodenas, M. Van Dalen, E. García-Pérez, P. Serra-Crespo, B. Zornoza, F. Kapteijn, J. Gascon, Visualizing MOF mixed matrix membranes at the nanoscale: Towards structure-performance relationships in CO2/CH4 separation over NH2-MIL-53(Al)@PI, Adv. Funct. Mater. 24 (2014) 249–256. doi:10.1002/adfm.201203462.

[56] X.Y. Chen, V.T. Hoang, D. Rodrigue, S. Kaliaguine, Optimization of continuous phase in amino-functionalized metal-organic framework (MIL-53) based co-polyimide mixed matrix membranes for CO 2/CH4 separation, RSC Adv. 3 (2013) 24266–24279. doi:10.1039/c3ra43486a.

[57] A. Ebadi Amooghin, M. Omidkhah, A. Kargari, The effects of aminosilane grafting on NaY zeolite-Matrimid®5218 mixed matrix membranes for $CO_2/CH_4$ separation,
J. Memb. Sci. 490 (2015) 364–379. doi:10.1016/j.memsci.2015.04.070.

[58] M. Loloei, M. Omidkhah, A. Moghadassi, A.E. Amooghin, Preparation and characterization of Matrimid® 5218 based binary and ternary mixed matrix membranes for CO2 separation, Int. J. Greenh. Gas Control. 39 (2015) 225–235. doi:http://dx.doi.org/10.1016/j.ijggc.2015.04.016.

[59] S. Keskin, S. D., Selecting metal organic frameworks as enabling materials in mixed matrix membranes for high efficiency natural gas purification, Energy Environ. Sci. 3 (2010) 343–351.

[60] M. Valero, B. Zornoza, C. Téllez, J. Coronas, Mixed matrix membranes for gas separation by combination of silica MCM-41 and MOF NH2-MIL-53(Al) in glassy polymers, Microporous Mesoporous Mater. 192 (2014) 23–28. doi:10.1016/j.micromeso.2013.09.018.

[61] Y. Liu, D. Peng, G. He, S. Wang, Y. Li, H. Wu, Z. Jiang, Enhanced CO2 permeability of membranes by incorporating polyzwitterion@cnt composite particles into polyimide matrix, ACS Appl. Mater. Interfaces. 6 (2014) 13051–13060. doi:10.1021/am502936x.

[62] A. Ebadi Amooghin, M. Omidkhah, A. Kargari, Enhanced $CO_2$ transport properties of membranes by embedding nano-porous zeolite particles into Matrimid®5218 matrix, RSC Adv. 5 (2015) 8552–8565. doi:10.1039/C4RA14903C.

[63] M.W. Anjum, F. Vermoortele, A.L. Khan, B. Bueken, D.E. De Vos, I.F.J. Vankelecom, Modulated UiO-66-Based Mixed-Matrix Membranes for CO2 Separation, ACS Appl. Mater. Interfaces. 7 (2015) 25193–25201. doi:10.1021/acsami.5b08964.

[64] X. Li, L. Ma, H. Zhang, S. Wang, Z. Jiang, R. Guo, H. Wu, X.Z. Cao, J. Yang, B. Wang, Synergistic effect of combining carbon nanotubes and graphene oxide in mixed matrix membranes for efficient CO2separation, J. Memb. Sci. 479 (2015) 1–10. doi:10.1016/j.memsci.2015.01.014.

[65] A. Sabetghadam, B. Seoane, D. Keskin, N. Duim, T. Rodenas, S. Shahid, S. Sorribas, C. Le Guillouzer, G. Clet, C. Tellez, M. Daturi, J. Coronas, F. Kapteijn, J. Gascon, Metal Organic Framework Crystals in Mixed-Matrix Membranes: Impact of the Filler Morphology on the Gas Separation Performance, Adv. Funct. Mater. 26 (2016) 3154–3163. doi:10.1002/adfm.201505352.

[66] A. Knebel, S. Friebe, N.C. Bigall, M. Benzaqui, C. Serre, J. Caro, Comparative Study of MIL-96(Al) as Continuous Metal-Organic Frameworks Layer and Mixed-Matrix Membrane, ACS Appl. Mater. Interfaces. 8 (2016) 7536–7544. doi:10.1021/acsami.5b12541.

[67] A. Ebadi Amooghin, M. Omidkhah, H. Sanaeepur, A. Kargari, Preparation and characterization of Ag+ ion-exchanged zeolite-Matrimid??5218 mixed matrix membrane for CO2/CH4 separation, J. Energy Chem. 25 (2016) 450–462. doi:10.1016/j.jechem.2016.02.004.

[68] X. Dong, Q. Liu, A. Huang, Highly permselective MIL-68(Al)/matrimid mixed matrix membranes for CO2/CH4 separation, J. Appl. Polym. Sci. 133 (2016) 1–8. doi:10.1002/app.43485.

[69] A. Fernández-Barquín, C. Casado-Coterillo, S. Valencia, A. Irabien, Mixed matrix membranes for O2/N2 separation: The influence of temperature, Membranes (Basel). 6 (2016). doi:10.3390/membranes6020028.

[70] R. Castro-Muñoz, V. Fíla, C.T. Dung, Mixed Matrix Membranes Based on PIMs for Gas Permeation: Principles, Synthesis, and Current Status, Chem. Eng. Commun. 204 (2017). doi:10.1080/00986445.2016.1273832.

[71] R. Castro-Muñoz, V. Fíla, Progress on incorporating zeolites in matrimid® 5218 mixed matrix membranes towards gas separation, Membr. 10.3390/membranes8020030. 8 (2018). doi:10.3390/membranes8020030.

[72] et al. Loloei, Mahsa, Improved CO2 separation performance of Matrimid®5218 membrane by addition of low molecular weight polyethylene glycol, Greenh. Gases Sci. Technol. 5 (2015) 1–15. doi:10.1002/ghg.

[73] R. Swaidan, X. Ma, E. Litwiller, I. Pinnau, High pressure pure- and mixed-gas separation of CO2/CH4 by thermally-rearranged and carbon molecular sieve membranes derived from a polyimide of intrinsic microporosity, J. Memb. Sci. 447 (2013) 387–394. doi:10.1016/j.memsci.2013.07.057.

[74] L.N. Yang, Z.Z., Song, Q.W., He, CO2 capture with PEG, in: L.N. Yan, Z.Z., Song, Q.W., He (Ed.), Capture Util. Carbon Dioxide with Polyethyl. Glycol, Springer Netherlands, Switzerland, 2012.

[75] A.I. Escudero, S. Espatolero, L.M. Romeo, Oxy-combustion power plant integration in an oil refinery to reduce CO2emissions, Int. J. Greenh. Gas Control. 45 (2016) 118–129. doi:10.1016/j.ijggc.2015.12.018.

[76] W. Yave, A. Car, S.S. Funari, S.P. Nunes, K.V. Peinemann, CO2-Philic polymer membrane with extremely high separation performance, Macromolecules. 43 (2010) 326–333. doi:10.1021/ma901950u.

[77] T. Khosravi, M. Omidkhah, Preparation of $CO_2$ -philic polymeric membranes by blending poly(ether-b-amide-6) and PEG/PPG-containing copolymer, RSC Adv. 5 (2015) 12849–12859. doi:10.1039/C4RA14168G.

[78] R. Xing, W.S.W. Ho, Synthesis and characterization of crosslinked polyvinylalcohol/polyethyleneglycol blend membranes for CO2/CH4separation, J. Taiwan Inst. Chem. Eng. 40 (2009) 654–662. doi:10.1016/j.jtice.2009.05.004.

[79] P. Hrabánek, A. Zikánová, B. Bernauer, V. Fíla, M. Kočiřík, Butane isomer separation with composite zeolite MFI mebranes, Desalination. 245 (2009) 437–443. doi:10.1016/j.desal.2009.02.006.

[80] M.L. Cecopieri-G??mez, J. Palacios-Alquisira, J.M. Dom??nguez, On the limits of gas separation in CO2/CH4, N2/CH4 and CO2/N2 binary mixtures using polyimide membranes, J. Memb. Sci. 293 (2007) 53–65. doi:10.1016/j.memsci.2007.01.034.

[81] T. Visser, N. Masetto, M. Wessling, Materials dependence of mixed gas plasticization behavior in asymmetric membranes, J. Memb. Sci. 306 (2007) 16–28. doi:10.1016/j.memsci.2007.07.048.

[82] O.C. David, D. Gorri, A. Urtiaga, I. Ortiz, Mixed gas separation study for the hydrogen recovery from H2/CO/N2/CO2 post combustion mixtures using a Matrimid membrane, J. Memb. Sci. 378 (2011) 359–368. doi:10.1016/j.memsci.2011.05.029.

[83] O.C. David, D. Gorri, K. Nijmeijer, I. Ortiz, A. Urtiaga, Hydrogen separation from multicomponent gas mixtures containing CO, N2 and CO2 using matrimid asymmetric hollow fiber membranes, Procedia Eng. 44 (2012) 1117–1118. doi:10.1016/j.proeng.2012.08.696.

[84] G. Dong, H. Li, V. Chen, Plasticization mechanisms and effects of thermal annealing of Matrimid hollow fiber membranes for CO2 removal, J. Memb. Sci. 369 (2011) 206–220. doi:10.1016/j.memsci.2010.11.064.

[85] A. Bos, I.G.M. Pünt, M. Wessling, H. Strathmann, CO2-induced plasticization phenomena in glassy polymers, J. Memb. Sci. 155 (1999) 67–78. doi:10.1016/S0376-7388(98)00299-3.

[86] Y. Zhang, K.J. Balkus, I.H. Musselman, J.P. Ferraris, Mixed-matrix membranes composed of Matrimid?? and mesoporous ZSM-5 nanoparticles, J. Memb. Sci. 325 (2008) 28–39. doi:10.1016/j.memsci.2008.04.063.

[87] A.L. Khan, X. Li, I.F.J. Vankelecom, SPEEK/Matrimid blend membranes for CO2 separation, J. Memb. Sci. 380 (2011) 55–62. doi:10.1016/j.memsci.2011.06.030.

[88] H. Lin, B.D. Freeman, Gas solubility, diffusivity and permeability in poly(ethylene oxide), J. Memb. Sci. 239 (2004) 105–117. doi:10.1016/j.memsci.2003.08.031.

[89] A. Bos, I.G.M. Pünt, M. Wessling, H. Strathmann, Suppression of CO2-plasticization by semiinterpenetrating polymer network formation, J. Polym. Sci. Part B Polym. Phys. 36 (1998) 1547–1556. doi:10.1002/(SICI)1099-0488(19980715)36:9<1547::AID-POLB12>3.0.CO;2-5.

[90] T.M. Sridhar, S., Veerapur, R. S., Patil, M. B., Gudasi, K. B., Aminabhavi, Matrimid Polyimide Membranes for the Separation of Carbon Dioxide from Methane, J. Appl. Polym. Sci.,. 106 (2007) 1585–1594.

[91] S.S. Hosseini, T.S. Chung, Carbon membranes from blends of PBI and polyimides for N2/CH4 and CO2/CH4 separation and hydrogen purification, J. Memb. Sci. 328 (2009) 174–185. doi:10.1016/j.memsci.2008.12.005.

[92] L. He, R. Xue, D. Yang, Y. Liu, R. Song, Effects of Blending Chitosan With Peg on Surface Morphology, Crystallization and Thermal Properties, Chinese J. Polym. Sci. 27 (2009) 501. doi:10.1142/S0256767909004175.

[93] H. Lin, B.D. Freeman, Materials selection guidelines for membranes that remove CO 2 from gas mixtures, 739 (2005) 57–74. doi:10.1016/j.molstruc.2004.07.045.

[94] H. Lin, B.D. Freeman, Gas permeation and diffusion in crosslinked poly(ethylene glycol diarylate), Macromolecules. 38 (2006) 8394–8407. doi:10.1021/ma051686o.

[95] F. Aziz, A.F. Ismail, Preparation and characterization of cross-linked Matrimid?? membranes using para-phenylenediamine for O2/N2 separation, Sep. Purif. Technol. 73 (2010) 421–428. doi:10.1016/j.seppur.2010.05.002.

[96] J. Zhang, F. Han, X. Wei, L. Shui, H. Gong, P. Zhang, Spectral studies of hydrogen bonding and interaction in the absorption processes of sulfur dioxide in poly(ethylene glycol) 400 + Water binary system, Ind. Eng. Chem. Res. 49 (2010) 2025–2030. doi:10.1021/ie9014759.

[97] Y. Zhang, I.H. Musselman, J.P. Ferraris, K.J. Balkus, Gas permeability properties of Matrimid?? membranes containing the metal-organic framework Cu-BPY-HFS, J. Memb. Sci. 313 (2008) 170–181. doi:10.1016/j.memsci.2008.01.005.

[98] J.S. Gregg, R.J. Andres, G. Marland, China: Emissions pattern of the world leader in CO2 emissions from fossil fuel consumption and cement production, Geophys. Res. Lett. 35 (2008) 2–6. doi:10.1029/2007GL032887.

[99] C. Le Quéré, R.J. Andres, T. Boden, T. Conway, R.A. Houghton, J.I. House, G. Marland, G.P. Peters, G.R. Van Der Werf, A. Ahlström, R.M. Andrew, L. Bopp, J.G. Canadell, P. Ciais, S.C. Doney, C. Enright, P. Friedlingstein, C. Huntingford, A.K. Jain, C. Jourdain, E. Kato, R.F. Keeling, K. Klein Goldewijk, S. Levis, P. Levy, M. Lomas, B. Poulter, M.R. Raupach, J. Schwinger, S. Sitch, B.D. Stocker, N. Viovy, S. Zaehle, N. Zeng, The global carbon budget 1959-2011, Earth Syst. Sci. Data. 5 (2013) 165–185. doi:10.5194/essd-5-165-2013.

[100] I.U.S. Energy, Electricity Generation Year: 2016, International Energy statistic Database., (2016). http://www.eia.gov/electricity/ (accessed May 20, 2008).

[101] J.D. Figueroa, T. Fout, S. Plasynski, H. McIlvried, R.D. Srivastava, Advances in CO2 capture technology-The U.S. Department of Energy's Carbon Sequestration Program, Int. J. Greenh. Gas Control. 2 (2008) 9–20. doi:10.1016/S1750-5836(07)00094-1.

[102] P. Luis, T. Van Gerven, B. Van Der Bruggen, Recent developments in membrane-based technologies for CO 2 capture, Prog. Energy Combust. Sci. 38 (2012) 419–448. doi:10.1016/j.pecs.2012.01.004.

[103] R. Castro-Muñoz, V. Fíla, C.T. Dung, Mixed Matrix Membranes Based on PIMs for Gas Permeation: Principles, Synthesis, and Current Status, Chem. Eng. Commun. 204 (2017) 295–309. doi:10.1080/00986445.2016.1273832.

[104] J. Ismail, A. F., Jaafar, Matrimid® Membranes, in: L. Drioli, E., Giorno (Ed.), Enyclopedia Membr., Springer-Verlag Berlin Heidelberg, 2015: pp. 1–3. doi:DOI 10.1007/978-3-642-40872-4_349-6.

[105] R. Castro-Muñoz, V. Martin-Gil, M.Z. Ahmad, V. Fíla, Matrimid® 5218 in preparation of membranes for gas separation - current state-of-the-art, Chem. Eng. Commun. 205 (2018) 161–196. doi:http://dx.doi.org/10.1080/00986445.2017.1378647.

[106] J. Peter, K. V. Peinemann, Multilayer composite membranes for gas separation based on crosslinked PTMSP gutter layer and partially crosslinked Matrimid?? 5218 selective layer, J. Memb. Sci. 340 (2009) 62–72. doi:10.1016/j.memsci.2009.05.009.

[107] Y. Xiao, Y. Dai, T.S. Chung, M.D. Guiver, Effects of brominating Matrimid polyimide on the physical and gas transport properties of derived carbon membranes, Macromolecules. 38 (2005) 10042–10049. doi:10.1021/ma051354j.

[108] S.M. Davoodi, M. Sadeghi, M. Naghsh, A. Moheb, Olefin–paraffin separation performance of polyimide Matrimid®/silica nanocomposite membranes, RSC Adv. 6 (2016) 23746–23759. doi:10.1039/C6RA00553E.

[109] Y. Xiao, T.S. Chung, M.L. Chng, S. Tamai, A. Yamaguchi, Structure and properties relationships for aromatic polyimides and their derived carbon membranes: Experimental and simulation approaches, J. Phys. Chem. B. 109 (2005) 18741–18748. doi:10.1021/jp050177l.

[110] R. Castro-Muñoz, V. Fila, Z. Ahmad, Enhancing the CO2 Separation Performance of Matrimid 5218 Membranes for CO2/CH4 Binary Mixtures, Chem. Eng. Technol. (2019) 645–654. doi:10.1002/ceat.201800111.

[111] S. Matteucci, V.A. Kusuma, S.D. Kelman, B.D. Freeman, Gas transport properties of MgO filled poly(1-trimethylsilyl-1-propyne) nanocomposites, Polymer (Guildf). 49 (2008) 1659–1675. doi:10.1016/j.polymer.2008.01.004.

[112] B. Zornoza, S. Irusta, C. Téllez, J. Coronas, Mesoporous silica sphere-polysulfone mixed matrix membranes for gas separation, Langmuir. 25 (2009) 5903–5909. doi:10.1021/la900656z.

[113] J. Ma, Y. Ying, Q. Yang, Y. Ban, H. Huang, X. Guo, Y. Xiao, D. Liu, Y. Li, W. Yang, C. Zhong, Mixed-matrix membranes containing functionalized porous metal – organic polyhedrons, Chem. Commun. 51 (2015) 4249–4251. doi:10.1039/C5CC00384A.

[114] R. Castro-Muñoz, V. Fíla, V. Martin-Gil, C. Muller, Enhanced CO2 permeability in Matrimid ® 5218 mixed matrix membranes for separating binary CO2/CH 4 mixtures, Sep. Purif. Technol. 210 (2019) 553–562. doi:10.1016/j.seppur.2018.08.046.

[115] T.H. Kim, W.J. Koros, G.R. Husk, K.C. O'Brien, Relationship between gas separation properties and chemical structure in a series of aromatic polyimides, J. Memb. Sci. 37 (1988) 45–62. doi:10.1016/S0376-7388(00)85068-1.

[116] J.O. Hsieh, K.J. Balkus, J.P. Ferraris, I.H. Musselman, MIL-53 frameworks in mixed-matrix membranes, Microporous Mesoporous Mater. 196 (2014) 165–174. doi:10.1016/j.micromeso.2014.05.006.

[117] B.W. Rowe, B.D. Freeman, D.R. Paul, Physical aging of ultrathin glassy polymer films tracked by gas permeability, Polymer (Guildf). 50 (2009) 5565–5575. doi:10.1016/j.polymer.2009.09.037.

[118] J.G. Afonso, C.A.M & Crespo, ed., Green Separation Processes: Fundamentals and Applications, 1st Ed., Wiley-VCH, Weinheim, Germany, 2015.

[119] A. Figoli, S. Santoro, F. Galiano, A. Basile, Pervaporation membranes: preparation, characterization, and application, in: A. Basile, A. Figoli, M. Khayet (Eds.), Pervaporation, Vap. Permeat. Membr. Distill., First edit, Elsevier Ltd., Cambridge UK, 2015: pp. 281–304.

[120] R.W. Baker, Membrane Technology and Applications, 2nd Ed., John Wiley & Sons, New York, 2007.

[121] F. Galiano, F. Falbo, A. Figoli, Polymeric Pervaporation Membranes : Organic-Organic Separation, in: O. Visakh, P. Nazarenko (Eds.), Nanostructured Polym. Membr., Scrivener Publishing LLC, Massachusetts, United States, 2016: pp. 281–304.

[122] A. Kudasheva, S. Sorribas, B. Zornoza, C. Téllez, J. Coronas, Pervaporation of water/ethanol mixtures through polyimide based mixed matrix membranes containing ZIF-8, ordered mesoporous silica and ZIF-8-silica core-shell spheres, J. Chem. Technol. Biotechnol. 90 (2015) 669–677. doi:10.1002/jctb.4352.

[123] Y. Han, K. Wang, J. Lai, Y. Liu, Hydrophilic chitosan-modi fi ed polybenzoimidazole membranes for pervaporation dehydration of isopropanol aqueous solutions, J. Memb. Sci. 463 (2014) 17–23. doi:10.1016/j.memsci.2014.03.052.

[124] D.W. Mangindaan, G. Min Shi, T.S. Chung, Pervaporation dehydration of acetone using P84 co-polyimide flat sheet membranes modified by vapor phase crosslinking, J. Memb. Sci. 458 (2014) 76–85. doi:10.1016/j.memsci.2014.01.030.

[125] H. Badiger, S. Shukla, S. Kalyani, S. Sridhar, Thin film composite sodium alginate membranes for dehydration of acetic acid and isobutanol, J. Appl. Polym. Sci. 131 (2014) 1–9. doi:10.1002/app.40018.

[126] Y.K. Ong, G.M. Shi, N.L. Le, Y.P. Tang, J. Zuo, S.P. Nunes, T.S. Chung, Recent membrane development for pervaporation processes, Prog. Polym. Sci. 57 (2016) 1–31. doi:10.1016/j.progpolymsci.2016.02.003.

[127] W. Zhang, Y. Ying, J. Ma, X. Guo, H. Huang, D. Liu, C. Zhong, Mixed matrix membranes incorporated with polydopamine-coated metal-organic framework for dehydration of ethylene glycol by pervaporation, J. Memb. Sci. 527 (2017) 8–17. doi:http://dx.doi.org/10.1016/j.memsci.2017.01.001.

[128] N.S. Prasad, S. Moulik, S. Bohra, K.Y. Rani, S. Sridhar, Solvent resistant chitosan/poly(ether-block-amide) composite membranes for pervaporation of n-methyl-2-pyrrolidone/water mixtures, Carbohydr. Polym. 136 (2016) 1170–1181. doi:10.1016/j.carbpol.2015.10.037.

[129] Y.J. Han, W.C. Su, J.Y. Lai, Y.L. Liu, Hydrophilically surface-modified and crosslinked polybenzimidazole membranes for pervaporation dehydration on tetrahydrofuran aqueous solutions, J. Memb. Sci. 475 (2015) 496–503. doi:10.1016/j.memsci.2014.10.050.

[130] C. Shin, X.C. Chen, J.M. Prausnitz, N.P. Balsara, Effect of block copolymer morphology controlled by casting-solvent quality on pervaporation of butanol/water mixtures, J. Memb. Sci. 523 (2017) 588–595. doi:10.1016/j.memsci.2016.09.054.

[131] F. Qin, S. Li, P. Qin, M. Nazmul, T. Tan, A PDMS membrane with high pervaporation performance for the separation of furfural and its potential in industrial application, Green Chem. 16 (2014) 1262–1273. doi:10.1039/c3gc41867g.

[132] N.R. Singha, P. Das, S.K. Ray, Recovery of pyridine from water by pervaporation using filled and crosslinked EPDM membranes, J. Ind. Eng. Chem. 19 (2013) 2034–2045. doi:10.1016/j.jiec.2013.03.017.

[133] D. Manjunath, M. Madhumala, S. Kalyani, R. Prasad, S. Sridhar, Extraction of Tetrahydrofuran and Ethylene Dichloride Solvents from Aqueous Solutions by Pervaporation through Thin Film Composite PDMS Membranes Extraction, Sep. Sci. Technol. 48 (2013) 706–715. doi:10.1080/01496395.2012.710700.

[134] J. nan Shen, Y. xia Chu, H. min Ruan, L. guang Wu, C. jie Gao, B. Van der Bruggen, Pervaporation of benzene/cyclohexane mixtures through mixed matrix membranes of chitosan and Ag+/carbon nanotubes, J. Memb. Sci. 462 (2014) 160–169. doi:10.1016/j.memsci.2014.03.040.

[135] L. Wang, X. Han, J. Li, D. Zheng, L. Qin, Modified MCM-41 silica spheres filled polydimethylsiloxane membrane for dimethylcarbonate/methanol separation via pervaporation, J. Appl. Polym. Sci. 127 (2013) 4662–4671. doi:10.1002/app.38046.

[136] S. Zereshki, A. Figoli, S.S. Madaeni, S. Simone, M. Esmailinezhad, E. Drioli, Pervaporation separation of MeOH / MTBE mixtures with modified PEEK membrane : Effect of operating conditions, J. Memb. Sci. 371 (2011) 1–9. doi:10.1016/j.memsci.2010.11.068.

[137] R. Castro-Muñoz, F. Galiano, V. Fíla, E. Drioli, A. Figoli, Matrimid®5218 dense membrane for the separation of azeotropic MeOH-MTBE mixtures by pervaporation, Sep. Purif. Technol. 199 (2018) 27–36. doi:10.1016/j.seppur.2018.01.045.

[138] D. Cai, S. Hu, Q. Miao, C. Chen, H. Chen, C. Zhang, P. Li, P. Qin, T. Tan, Bioresource Technology Two-stage pervaporation process for effective in situ removal acetone-butanol-ethanol from fermentation broth, Bioresour. Technol. 224 (2017) 380–388. doi:10.1016/j.biortech.2016.11.010.

[139] R.D. Offeman, C.N. Ludvik, Poisoning of mixed matrix membranes by fermentation components in pervaporation of ethanol, J. Memb. Sci. 367 (2011) 288–295. doi:10.1016/j.memsci.2010.11.005.

[140] X. Zhan, J.D. Li, C. Fan, X.L. Han, Pervaporation separation of ethanol/water mixtures with chlorosilane modified silicalite-1/PDMS hybrid membranes, Chinese J. Polym. Sci. (English Ed. 28 (2010) 625–635. doi:10.1007/s10118-010-9136-4.

[141] P. Chuntanalerg, S. Kulprathipanja, T. Chaisuwan, P. Aungkavattana, K. Hemra, S. Wongkasemjit, Performance polybenzoxazine membrane and mixed matrix membrane for ethanol purification via pervaporation applications, J. Chem. Technol. Biotechnol. 91 (2016) 1173–1182. doi:10.1002/jctb.4704.

[142] F. Xiangli, Y. Chen, W. Jin, N. Xu, Polydimethylsiloxane (PDMS)/ Ceramic Composite Membrane with High Flux for Pervaporation of Ethanol - Water Mixtures, Ind. Eng. Chem. Res. 46 (2007) 2224–2230. doi:10.1021/ie0610290.

[143] J. Goldemberg, J. Goldemberg, Ethanol for a Sustainable Energy Future, Sci. 315 (2007) 808–810. doi:10.1126/science.1137013.

[144] S. Santoro, F. Galiano, J.C. Jansen, A. Figoli, Strategy for scale-up of SBS pervaporation membranes for ethanol recovery from diluted aqueous solutions, Sep. Purif. Technol. 176 (2017) 252–261. doi:10.1016/j.seppur.2016.12.018.

[145] Y. Lin, S. Tanaka, Ethanol fermentation from biomass resources: Current state and prospects, Appl. Microbiol. Biotechnol. 69 (2006) 627–642. doi:10.1007/s00253-005-0229-x.

[146] M. Balat, H. Balat, Recent trends in global production and utilization of bio-ethanol fuel, Appl. Energy. 86 (2009) 2273–2282. doi:10.1016/j.apenergy.2009.03.015.

[147] RFA, World Fuel Ethanol Production, Renew. Fuels Assoc. (2017). http://www.ethanolrfa.org/resources/industry/statistics/#1454098996479-8715d404-e546 (accessed January 22, 2018).

[148] P.R. Lennartsson, P. Erlandsson, M.J. Taherzadeh, Integration of the first and second generation bioethanol processes and the importance of by-products, Bioresour. Technol. 165 (2014) 3–8. doi:10.1016/j.biortech.2014.01.127.

[149] Z. Lei, C. Li, B. Chen, Extractive Distillation: A Review, Sep. Purif. Rev. 32 (2003) 121–213. doi:10.1081/SPM-120026627.

[150] G.D.A. Onuki S., Koziel J.A., van Leeuwen J., Jenks W. S., Ethanol production, purification, and analysis techniques: a review, Agric. Biosyst. Eng. 1 (2008) 1–11.

[151] J.-H. Chang, J.-K. Yoo, S.-H. Ahn, K.-H. Lee, S.-M. Ko, Simulation of pervaporation process for ethanol dehydration by using pilot test results, Korean J. Chem. Eng. 15 (1998) 28–36. doi:10.1007/BF02705302.

[152] W. Kujawski, S.R. Krajewski, Sweeping gas pervaporation with hollow-fiber ion-exchange membranes, Desalination. 162 (2004) 129–135. doi:10.1016/S0011-9164(04)00036-0.

[153] P. Shao, R.Y.M. Huang, Polymeric membrane pervaporation, J. Memb. Sci. 287 (2007) 162–179. doi:10.1016/j.memsci.2006.10.043.

[154] J. Fontalvo, P. Cuellar, J.M.K. Timmer, M.A.G. Vorstman, J.G. Wijers, J.T.F. Keurentjes, Comparing pervaporation and vapor permeation hybrid distillation processes, Ind. Eng. Chem. Res. 44 (2005) 5259–5266. doi:10.1021/ie049225z.

[155] G. Jyoti, A. Keshav, J. Anandkumar, Review on Pervaporation: Theory, Membrane Performance, and Application to Intensification of Esterification Reaction, J. Eng. (United States). 2015 (2015). doi:10.1155/2015/927068.

[156] S. Chovau, D. Degrauwe, B. Van Der Bruggen, Critical analysis of techno-economic estimates for the production cost of lignocellulosic bio-ethanol, Renew. Sustain. Energy Rev. 26 (2013) 307–321. doi:10.1016/j.rser.2013.05.064.

[157] P. Peng, B. Shi, Y. Lan, A Review of Membrane Materials for Ethanol Recovery by Pervaporation, Sep. Sci. Technol. 46 (2011) 234–246. doi:10.1080/01496395.2010.504681.

[158] W. Qiu, M. Kosuri, F. Zhou, W.J. Koros, Dehydration of ethanol-water mixtures using asymmetric hollow fiber membranes from commercial polyimides, J. Memb. Sci. 327 (2009) 96–103. doi:10.1016/j.memsci.2008.11.029.

[159] Y.M. Xu, T.S. Chung, High-performance UiO-66/polyimide mixed matrix membranes for ethanol, isopropanol and n-butanol dehydration via pervaporation, J. Memb. Sci. 531 (2017) 16–26. doi:10.1016/j.memsci.2017.02.041.

[160] L.L. Xia, C.L. Li, Y. Wang, In-situ crosslinked PVA/organosilica hybrid membranes for pervaporation separations, J. Memb. Sci. 498 (2016) 263–275. doi:10.1016/j.memsci.2015.10.025.

[161] S. Xu, L. Shen, C. Li, Y. Wang, Y. Wang, Properties and pervaporation performance of poly(vinyl alcohol) membranes crosslinked with various dianhydrides, J. Appl. Polym. Sci. 135 (2018) 15–19. doi:10.1002/app.46159.

[162] J. Crespo, C. Brazinha, Fundamentals of pervaporation, in: A. Basile, A. Figoli, M. Khayet (Eds.), Pervaporation, Vap. Permeat. Membr. Distill., Elsevier Ltd., Cambridge UK, 2015: pp. 1–17.

[163] B. Bolto, M. Hoang, Z. Xie, A review of membrane selection for the dehydration of aqueous ethanol by pervaporation, Chem. Eng. Process. Process Intensif. 50 (2011) 227–235. doi:10.1016/j.cep.2011.01.003.

[164] J. Nilsen-nygaard, S.P. Strand, K.M. Vårum, K.I. Draget, C.T. Nordgård, Chitosan: Gels and Interfacial Properties, (2015) 552–579. doi:10.3390/polym7030552.

[165] N. Wynn, Pervaporation comes of Age., 2001. http://people.clarkson.edu/~wwilcox/Design/pervapn.pdf.

[166] R.D. Noble, Perspectives on mixed matrix membranes, J. Memb. Sci. 378 (2011) 393–397. doi:10.1016/j.memsci.2011.05.031.

[167] J.G. Wijmans, R.W. Baker, The solution-diffusion model: a review, J. Memb. Sci. 107 (1995) 1–21. doi:10.1016/0376-7388(95)00102-I.

[168] S.L. Wee, C.T. Tye, S. Bhatia, Membrane separation process-Pervaporation through zeolite membrane, Sep. Purif. Technol. 63 (2008) 500–516. doi:10.1016/j.seppur.2008.07.010.

[169] L. Ying, Y. Wang, T. Chung, X. Yi, J. Lai, Polyimides membranes for pervaporation and biofuels separation, Prog. Polym. Sci. 34 (2009) 1135–1160. doi:10.1016/j.progpolymsci.2009.06.001.

[170] T.C. Bowen, R.D. Noble, J.L. Falconer, Fundamentals and applications of pervaporation through zeolite membranes, J. Memb. Sci. 245 (2004) 1–33. doi:10.1016/j.memsci.2004.06.059.

[171] C.J. Rhodes, Properties and applications of zeolites, Sci. Prog. 93 (2010) 223–284. doi:10.3184/003685010X12800828155007.

[172] E. Okumuş, T. Gürkan, L. Yilmaz, Effect of fabrication and process parameters on the morphology and performance of a PAN-based zeolite-filled pervaporation membrane, J. Memb. Sci. 223 (2003) 23–38. doi:10.1016/S0376-7388(03)00287-4.

[173] Z. Huang, H.M. Guan, W.L. Tan, X.Y. Qiao, S. Kulprathipanja, Pervaporation study of aqueous ethanol solution through zeolite-incorporated multilayer poly(vinyl alcohol) membranes: Effect of zeolites, J. Memb. Sci. 276 (2006) 260–271. doi:10.1016/j.apcatb.2005.10.011.

[174] Z. Huang, Y. Shi, R. Wen, Y.H. Guo, J.F. Su, T. Matsuura, Multilayer poly(vinyl alcohol)-zeolite 4A composite membranes for ethanol dehydration by means of pervaporation, Sep. Purif. Technol. 51 (2006) 126–136. doi:10.1016/j.seppur.2006.01.005.

[175] S. Amnuaypanich, J. Patthana, P. Phinyocheep, Mixed matrix membranes prepared from natural rubber/poly(vinyl alcohol) semi-interpenetrating polymer network (NR/PVA semi-IPN) incorporating with zeolite 4A for the pervaporation dehydration of water-ethanol mixtures, Chem. Eng. Sci. 64 (2009) 4908–4918. doi:10.1016/j.ces.2009.07.028.

[176] P. Amnuaypanich, S., Naowanon, T., Wongthep, W., Phinyocheep, Highly Water-Selective Mixed Matrix Membranes from Natural Rubber-blend-poly(acrylic acid) (NR-blend-PAA) Incorporated with Zeolite 4A for the Dehydration of Water–Ethanol Mixtures through Pervaporation, J. Appl. Polym. Sci. 124 (2012) E319–E329.

[177] H.M. Guan, T.S. Chung, Z. Huang, M.L. Chng, S. Kulprathipanja, Poly(vinyl alcohol) multilayer mixed matrix membranes for the dehydration of ethanol-water mixture, J. Memb. Sci. 268 (2006) 113–122. doi:10.1016/j.memsci.2005.05.032.

[178] G. Lin, M. Abar, L.M. Vane, Mixed Matrix Silicone and Fluorosilicone/Zeolite 4A Membranes for Ethanol Dehydration by Pervaporation, Sep. Sci. Technol. (Philadelphia, PA, U. S.). 48 (2013) 523–536. doi:10.1080/01496395.2012.719057.

[179] Y.L. Liu, C.Y. Hsu, Y.H. Su, J.Y. Lai, Chitosan-silica complex membranes from sulfonic acid functionalized silica nanoparticles for pervaporation dehydration of ethanol-water solutions, Biomacromolecules. 6 (2005) 368–373. doi:10.1021/bm049531w.

[180] L.M. Vane, V. V. Namboodiri, T.C. Bowen, Hydrophobic zeolite-silicone rubber mixed matrix membranes for ethanol-water separation: Effect of zeolite and silicone component selection on pervaporation performance, J. Memb. Sci. 308 (2008) 230–241. doi:10.1016/j.memsci.2007.10.003.

[181] L.M. Vane, V. V. Namboodiri, R.G. Meier, Factors affecting alcohol-water pervaporation performance of hydrophobic zeolite-silicone rubber mixed matrix membranes, J. Memb. Sci. 364 (2010) 102–110. doi:10.1016/j.memsci.2010.08.006.

[182] H. Sun, L. Lu, X. Chen, Z. Jiang, Pervaporation dehydration of aqueous ethanol solution using H-ZSM-5 filled chitosan membranes, Sep. Purif. Technol. 58 (2008) 429–436. doi:10.1016/j.seppur.2007.09.012.

[183] S.G. Adoor, L.S. Manjeshwar, S.D. Bhat, T.M. Aminabhavi, Aluminum-rich zeolite beta incorporated sodium alginate mixed matrix membranes for pervaporation dehydration and esterification of ethanol and acetic acid, J. Memb. Sci. 318 (2008) 233–246. doi:10.1016/j.memsci.2008.02.043.

[184] S.D. Bhat, T.M. Aminabhavi, Pervaporation-Aided Dehydration and Esterification of Acetic Acid with Ethanol Using 4A Zeolite-Filled Cross-linked Sodium Alginate-Mixed Matrix Membranes, J. Appl. Polym. Sci. 113 (2009) 157–168. doi:10.1002/app.29545.

[185] J.H. Choi, J. Jegal, W.N. Kim, H.S. Choi, Incorporation of Multiwalled Carbon Nanotubes into Poly(vinyl alcohol) Membranes for Use in the Pervaporation of Water/Ethanol Mixtures, J. Appl. Polym. Sci. 111 (2008) 2186–2193.

[186] D. Yang, J. Li, Z. Jiang, L. Lu, X. Chen, Chitosan/TiO2 nanocomposite pervaporation membranes for ethanol dehydration, Chem. Eng. Sci. 64 (2009) 3130–3137. doi:10.1016/j.ces.2009.03.042.

[187] A.M. Hu W.W., Zhang, X.H., Zhang, Q. G., Liu, Q. L., Zhu, Pervaporation Dehydration of Water/Ethanol/Ethyl Acetate Mixtures Using Poly(vinyl alcohol)–Silica Hybrid Membranes, J. Appl. Polym. Sci. 126 (2012) 778–787.

[188] F.U. Nigiz, H. Dogan, N.D. Hilmioglu, Pervaporation of ethanol/water mixtures using clinoptilolite and 4A filled sodium alginate membranes, Desalination. 300 (2012) 24–31. doi:10.1016/j.desal.2012.05.036.

[189] G.M. Shi, T. Yang, T.S. Chung, Polybenzimidazole (PBI)/zeolitic imidazolate frameworks (ZIF-8) mixed matrix membranes for pervaporation dehydration of alcohols, J. Memb. Sci. 415–416 (2012) 577–586. doi:10.1016/j.memsci.2012.05.052.

[190] R.Y.M. Huang, R. Pal, G.Y. Moon, Characteristics of sodium alginate membranes for the pervaporation dehydration of ethanol-water and isopropanol-water mixtures, J. Memb. Sci. 160 (1999) 101–113. doi:10.1016/S0376-7388(99)00071-X.

[191] V. Datsyuk, M. Kalyva, K. Papagelis, J. Parthenios, D. Tasis, A. Siokou, I. Kallitsis, C. Galiotis, Chemical oxidation of multiwalled carbon nanotubes, Carbon N. Y. 46 (2008) 833–840. doi:10.1016/j.carbon.2008.02.012.

[192] D. Vairavapandian, P. Vichchulada, M.D. Lay, Preparation and modification of carbon nanotubes: Review of recent advances and applications in catalysis and sensing, Anal. Chim. Acta. 626 (2008) 119–129. doi:10.1016/j.aca.2008.07.052.

[193] Q. Wan, C. Ramsey, G. Baran, Thermal pretreatment of silica composite filler materials, J. Therm. Anal. Calorim. 99 (2010) 237–243. doi:10.1007/s10973-009-0139-8.

[194] K. Sunitha, S. V. Satyanarayana, S. Sridhar, Phosphorylated chitosan membranes for the separation of ethanol-water mixtures by pervaporation, Carbohydr. Polym. 87 (2012) 1569–1574. doi:10.1016/j.carbpol.2011.09.054.

[195] V.T. Magalad, G.S. Gokavi, K.V.S.N. Raju, T.M. Aminabhavi, Mixed matrix blend membranes of poly(vinyl alcohol)-poly(vinyl pyrrolidone) loaded with phosphomolybdic acid used in pervaporation dehydration of ethanol, J. Memb. Sci. 354 (2010) 150–161. doi:10.1016/j.memsci.2010.02.055.

[196] P. Wei, X. Qu, H. Dong, L. Zhang, H. Chen, C. Gao, Silane-modified NaA zeolite/PAAS hybrid pervaporation membranes for the dehydration of ethanol, J. Appl. Polym. Sci. 128 (2013) 3390–3397. doi:10.1002/app.38555.

[197] J. Lawler, Incorporation of Graphene-Related Carbon Nanosheets in Membrane Fabrication for Water Treatment: A Review, Membranes (Basel). 6 (2016) 57. doi:10.3390/membranes6040057.

[198] S.P. Dharupaneedi, R. V. Anjanapura, J.M. Han, T.M. Aminabhavi, Functionalized graphene sheets embedded in chitosan nanocomposite membranes for ethanol and isopropanol dehydration via pervaporation, Ind. Eng. Chem. Res. 53 (2014) 14474–14484. doi:10.1021/ie502751h.

[199] S. Panahian, A. Raisi, A. Aroujalian, Multilayer mixed matrix membranes containing modified-MWCNTs for dehydration of alcohol by pervaporation process, Desalination. 355 (2015) 45–55. doi:10.1016/j.desal.2014.10.027.

[200] Y. Zhang, H., Wang, Poly(vinyl alcohol)/ZIF-8 NH2 Mixed Matrix Membranes for Ethanol Dehydration via Pervaporation, AIChE J. 62 (2016) 1728–1739.

[201] P. Delgado, M.T. Sanz, S. Beltrán, Pervaporation study for different binary mixtures in the esterification system of lactic acid with ethanol, Sep. Purif. Technol. 64 (2008) 78–87. doi:10.1016/j.seppur.2008.08.002.

[202] A. Penkova, G. Polotskaya, A. Toikka, Pervaporation composite membranes for ethyl acetate production, Chem. Eng. Process. Process Intensif. 87 (2015) 81–87. doi:10.1016/j.cep.2014.11.015.

[203] Ó. de la Iglesia, S. Sorribas, E. Almendro, B. Zornoza, C. Téllez, J. Coronas, Metal-organic framework MIL-101(Cr) based mixed matrix membranes for esterification of ethanol and acetic acid in a membrane reactor, Renew. Energy. 88 (2016) 12–19. doi:10.1016/j.renene.2015.11.025.

[204] M. Zhang, L. Chen, Z. Jiang, J. Ma, Effects of Dehydration Rate on the Yield of Ethyl Lactate in a Pervaporation-Assisted Esterification Process, Ind. Eng. Chem. Res. 54 (2015) 6669–6676. doi:10.1021/acs.iecr.5b01199.

[205] C.S.M. Pereira, V.M.T.M. Silva, S.P. Pinho, A.E. Rodrigues, Batch and continuous studies for ethyl lactate synthesis in a pervaporation membrane reactor, J. Memb. Sci. 361 (2010) 43–55. doi:10.1016/j.memsci.2010.06.014.

[206] E. Sert, F.S. Atalay, N-Butyl acrylate production by esterification of acrylic acid with n-butanol combined with pervaporation, Chem. Eng. Process. Process Intensif. 81 (2014) 41–47. doi:10.1016/j.cep.2014.04.010.

[207] K. Liu, X. Feng, Z. Tong, L. Li, Removal of trace water from organic mixtures by pervaporation separation during butyl acetate production via esterification, Sep. Sci. Technol. 40 (2005) 2021–2033. doi:10.1081/SS-200068429.

[208] G. Liu, S. Guo, B. He, J. Li, X. Qian, Synthesis of Butyl Acetate in a Membrane Reactor in a Flow-Through Mode, Int. J. Chem. React. Eng. 14 (2016) 579–585. doi:10.1515/ijcre-2015-0198.

[209] D.J. Benedict, S.J. Parulekar, S.P. Tsai, Pervaporation-assisted esterification of lactic and succinic acids with downstream ester recovery, J. Memb. Sci. 281 (2006) 435–445. doi:10.1016/j.memsci.2006.04.012.

[210] V.S. Chandane, A.P. Rathod, K.L. Wasewar, Coupling of in-situ pervaporation for the enhanced esterification of propionic acid with isobutyl alcohol over cenosphere based catalyst, Chem. Eng. Process. Process Intensif. 119 (2017) 16–24. doi:10.1016/j.cep.2017.05.015.

[211] P.M. Budd, N.M.P.S. Ricardo, J.J. Jafar, B. Stephenson, R. Hughes, Zeolite/Polyelectrolyte Multilayer Pervaporation Membranes for Enhanced Reaction Yield, Ind. Eng. Chem. Res. 43 (2004) 1863–1867. doi:10.1021/ie034142o.

[212] J.J. Jafar, P.M. Budd, R. Hughes, Enhancement of esterification reaction yield using zeolite A vapour permeation membrane, J. Memb. Sci. 199 (2002) 117–123. doi:10.1016/S0376-7388(01)00683-4.

[213] D.J. Benedict, S.J. Parulekar, S.P. Tsai, Esterification of lactic acid and ethanol with/without pervaporation, Ind. Eng. Chem. Res. 42 (2003) 2282–2291. doi:10.1021/ie020850i.

[214] J. Ma, M. Zhang, L. Lu, X. Yin, J. Chen, Z. Jiang, Intensifying esterification reaction between lactic acid and ethanol by pervaporation dehydration using chitosan-TEOS hybrid membranes, Chem. Eng. J. 155 (2009) 800–809. doi:10.1016/j.cej.2009.07.044.

[215] S. Sorribas, A. Kudasheva, E. Almendro, B. Zornoza, Ó. De, C. Téllez, J. Coronas, Pervaporation and membrane reactor performance of polyimide based mixed matrix membranes containing MOF HKUST-1, Chem. Eng. Sci. 124 (2015) 37–44. doi:10.1016/j.ces.2014.07.046.

[216] N.C. Burtch, H. Jasuja, K.S. Walton, Water stability and adsorption in metal-organic frameworks, Chem. Rev. 114 (2014) 10575–10612. doi:10.1021/cr5002589.

[217] N. Ko, P.G. Choi, J. Hong, M. Yeo, S. Sung, K.E. Cordova, H.J. Park, J.K. Yang, J. Kim, Tailoring the water adsorption properties of MIL-101 metal–organic frameworks by partial functionalization, J. Mater. Chem. A. 3 (2015) 2057–2064. doi:10.1039/C4TA04907A.

[218] X. Zhan, J. Li, J. Chen, J. Huang, Pervaporation of ethanol/ water mixtures with high flux by zeolite-filled PDMS/PVDF composite membranes, Chinese J. Polym. Sci. 27 (2009) 771–780.

[219] S. Yi, Y. Su, Y. Wan, Preparation and characterization of vinyltriethoxysilane (VTES) modified silicalite-1/PDMS hybrid pervaporation membrane and its application in ethanol separation from dilute aqueous solution, J. Memb. Sci. 360 (2010) 341–351. doi:10.1016/j.memsci.2010.05.028.

[220] P. Peng, B. Shi, Y. Lan, Preparation of PDMS—Silica Nanocomposite Membranes with Silane Coupling for Recovering Ethanol by Pervaporation, Sep. Sci. Technol. 46 (2011) 420–427. doi:10.1080/01496395.2010.527896.

[221] X. Zhan, J. Lu, T. Tan, J. Li, Mixed matrix membranes with HF acid etched ZSM-5 for ethanol/water separation: Preparation and pervaporation performance, Appl. Surf. Sci. 259 (2012) 547–556. doi:10.1016/j.apsusc.2012.05.167.

[222] T.C. Bowen, R.G. Meier, L.M. Vane, Stability of MFI zeolite-filled PDMS membranes during pervaporative ethanol recovery from aqueous mixtures containing acetic acid, J. Memb. Sci. 298 (2007) 117–125. doi:10.1016/j.memsci.2007.04.007.

[223] H. Zhou, Y. Su, X. Chen, Y. Wan, Separation of acetone, butanol and ethanol (ABE) from dilute aqueous solutions by silicalite-1/PDMS hybrid pervaporation membranes, Sep. Purif. Technol. 79 (2011) 375–384. doi:10.1016/j.seppur.2011.03.026.

[224] I.L. Borisov, G.S. Golubev, V.P. Vasilevsky, A. V. Volkov, V. V. Volkov, Novel hybrid process for bio-butanol recovery: Thermopervaporation with porous condenser assisted by phase separation, J. Memb. Sci. 523 (2017) 291–300. doi:10.1016/j.memsci.2016.10.009.

[225] P. Luis, B. Van Der Bruggen, The driving force as key element to evaluate the pervaporation performance of multicomponent mixtures, Sep. Purif. Technol. 148 (2015) 94–102. doi:10.1016/j.seppur.2015.05.006.

[226] F.N. M. Winterberg, E. Schulte-Korne, U. Peters, Methyl Tert-Butyl Ether, Ullmann's Encycl. Ind. Chem. (2010) 413–454. doi:10.1002/14356007.a16.

[227] S. Sridhar, B. Smitha, A. Shaik, Pervaporation – Based Separation of Methanol / MTBE Mixtures — A Review, 2119 (2017). doi:10.1081/SPM-200054949.

[228] G. Khatinzadeh, M. Mahdyarfar, A. Mehdizadeh, Pervaporation ( PV ) Separation of Methanol / Methyl Tert-butyl Ether Mixtures in Low Permeate Pressure Conditions, 7 (2017) 43–48.

[229] S. Cao, Y. Shi, G. Chen, Influence of acetylation degree of cellulose acetate on pervaporation properties for MeOH / MTBE mixture, 165 (2000) 89–97.

[230] H. Wu, X. Fang, X. Zhang, Z. Jiang, B. Li, X. Ma, Cellulose acetate – poly ( N-vinyl-2-pyrrolidone ) blend membrane for pervaporation separation of methanol / MTBE mixtures, 64 (2008) 183–191. doi:10.1016/j.seppur.2008.09.013.

[231] J. Rhim, Y. Kim, Pervaporation Separation of MTBE – Methanol Mixtures Using Cross-linked PVA Membranes, (1999) 1699–1707.

[232] M. Peivasti, A. Madandar, T. Mohammadi, Effect of operating conditions on pervaporation of methanol / methyl tert -butyl ether mixtures, 47 (2008) 1069–1074. doi:10.1016/j.cep.2007.08.005.

[233] S. Zereshki, A. Figoli, S.S. Madaeni, S. Simone, E. Drioli, Pervaporation Separation of Methanol / Methyl tert -Butyl Ether with Poly ( lactic acid ) Membranes, J. Appl. Polym. Sci. 118 (2010) 1364–1371. doi:10.1002/app.

[234] G.L. Han, Q.G. Zhang, A.M. Zhu, Q.L. Liu, Pervaporation separation of methanol/methyl tert-butyl ether mixtures using polyarylethersulfone with cardo membranes, Sep. Purif. Technol. 107 (2013) 211–218. doi:10.1016/j.seppur.2013.01.039.

[235] G. Gozzelino, G. Malucelli, Permeation of methanol / methyl- t -butyl ether mixtures through poly ( ethylene-co-vinyl acetate ) films, 235 (2004) 35–44. doi:10.1016/j.colsurfa.2004.01.004.

[236] K. Zhou, Q. Gen, G.L. Han, A.M. Zhu, Q. Lin, Pervaporation of water – ethanol and methanol – MTBE mixtures using poly ( vinyl alcohol )/ cellulose acetate blended membranes, J. Memb. Sci. 448 (2013) 93–101. doi:10.1016/j.memsci.2013.08.005.

[237] M. Villegas, A.I. Romero, M.L. Parentis, E.F.C. Vidaurre, J.C. Gottifredi, Chemical Engineering Research and Design Acrylic acid plasma polymerized poly ( 3-hydroxybutyrate ) membranes for methanol / MTBE separation by pervaporation, Chem. Eng. Res. Des. 109 (2016) 234–248. doi:10.1016/j.cherd.2016.01.018.

[238] S. Ray, S.K. Ray, Synthesis of highly methanol selective membranes for separation of methyl tertiary butyl ether ( MTBE )– methanol mixtures by pervaporation, 278 (2006) 279–289. doi:10.1016/j.memsci.2005.11.011.

[239] L. Ying, T. Chung, R. Rajagopalan, Dehydration of alcohols by pervaporation through polyimide Matrimid ( R ) asymmetric hollow fibers with various modifications Dehydration of alcohols by pervaporation through polyimide Matrimid  asymmetric hollow fibers with various modifications, (2008). doi:10.1016/j.ces.2007.09.026.

[240] L.Y. Jiang, T. Chung, R. Rajagopalan, Matrimid / MgO Mixed Matrix Membranes for Pervaporation, AIChE J. 53 (2007) 1745–1757. doi:10.1002/aic.

[241] L.S. White, A.R. Nitsch, Solvent recovery from lube oil filtrates with a polyimide membrane, J. Memb. Sci. 179 (2000) 267–274. doi:10.1016/S0376-7388(00)00517-2.

[242] I. Soroko, M.P. Lopes, A. Livingston, The effect of membrane formation parameters on performance of polyimide membranes for organic solvent nanofiltration (OSN): Part A. Effect of polymer/solvent/non-solvent system choice, J. Memb. Sci. 381 (2011) 152–162. doi:10.1016/j.memsci.2011.07.027.

[243] G. Wang, Hua, Yeager, Solvent-resistant membranes from solvent-inert polyimides and polyketones, US 20070056901 A1, 2007.

[244] Y. Zhang, I.H. Musselman, J.P. Ferraris, K.J. Balkus, Gas permeability properties of mixed-matrix matrimid membranes containing a carbon aerogel: A material with both micropores and mesopores, Ind. Eng. Chem. Res. 47 (2008) 2794–2802. doi:10.1021/ie0713689.

[245] K. Fatyeyeva, A. Dahi, C. Chappey, RSC Advances E ff ect of cold plasma treatment on surface properties and gas permeability of polyimide fi lms, (2014) 31036–31046. doi:10.1039/C4RA03741C.

[246] R. Ravindra, S. Sridhar, A.A. Khan, Separation Studies of Hydrazine from Aqueous Solutions by Pervaporation, (1999) 1969–1980.

[247] W.-F. Su, Principles of Polymer Design and Synthesis, 82 (2013). doi:10.1007/978-3-642-38730-2.

[248] C.M. Hansen, Hansen solubility parameters: A user's book, 2nd Editio, CRC Press, Taylor & Francis Group, New York, 2007.

[249] P. Musto, M. Galizia, P. La Manna, M. Pannico, G. Mensitieri, Diffusion and molecular interactions in a methanol/polyimide system probed by coupling time-resolved FTIR spectroscopy with gravimetric measurements, Front Chem. 2 (2014) 2. doi:10.3389/fchem.2014.00002.

[250] M.M. Nakagawa Kanji, Process for producing ether compound, U.S. Patent 5292963 A, 1994.

[251] B. Shi, Y. Wu, J. Liu, Vapor permeation separation of MeOH/MTBE through polyimide/sulfonated poly(ether-sulfone) hollow-fiber membranes, Desalination. 161 (2004) 59–66. doi:10.1016/S0011-9164(04)90040-9.

[252] T.E.V. Duggal A., Dependence of diffusive permeation rates and selectivities on upstream and downstream pressures : VI. Experimental results for the water/ethanol system, J. Memb. Sci. 27 (1986) 13–30.

[253] A. Figoli, P. Vandezande, F. Galiano, S. Zereshki, Polymeric Pervaporation Membranes: Organic-Organic Separation, in: N.O. Visakh P.M. (Ed.), Nanostructured Polym. Membr., First edit, Scrivener Publishing LLC, 201AD: pp. 281–304.

[254] R. Kopec, M. Meller, W. Kujawski, J. Kujawa, Polyamide-6 based pervaporation membranes for organic-organic separation, Sep. Purif. Technol. 110 (2013) 63–73. doi:10.1016/j.seppur.2013.03.007.

[255] X. Ma, C. Hu, R. Guo, X. Fang, H. Wu, Z. Jiang, HZSM5-filled cellulose acetate membranes for pervaporation separation of methanol/MTBE mixtures, Sep. Purif. Technol. 59 (2008) 34–42. doi:10.1016/j.seppur.2007.05.023.

[256] G.L. Han, K. Zhou, A.N. Lai, Q.G. Zhang, A.M. Zhu, Q. Lin, [ Cu 2 ( bdc ) 2 ( bpy )] n / SPES-C mixed matrix membranes for separation of methanol / methyl tert-butyl ether mixtures, J. Memb. Sci. 454 (2014) 36–43. doi:10.1016/j.memsci.2013.11.049.

[257] Y. Wang, L. Yang, G. Luo, Y. Dai, Preparation of cellulose acetate membrane filled with metal oxide particles for the pervaporation separation of methanol / methyl tert -butyl ether mixtures, Chem. Eng. J. 146 (2009) 6–10. doi:10.1016/j.cej.2008.05.009.

[258] P.T. Anastas, J.C. Warner, Green Chemistry: Theory and Practice, Oxford University Press, New York, 1998.

[259] R. Castro-Muñoz, F. Galiano, V. Fíla, E. Drioli, A. Figoli, Mixed matrix membranes ( MMMs ) for ethanol purification through pervaporation : current state of the art, Rev. Chem. Eng. https//doi.org/10.1515/revce-2017-0115. (2018). doi:https://doi.org/10.1515/revce-2017-0115.

[260] M. Amirilargani, B. Sadatnia, Poly ( vinyl alcohol )/ zeolitic imidazolate frameworks ( ZIF-8 ) mixed matrix membranes for pervaporation dehydration of isopropanol, J. Memb. Sci. 469 (2014) 1–10. doi:10.1016/j.memsci.2014.06.034.

[261] V. Van Hoof, C. Dotremont, A. Buekenhoudt, Performance of Mitsui NaA type zeolite membranes for the dehydration of organic solvents in comparison with commercial polymeric pervaporation membranes, Sep. Purif. Technol. 48 (2006) 304–309. doi:10.1016/j.seppur.2005.06.019.

[262] H.K. Dave, K. Nath, Graphene oxide incorporated novel polyvinyl alcohol composite membrane for pervaporative recovery of acetic acid from vinegar wastewater, J. Water Process Eng. 14 (2016) 124–134. doi:10.1016/j.jwpe.2016.11.002.

[263] N. Wang, S. Ji, J. Li, R. Zhang, G. Zhang, Poly(vinyl alcohol)-graphene oxide nanohybrid “pore-filling” membrane for pervaporation of toluene/n-heptane mixtures, J. Memb. Sci. 455 (2014) 113–120. doi:10.1016/j.memsci.2013.12.023.

[264] W.S. Hummers, R.E. Offeman, Preparation of Graphitic Oxide, J. Am. Chem. Soc. 80 (1958) 1339. doi:10.1021/ja01539a017.

[265] S. Kashyap, S.K. Pratihar, S.K. Behera, Strong and ductile graphene oxide reinforced PVA nanocomposites, J. Alloys Compd. 684 (2016) 254–260. doi:10.1016/j.jallcom.2016.05.162.

[266] G. Wang, Z. Yang, X. Li, C. Li, Synthesis of poly(aniline-co-o-anisidine)-intercalated graphite oxide composite by delamination/reassembling method, Carbon N. Y. 43 (2005) 2564–2570. doi:10.1016/j.carbon.2005.05.008.

[267] S. Stankovich, D.A. Dikin, R.D. Piner, K.A. Kohlhaas, A. Kleinhammes, Y. Jia, Y. Wu, S.B.T. Nguyen, R.S. Ruoff, Synthesis of graphene-based nanosheets via chemical reduction of exfoliated graphite oxide, Carbon N. Y. 45 (2007) 1558–1565. doi:10.1016/j.carbon.2007.02.034.

[268] R. Zhang, X. Xu, B. Cao, P. Li, Fabrication of high-performance PVA / PAN composite pervaporation membranes crosslinked by PMDA for wastewater desalination, Pet. Sci. 15 (2018) 146–156. doi:10.1007/s12182-017-0204-z.

[269] X. Qian, N. Li, Q. Wang, S. Ji, Chitosan/graphene oxide mixed matrix membrane with enhanced water permeability for high-salinity water desalination by pervaporation, Desalination. 438 (2018) 83–96. doi:10.1016/j.desal.2018.03.031.

[270] E.A. Feijani, A. Tavassoli, H. Mahdavi, H. Molavi, Effective gas separation through graphene oxide containing mixed matrix membranes, J. Appl. Polym. Sci. 135 (2018) 1–11. doi:10.1002/app.46271.

[271] K. Krishnamoorthy, M. Veerapandian, K. Yun, S.J. Kim, The chemical and structural analysis of graphene oxide with different degrees of oxidation, Carbon N. Y. 53 (2013) 38–49. doi:10.1016/j.carbon.2012.10.013.

[272] D.R. Dreyer, S. Park, C.W. Bielawski, R.S. Ruoff, The chemistry of Graphite oxide, Chem. Soc. Rev. 39 (2010) 228–240. doi:10.1039/b917103g.

[273] R. Zhang, B. Liang, T. Qu, B. Cao, P. Li, High-performance sulfosuccinic acid cross-linked PVA composite pervaporation membrane for desalination, Environ. Technol. (United Kingdom). 3330 (2017) 1–9. doi:10.1080/09593330.2017.1388852.

[274] S.P. Dharupaneedi, R. V. Anjanapura, J.M. Han, T.M. Aminabhavi, Functionalized graphene sheets embedded in chitosan nanocomposite membranes for ethanol and isopropanol dehydration via pervaporation, Ind. Eng. Chem. Res. 53 (2014) 14474–14484. doi:10.1021/ie502751h.

[275] B. Feng, K. Xu, A. Huang, Synthesis of graphene oxide/polyimide mixed matrix membranes for desalination, RSC Adv. 7 (2017) 2211–2217. doi:10.1039/C6RA24974D.

[276] X. Zhao, O. Zhang, D. Chen, Enhanced Mechanical Properties of Graphene-Based Poly(vinyl alcohol) Composites, Macromolecules. 43 (2010) 2357–2363. doi:10.1021/ma902862u.

[277] S. Zereshki, A. Figoli, S.S. Madaeni, S. Simone, J.C. Jansen, M. Esmailinezhad, E. Drioli, Poly(lactic acid)/poly(vinyl pyrrolidone) blend membranes: Effect of membrane composition on pervaporation separation of ethanol/cyclohexane mixture, J. Memb. Sci. 362 (2010) 105–112. doi:10.1016/j.memsci.2010.06.025.

[278] D.S.M. Constantino, R.P.V. Faria, A.M. Ribeiro, J.M. Loureiro, A.E. Rodrigues, Performance Evaluation of Pervaporation Technology for Process Intensification of Butyl Acrylate Synthesis, Ind. Eng. Chem. Res. 56 (2017) 13064–13074. doi:10.1021/acs.iecr.7b01328.

[279] T.F. Ceia, A.G. Silva, C.S. Ribeiro, J. V. Pinto, M.H. Casimiro, A.M. Ramos, J. Vital, PVA composite catalytic membranes for hyacinth flavour synthesis in a pervaporation membrane reactor, Catal. Today. 236 (2014) 98–107. doi:10.1016/j.cattod.2014.02.052.

[280] S. Homaeigohar, M. Elbahri, Graphene membranes for water desalination, NPG Asia Mater. 9 (2017) e427. doi:10.1038/am.2017.135.

[281] R.R. Nair, H.A. Wu, P.N. Jayaram, I.V. Grigorieva, A.K. Geim, Unimpeded Permeation of Water Through Helium-Leak–Tight Graphene-Based Membranes, Science (80-. ). 335 (2012) 442–445.

[282] K. Huang, G. Liu, W. Jin, Vapor transport in graphene oxide laminates and their application in pervaporation, Curr. Opin. Chem. Eng. 16 (2017) 56–64. doi:10.1016/j.coche.2017.04.009.

[283] S. Kumar Kannam, B.D. Todd, J.S. Hansen, P.J. Daivis, Slip length of water on graphene: Limitations of non-equilibrium molecular dynamics simulations, J. Chem. Phys. 136 (2012). doi:10.1063/1.3675904.

[284] W.S. Hung, Q.F. An, M. De Guzman, H.Y. Lin, S.H. Huang, W.R. Liu, C.C. Hu, K.R. Lee, J.Y. Lai, Pressure-assisted self-assembly technique for fabricating composite membranes consisting of highly ordered selective laminate layers of amphiphilic graphene oxide, Carbon N. Y. 68 (2014) 670–677.

## Abbreviations

$CO_2$: Carbon dioxide

$CO_2$: methane

DSC: Differential scanning calorimetry

EDX: Dispersive X-ray spectroscopy

FESEM: Field emission scanning electron microscopy

FTIR:Fourier transform infrared

GO:Graphene oxide

MMMs: mixed matrix membranes

MOF: Metal-organic framework

MeOH:methanol

MTBE: methyl *tert*-butyl ether

PVA: poly(vinyl alcohol)

PV:Pervaporation

PEG: Poly ethylene glycol

SEM: Scanning electron microscopy

TGA: Thermal gravimetric analysis

XRD:X-ray diffraction

ZIF: Zeolitic imidazolate framework

## Units

Permeability: Barrer

[1 x $10^{-10}$ $cm^3$ (STP) cm $cm^{-2}$ $s^{-1}$ cm $Hg^{-1}$]

Separation factor : [-]

Permeate flux: kg $m^{-2}$ $h^{-1}$

Swelling degree: %

Temperature: ◦C

Tg: ◦C

Pressure: bar

Total flow : mL $min^{-1}$

Thickness: μm

Young`s modulus: N $mm^{-2}$

Elongation at break: %

**BIOGRAPHY**

**Roberto Castro-Muñoz** was born on March 9th, 1988 in Mexico City, Mexico. He attended the Center of Scientific and Technological studies (CECYT No. 1) from *National Polytechnic Institute (IPN)*, Mexico City from the tender age of 15. He later studied the bachelor in Food engineering in Unidad Profesional Interdisciplinaria de Biotecnologia (UPIBI) from *National Polytechnic Institute (IPN)*. He was ranked within the three best students of his generation. After, he joined the transnational petrochemical MEXICHEM Company as a Process Engineer, in which he was commissioned in the department of synthesis of sodium phosphates food grade (D-28 department). One year later, he studied the MSc in Bioprocesses in UPIBI-IPN. The thesis was titled 'Effect of spray drying on the stability of bioactive compounds of purple cactus pear *Opuntia ficus-indica*'. Meantime, he performed a research internship at Institute on Membrane Technology (ITM-CNR), Italy. He defended his research thesis with Honors and awarded by *National Polytechnic Institute* as the best academic performance student.

In 2014, he studied his first Ph.D. in Sciences in Bioprocesses at UPIBI-IPN. He worked on the 'Evaluation of the cooking wastewaters from Nixtamalization process using membrane technology'. In 2015, Roberto was selected and awarded to study the European Union Joint Doctorate 'Erasmus Mundus Doctorate in Membrane Engineering, having as home institution University of Chemistry and Technology Prague, Czech Republic. His hosting institutions, University of Calabria and Institute on Membrane Technology (ITM-CNR), Italy and University of Zaragoza, Spain. His main research activities are oriented to the synthesis and preparation of mixed matrix membranes for gas separation and pervaporation.

To date, he has authored over 38 scientific papers, 8 book chapters in the field of membrane technologies, and their application to environmental and food technology. He is a member of the national research council (SNI 1) of Mexico awarded by CONACYT.

# *Publications related to this thesis*

i) **Castro-Muñoz, R**., Martin-Gil V., Ahmad M.Z., Fíla, V. (2018). Matrimid® 5218 in preparation of membranes for gas separation - current state-of-the-art. *Chemical Engineering Communications*, 205 (2), 161-196.

ii) **Castro-Muñoz, R**., Fíla, V., & Dung, C. T. (2017). Mixed Matrix Membranes Based on PIMs for Gas Permeation: Principles, Synthesis, and Current Status. *Chemical Engineering Communications*, 204(3), 295–309.

iii) Favvas E.P., Figoli A., **Castro-Muñoz R**., Fíla V., He X. (2018). **Chapter 1**: Polymeric membrane materials for $CO_2$ separations. In *Current Trends and Future Developments on (Bio-) Membranes* (Eds. Basile A, Favvas A.), Elsevier, 1-668.

iv) **Castro-Muñoz, R.**; Fíla, V. (2018). Progress on Incorporating Zeolites in Matrimid®5218 Mixed Matrix Membranes towards Gas Separation. *Membranes*, 8, 30.

v) **Castro-Muñoz, R.**, Fíla, V., Ahmad M.Z. (2019). Enhancing $CO_2$ separation performance of Matrimid® 5218 membranes for $CO_2/CH_4$ binary mixtures. *Chemical Engineering & Technology*, 42, 645-654

vi) **Castro-Muñoz, R.**, Fíla, V., Martin-Gil, Muller C. (2019). Enhanced $CO_2$ permeability in Matrimid® 5218 mixed matrix membranes for separating binary $CO_2/CH_4$ mixtures. *Separation and Purification Technology*, 210, 553-562.

vii) **Castro-Muñoz, R.**, Galiano F., Fíla V., Drioli E., Figoli A. (2018). Mixed matrix membranes (MMMs) for ethanol purification through pervaporation: Current state of the art. *Reviews in Chemical Engineering, In Press*.

viii) **Castro-Muñoz, R.**, de la Iglesia Ó., Fíla V., Téllez C., Coronas J. (2018). Pervaporation-Assisted Esterification Reactions by Means of Mixed Matrix Membranes. *Industrial & Engineering Chemistry Research*, 57, 15998-16011.

ix) **Castro-Muñoz, R.**, Galiano F., Fíla V., Drioli E., Figoli A. (2018). Matrimid®5218 dense membrane for the separation of azeotropic MeOH-MTBE mixtures by pervaporation. *Separation and Purification Technology, 199, 27-36.*

x) **Castro-Muñoz, R.**, Buera-González J., de la Iglesia Ó., Galiano F., Fíla V., Rubio C., Figoli A., Téllez C., Coronas J. (2019). Towards the dehydration of ethanol using pervaporation cross-linked poly(vinyl alcohol)/graphene oxide membranes. *Journal of Membrane Science, Accepted.*

xi) **Castro-Muñoz R.** & Fíla V. (2019) Effect of the ZIF-8 distribution in mixed matrix membranes based on Matrimid® 5218 towards $CO_2$ separation. *Chemical Engineering & Technology, Accepted*

xii) **Castro-Muñoz R.,** Ahmad Z., Fíla V. (2019). Enhanced $CO_2$ separation performance of Matrimid® 5218 for $CO_2/CH_4$ binary mixtures. *Chemical Engineering & Technology*, 42, 645-654.

## *Selected conference abstracts*

**i)** **Castro-Muñoz R.,** de la Iglesia O., Fíla V., Téllez C., Coronas J. Hydrophilic materials embedded into polyimides for pervaporation applications. **MELPRO 2018,** Prague, Czech Republic.

**ii)** Castro-Muñoz R., Galiano F., Fíla V., Drioli. E., Figoli A. Matrimid®5218 dense membrane for the separation of azeotropic MeOH-MTBE mixtures by pervaporation , **EUROMEMBRANE 2018,** Valencia, Spain.

iii) Castro-Muñoz R., Fíla V. Enhancement of $CO_2$ separation performance in Matrimid® 5218-PEG 200 membranes by incorporating metal organic frameworks (ZIF-8),**CHISA 2018,** Prague, Czech Republic.

# *Acknowledgments*

I would like to acknowledge the European Commission - Education, Audiovisual and Culture Executive Agency (EACEA) for my PhD scholarship under the program: Erasmus Mundus Doctorate in Membrane Engineering – **EUDIME** (FPA **No 2011-0014**, Edition V, http:/eudime.unical.it). Moreover, I thank the UCT Prague for awarded me three continuous Internal Gran Agency (IGA) (**MSMT No 20-SVV/2017, MSMT No 21-SVV/2018** & **MSMT No 22-SVV/2019**) and three **Emila Votočka** stipendium 2017, 2018, 2019. Acknowledgement also to the financial assistance of Operational Programme Prague – Competitiveness (CZ.2.16/3.1.00/24501) and "National Program of Sustainability" (NPU I LO1613) MSMT-43760/2015.

To my main supervisor Prof. Vlastimil Fíla, who gave me always the support, follow and help over these three years PhD time. ….Děkuji!!! …. Thank you for your positive feedback when I requested something (when everything was in Czech). Also, thank you for your good mood and happiness (always smiling).

To Prof. Alberto Figoli and Dr. Francesco Galiano…..Grazie mille!!!.... Thank you so much for hosting me in the beautiful Calabria and always following me during my mobility. Moreover, thank you for teaching me how another membrane process is working…. Pervaporation.

To Prof. Joaquín Coronas and Prof. Carlos Téllez ….. Muchisimas gracias!!!.... Thank you so much for hosting, following and supervising me at INA-Unizar. Moreover, thank you for teaching me how to be more professional, efficient and fast in the research field. Your contribution to my professional growth is highly thanked.

To Dr. Óscar de la Iglesia and Juan Buera-González ….. Muchisimas gracias!!! Thanks a lot for your contribution in our work done at INA. More than this, thank you for your friendship during this time we were working together.